



HAL
open science

The CaV β 1 isoforms: role in neuromuscular junction formation and implication in Myotonic Dystrophy type 1 pathophysiology

Amélie Vergnol

► **To cite this version:**

Amélie Vergnol. The CaV β 1 isoforms: role in neuromuscular junction formation and implication in Myotonic Dystrophy type 1 pathophysiology. Cellular Biology. Sorbonne Université, 2024. English. NNT: 2024SORUS305 . tel-04833678

HAL Id: tel-04833678

<https://theses.hal.science/tel-04833678v1>

Submitted on 12 Dec 2024

HAL is a multi-disciplinary open access archive for the deposit and dissemination of scientific research documents, whether they are published or not. The documents may come from teaching and research institutions in France or abroad, or from public or private research centers.

L'archive ouverte pluridisciplinaire **HAL**, est destinée au dépôt et à la diffusion de documents scientifiques de niveau recherche, publiés ou non, émanant des établissements d'enseignement et de recherche français ou étrangers, des laboratoires publics ou privés.



Ecole Doctorale Complexité du Vivant – ED515
INSERM UMR-S 974 – Centre de Recherche en Myologie

THESE DE DOCTORAT

En vue de l'obtention du grade de Docteur de Sorbonne Université

Présentée par Amélie VERGNOL

Les isoformes $Ca_v\beta 1$: rôle dans la formation de la jonction neuromusculaire et implication dans la physiopathologie de la Dystrophie Myotonique de type 1

Soutenue publiquement le 12 septembre 2024

Composition du jury :

Isabelle MARTY	Directrice de Recherche	Présidente du jury
Bruno ALLARD	Professeur	Rapporteur
Laurent SCHAEFFER	Professeur	Rapporteur
Vanessa RIBES	Chargée de Recherche	Examinatrice
Mario GOMES-PEREIRA	Directeur de Recherche	Examineur
Dario COLETTI	Maître de Conférence	Représentant de l'établissement
France PIETRI-ROUXEL	Directrice de Recherche	Directrice de thèse
Sestina FALCONE	Chargée de Recherche	Directrice de thèse

"It always seems impossible until it's done."

Nelson Mandela

REMERCIEMENTS

Tout d'abord, je tiens à remercier les membres de mon jury pour avoir accepté d'évaluer mon travail. Je remercie le Pr Bruno Allard et le Pr Laurent Schaeffer d'avoir accepté d'être rapporteurs de ma thèse, et pour le temps consacré à son évaluation, ainsi que Dr Isabelle Marty, Dr Vanessa Ribes, Dr Mario Gomes-Pereira et Dr Dario Coletti d'en être les examinateurs.

Je remercie chaleureusement mes deux directrices de thèse. France, merci de m'avoir accueillie dans ton équipe et d'avoir toujours cru en moi et en mes idées, et ce depuis mon stage de master 2. Tu m'as poussé à prendre confiance en moi et à grandir scientifiquement à travers les défis rencontrés. Sestina, je suis profondément reconnaissante pour ta disponibilité et le soutien inestimable que tu m'as offert tant sur le plan scientifique que personnel, tes réflexions et conseils ont été essentiels tout au long de ces 4 ans de thèse !

Merci infiniment à Stéphanie, ton soutien a été plus que précieux dans la dernière ligne droite de cette thèse et ta passion pour la JNM a été vraiment contagieuse !! Merci pour ton expertise et ta bonne humeur. Tu m'as donné le boost dont j'avais besoin pour aller jusqu'au bout et je t'en suis vraiment reconnaissante.

Merci à mes collaborateurs pour m'avoir apporté leur expertise dans ce travail de thèse : Alain Sureau, Denis Furling et Geneviève Gourdon pour la partie DM1, Eric Allemand pour la partie Nanopore et Eric Bastché pour tout l'analyse épigénétique de l'activité des promoteurs de *Cacnb1*. Et plus généralement pour m'avoir accordé de votre temps pour toutes ces discussions scientifiques stimulantes et enrichissantes.

J'adresse toute ma gratitude aux personnes qui m'ont accompagnées dans la réalisation de ce travail et en particulier Christel, tu as toujours été attentionnée à mon égard, et tu m'as apporté une aide énorme aussi bien pour les manip que sur un plan émotionnel pendant des périodes de doute. Merci aussi pour tes précieux conseils scientifiques et ton expertise que tu es toujours prête à partager ! Merci Massiré pour ton encadrement, toute ton aide, et pour avoir bravé toutes les fouilles archéologiques du -80°C que je t'ai fait subir. A Cécile pour m'avoir apporté ton aide sans hésitation à chacun de mes nombreux moments désespoirs de clonages pour lesquels la lune n'était sûrement pas assez bien alignée avec je ne sais quel astre, merci !

A ma partenaire de galères, Inès évidemment ! A nos innombrables soirées et weekend passés au labo, tu as le don de transformer n'importe quelle situation pour la rendre plus légère par ton rire et ta pétillance (nouveau mot à ajouter au dictionnaire oui), et vu nos galères ça n'est pas peu dire, merci pour ton soutien à toute épreuve ! Le merge n'est pas encore fini, mais promis maintenant ça ne sera que pour du positif. Tu vas déchirer cette dernière année de thèse, tu peux déjà être tellement fière

de toi, je le suis. MT, tu as été une vraie bouffée d'air frais, toujours positive et enthousiaste, un vrai bonheur. Tu m'as apporté énormément, au 105 et ensuite encore depuis l'autre bout du globe. Merci pour tout Habibi tu es une personne incroyable. Lulu, tu es là depuis mon premier jour !! Je suis si contente que tu sois revenue au 105 pour également terminer cette aventure à tes côtés et toujours avec ton énergie inépuisable pour organiser 1000 choses (à quand la prochaine soirée, expo ou je ne sais quel évènement, évidemment suivi d'un brunch ??). Merci pour touuuute ton aide et pour ton soutien énorme au quotidien, toujours présente à mes côtés, merci merci merci. Maxime et Aly, le binôme infernal, quand ce n'est pas l'un qui m'embête c'est l'autre, avouez, vous aviez un planning secret pour ça ? Toujours à m'embêter oui, mais toujours présents dès que j'appelai au secours (en particulier pour mes manip souris !). Et puis entre le temps démesuré que tu as passé sur mes JNM Aly et les manip foireuses que je t'ai refilé sur cette fin de thèse Maxime, vous avez été plus qu'incroyables, merci ! Aurélie, un grand merci à toi aussi pour ta gentillesse et ta présence sur laquelle j'ai pu compter dès ton arrivée. Sonia, tu as littéralement volé à mon secours, je n'en reviens toujours pas je t'en suis tellement reconnaissante. Promis j'ai bien mangé ce midi, et ce soir aussi ;) . Je voulais aussi mentionner Pierrot, au-delà de tes vanes incessantes, tu m'as beaucoup boosté pour que je prenne du recul sur le chemin parcouru et les obstacles surmontés, merci à toi pour tout cela. Maintenant il faudra trouver quelqu'un d'autre à blâmer pour le bazar de la salle de culture (non, pas Inès, je te vois venir) !

Un énorme merci à tous les copains du 2^{ème} étage, anciens et actuels, que ce soit au labo ou en dehors, lors de nos périples à Nice, en Grèce, en weekend au fin fond du 77, ou simplement autour d'un verre (ou de burgers, je n'oublie pas les burgers MT), vous avez rendu cette thèse mémorable. Je pense notamment à Chiara, Mathilde, Anne, Marie, Zoheir, Arielle, Cynthia, Jérôme, Chloé, Alessandra mais aussi aux pirates : Odessa, Axel, Chloé, Nicolas, Marius, Morgane, Benoît, Alexandra. Votre présence au cours de ma thèse a été très importante pour moi, merci pour ces moments si précieux.

En dehors de cette aventure professionnelle (qui m'a amené à des rencontres qui ne se limiteront sûrement pas à ce cadre), ces années de thèse ont également été marquées par le soutien de ma famille et de mes amis. Un grand merci à mes parents, mon frère et ma sœur pour m'avoir encouragé, accompagné (et supporté !!) tout au long de mon parcours.

Merci également à mes amis : Flora, Mélody, Raph, Gaël et Antoine, pour m'avoir écouté me plaindre à de si nombreuses reprises mais surtout pour tous ces moments partagés et pour votre soutien sans faille. Je pense aussi à Pauline, Alice, merci pour votre patience et votre soutien pendant cette période plus que tumultueuse. Et également à mes colocs Camille et Nabelle qui ont vécu et m'ont soutenu en direct dans mes paniques de fin de thèse, promis maintenant le salon va redevenir un salon et non plus un chaos de paperasse scientifique. Antoine, merci d'avoir été présent sur cette fin de thèse, tu m'as permis de souffler et garder le cap !

Et pour finir par ça car c'était fou, mes héros de fin de thèse : Sonia, Lulu, Massiré, you saved me !!

RESUME

Quatre protéines $Ca_v\beta$ ($Ca_v\beta 1$ à $Ca_v\beta 4$) sont connues comme des sous-unités régulatrices des canaux Calcium (Ca^{2+}) dépendants du voltage (Voltage-gated Ca^{2+} Channels, VGCC), chacune ayant des profils d'expression spécifiques selon leur fonction. Bien qu'elles soient principalement reconnues pour leur rôle dans la régulation des VGCC, les protéines $Ca_v\beta$ peuvent également agir indépendamment de ces canaux, en tant que régulateurs de l'expression génique. Parmi ces protéines, $Ca_v\beta 1$ est exprimée dans le muscle squelettique sous différentes isoformes. L'isoforme adulte constitutive, $Ca_v\beta 1D$, est localisée au niveau du sarcolemme et plus précisément à la triade, où elle joue un rôle crucial dans la régulation de Ca_v1 et ainsi du mécanisme de Couplage Excitation-Contraction (CEC), essentiel à la contraction musculaire.

Dans cette thèse, nous nous sommes concentrés sur les isoformes embryonnaires/périnatales de $Ca_v\beta 1$, moins étudiées, y compris la $Ca_v\beta 1E$ précédemment décrite. Nous avons étudié leurs rôles dans le système neuromusculaire. En effet, la protéine $Ca_v\beta 1$ s'est révélée essentielle au développement de la jonction neuromusculaire (JNM), mais l'implication spécifique de ses isoformes y reste encore inconnue. Notre étude a donc évalué le rôle des isoformes $Ca_v\beta 1$ à différents stades de la formation, de la maturation et de maintenance de la JNM. Parallèlement, étant donné la dérégulation de $Ca_v\beta 1$ dans la dystrophie myotonique de type 1 (DM1), nous avons exploré son rôle fonctionnel dans ce contexte pathologique.

Nous avons tout d'abord identifié $Ca_v\beta 1A$ comme une isoforme exprimée pendant l'embryogenèse et les stades périnataux. Nos résultats ont révélé que l'expression des isoformes $Ca_v\beta 1$ est régulée par l'activation différentielle des promoteurs au cours du développement : un promoteur dans l'exon1 (Prom1) contrôle l'expression de $Ca_v\beta 1A/E$, tandis qu'un promoteur dans l'exon2B (Prom2) contrôle l'expression de $Ca_v\beta 1D$. Il est intéressant de noter qu'un endommagement du nerf déclenche une réactivation du Prom1, conduisant à la réexpression des transcrits de $Ca_v\beta 1A/E$.

De plus, nous avons découvert que les isoformes embryonnaires/périnatales de $Ca_v\beta 1$ sont impliquées dans l'agrégation des RACH (Récepteur à l'Acétylcholine) dans un système de myotubes *in vitro* et que leur expression postnatale influence la maturation/stabilité de la JNM. Dans le contexte pathologique de la DM1, nous avons observé une augmentation de l'expression de $Ca_v\beta 1A/E$, qui semble atténuer la myotonie, un symptôme caractéristique de cette pathologie. De plus, nous avons trouvé que la modulation de leur expression est liée aux protéines MuscleBlind Like (MBNL), centrales dans la physiopathologie de la DM1.

En conclusion, ce travail de thèse a permis de clarifier les connaissances sur les différentes isoformes de $Ca_v\beta 1$ dans le muscle squelettique et d'apporter de nouveaux éléments sur leur rôle dans deux contextes indépendants : le développement de la JNM et de la physiopathologie de la DM1. Comprendre la régulation des isoformes protéiques de $Ca_v\beta 1$ dans le muscle squelettique est essentiel pour déchiffrer les mécanismes de l'homéostasie musculaire et potentiellement identifier de nouvelles approches thérapeutiques pour faire face aux pathologies musculaires.

Mots clés : $Ca_v\beta 1$, isoformes, Jonction NeuroMusculaire (JNM), pré-empainte, Dytrophie Myotonique de type 1 (DM1), Muscleblind Like (MBNL)

ABSTRACT

Four $\text{Ca}_v\beta$ proteins ($\text{Ca}_v\beta 1$ to $\text{Ca}_v\beta 4$) are described as regulatory subunit of Voltage-gated Ca^{2+} channel (VGCC), each exhibiting specific expression pattern in excitable cells based on their function. While primarily recognized for their role in VGCC regulation, $\text{Ca}_v\beta$ proteins also function independently of channels, acting as regulators of gene expression. Among these, $\text{Ca}_v\beta 1$ is expressed in skeletal muscle as different isoforms. The adult constitutive isoform, $\text{Ca}_v\beta 1D$, is located at the sarcolemma and more specifically at the triad, where it plays a crucial role in regulating Ca_v1 to control Excitation-Contraction Coupling (ECC) mechanism, essential for muscle contraction.

In this thesis, we further explored the less studied $\text{Ca}_v\beta 1$ isoforms, with a particular focus on embryonic/perinatal variants, including the previously described $\text{Ca}_v\beta 1E$. We investigated their roles in the neuromuscular system. Indeed, $\text{Ca}_v\beta 1$ proteins have been shown to be crucial for neuromuscular junction (NMJ) development, though the involvement of specific isoform still remains unclear. Our investigation assessed the role of $\text{Ca}_v\beta 1$ isoforms at different stages of NMJ formation, maturation and maintenance. Additionally, given the deregulation of $\text{Ca}_v\beta 1$ in Myotonic Dystrophy Type 1 (DM1), we explored its functional role in this muscular pathological context.

First, we identified $\text{Ca}_v\beta 1A$ as another isoform expressed during embryogenesis and perinatal stages. Our findings revealed that $\text{Ca}_v\beta 1$ isoforms expressions are regulated by the differential activation of promoters during development: a promoter in exon1 (Prom1) drives $\text{Ca}_v\beta 1A/E$ expressions, while a promoter in exon2B (Prom2) controls $\text{Ca}_v\beta 1D$ expression. Interestingly, nerve damage in adult muscle triggers a shift toward the Prom1 activation and leading to the re-expression of $\text{Ca}_v\beta 1A/E$ transcripts.

Furthermore, we found that $\text{Ca}_v\beta 1$ embryonic/perinatal isoforms are involved in the proper *in vitro* Acetylcholine Receptor (AChR) aggregation and that their postnatal expressions influence NMJ maturation/maintenance. In the pathological context of DM1, we observed the increased expression of $\text{Ca}_v\beta 1A/E$, which appears to mitigate myotonia symptoms. In addition, we found that the modulation of their expression is linked with MuscleBlind Like (MBNL) proteins, which are central in the pathophysiology of DM1.

In conclusion, this thesis work has clarified knowledge of the various $\text{Ca}_v\beta 1$ isoforms in skeletal muscle and provides new insights into their role in two independent contexts of NMJ development and DM1 pathophysiology. Understanding $\text{Ca}_v\beta 1$ protein regulation in skeletal muscle is essential to decipher muscle homeostasis mechanisms and potentially identify new therapeutic targets to face muscular disorders.

Key words: $\text{Ca}_v\beta 1$, isoforms, NeuroMuscular Junction (NMJ), pre-patterning, Myotonic Dystrophy Type 1 (DM1), Muscleblind Like (MBNL)

ABBREVIATIONS

AAV: Adeno-Associated-Virus	CSD: Chromo Shadow Domain
ABP: AID-binding pocket	cTNT: cardiac Troponin T
ACh: AcetylCholine	DGC: Dystrophin-Glycoprotein Complex
AChE: AcetylCholineEsterase	DHPR: Dihydropyridine Receptor (Ca _v 1.1)
AChR: AcethylCholine Receptor	DICR: Depolarization-Induced Ca ²⁺ Release
ADP: Adenosine DiPhosphate	DM1: Myotonic Dystrophy Type 1
AID: Alpha Interaction Domain	DM: Myotonic Dystrophy
APA: Alternative PolyAdenylation	ECC: Excitation Contraction-Coupling
AP: Action Potential	EDL: Extensor Digitorum Longus
ASD: Autism Spectrum Disorder	ENMG: Electroneuromyogram
ATP: Adenosine TriPhosphate	ER: Endoplasmic Reticulum
ATPase: Adenosine TriPhosphatase	FBS: Fetal Bovine Serum
BID: Beta Interaction Domain	GAS: Gastrocnemius
Ca ²⁺ : Calcium	GDF5: Growth Differentiation Factor 5
CELF: CUG-BP, Elav-like Family	GK: Guanylate Kinase
CHCB2/HP1 γ : CHromo Box protein 2/Heterochromatin Protein 1 γ	HCM: Hypertrophic CardioMyopathy
CICR: Ca ²⁺ Induced Ca ²⁺ Release	HD: HomeoDomain
Cl ⁻ : Chloride	HSA: Human Skeletal alpha-Actin
CLIP: CrossLinking ImmunoPrecipitation	HSA ^{LR} : HSA Long Repeats
CLIPseq: CLIP sequencing	HVA: High-Voltage-Activated
CMAP: Compound Muscle Activity Potential	IF: ImmunoFluorescence
CNS: Central Nervous System	IM: Intramuscular
CRC: Ca ²⁺ Release Complex	IP3: Inositol 3-Phosphate
CREB: Cyclic AMP Response Element Binding	IP3R: IP3 Receptor
	KD: Knock Down

KO: Knock Out

Lrp4: Low-density lipoprotein receptor-related protein 4

LTCC: L-Type Ca^{2+} Channel

LVA: Low-Voltage-Activated

MAGUK: Membrane-Associated GUanylate Kinase

MBNL: MuscleBlind-Like

MBNL1: MuscleBlind-Like 1

MBNL2: MuscleBlind-Like 2

MBNL3: MuscleBlind-Like 3

Mdg: Muscular Dysgenesis

MEF2: Myocyte Enhancer Factor 2

MH: Malignant Hyperthermia

MHC: Myosin Heavy Chain

MPC: Muscle Precursor Cell

MRFs: Myogenic Regulatory Factors

MuSC: Muscle Satellite Cells

MuSK: Muscle Specific Kinase

Na^+ : sodium

NLS: Nuclear Localization Sequence

NMJ: Neuromuscular junction

ORF: Open Reading Frame

Pax3: Paired box gene 3

PBS: Phosphate-buffered saline

PCR: Polymerase Chain Reaction

PFA: Paraformaldehyde

Pi: inorganic Phosphate

PST: Proline/Serine/Threonine

qPCR: quantitative PCR

RMSD: Root Mean Square Deviation

RNAseq: RNA sequencing

RT: Reverse Transcription

RyR1: Ryanodine Receptor 1

SERCA: SarcoEndoplasmic Reticulum Ca^{2+} ATPase

SH3: Src Homology 3

SOL: Soleus

SPF: Specific-pathogen-free

SR: Sarcoplasmic Reticulum

STAC3: SH3 and cysteine-rich domain-containing protein 3

TA: Tibialis Anterior

TCF4: T-Cell Factor 4

T-tubule: Transverse-tubule

TU: Transcriptional Unit

UTR: Untranslated region

VDA: Voltage-Dependent Activation

VDCC: Voltage-Dependent Ca^{2+} Channels

Vg: Vector genomes

VGCC: Voltage Gated Ca^{2+} Channel

VDI: Voltage-Dependant Inactivation

WT: Wild-Type

ZnF: Zinc-Finger

FIGURES AND TABLE LIST

Figure 1. Skeletal muscle organization.....	4
Figure 2. Myogenesis.	5
Figure 3. Sarcomeres during contraction.....	9
Figure 4. Detailed muscle organization and ultrastructure of muscle fiber components.	10
Figure 5. Variation of membrane potential during depolarization.....	13
Figure 6. Skeletal muscle ECC process: overview.....	14
Figure 7. Myofilaments during muscle contraction process: the cross-bridge cycle.....	15
Figure 8. Structure and functional domains of $Ca_v1.1$ channel with a particular focus on α_1s within the cell membrane, highlighting its critical domains.....	16
Figure 9. Arrangement in tetrads and interaction of $Ca_v1.1$ and RyR1 within muscle cells.	18
Figure 10. Neuromuscular Junction in mammals.....	20
Figure 11. Molecular mechanism of the Agrin-Lrp4-MuSK signalling.....	21
Figure 12. Development and maturation of AChR at the NMJ.	25
Figure 13. LVA and HVA Ca^{2+} channels and their current types, subunit composition and associated genes.	28
Figure 14. Functional domains and key sites of $Ca_v\beta_1$ proteins.	30
Figure 15. Ca_v -independent $Ca_v\beta s$ functions in regulating gene expression.....	37
Figure 16. Molecular pathogenesis of DM1.....	45
Figure 17. MBNL gene and protein domain structure.	46
Figure 18. Binding of MBNL proteins to mRNA.....	47
Figure 19. Different transcripts from different tissues are incorrectly spliced, causing most DM1 symptoms.....	52
Figure 20. Identification of a putative new $Ca_v\beta_1$ isoform: $Ca_v\beta_{1early}$	105
Figure 21. shMbnl1 model recapitulating DM1 features.....	109
Figure 22. MBNL1 regulates embryonic $Ca_v\beta_1$ isoforms expression.	110
Figure 23. Downregulating embryonic $Ca_v\beta_1$ isoforms in shMbnl1 model exacerbates myotonia. ...	112

Figure 24. Effect of embryonic Cav β 1 isoforms downregulation on myotonia-related molecular defects.	114
Figure 25. MBNL3 regulates embryonic Cacnb1 isoforms expression through their 3'UTR.....	116
Figure 26. Cacnb1 promoters display physical interaction with two enhancer domains.	122
Figure 27. Lack of activating epigenetic marks at the e6289 enhancer region.	123
Figure 28. Lack of activating epigenetic marks at the e6307 enhancer region.	124
Table 1. Tissue distribution of Cav β isoforms	29
Table S1. Primer list for RT-PCR, RT-qPCR, Triplex RT-PCR and CHIP-qPCR.....	132
Table S2. Primer list for Nanopore.....	133
Table S3. Primary antibodies.....	134
Table S4. Secondary antibodies.....	135

TABLE OF CONTENTS

GENERAL INTRODUCTION	1
CHAPTER 1: The neuromuscular system.....	3
I- Skeletal muscle.....	3
a) Skeletal muscle development	4
b) Histological, structural and functional features of skeletal muscle	7
II- Excitation Contraction Coupling (ECC)	11
a) Chronological discoveries.....	12
b) Neuromuscular transmission	12
c) ECC molecular components	15
III- The neuromuscular junction (NMJ).....	19
a) AP transmission to the muscle	19
b) Molecular actors at the NMJ	20
c) NMJ formation, maturation and maintenance	22
CHAPTER 2: Cavβ proteins	28
I- Cavβ proteins.....	29
a) Cav β isoforms	29
b) Structural features of Cav β proteins	30
II- Cavβ regulation of HVA Ca²⁺ channels.....	31
a) Plasma membrane expression of Cav α 1	31
b) HVA Ca ²⁺ channel gating properties	31
c) RGK inhibition of HVA Ca ²⁺ channels.....	32
III- Cavβ1 & ECC	33
a) Tetrad formation	33
b) Voltage sensing and charge movement	34
c) Interaction with RyR1	34
IV- Cav-independent Cavβ function: Regulation of gene expression	35
a) Nuclear localization	35
b) Ca ²⁺ mediated modulation of gene expression	36
c) Interaction with transcription factors	38
d) Interaction with regulatory DNA sequence.....	39
V- Cavβ associated disorders.....	40
a) Cav β as Cav regulatory subunit.....	40
b) Cav-independent disorders	41
CHAPTER 3: MuscleBlind Like (MBNL) proteins & Myotonic Dystrophy Type 1	43
I- Dystrophy Myotonic Type 1.....	43
a) Generalities	43
b) Pathophysiology: DM1 as a toxic RNA disorder	44
II- MBNL proteins.....	44
a) Generalities on MBNL proteins	45
b) MBNLs as key players in mRNA processing	47
c) MBNL and CELF proteins: antagonist role in RNA processing	49
III- Differential implication of MBNL proteins in DM1 physiopathology.....	50
a) DM1 skeletal muscle defects.....	50
b) DM1 cognitive impairments	51
c) DM1 cardiac defects.....	52
RATIONAL FOR THE CURRENT STUDY & THESIS OBJECTIVES	53

MATERIALS AND METHODS.....	55
Biological material.....	57
I- Plasmids.....	57
II- AAV production.....	57
Mouse experimental models.....	57
I- Animals and ethics.....	57
II- <i>In vivo</i> procedures.....	58
a) Injection procedures.....	58
b) Denervation procedures.....	58
c) Functional analyses.....	59
<i>In vitro</i> procedures.....	59
I- C2C12 muscle cell line, transfection and luciferase assay.....	59
II- Primary cells, transduction and high differentiation induction.....	60
Gene expression analyses.....	60
I- RNA isolation and gene expression analyses.....	60
II- Nanopore sequencing.....	61
III- ChIP experiments.....	61
Protein analyses.....	62
I- Immunoblotting.....	62
II- Immunofluorescence (IF) and image acquisition.....	63
a) Muscle cryosections.....	63
b) Isolated fibers.....	63
c) Primary myotubes.....	63
Statistical analyses.....	64
RESULTS.....	65
CHAPTER 1 - Identification and characterization of Cavβ1 embryonic isoforms in skeletal muscle: Implication for neuromuscular junction (NMJ) formation, maturation and maintenance.....	67
I- Chapter abstract.....	67
II- Results.....	68
a) Article in preparation.....	68
b) Additional results.....	105
CHAPTER 2 - Regulation of Cavβ1 isoforms expression by MBNLs and involvement in Myotonic Dystrophy Type 1.....	107
I- Introduction.....	107
II- Results.....	108
a) shMbnl1, a DM1 model?.....	108
b) Role of Cav β 1 in DM1 features.....	110
c) MBNL3 involvement in Cav β 1 isoform regulation.....	115
d) Mechanistic of the regulation of Cav β 1 expression by MBNLs.....	115

GENERAL DISCUSSION	117
Ca_vβ1 isoforms characterization	119
I- Deciphering Ca _v β1 isoforms: identification/characterization	119
II- Ca _v β1early isoform	120
Regulation of Ca_vβ1 isoforms expression	121
I- Promoter regulation	121
II- 3'-UTR regulation	125
Ca_vβ1 role in NMJ processes	125
I- Ca _v β1 effect on AChR aggregation	125
a) Hypothesis on the regulation of upstream molecular players	125
b) A Ca ²⁺ related process?	126
II- Ca _v β1 effect on NMJ maturation/maintenance	126
III- Limitations of the highly-differentiated myotube model	127
Ca_vβ1s & DM1 pathophysiology	128
I- The shMbnl1 model.....	128
II- Ca _v β1 protective effect on myotonia?	128
III- MBNL1.....	129
IV- MBNL3.....	129
Which of the embryonic Ca_vβ1 isoform is involved in the different described processes?	130
I- In NMJ formation, maturation and maintenance.....	130
II- In DM1 pathophysiology	130
III- In ECC during embryogenesis.....	131
Supplementary data	132
REFERENCES	137
APPENDICES	163
Mini review – Vergnol et al. 2022	165
2 nd author publication – Traoré et al. 2024.....	173

GENERAL INTRODUCTION

CHAPTER 1: The neuromuscular system

Skeletal muscle is the most abundant tissue of the body with approximately 40-45% of the total body mass. It is primarily composed of cells with the unique ability to contract and generate movement and force. There are three types of muscle: cardiac, smooth and skeletal. Cardiac and smooth muscles handle involuntary contractions while skeletal muscles control voluntary movements. The heart pumps blood with regular beats to ensure proper oxygenation of the organs. Smooth muscles manage the contractions of the gastrointestinal, reproductive, urinary, and vascular systems. Skeletal muscles, besides enabling voluntary movements, are also responsible for energy expenditure, supporting skeletal structure and maintaining posture.

The neuromuscular system connects motor nerves to muscles (peripheral nervous system), turning signals from the central nervous system into muscle movement through electrical stimulation from the spinal cord. This system is essential for initiating all body movements, whether voluntary or involuntary.

As my research project focuses on skeletal muscle, we will focus on this tissue for this manuscript.

I- Skeletal muscle

Skeletal muscle is a highly organized tissue that encompasses muscle fibers, which are the contractile units, vasculature for proper oxygenation, nerves triggering electrical activity and connective tissue maintaining joined structures. It has a cable-like arrangement: parallel muscle fibers (or myofibers) are bundled together into fascicles and these parallel fascicles are grouped to form the muscle. Each compartment is enclosed by a supportive conjunctive tissue: the endomysium surrounds each myofiber, the perimysium delimits the muscle fascicles, and the epimysium covers the entire muscle. Blood vessels cross the epimysium and give rise to a fine network of capillaries that reach the perimysium and the endomysium of each myofiber to ensure their vascularization. Similarly, nerves cross the perimysium and arborize the myofibers, forming neuromuscular junctions (NMJ) that innervate each myofiber. The epimysium, therefore containing capillaries and nerves, is located above the plasma membrane of the muscle fiber called sarcolemma (**Fig. 1**).

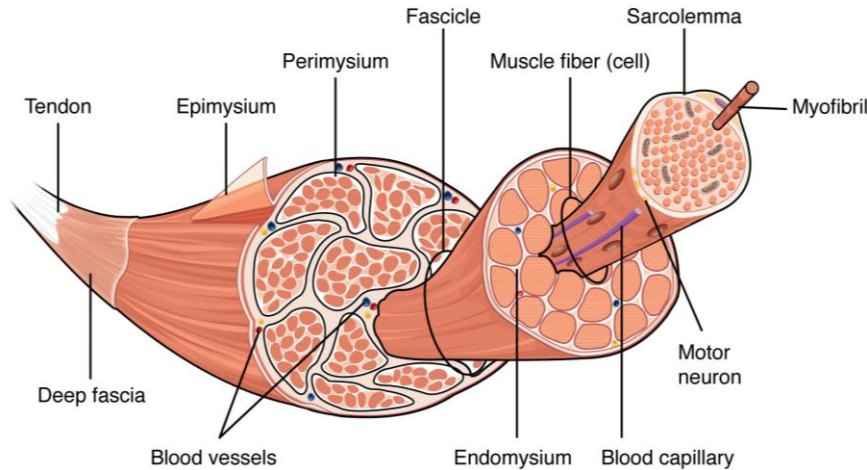


Figure 1. Skeletal muscle organization.

Skeletal muscle structure with muscle fibers, vasculature (for muscle oxygenation), nerves (for electrical activity), and connective tissue layers: endomysium surrounding each myofibers, perimysium delimiting muscle fascicules, and epimysium covering the entire muscle. From <https://sciencediagrams.com/skeletal-muscle/>.

a) Skeletal muscle development

Myogenesis:

Myogenesis is the process by which skeletal muscle tissue formation occurs during embryogenesis and during regeneration after muscle damage. Skeletal muscle is a tissue originating from the mesoderm and more specifically from the dermomyotome where are located the muscle precursor cells (Buckingham et al., 2003). There are two successive waves of myogenesis: the embryonic myogenesis which implements muscle architecture, begins around embryonic day 10.5 (codified with the E letter followed by the number of days post-fecundation, here 10.5) in mice and ends approximately at E14.5 while the fetal myogenesis is responsible for muscle growth and further differentiation, from E14.5 to birth. Postnatally, the muscle tissue continues to mature for 2-3 weeks.

During the embryonic myogenesis, progenitor cells (identified by the expression of paired box gene 3 -Pax3) undergoes delamination from the dermomyotome and migration toward the limb buds (Bober et al., 1994). These undifferentiated mononucleated cells are known as embryonic myoblasts, which proliferate and begin to differentiate: they irreversibly cease division and fuse to form multi-nucleated myotubes. At this stage, the nuclei are centrally positioned, their migration toward the cell periphery takes place during differentiation into myofibers. The fetal myogenesis begins around E14.5 in mice with the second wave of differentiation of progenitor cells giving rise to the fetal myoblasts that fuse either to the embryonic fi* * *

figurebers or to each other, in both cases giving rise to secondary fibers. By E16, the pool of Muscle Satellite Cells (MuSC) is established on the surface of the muscle fibers (**Fig. 2**).

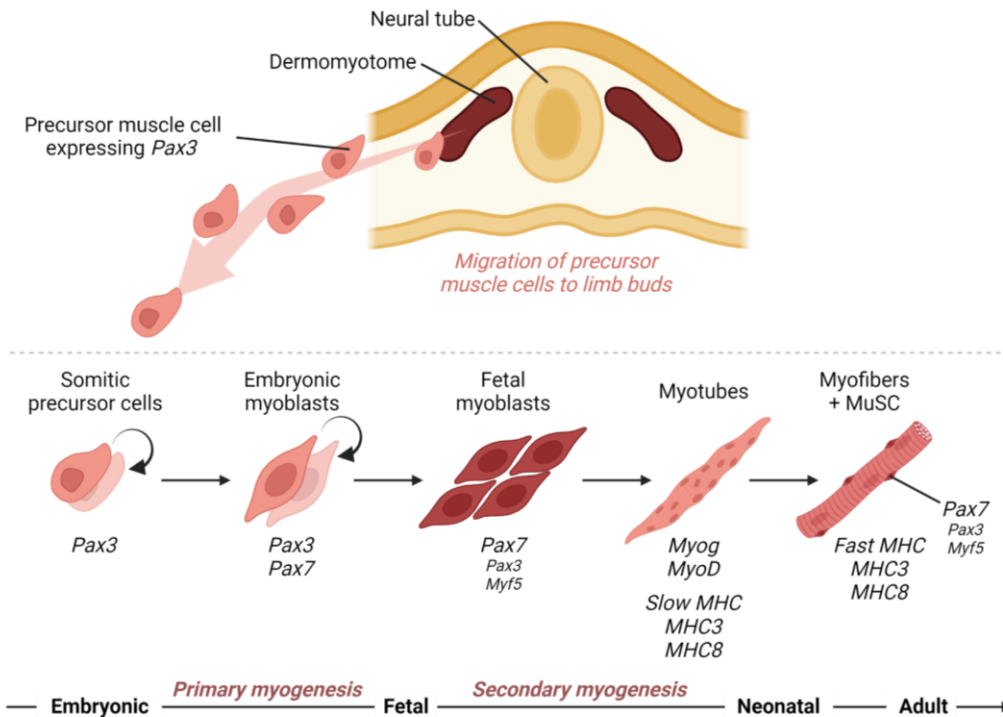


Figure 2. Myogenesis.

The muscle precursor cells migrate from the dermomyotome to the limb buds, and follow different stages of differentiation including a primary and secondary myogenesis during the embryonic and foetal stages, continuing through neonatal and adult periods (created with BioRender.com).

The embryonic and fetal myoblasts are distinct populations that undergo differentiation successively, both originate from Pax3+ progenitors but the fetal myoblasts differ by the higher expression of Pax7 and decreased expression of Pax3. Myogenesis is controlled by transcription factors of the Muscle Regulatory Factors (MRFs) family, which includes 4 proteins: the determination factors MyoD, Myf5, MRF4 and the differentiation factor myogenin, all characterized by a strict spatiotemporal pattern of expression. Together, these proteins initiate the myogenic program, heading undifferentiated cells toward skeletal muscle lineage and ending with a fully mature skeletal muscle tissue. Furthermore, all four MRFs can induce lineage reprogramming of fibroblasts to myoblasts (Braun et al., 1992; Davis et al., 1987).

These molecular events are crucial for the perinatal muscle growth and for adult muscle homeostasis. Indeed, the same myogenic process is recapitulated in adult skeletal muscle after injury, leading to tissue regeneration (Chargé and Rudnicki, 2004). After a phase characterized by necrosis of the injured myofibers and immune response activation, adult muscle regeneration goes through the activation of satellite cells, which are processed toward new fiber formation. Similarly to what happens during muscle development, the myogenic cells proliferate and either fuse to each other's or to pre-existing fibers, to repair the injured muscle (Chargé and Rudnicki, 2004).

Regulation of myogenesis by MRFs proteins:

MRFs proteins are transcription factors that evolved from a single ancestral gene (Atchley et al., 1994). They are basic helix-loop-helix proteins (bHLH) that bind to E-box consensus sequences (CANNTG), sequences characteristically present in the regulatory regions of muscle-specific genes (Berkes and Tapscott, 2005). The bHLH region's structural similarities provide a high degree of functional overlap, but MRFs have been able to acquire specialized roles thanks to the evolutionary divergence of their other domains.

Further studies demonstrated both the overlapping and the specific functions of MRFs through the use of genetically modified models. Individual Myf5 or MyoD genetic ablation does not lead to an obvious muscle phenotype (Braun et al., 1992; Rudnicki et al., 1992) but the double *MyoD/Myf5*-null mice lack essentially all skeletal muscle tissue at birth (Kassar-Duchossoy et al., 2004; Rudnicki et al., 1993) suggesting their redundant role in muscle development during embryogenesis but the necessary presence of at least one of these two factors. Mice harbouring single mutation of MRF4 show altered morphologies but no catastrophic phenotypes (Yoon et al., 1997). The main highly deleterious MRF gene-depleted model is the myogenin depleted mouse that dies at birth due to muscle insufficiency. In this model myoblasts are present, indicating that myogenin is dispensable for establishing the myogenic lineage but is critical for terminal differentiation (Hasty et al., 1993; Nabeshima et al., 1993; Venuti et al., 1995).

While MRFs proteins are mainly expressed during developmental and regenerative myogenesis, Myf5, MyoD and myogenin expression decreases at very low levels once differentiation is complete. Indeed, muscle innervation state strongly regulates their expression (Eftimie et al., 1991; Weis, 1994). The exception is MRF4 which is the more expressed MRFs in healthy adult skeletal muscle (Zammit, 2017), where it plays an important role in regulating adult muscle homeostasis. When decreasing MRF4 levels by RNAi tools *in vivo*, it promotes muscle growth and Moretti and colleagues showed in 2016 that this regulation relies on the negative regulation of MRF4 on Myocyte Enhancer Factor 2 (MEF2) family of proteins. Moretti's work established MEF2 proteins as modulators of muscle homeostasis and hypertrophy, responsible for the expression of numerous muscle-specific genes including those coding for sarcomeric proteins, Excitation-Contraction Coupling (ECC) machinery and energy metabolism (Moretti et al., 2016). More broadly, this study proposes a model in which in normal muscle homeostasis, MRF4 functions to suppress the activation of hypertrophic-genes mediated by MEF2.

Regulation of myogenesis by muscle activity:

Spontaneous muscle contractions begins around E14.5 in mice (Kodama and Sekiguchi, 1984), a phenomenon that has also been observed *in vitro* in myotubes that have differentiated sufficiently. Spontaneous electrical activity, associated with Calcium (Ca^{2+}) transients, can be measured in 3- to 5-day-differentiated myotubes *in vitro* but with no link to noticeable contractions at these times. In

contrast, after a few days, these same changes in membrane potential leads to twitch contractions, demonstrating the maturation of the ECC machinery (Grouselle et al., 1991; Lorenzon et al., 2002).

Importantly, such release of Ca^{2+} plays a role in a variety of molecular pathways important for muscle development like proliferation, migration and fusion of myoblasts, but it also participate in activating transcription of myogenic factors among which myogenin and MEF2 (Benavides Damm and Egli, 2014). Movement during development triggers mechanotransduction, a process by which mechanical stimuli are sensed and converted into an appropriate biological response. Ca^{2+} is known to be a major actor of such mechanism and is therefore going to participate through this means to the aforementioned processes of muscle development.

b) Histological, structural and functional features of skeletal muscle

Myosin isoforms & Fiber types:

The skeletal muscle is consisting of two types of muscle fibers: slow-twitch fibers and fast-twitch fibers. The slow-twitch fibers, also known as type I fibers are responsible for endurance; they are small and highly vascularized. They encompass many mitochondria and low glycogen stores. Conversely, the fast-twitch fibers, or type II fibers, allow some powerful bursts of energy but during shorter periods of time. These fibers are wider and with lower vascularity than the slow-twitch ones, poor in their mitochondria content but rich in glycogen. Glycogen is a complex form of carbohydrate stored in the muscle and the liver. It consists of long glucose chains that, when broken down, offer a quick and effective source of energy for movement. *Extensor Digitorum Longus* (EDL), *Tibialis Anterior* (TA) or *Gastrocnemius* (GAS) are examples of hindlimb fast-twitch muscles while *Soleus* (SOL) is a slow-twitch muscle.

The slow and fast-twitch fibers difference relies on their myosin composition (Pette and Staron, 2000; Reggiani et al., 2000). Myosin is a polypeptide made up of 6 subunits including two heavy chains and four light chains, Myosin Heavy Chain (MHC) isoforms are used as the more suitable markers for distinguishing across fiber types. We can delineate “pure” and “hybrid” fiber types based on whether they include a single or multiples MHC isoforms respectively (Medler, 2019). Four pure fiber types are described including one slow type I fiber (with MHC-I β isoform), and three fast types: IIA (with MHCIIa), IID (with MHCIIId) and IIB (with MHCIIb).

Fiber type identity is first established during embryonic development. However, fiber-type remodeling (or fiber-type transition) can occur in adult skeletal muscle as an adaptation to exercise or during aging (Blaauw et al., 2013; Larson et al., 2019). Many inherited myopathies are also described as affecting fiber type composition of muscle (Talbot and Maves, 2016).

Myofibrils & Sarcomeres:

The muscle fibers (or myofibers) are divided into multiple myofibrils (1-2 μ m in diameter) known as the contractile elements of the muscle cells. Each myofibril is divided into successive structural units called sarcomeres, the smallest contractile unit of the myofiber. Each sarcomere can be divided into different fragments: in the center, a dark band (A band) which is slightly lighter in the middle (H band). On each side of the central dark band, light bands are called I bands. Each sarcomere is delimited by two Z lines (or Z disks) (Au, 2004; Clark et al., 2002) (**Fig. 3**).

The sarcomere consists of different myofilaments: thick filaments and thin filaments. Their association is responsible for the dark/light colours observed in light and electron microscopy (**Fig. 3**), characteristic of the banding aspect of striated muscles: the lateral light bands (I bands) are the thin filaments while the dark central band (A band) is a superposition of both thick and thin protein filaments. The central H band is lighter because of the absence of thin filaments, only thick filaments are present (**Fig. 3**).

Thick filaments are made up of a tail and a head of myosin and thin filaments that are composed of actin (double helix structure) together with tropomyosin and troponin proteins. Actin presents a myosin binding site that is hidden by tropomyosin when the muscle is resting. Tropomyosin is a protein located in the grooves of actin double helix, forming a continuous strand along the whole thin filament. When the muscle is resting, tropomyosin covers its actin binding sites. Troponin is a complex protein including three chains known respectively as Troponin-T that associates with tropomyosin, Troponin-I with an Adenosine TriPhosphatase (ATPase) activity and Troponin-C which possesses four Ca²⁺ binding sites (Johnston et al., 2018).

As mentioned earlier, myofibrils are the contractile elements of the muscle: sarcomeres can be shortened by approximately 70% of their original length during contraction, due to the sliding of thin filaments, tethered at one end to the Z-line, into thick filaments. Under muscle contraction the light I band disappears and the dark A bands gets closer (**Fig. 3**). The mechanism of contraction will be described in the next part.

Triads:

Muscle fiber's cytoplasm is called sarcoplasm, it contains the cytoskeleton, the glycogen stores, and the organelles responsible for its functioning. Among these organelles, we can mention the Endoplasmic Reticulum (ER) and more specifically the Sarcoplasmic Reticulum (SR), and mitochondria. SR is a specialized compartment of the ER which can be divided into the terminal SR cisternae responsible for Ca²⁺ storage/release and the longitudinal SR which is the site of Ca²⁺ uptake (Flucher et al., 1994). Mitochondrion is another important organelle since it produces Adenosine TriPhosphate (ATP) for cell energy. Both Ca²⁺ and ATP are directly used by the myofiber to contract its myofibrils.

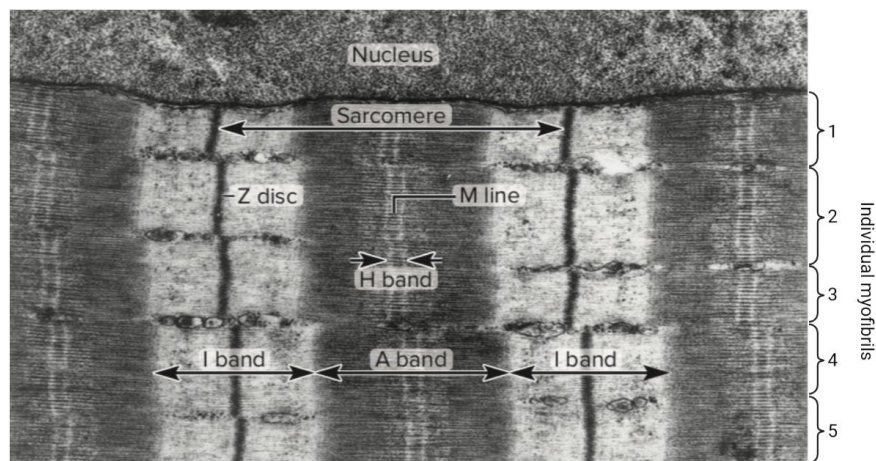
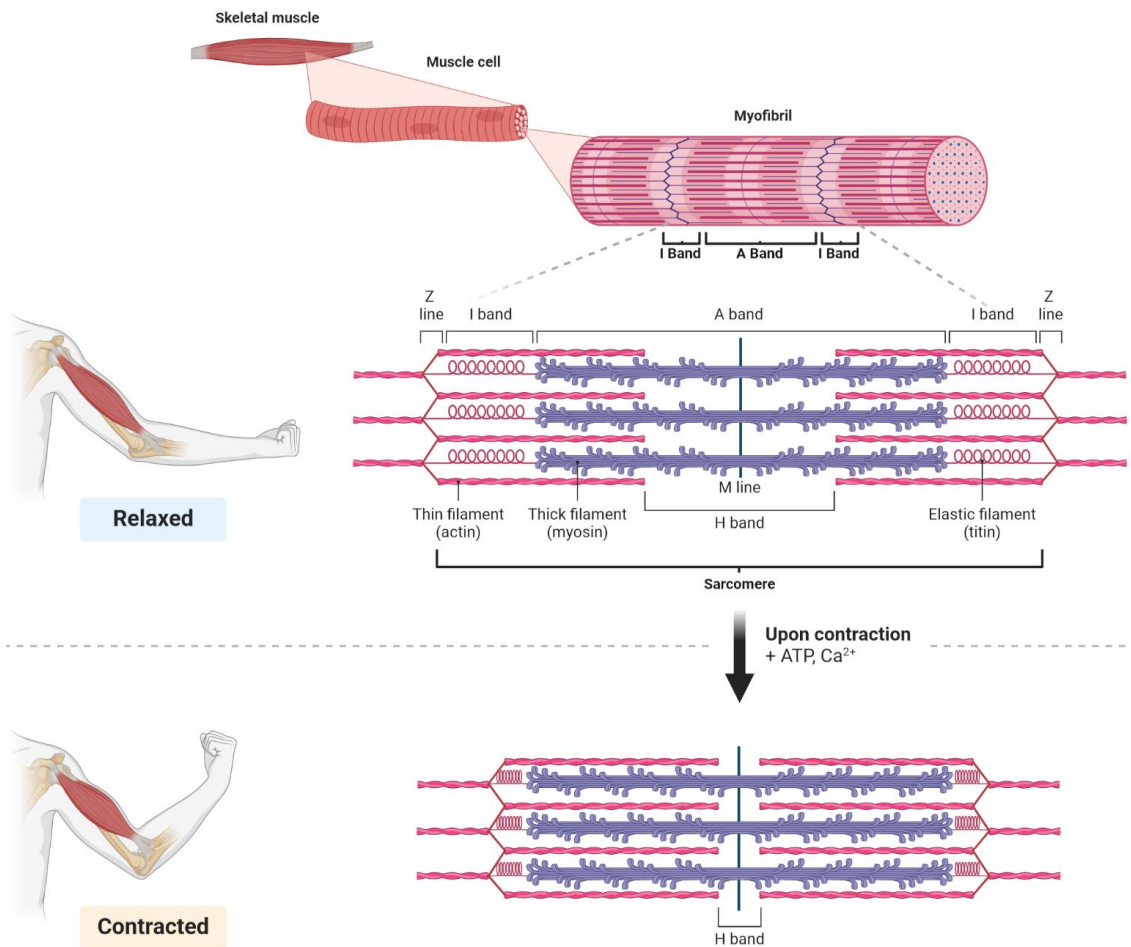


Figure 3. Sarcomeres during contraction.

Skeletal muscle is structured as a cable-like arrangement with myofibers bundled together. Each myofiber is divided into successive contractile units called sarcomeres divided into I, A and H bands as well and Z lines. I and H bands contain only actin and only myosin filaments, respectively. A band regroups both actin and myosin filaments. Z-lines constitute the boundaries of each sarcomere. During contraction, actin and myosin filaments slide past each others leading to the shortening of the sarcomere: I bands disappears and H band shortens (created with BioRender.com). Photo by Don W. Fawcett. Total figure from K.S. Saladin, *Anatomy & Physiology—The Unity of Form and Function*, 8th ed., McGraw-Hill, 2018

As described above, the muscle fiber is surrounded by a membrane called the sarcolemma. This membrane presents tubular invaginations known as Transverse-tubules (T-tubules), evenly distributed along the muscle fiber, penetrating deeply into it. T-tubules are a specificity of striated muscles, they are central in the regulation of SR Ca^{2+} store. Thanks to the presence of ion channels, transporters and pumps, they play a fundamental role in the rapid transmission of the Action Potential (AP) into the cell. One T-tubule surrounded by two terminal SR cisternae forms a triad (**Fig. 4**), a highly specialized membrane structure essential for muscle contraction through ECC. ECC mechanism will be deeply recapitulated in the next section of this manuscript but it is important to note the presence of ECC-specialized proteins at the triad: the Ryanodine Receptor-1 (RyR1) located at the SR membrane, and the Dihydropyridine Receptor (DHPR or Ca_v1) found predominantly at T-tubule membrane, the minor remaining portion being found throughout the sarcolemma (Jorgensen et al., 1989; Piétri-Rouxel et al., 2010).

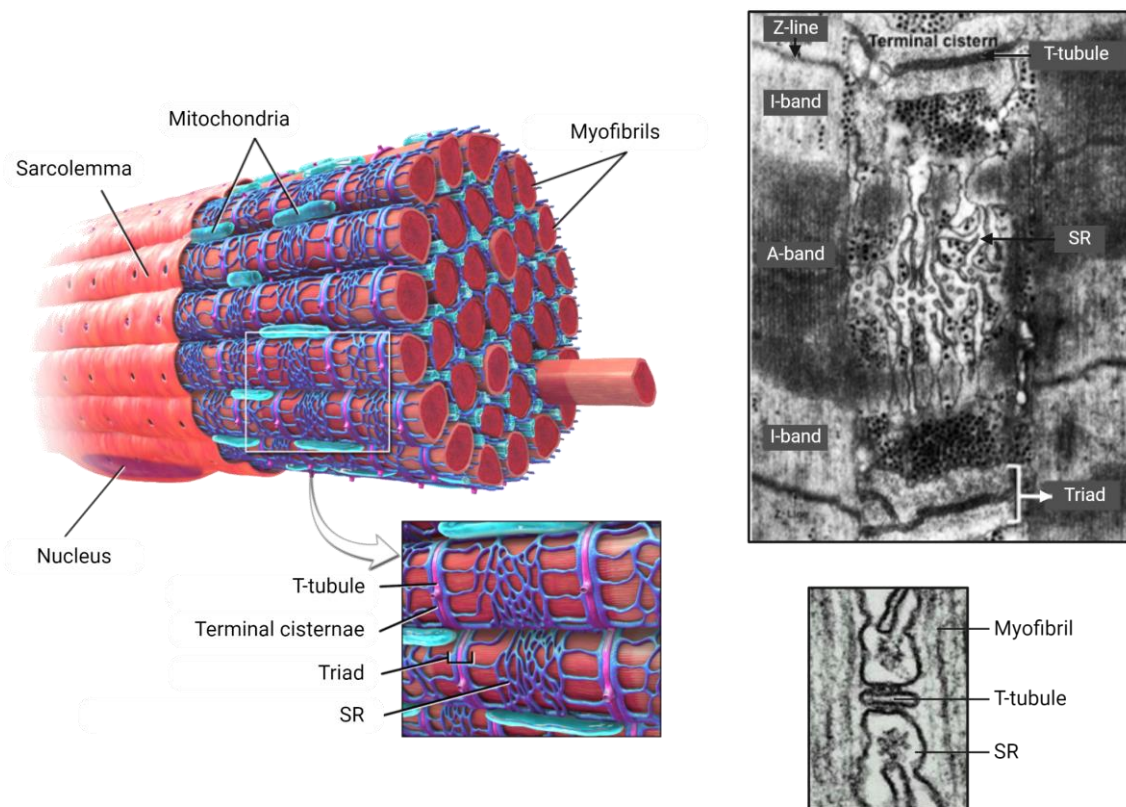


Figure 4. Detailed muscle organization and ultrastructure of muscle fiber components.

This figure provides a comprehensive overview of the microscopic anatomy of a muscle fiber, emphasizing the role of the triad in muscle contraction. Modified from Blausen.com staff (2014). "Medical gallery of Blausen Medical 2014". *WikiJournal of Medicine*, https://vmicro.iusm.iu.edu/hs_vm/docs/lab4_3.htm and *Molecular Biology of the Cell*, 4th Edition.

Along embryogenesis in mice, the development of triads implies the concomitant SR and T-tubules biogenesis. SR develops first from the tubular ER (Kilarski and Jakubowska, 1979) which progresses into reticular structures surrounding the myofibrils as early as E14 (Luff and Atwood, 1971), time where the first RyR1 clusters are observable, before becoming more and more abundant at E16 (Takekura et al., 2001). The first T-tubules originates from the sarcolemma at E15 and extend deeper within the

myofiber, in longitudinal position, as embryonic development continues. While both SR and T-tubule amount increases progressively, the two structures begin to increase their contact sites over time, forming the first triads at the junction of A and I bands of myofibrils. The $Ca_v1.1$ channels are initially equally distributed along the sarcolemma before becoming mainly restricted to the T-tubules system once triads formation occurs (Romey et al., 1989). Transversal positioning of the T-tubules (and subsequently, the triads) is achieved during postnatal period and is completed three weeks after birth (Franzini-Armstrong, 1991; Takekura et al., 2001).

The direct interaction between RyR1 at the SR membrane, and $Ca_v1.1$ at the T-tubule membrane as early as the first SR docking junctions are observed, raised the question of the role of such assembly in the formation of the triad (Yuan et al., 1991). However, studies in dysgenic and dyspedic mice, genetically ablated for $Ca_v1.1$ and RyR1 respectively, did not reveal any abnormal SR-T-tubule junction (Franzini-Armstrong et al., 1991; Powell and Fambrough, 1973; Takeshima et al., 1994). The same observation was made later with RyR1- $Ca_v1.1$ double Knock Out (KO) mice (Felder et al., 2002) leading to the conclusion that SR-T-tubule docking is independent of the presence of these two proteins. Moreover, both calsequestrin and triadin, two broadly characterized proteins of the SR-membrane junction, were described to remain properly targeted and their structural organization to be unaffected as well. Both SR surface junction morphology and molecular composition were not affected by the lack of RyR1 and $Ca_v1.1$ (Felder et al., 2002).

The molecular characterization of T-tubule biogenesis and triad formation still remains unclear up today. Pioneer studies showed a clustering and accumulation of caveolae at the sarcoplasm (Franzini-Armstrong, 1991; Parton et al., 1997). Later, Bin1 (Apmhophysin-2) has been pointed out as a factor required for normal T-tubule formation (Lo et al., 2021) and a recent study showed that Caveolin-3 (Cav3) and Bin1 form ring-like structures from which tubes with abundant $Ca_v1.1$ arise (Lemerle et al., 2023). Additionally, Bin1 was depicted to be required for triad formation with N-WASP in myofibers differentiated *in vitro* (Falcone et al. 2014). Several conditions with impairment of either Cav3 or Bin1 have been reported to be associated with T-tubule and triad defects (Fugier et al., 2011; Nicot et al., 2007). In short, Cav3 and Bin1 are the two main factors regulating T-tubule biogenesis by controlling the Caveolae formation and the membrane tubulation respectively.

II- Excitation Contraction Coupling (ECC)

The nervous system controls muscle movements by regulating contraction or relaxation of myofibers. The process that transduces fiber depolarization upon nerve stimulation into muscle contraction is called Excitation Contraction-Coupling. This is accomplished through a special synapse: the NMJ, which is a communication zone between the nerve, that sends the contraction signal (nerve stimulation), and the muscle that contracts in response.

a) Chronological discoveries

Along the XVIIIth century, the question of the mechanisms at work to induce the muscular movement was widely debated by the scientific world and more deeply by the naturalists. A first hypothesis was that the nerves were hollow and conducted a fluid or a gas that filled the muscles, initiating their increased size and their contraction. This theory was refuted by Jan Swammerdam and other lines of research appeared, including chemistry and then electricity. In 1780, an anatomist named Luigi Galvani hypothesized the existence of an “animal electricity” (Galvani et al., 1791) and together with Alessandro Volta, a physician, they proved that the muscles are not properly producing the electrical influx but are able to transduce it to contraction.

Edgar Douglas Adrian was awarded in 1932 by the Nobel prize in Physiology for the discovery of a “uniform-size electrical signal” produced by the neurons. Twenty years later, Sandow demonstrated the existence of a bridge between electrical activity and contraction (Sandow, 1952), and a study published in 1960 showed a change in the membrane potential as the initiating step leading to the ECC (Hodgkin and Horowicz, 1960). Electronic microscopy helped later with the understanding of this mechanism by allowing the visualization of the triads (**Fig. 4**) that were suggested to be of importance for muscle contraction (Porter and Palade, 1957). T-tubule were soon characterized as the element transmitting the electrical impulse to the muscle (Andersson-Cedergren, 1959).

The crucial role of Ca^{2+} in muscle contraction (Weber, 1959) and the importance of its release and reuptake from the SR (Podolsky and Costantin, 1964) as well as its mechanical way of action (Ebashi et al., 1967; Ebashi and Ebashi, 1964) was studied extensively during the 1960s.

In the early 1980s, the two key molecular components of the ECC system were identified: Ca_v1 and RyR.

b) Neuromuscular transmission

From nerve influx...

The nerve impulse takes its origin in the frontal lobe and motor cortical regions of the brain (Dum and Strick, 2002), goes through the spinal cord and propagates by membrane depolarization along the axons of the motor neurons to reach the terminal end of the motor axon for final transmission to the muscle. Membrane depolarization is a shift in electrical charge distribution through the membrane, depending on ions flow and therefore on the ability of voltage-gated channels to regulate the flow of ions (sodium Na^+ , potassium K^+ , Chloride Cl^- and Calcium Ca^{2+}) across the cell membrane.

At rest, the electrical potential difference through the membrane (called “resting potential”) is negative, meaning that the inside of the cell membrane is negatively charged compared to the outside. The muscle resting potential is typically around -85mV , mainly carried by CLC1, allowing a “passive” adjustment of membrane potential (Brenes et al., 2023). When reaching the motor nerve terminal, the AP is transmitted to the muscle by the liberation of neurotransmitters that will be captured by the post-synaptic muscle membrane and lead to the creation of a muscle membrane depolarization that will itself propagate as an AP across the sarcolemma: voltage-gated Na^+ channel ($\text{Na}_v1.4$) opens to drive the influx of Na^+ ions causing an increase in membrane potential. When exceeding a specific threshold (around -65mV), this local depolarization leads to the exacerbation of ions flux and depolarization is propagated as an AP over the entire the myofiber surface. When the membrane potential reaches about $+35\text{mV}$, repolarization occurs as K^+ channels open, and $\text{Na}_v4.1$ channels close, allowing K^+ ions to leave the cell, and stopping Na^+ ions to enter the cell, carrying positive charges out. In addition, Cl^- influx through CLC1 contributes to the repolarization, bringing the membrane potential back toward its resting voltage (Brenes et al., 2023). A brief period of hyperpolarization occurs before the membrane potential returns to its resting state (Fig. 5). Overall, the wave of depolarization, followed by repolarization, allows the action potential to travel efficiently along the axon, ultimately leading to the transmission of neural signals to the target muscles or tissues.

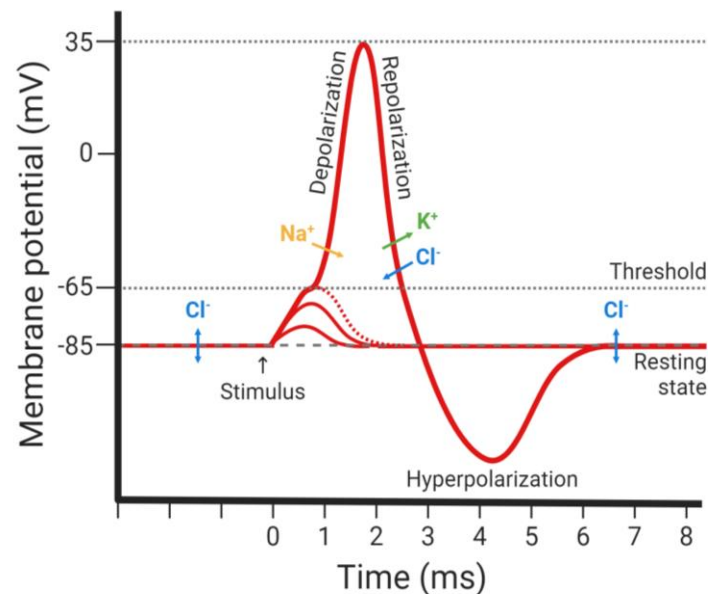


Figure 5. Variation of membrane potential during depolarization.

Skeletal muscle cells exhibit a negative electrical membrane potential at rest (-85mV) meaning that inside of the cell is negatively charged compared to the outside, due to a balance mainly adjusted by Cl^- conductance. Na^+ entry leads to membrane depolarization while K^+ exit and Cl^- entry from the cell trigger repolarization. A brief hyperpolarization occurs before returning to membrane resting state (created with BioRender.com).

While sarcolemma depolarization reaches the T-tubules, $\text{Ca}_v1.1$ conformation is modified through charge movement. This conformational changing leads to the interaction of $\text{Ca}_v1.1\beta1$ subunit with RyR1 at the surface of the RS terminal cisternae and RyR1 channel opens to release Ca^{2+} into the sarcoplasm (**Fig. 6**).

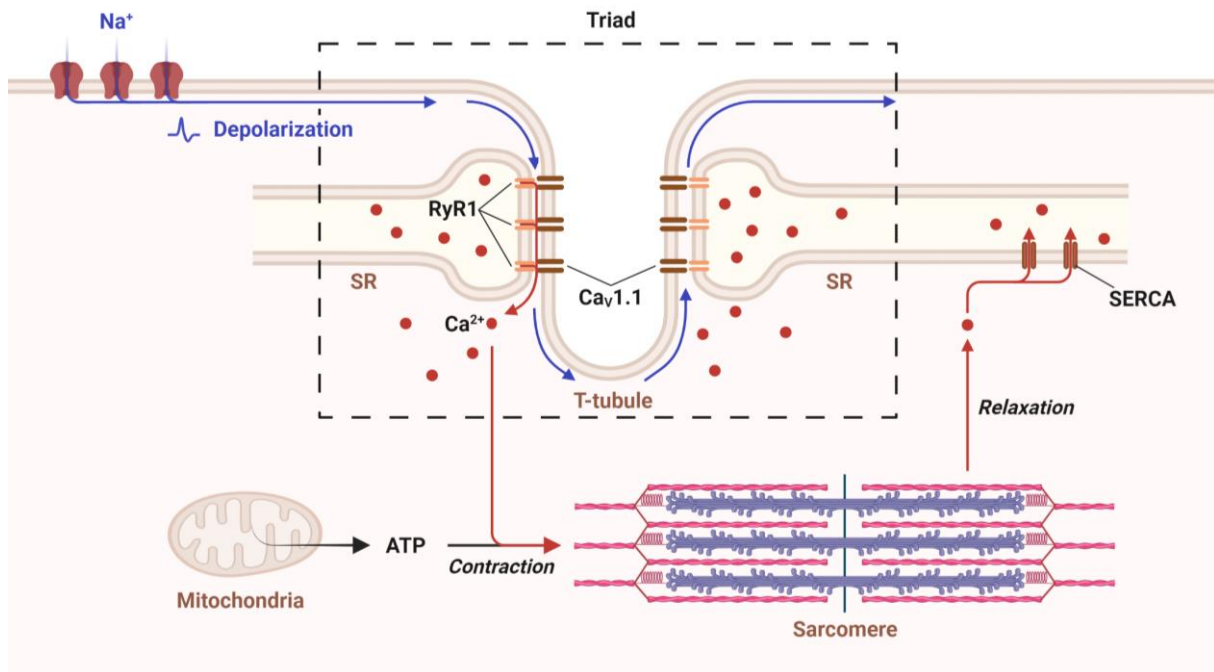


Figure 6. Skeletal muscle ECC process: overview.

The triad is a structure composed of one t-tubule flanked by two terminal SR cisternae. Membrane depolarization, triggered by the opening of Na^+ channels, allows the action potential to efficiently travel along the sarcolemma and reach the t-tubule. At t-tubule membrane, this depolarization induces $\text{Ca}_v1.1$ Ca^{2+} channel to interact with RyR1 on the SR surface, leading to the release of calcium from the SR. Ca^{2+} , along with ATP produced by mitochondria, is used by the sarcomere to induce muscle contraction (created with BioRender.com).

...to muscle contraction:

The Ca^{2+} release into the sarcoplasm is the first step of the contraction process. Indeed, to allow muscle contraction, tropomyosin must change conformation and induce its removal from a portion of actin which becomes exposed and accessible to myosin heads binding. This change of tropomyosin conformation is regulated by Troponin-C when Ca^{2+} is high. Simultaneously, ATP is hydrolysed into ADP (Adenosine DiPhosphate) + Pi (inorganic phosphate). These two conditions are needed to have the formation of a bridge between the actin filament and the myosin head. When Pi is released, myosin changes conformation resulting in the power stroke that triggers myosin and actin filaments to slide past each other. ADP is released, the myosin head is removed from actin and a new ATP molecule binds and is hydrolyzed in his turn: the consecutive attachment and detachment of the myosin head to the actin filament ensures the sliding of fine filaments along the thick ones ensuring a proper muscle contraction. This repetitive process is known as the cross-bridge cycle (**Fig. 7**). The limiting factors are the amount of ATP and Ca^{2+} in the sarcoplasm. If Ca^{2+} release from the SR triggers muscle contraction,

muscle relaxation occurs through Ca^{2+} reuptake in the SR through a Ca^{2+} pump known as SERCA for SarcoEndoplasmic Reticulum Ca^{2+} ATPase (Fig. 5).

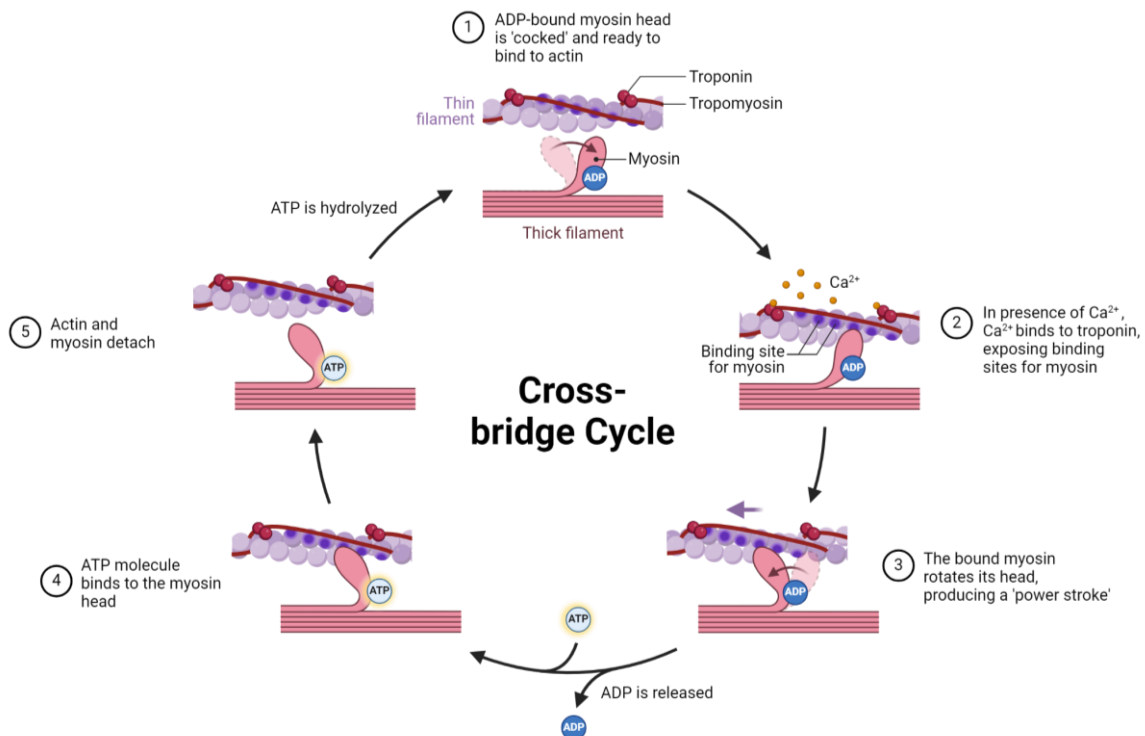


Figure 7. Myofilaments during muscle contraction process: the cross-bridge cycle.

Sliding filament model of muscle contraction. In step 1, the muscle is at rest with the myosin head bound to ADP and P_i , while tropomyosin covers the actin's binding sites. In step 2, Ca^{2+} released from the SR binds to the troponin complex, causing tropomyosin to move and expose the myosin-binding sites on actin. In step 3, the myosin head binds to actin, forming a cross-bridge. This leads to step 4, in which the release of ADP and P_i triggers the power stroke that triggers myosin and actin filaments to slide past each other, resulting in muscle contraction. In the final step, ATP binds to the myosin head, causing it to detach from actin. The ATP is then hydrolyzed to reset the myosin head, ready it for another cycle of contraction (from BioRender.com).

c) ECC molecular components

Interestingly, the content of ECC molecular components differs among muscles and more specifically the different partners vary considering slow- or fast-fibers: $\text{Ca}_v1.1$ and RyR1 content is higher in fast-twitch fibers compared to slow-twitch ones. These differences explain the inequivalent Ca^{2+} handling among fiber types, the more these Ca^{2+} Release Complex (CRC) proteins are present, the greater is the efficiency of Ca^{2+} transients, the faster are the fibers (Calderón et al., 2014).

Ca_v1 :

The Ca_v1 family is also known as DHPs (DiHydroPyridine Receptor, the historical name) because of their pharmacological sensitivity to dihydropyridine drugs (Tanabe et al., 1987). These are protein complexes structured by an assembly of several subunits: the principal α_1 -subunit (holding the pore channel property) and the γ_1 -subunit are both transmembrane proteins, one extracellular α_2 -subunit and one intracellular β_1 -subunit (Buraei and Yang, 2010). Ca_v1 family is subdivided into $\text{Ca}_v1.1$ in the

skeletal muscle, $\text{Ca}_v1.2$ in the heart and smooth muscle, $\text{Ca}_v1.3$ in the inner ear and $\text{Ca}_v1.4$ in the retina (Dolphin, 2021), accordingly to the $\text{Ca}_v\alpha_1$ subunit: $\text{Ca}_v\alpha_{1s}$, $\text{Ca}_v\alpha_{1c}$, $\text{Ca}_v\alpha_{1d}$ and $\text{Ca}_v\alpha_{1f}$ respectively (Ertel et al., 2000).

All Ca_v1 channels respond to membrane depolarization. However, the way they respond to these changes in membrane potential differs: in the heart and smooth muscle, $\text{Ca}_v1.2$ isoform allows Ca^{2+} entry (it functions through its L-Type Ca^{2+} Channel (LTCC) role) leading to a Ca^{2+} Induced Ca^{2+} Release (CICR) muscle contraction. In contrast, isolated frog skeletal muscle continues to contract for ten minutes even when Ca^{2+} influx is prevented (Armstrong et al., 1972). Indeed, the skeletal muscle $\text{Ca}_v1.1$ isoform primarily does not function as a Ca^{2+} channel but as a voltage sensor leading to a Depolarization-Induced Ca^{2+} Release (DICR) muscle contraction.

In skeletal muscle, the specific Ca_v1 isoform is $\text{Ca}_v1.1$. This complex is composed of four subunits among which α_{1s} , responsible for the voltage sensor activity, is the key component for ECC. This core protein channel contains four homologous repeats (I-IV), connected through cytoplasmic loops (Buraei and Yang, 2010) (Fig. 8). Among the three other subunits, only $\text{Ca}_v\beta_1$ is described to be essential for ECC whereas $\alpha_2\delta$ and γ only play a minor role in regulating $\text{Ca}_v1.1$ (Ahern et al., 2001; Obermair et al., 2005).

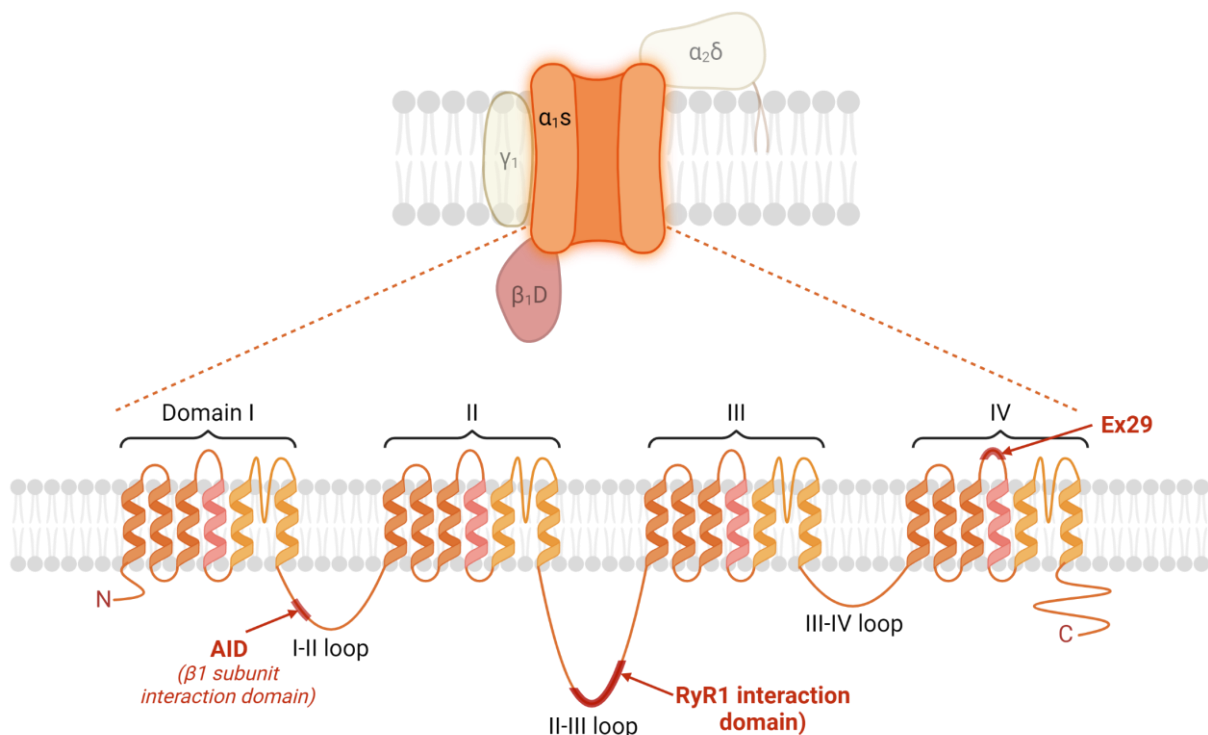


Figure 8. Structure and functional domains of $\text{Ca}_v1.1$ channel with a particular focus on α_{1s} within the cell membrane, highlighting its critical domains.

The top portion shows the arrangement of the five subunits composing $\text{Ca}_v1.1$: α_{1s} , $\alpha_2\delta$, β_1D , γ_1 , and α_{1s} , embedded in the plasma membrane. The bottom portion zooms in on the α_{1s} subunit, which is structured around four homologous repeat domains (I to IV). Key domains are indicated with as the β_1 subunit interaction domain (AID) in the I-II intracellular loop and the RyR1 interaction domain in the II-III intracellular loop. These regions are critical for the channel's function and interaction with other proteins involved in excitation-contraction coupling. The position of exon29-encoded domain is indicated, this exon being alternatively spliced in the embryonic *Cacna1s* isoform and excluded in some pathologies, leading to the retention of *Cacna1s* embryonic isoform (created with BioRender.com).

It is important to mention that the mature skeletal muscle $\text{Ca}_v1.1$ functions mainly through its role of depolarization sensor to trigger ECC and therefore displays only small LTCC currents. However, during embryogenesis the main α_{1s} subunit exon29 is alternatively spliced, giving rise to a $\text{Ca}_v1.1e$ channel, which presents an additional sizeable LTCC, required for muscle development (Benedetti et al., 2015; Tuluc et al., 2009). Some pathologies are linked to the mis-splicing of $\text{Ca}_v1.1$ exon29, resulting in the retention of its embryonic form (Δ exon29) in adult muscle. This will be explored further in Chapter 3.

RyR:

RyR is a Ca^{2+} release channel purified and identified in the 1980s (Inui et al., 1987; Meissner, 1986) as a protein with high affinity for the plant-derived alkaloid compound ryanodine. RyRs are found as homotetramers of approximately 550kDa in intracellular membranes like the ER where they are responsible for the Ca^{2+} release. In mammalian, three genes encode three RyRs: RyR1 and RyR2 are mainly expressed in skeletal muscle and in cardiac tissue, respectively, while RyR3, first identified in the brain, is present in a wider variety of tissue (Dulhunty, 2006).

Mutations in RyR1 are coupled with a dysregulation of Ca^{2+} in skeletal muscle which causes several myopathies. Depending on the effect of the mutation, these pathologies can be associated with an excessive activation of RyR1 after membrane depolarization, a leak in RyR1 channel leading to depletion in SR Ca^{2+} store or a deficit in ECC (Hernández-Ochoa et al., 2016).

Interaction between $\text{Ca}_v1.1$ and RyR1 in skeletal muscle:

Mouse models recapitulating a non-functional ECC complex, due to $\text{Ca}_v1.1$ and/or RyR1 highly deleterious mutations, display a complete absence of muscle contractibility and death at birth dependent on respiratory failure and asphyxia. This applies for the dysgenic model, carrying the muscular dysgenesis (mdg)-associated mutation α_{1s} -null (Beam et al., 1986; Knudson et al., 1989), and the dyspedic mice (RyR1-null model) (Takekura et al., 1995).

Briefly, three prerequisites are needed to ensure a proper skeletal muscle ECC: 1) $\text{Ca}_v1.1$ and RyR1 have to be correctly expressed and localized at the triad, 2) $\text{Ca}_v1.1$ needs to be able to ensure the charge movement and 3) $\text{Ca}_v1.1$ must be organized in tetrads, cooperatively associated with RyR1 tetramers. The correct expression and localization of $\text{Ca}_v1.1$ and RyR1, includes the suitable synthesis of these channels but also their precise positioning within the specialized triadic structure. To ensure a correct localization, both $\text{Ca}_v1.1$ and RyR1 channels have targeting signals that direct their positioning into T-tubule and SR membrane respectively. Noteworthy, $\text{Ca}_v\beta 1$ subunit is essential for $\text{Ca}_v1.1$ docking (Brice et al., 1997).

The second mentioned prerequisite for a proper ECC is the $\text{Ca}_v1.1$ -dependent charge movement. The charge movement is associated with the rearrangement of $\text{Ca}_v1.1$ conformation following electrical stimulation. Indeed, depolarization is a change in voltage running across the sarcolemma and when this change occurs at a Ca_v1 position, specific charged amino acids of the $\text{Ca}_v1.1$ transmembrane segment are repositioned, allowing $\text{Ca}_v1.1$ II-III loop to contact RyR1 (**Fig. 8**) and transduce the depolarization signal triggering Ca^{2+} release. A correct charge movement testifies of the proper $\text{Ca}_v1.1$ associated structure-function.

The importance of the structural conformation of ECC components for their appropriate physical interaction was more deeply investigated through electron microscopy images which revealed that RyR1 tetramers align with $\text{Ca}_v1.1$, itself arranged into groups of four called “tetrads”, in the T-tubule membrane: each of the four alternating RyR1 subunit is occupied by a $\text{Ca}_v1.1$ protein (Block et al., 1988) (**Fig. 9**). This tetrad arrangement is unique to skeletal muscle, and is not found in the heart. This organization ensure a close proximity of these channels, allowing a direct mechanical coupling and signal transduction. The specific individual role of charge movement and tetrad formation on ECC, depending on $\text{Ca}_v1.1$ interaction with RyR1, has been investigated. It has been demonstrated that when restored in *relaxed* zebrafish (no Ca^{2+} transient), charge movement rescued the Ca^{2+} transient only partially, while when both charge movement and $\text{Ca}_v1.1$ tetrad organization were restored it resulted in a total rescue in Ca^{2+} transient and zebrafish motility (Dayal et al., 2022). The direct impact of tetrad organization on ECC has not been tested independently of the charge movement.

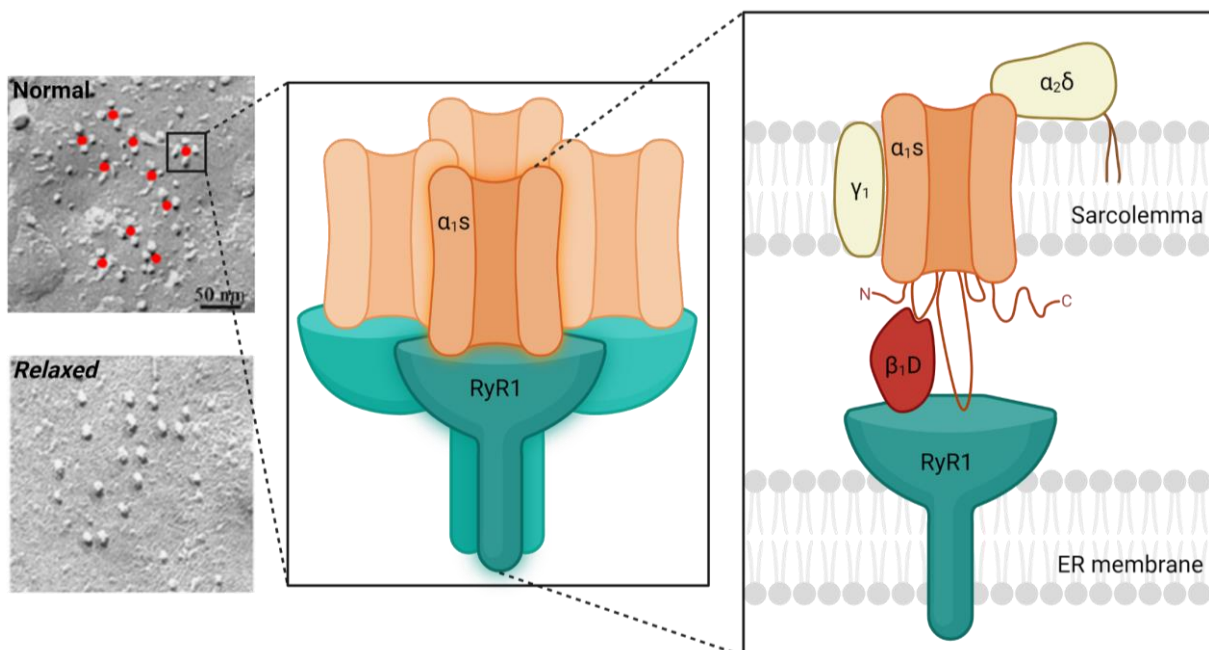


Figure 9. Arrangement in tetrads and interaction of $\text{Ca}_v1.1$ and RyR1 within muscle cells.

Left: electron microscopy images (Dayal et al. 2022) showing $\text{Ca}_v1.1$ channels arranged in tetrads (indicated by red dots) in normal condition while not organized in “relaxed” ($\text{Ca}_v\beta1$ -null mutant) muscle cells. Center: tetrad organizations composed by RyR1 tetramers closely associated with $\text{Ca}_v1.1$, itself arranged into groups of four. Right: this organization is necessary for their physical coupling (created with BioRender.com).

Among the three mentioned and described prerequisites for a proper ECC in skeletal muscles, the role of Cav1.1 β 1 subunit is crucial: this subunit accurately induces Cav1.1 targeting in the sarcolemma and at the triad, is able to trigger its organization into tetrads and is also required for charge movement facilitation. These roles in ECC mechanism will be further described in Chapter 2 of this manuscript.

Years after the characterization of Cav1.1 and RyR1, another protein has been demonstrated to be crucial for ECC by allowing a proper Cav1.1-RyR1 interaction: STAC3 (for Src Homology 3 (SH3) and cysteine-rich domain-containing protein 3) is a protein interacting with Cav1.1 at the triad that is essential for regulating the voltage response of the Ca²⁺ channel. Indeed, Horstick and colleagues characterized in 2013 a zebrafish mutant model underlying the same defective ECC phenotype as dysgenic and dyspedic mouse models and a genetic screening leads to the identification of the causative mutation in the STAC3 gene (Horstick et al., 2013). The STAC3-null mice were also characterized the same year with a disrupted ECC mechanism leading to a perinatal lethality (Nelson et al., 2013). These studies were the first ones to point STAC3 as essential for ECC.

III- The neuromuscular junction (NMJ)

The NMJ is a neurochemical synapse with a highly specialized anatomical and molecular structure enabling neuromuscular transmission. It is composed of a tripartite synapse formed by the presynaptic nerve ending of motor axon, the postsynaptic skeletal muscle fiber and specialized glial cells named terminal Schwann cells, which cap the nerve ending. These three elements interact to support the proper NMJ function (Ko and Robitaille, 2015). The gap between the pre- and the post-synaptic elements is called the synaptic cleft.

In mammal adult muscles, the area occupied by NMJ is less than 0.01-0.1% of the total surface of the muscle and these post-synaptic sites are highly specialized to ensure the proper transmission of electrical influx transmitted by the nerve.

a) AP transmission to the muscle

The nerve influx induces the increase of Ca²⁺ inside axonal termination and presynaptic zone which is rich in synaptic vesicles containing AcetylCholine (ACh), the key neurotransmitter for brain functions and muscle contraction. It leads to the exocytosis of the ACh-containing synaptic vesicles and the liberation of the neurotransmitter into the synaptic cleft, activating its specific nicotinic receptor, the acetylcholine receptor (nAChR) on the post-synaptic membrane (**Fig. 10**).

The reversibly bound ACh is then released from its receptor, and the excess ACh is hydrolyzed into acetate and choline by the AcetylCholineEsterase (AChE), an enzyme specific to the synaptic cleft. Free choline is then re-uptake by the end of nerve terminal via the choline transporter, and recycled to generate new ACh molecules locally in synaptic vesicles.

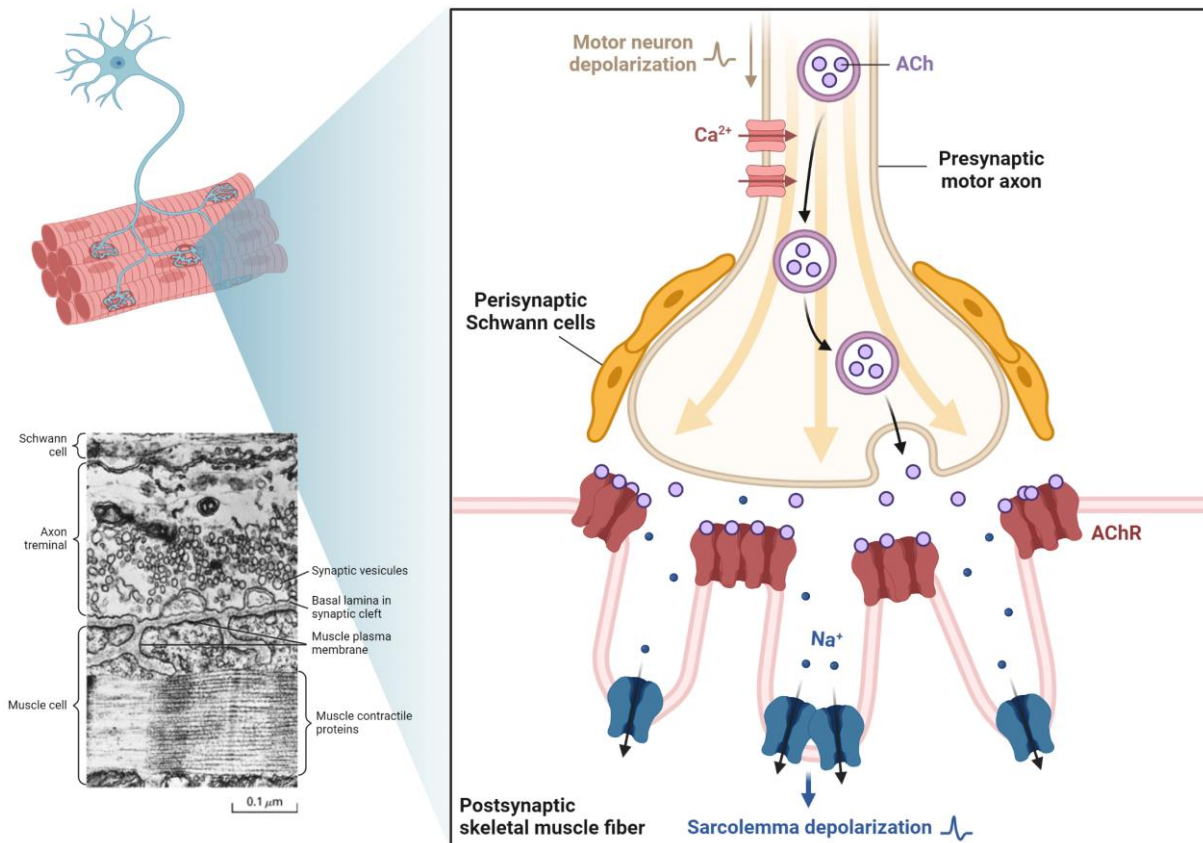


Figure 10. Neuromuscular Junction in mammals.

Nerve depolarization via Ca^{2+} entry promotes the fusion of AChR vesicles with the terminal nerve membrane and the release of ACh in the synaptic cleft. ACh binds to the AChR in the post-synaptic sarcolemma membrane, causing membrane depolarization and, ultimately, muscle contraction (created with BioRender.com). Electron microscopy image is from https://www.zoology.ubc.ca/~gardner/chemical_synapses%20-%20postsynaptic.htm.

When the nerve AP is transmitted to the muscle through the activation of AChR receptor channel, triggering muscle membrane depolarization down to the bottom of the sub-synaptic folds, Na^{+} channel opens when they exceed a specific threshold (around $-65mV$). This local depolarization then leads to the propagation of depolarization across the entire surface of the myofiber (**Fig. 10**).

b) Molecular actors at the NMJ

Agrin:

Agrin is a heparan sulphate proteoglycan that exists as several isoforms, whose expression depends on cell type. The neural secreted isoform is named Z⁺ agrin or neural agrin and is specific to motor neurons (Bezakova and Ruegg, 2003). Its role is crucial for NMJ formation: genetically depleted models are lethal due to the deficient formation of NMJ (Gautam et al., 1999). Conversely, gain-of-function studies demonstrated that agrin can function as a nerve substitute for the organization of a complex post-synaptic apparatus *in vivo* (Sanes and Lichtman, 2001).

The role of neural agrin in NMJ formation goes through its ability to trigger the aggregation of AChR, as well as other proteins of the postsynaptic apparatus, when released from the nerve terminal. During

development, the mechanism by which neural agrin induces aggregation and clustering of aneural AChR implies a signalling involving the Lrp4 protein (Low-density lipoprotein receptor-related protein 4) and its co-receptor MuSK (Muscle Specific Kinase), concentrated in the centre of the muscle fiber.

Lrp4-MuSK signalling:

Neural agrin released from the nerve terminals, binds several molecules at the myotube surface, including the transmembrane protein Lrp4 via its β 1 propeller domain and two Agrin-Lrp4 dimers are assembled on the surface of muscle cells: this tetrameric complex then activates its co-receptor MuSK through transphosphorylation of its tyrosine kinase domain in position Tyrosine Y553. The subsequent recruitment of DOK7 (Docking protein 7), a muscle cytoplasmic kinase, enables full activation of MuSK by binding to its extracellular juxta-membrane domain, which further enhances MuSK kinase activity (Eguchi et al., 2016; Inoue et al., 2009). The decisive role of Dok7 in the formation of NMJs has been demonstrated in mice lacking DOK7 that fail to cluster AChR and to form neuromuscular synapses (Inoue et al., 2009; Okada et al., 2006). DOK7 is sufficient on its own to activate MuSK outside of agrin/Lrp4/MuSK signalling (Bergamin et al., 2010; Okada et al., 2006). When active, MuSK initiates several downstream signalling cascades, among which Rapsyn recruitment. Rapsyn plays a crucial role in AChR aggregation by anchoring the complex to the cytoskeleton, therefore stabilizing AChR at the NMJ (Moransard et al., 2003; Oury et al., 2019) (**Fig. 11**).

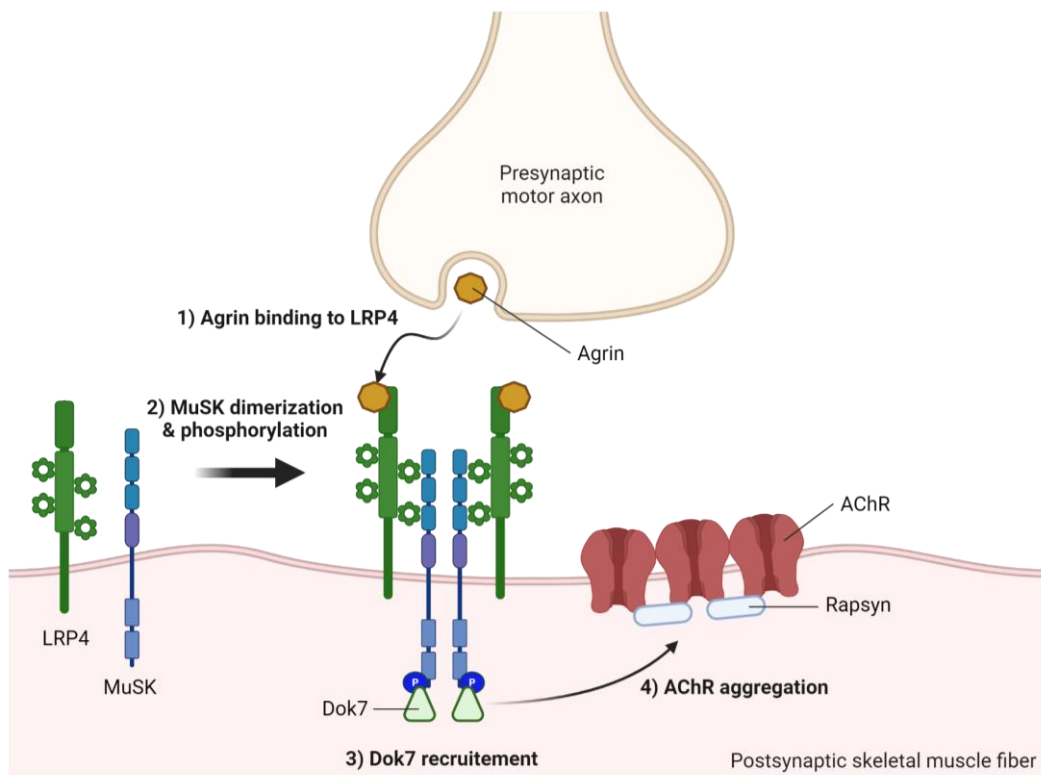


Figure 11. Molecular mechanism of the Agrin-Lrp4-MuSK signalling.

Agrin, released from the presynaptic motor axon, binds to LRP4 on the postsynaptic skeletal muscle fiber. This induces MuSK dimerization and phosphorylation, which triggers its activation. Dok7 is recruited to MuSK extracellular juxta-membrane domain, which enable its full activation and enhances its kinase activity. Downstream signaling pathways, including rapsyn recruitment, are triggered to induce AChR aggregation (created with BioRender.com).

nAChR

The nicotinic AChR is a complex of proteins forming a heteropentamer with two α , one β , one δ and one γ subunits in fetal muscle tissue. After birth, the γ -subunit is replaced by ϵ -subunit, the importance of this change will be described below in this chapter.

During mammalian development, the transcription of AChR subunit genes begins as early as myotubes are formed. After AChR subunit translation and assembling into $\alpha_2\beta\gamma\delta$ heteropentamers, they insert into the sarcolemma but at very early embryonic stages their density does not exceed $\approx 1\ 000$ AChR by μm^2 of muscle membrane. The gathering of AChR into concentrated regions is called clustering. The highly specialized portion of sarcolemma at the NMJ reaches more than 10 000 AChR by μm^2 while in the extra-synaptic membrane this density drops to less than $10\mu\text{m}^{-2}$.

Upon denervation, traumatic or pathologic nerve damage (nerve injury, motor neuron disorders, etc.) the fetal AChR is re-expressed as an attempt by the muscle to increase its sensitivity to ACh and as a try to maintain a functional nerve influx to the sarcolemma. This re-expression of the fetal γ -subunit in adult muscle after denervation has been observed in several mammalian species like in rat, mouse and in humans, and also in chicken (Cetin et al., 2020), specifically in type I muscle fibers (Gattenlöhner et al., 2002).

Wnt signalling:

While agrin is essential for AChR clustering in NMJ formation, Wnt signalling, in a modulatory manner, is also involved in AChR aggregation. In vertebrates, the role of Wnt proteins in the NMJ's overall formation is complex due to the multiple Wnt genes included in the Wnt family, among which great functional heterogeneity has been observed. Wnt4, Wnt9a, Wnt9b, Wnt10b, Wnt16 and Wnt11 have been demonstrated to be involved in AChR aggregation in absence of neural agrin *in vitro* (Messéant et al., 2017; Zhang et al., 2012). In addition, some Wnts also act on the agrin-induced AChR clustering by promoting (Wnt3) or inhibiting it (Wnt3a, Wnt8a, Wnt7a and Wnt10b) (Li et al., 2018).

c) NMJ formation, maturation and maintenance

Before innervation:

At early embryonic stages, before innervation takes place (before E14,5 in mice), aneural AChR clusters aggregate in a large central region of the myotubes defining the location of the future NMJ: this phenomenon is known as muscle pre-patterning. This event is muscle-intrinsic and independent of innervation (Arber et al., 2002; Yang et al., 2001). This recruitment is linked to the capacity of post-synaptic proteins as Lrp4 and MuSK to synthesise and accumulate AChRs at the future synaptic zone (Bloch and Pumplin, 1988; Yang et al., 2001; Lin et al., 2001). AChR clusters being a hallmark of a highly differentiated postsynaptic apparatus, the common-sense hypothesis is that these aneural AChR clusters represent the first initiating events of the complex mechanism of NMJ formation.

Concurrently, the central nervous system develops, with the spinal cord in ventral position hosting the specification of motor neurons. These motor neurons are directed toward their muscle target by various molecular cues, which are received by the axonal growth cone, an actin-supported structure that grows toward its synaptic destination.

Initiation of muscle innervation:

During NMJ development, when innervation begins around E14, the axonal growth cones head sarcolemma and the first synaptic contacts are established. There is an apposition between the axonal growth cone of the motor neuron and the predefined sites of AChR aggregates on the myotube (pre-patterning) associated with Lrp4 and MuSK in the central zone of the muscle fiber. The motor axon then plays an active role in the development, maturation and stabilisation of the post-synaptic sites with, on one hand, the release of ACh which disperses the aneural AChRs and, on the other hand, neural agrin which activates the synthesis of AChR subunits in the sub-synaptic nuclei which are then addressed at the top of the crests of the sub-neuronal folds when muscle is mature (Ngo et al., 2007).

Agrin, released by the motor axon, has been suggested to initiate the formation of synaptic clusterization of AChR: this is the neurocentric model. However, as mentioned above, aneural AChR clusters can already be observed along a central band in muscle fiber before innervation begins as well as in primary myotubes cultured in presence of neural agrin (Lin et al., 2008). Besides, many *in vitro* studies using either myogenic cell lines (Pęziński et al., 2020; Weston et al., 2000) or primary cells (Chu et al., 1995; Pęziński et al., 2020) pointed out the existence of AChR clusters, termed “hot spots”, forming spontaneously on myotubes. In particular, Kummer and colleagues showed in 2004 elaborated branched AChR clusters formed on *in vitro* myotubes, surprisingly similar to a mature *in vivo* post-synaptic apparatus (Kummer et al., 2004). These studies were made either *in vivo* before innervation begins or *in vitro* without neural agrin addition therefore supporting the myocentric hypothesis according to which muscle-derived cues spatially restrict the nerve to form synapses from aneural AChR clusters.

Interestingly, nerve-muscle co-cultures showed that axons actually contact myotubes at random sites, disregarding the pre-existing primitive AChR clusters and, instead, new AChR clusters are formed at these nerve-muscle interaction spots (Anderson and Cohen, 1977; Frank and Fischbach, 1979). *In vivo* data later supported these *in vitro* studies by showing that AChR in zebrafish failed to cluster in the absence of motor neurons (Liu and Westerfield, 1992) therefore supporting the neurocentric hypothesis of NMJ formation.

In this context, the question of the role of muscle pre-patterning was addressed. It was suggested that muscle pre-patterning may contribute to guiding motor neuron growth broadly to the center of muscle fibers, but aneural AChR clusters do not necessarily guide a specific nerve to interact with a muscle fiber at a particular spot (Wu et al., 2010). Moreover, when the aneural AChR, constituting muscle pre-

patterning, is genetically removed, it results in an excessive nerve branching and abnormal NMJ formation (Liu et al., 2008). In regard to these affirmations giving a different role of the aneural versus nerve-induced AChR clusters, the transition from one to the other is suggested to be essential for the establishment of a functional synaptic connection between motor neurons and muscle fibers.

Role of ECC machinery in muscle pre-patterning:

The importance of muscle activity in AChR clustering at the muscle surface has been suggested as early as in the 1970s when myofiber activity stimulation *in vitro* has been associated with an alteration of AChR expression levels (Cohen and Fischbach, 1973). Dysgenic mice (Cav1.1-null) display an abnormal distribution of AChRs (Rieger et al., 1984) and since this model show a disrupted ECC, the challenge was to separate muscle electric activity from its contractile activity to decipher if only one or both mechanisms were involved in muscle patterning. Two teams investigated this aspect by taking advantage of mouse models genetically altered for molecular components of the ECC machinery to look into the relative effect of excitation versus contraction on AChR clustering (Chen et al., 2011; Kaplan et al., 2018). Interestingly, they showed that muscle pre-patterning was preserved in both dyspedic mice (RyR1-null) and in Cav1.1^{nc/nc} mice, a model with a non-conducting Cav1.1. However, in the RyR1^{-/-}; Cav1.1^{-/-} double KO, AChR patterning was severely affected, indicating that Ca²⁺ influx and release is crucial for a proper muscle pre-patterning during NMJ formation (Kaplan et al., 2018).

The regulation of muscle pre-patterning by the Ca²⁺-related muscle activity goes through the consecutive action of several molecular partners: when Ca²⁺ signalling is disrupted, this abolishes the inhibition of Myogenin transcription, known to act as a positive regulator on AChR and MuSK transcription (Tang et al., 2004; Tang and Goldman, 2006). Consequently, the loss of Ca²⁺ normal activity during development leads to aberrant MuSK and AChR expression resulting in abnormal AChR aggregation and finally altered muscle innervation (Chen et al., 2011; Tang et al., 2006).

Later stages of muscle innervation:

After innervation, the nerve releases factors inducing the full differentiation of the postsynaptic apparatus. This density of AChR is an important hallmark of a highly differentiated post synaptic NMJ membrane. Several events occur to reach such concentration after the docking of nerve to muscle: 1) the redistribution of AChRs from extra-synaptic to synaptic areas, participating to the clusters after arrival of the motor axon growth cone 2) stabilization of AChR after clustering, 3) specialization of sub-synaptic nuclei (Belotti and Schaeffer, 2020) in the transcription of AChR subunits (among other postsynaptic components) and, 4) repression of AChR subunit transcription at the non-synaptic nuclei (Sanes and Lichtman, 2001) (**Fig. 12**).

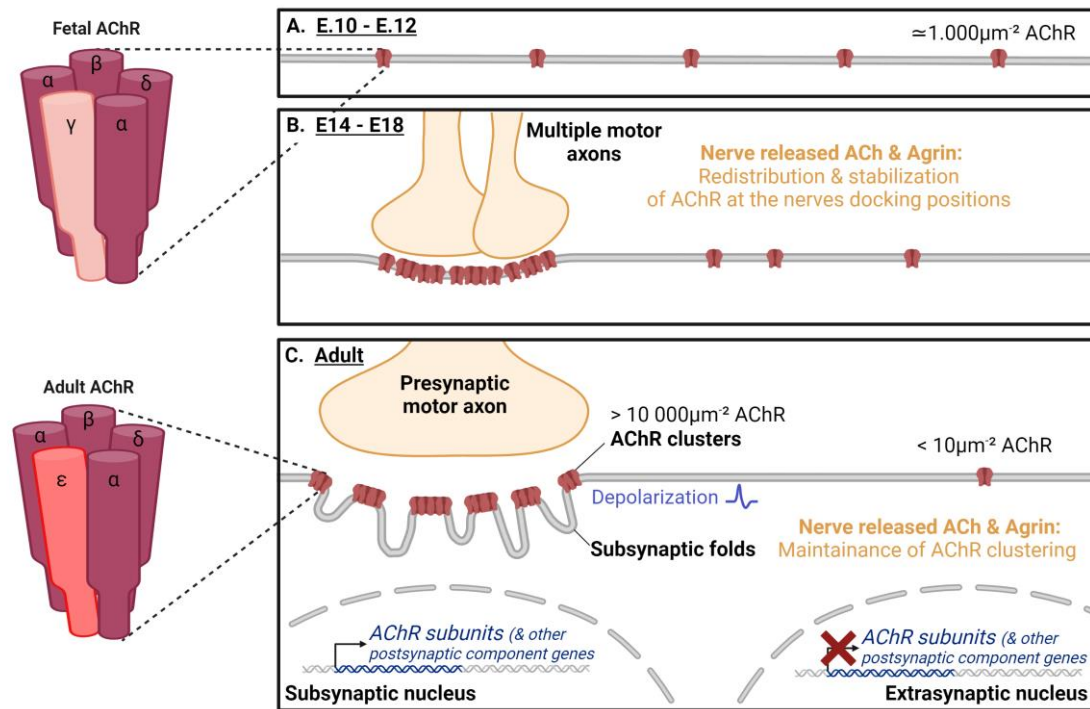


Figure 12. Development and maturation of AChR at the NMJ.

This figure illustrates the changes operating in AChR during NMJ development from fetal to adult stages. AChR switches from its embryonic $\alpha_2\beta\gamma\delta$ to its adult $\alpha_2\beta\epsilon\delta$ form at perinatal stages. Before innervation, AChRs are distributed along sarcolemma at low density. Between E14 and E18, agrin triggers the high clustering of AChRs under the nerve ending. In adult muscles, depolarization induces the release of ACh from the nerve ending, which activates postsynaptic AChRs located at the top of subsynaptic folds. This activation leads various signalling cascades, including the transcription of AChR and other post-synaptic components, coded by genes in subsynaptic nuclei (created with BioRender.com).

When the ECC machinery is mature, the release of ACh from the nerve causes muscle depolarization, itself leading to the dispersion of AChR aggregates that are not involved in synaptogenesis. Concurrently, neural agrin impedes the action of ACh in synaptic areas and stabilises neuronal AChR clusters (Kummer et al., 2006; Misgeld et al., 2005). The double role of agrin to 1) activate the Lrp4/MuSK complex and thus AChR aggregation, and 2) to counteract the “antisynaptogenic” effect of ACh and therefore stabilize of AChR aggregation, is primordial for the formation of the large oval-shaped plaques of uniformly distributed AChR. Such immature NMJs are innervated by multiple axons (E16-P14) and the size of the clusters increases as the muscle grows.

In adult muscle, the same mechanism of action of the nerve released ACh, through muscle depolarization, and Agrin through Lrp4/MuSK signalling, allow the maintenance of the AChR clustering pattern (Fig. 12).

Simultaneously, the nerve endings differentiate into synaptic boutons and progressively accumulate more and more ACh-rich synaptic vesicles. Interestingly, studies using mice lacking electrical activity are associated with defect in this nerve terminal differentiation, suggesting a role for synaptic transmission in this process (Misgeld et al., 2002; Pacifici et al., 2011). This was more deeply deciphered by a study published in 2019 by Kaplan and Flucher showing that $\text{Ca}_v1.1$ coordinates the presynaptic differentiation through the regulation of Ca^{2+} signalling (Kaplan and Flucher, 2019).

Another aspect of nerve differentiation during development is the axonal arborization, shown to be aberrantly extensive in models lacking genes necessary for muscle AChR patterning such as agrin, MuSK, Lrp4 and rapsyn (Li et al., 2018). Accordingly, in mice treated with blocking antibodies against Lrp4 or MuSK, presynaptic defects are observed (Shen et al., 2013; Viegas et al., 2012). This suggests that this axis regulates nerve end-plate differentiation. High differentiation of sarcolemma is mediated by the nerve terminal releasing factors, and reversely, there is also a retrograde signalling from the muscle to the nerve terminal, resulting in tightly coordinated differentiation of both pre-and post-synaptic components (Li et al., 2018).

Maturation and maintenance of the NMJ:

At birth the neuromuscular synapses are functional but their efficacy is insufficient for a proper motor activity. Their maturation, which is complete around 20 days after birth, enhances their efficacy. At birth, muscle expresses only the fetal AChR form $\alpha_2\beta\gamma\delta$, which will shift to the adult $\alpha_2\beta\epsilon\delta$ form gradually as post-natal innervation increases (Mishina et al., 1986; Missias et al., 1996). This event is transcriptionally regulated by MRF factors (Wang et al., 2003). Structural variations between the γ - and ϵ -subunits have been connected to a number of functional differences between fetal and adult AChRs: there is an higher affinity of ACh for the fetal AChR, associated with a longer opening time of the channel (Kopta and Steinbach, 1994; Nayak et al., 2014), but AChR conductance is higher in adult compared to fetal (Cetin et al., 2020). The switch from γ - ϵ -subunit also influences the stability of NMJ with AChR clusters becoming more resistant to disassembly: plaques disassemble rapidly after denervation in the first post-natal weeks while adult synaptic AChR remains clustered for many weeks after denervation (Sanes and Lichtman, 2001). In short, the shift from fetal to adult receptors enable functionally superior features and results in more stable and denser receptor aggregation, leading to improved synaptic transmission and muscle function.

Morphologically, AChR clusters undergo progressive perforation of AChR plaques to end up as a mammalian pretzel shape (Slater, 1982) innervated by a single axon (Li et al., 2018). The postsynaptic apparatus also matures at macroscopic level: the sarcolemma forms an hemicylindrical synaptic trough that embeds the nerve ending, increasing the contact surface between the axon and the muscle. It also acquires invaginations called neuronal folds. These modifications enhance the efficiency of neuromuscular transmission and ECC (P14).

The maintenance of NMJ in adult muscles involves a complex interplay of different factors.

1) Molecular interactions and signalling pathway: Agrin, Lrp4, MuSK and Dok7 integrity and their proper signalling are crucial to ensure an appropriate, dense and functional AChR clustering. Indeed, individual loss of the actors of this pathway post-natally after synapse maturation (i.e. by the mean of doxycycline-inducible Lrp4 deletion (Barik et al., 2014), electroporation of MuSK-targeting siRNA or

dsRNA (Kong et al., 2004) or MuSK conditional deletion (Hesser et al., 2006) leads to the destruction of NMJs.

2) Synaptic activity: when the nerve is damaged, the absence of neuronal stimulation causes AChRs to disperse.

3) Structural components like the Dystrophin-Glycoprotein Complex (DGC): this complex links the muscle cytoskeleton to the extracellular matrix and if several of its components are linked with NMJ formation or maturation, it also seems to play a role in its maintenance (Grady et al., 2000).

CHAPTER 2: Ca_vβ proteins

The Voltage Gated Ca²⁺ Channels (VGCCs) are crucial transducers of membrane depolarization into intracellular Ca²⁺ transients, which trigger many physiological events. Three families of VGCCs have been defined in mammals: Ca_v1, Ca_v2 and Ca_v3. Each of them is associated with tissue-specific functions. In muscles, Ca_v1 (described in the previous Chapter) is a L-Type Ca²⁺ channel (LTCC) mediating muscle contraction through ECC. Ca_v2 channels are expressed in the peripheral and central nervous system where they drive synaptic transmission through N-, P/Q- and R-type channels. Finally, Ca_v3 are T-type channels responsible for pacemaker and repetitive firing, meaning that it induces oscillatory transients in excitable cells and in particular in neurons (Dolphin, 2021).

Ca_v1 and Ca_v2 are High-Voltage-Activated (HVA) channels meaning that they require a high membrane potential to get activated, while Ca_v3 is a Low-Voltage-Activated channel family (LVA) (Catterall, 2011; Tsien et al., 1988; Zamponi et al., 2015). HVA are constituted by two transmembrane proteins: the main pore-forming subunit α₁ (Ca_vα₁) and the γ subunit (Ca_vγ), one extracellular α₂δ subunit (Ca_vα₂δ), and one intracellular Ca_vβ subunit. In contrast, LVA channels are only constituted by Ca_vα₁ (Rima et al., 2016). In total, several genes encode VGCC subunits: 10 Ca_vα₁, 4 Ca_vβ, 4 Ca_vα₁δ and 8 Ca_vγ genes have been enumerated (Rima et al., 2016) (**Fig. 13**).

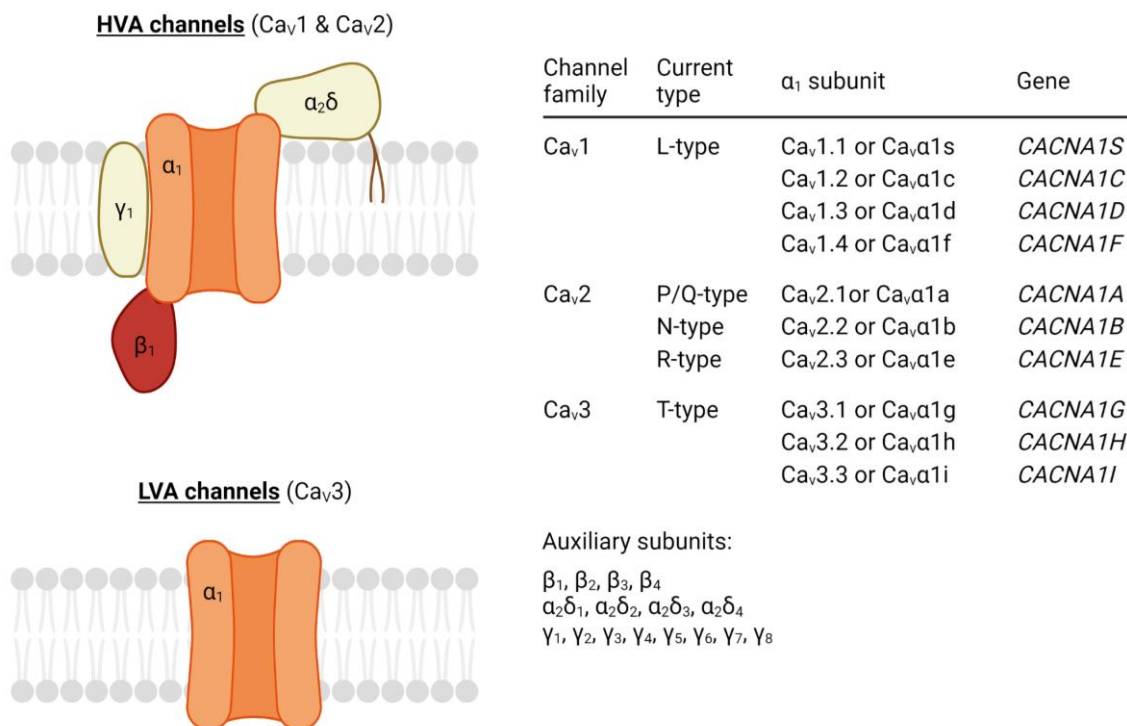


Figure 13. LVA and HVA Ca²⁺ channels and their current types, subunit composition and associated genes.

HVA channels (Ca_v1 and Ca_v2 channels) are composed of the pore channel α₁, and regulatory subunits α₂δ, β₁ and γ₁. In contrast LVA (Ca_v3 channels) are constituted of the pore channel α₁ only. In total, 10 genes code for 10 different α₁ subunits, with specific biophysical properties that results in distinct current types, classifying the channel family type. Table from Buraei et al. 2010 (created with BioRender.com).

A specificity of HVA channels compared with most voltage-gated ion channels is the primordial role played by the auxiliary $\text{Ca}_v\beta$ subunit. Indeed, if the $\text{Ca}_v\alpha_1$ subunit confers the biophysical and pharmacological properties of Ca_v , $\text{Ca}_v\beta$ is required for its correct membrane-targeting and for functional properties such as the fine-tuning channel gating (Lacerda et al., 1991). This Chapter 2 will focus on $\text{Ca}_v\beta$ proteins and the understanding of their biological functions, related or not to $\text{Ca}_v\alpha$.

I- $\text{Ca}_v\beta$ proteins

a) $\text{Ca}_v\beta$ isoforms

Expression and tissue distribution:

The first discovered and cloned $\text{Ca}_v\beta$ protein is the skeletal muscle $\text{Ca}_v\beta 1\text{D}$ isoform (Pragnell et al., 1991; Ruth et al., 1989), formerly known and referred as $\text{Ca}_v\beta 1\text{A}$ (Traoré et al., 2019). Further studies revealed the existence of four $\text{Ca}_v\beta$ proteins in mammalian: $\text{Ca}_v\beta 1$, $\text{Ca}_v\beta 2$, $\text{Ca}_v\beta 3$, and $\text{Ca}_v\beta 4$ encoded by four genes: *CACNB1*, *CACNB2*, *CACNB3*, and *CACNB4* respectively. Each $\text{Ca}_v\beta$ mRNA can undergo alternative splicing, therefore generating an extensive number of variants (Buraei and Yang, 2010). Splice variants originating from alternative exon splicing harbour different amino acidic compositions of their variable regions, leading to specificities in protein interaction (Obermair et al., 2010; Subramanyam et al., 2009), subcellular targeting properties, and cellular localization, all influencing the stability and activity of channel complexes (Campiglio et al., 2013). We can also mention the diversity of tissue distribution of $\text{Ca}_v\beta$ proteins, although particularly abundantly expressed in brain, heart and muscles, in other words, mostly in excitable tissues.

Gene name	$\text{Ca}_v\beta$ variants	Tissue distribution in mouse
CACNB1	$\beta 1\text{a}$	Skeletal muscle (during development, after nerve damage, data showed in this manuscript)
	$\beta 1\text{b}$	Heart, cerebellum, cerebral cortex, nerve, pancreas
	$\beta 1\text{c}$	Brain, spleen
	$\beta 1\text{d}$	Skeletal muscle (Traoré et al., 2019)
	$\beta 1\text{e}$	Skeletal muscle (during development, after nerve damage (Traoré et al., 2019))
CACNB2	$\beta 2\text{a}$	Heart, aorta, brain
	$\beta 2\text{b}$	Heart, aorta, brain
	$\beta 2\text{c}$	Heart, brain
	$\beta 2\text{d}$	Heart (during development)
	$\beta 2\text{e}$	Heart (during development)
CACNB3	$\beta 3$	Brain, heart, aorta, kidney, lung, muscle, spleen, thalamus, T-cells, trachea
	$\beta 3$ _truncated	Brain, heart and aorta
CACNB4	$\beta 4\text{a}$	Spinal cord, cerebellum
	$\beta 4\text{b}$	Spinal cord, forebrain

Table 1. Tissue distribution of $\text{Ca}_v\beta$ isoforms (modified from Buraei et Yang, 2010).

Ca_vβ-Ca_vα1 interaction:

A study analysing the amino acidic composition of Ca_vβ, identified a protein sequence consistent with a cytoplasmic localization of this subunit (Ruth et al., 1989). Indeed, the majority of Ca_vβs show a cytoplasmic distribution in the absence of Ca_vα1. However, when co-expressed with Ca_vα1, Ca_vβs localize to the plasma membrane due to their interaction (Buraei and Yang, 2010).

b) Structural features of Ca_vβ proteins

The core protein structure of Ca_vβ is defined by the presence of a Src homology 3 (SH3) and a guanylate kinase (GK) domains. These two highly conserved domains are connected by a variable HOOK region (**Fig. 14**). This SH3-HOOK-GK module constitutes the core of Ca_vβ protein making it as a member of the big membrane-associated guanylate kinase (MAGUK) family. In contrast, N-terminal and C-terminal domains of Ca_vβ are variable regions, considering their length and their amino acid sequence (Buraei and Yang, 2013, 2010).

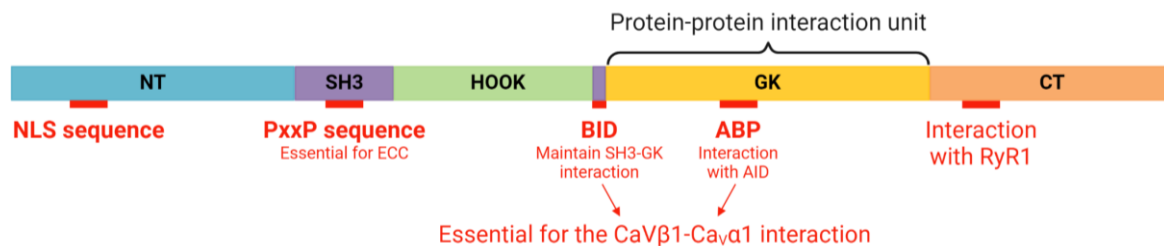


Figure 14. Functional domains and key sites of Ca_vβ1 proteins.

Schematic representation of Ca_vβ1 protein domains: N-Terminal (NT) domain with an NLS sequence, SH3 domain with PxxP sequence, essential for ECC mechanism, HOOK domain, GK domain, a protein-protein interaction unit containing the AID-Binding Pocket (ABP) site, essential for Ca_vβ1 interaction with Ca_vα1s, and the C-terminal (CT) domain, with the RyR1 interaction site (created with BioRender.com).

The SH3 domain is an interaction region found in a wide range of proteins. It contains a hydrophobic sequence that binds to its target proteins through a PxxP sequence. This SH3 domain presents a well-conserved fold of five consecutive β-strands. However, the PxxP sequence in Ca_vβ-SH3 domain is partially hidden due to a different folding of the protein: the five successive β-strands are interrupted by the HOOK region between the fourth and the fifth β-strand. Consequently, it might require a conformational change to expose this PxxP protein-protein interaction sequence (Buraei and Yang, 2013). Nevertheless, another study proved that this Ca_vβ-PxxP domain is actually active in skeletal muscle and is needed to ensure a proper ECC (Dayal et al., 2013) (**Fig. 14**).

GK stands for Guanylate kinase, a name reflecting the typical catalytic activity of the GK-domain: facilitating the transfer of a phosphate group from ATP to GMP, generating ADP and GDP. However, evolutionary modifications have rendered the GK domain in the MAGUK family inactive due to structural differences and the absence of essential catalytic residues. Instead, the MAGUK-GK domain has evolved into a protein-protein interaction unit. Specifically, in Ca_vβ, it contains a highly conserved group of residues known as Beta Interaction Domain (BID), which is determinant for Ca_vβ interaction

with the Cav-Alpha Interaction Domain (AID) (Buraei and Yang, 2013, 2010; Pragnell et al., 1991). Surprisingly, crystallography studies demonstrated that the AID does not directly binds the BID, but rather interact with an AID-binding pocket (ABP). Indeed, if mutations in either AID domain of Cav α 1 or BID domain of Cav β weaken their interaction and reduce the resulting Ca²⁺ channel current, mutations in the ABP can lead to a complete abolishment of AID-Cav β link (He et al., 2007).

The SH3 and GK domains of Cav β interact, with the last β -sheet of the SH3 domain playing a crucial role in strengthening this interaction. Interestingly, BID domain is crucial for maintaining this interaction which is demonstrated to be needed for the function of Cav β protein. Indeed, if BID mutations have only a mild impact on Cav α 1-Cav β interaction, they do alter Cav β folding which impacts the function of Cav β (Buraei and Yang, 2010) (**Fig. 14**).

II- Cav β regulation of HVA Ca²⁺ channels

a) Plasma membrane expression of Cav α 1

An *in vitro* study performed in COS cells showed that when Cav β is absent, Cav α 1 pore channel is unable to localize to the plasma membrane and that the transient expression of either Cav β 1b, Cav β 2a, Cav β 3 or Cav β 4 isoforms is able to rescue this phenotype. This study indicates that Cav β s act as chaperone proteins for Cav α 1 (Brice et al., 1997). One hypothesis for such a mechanism is suggested to be linked to an ER-retention signal which has been identified in Cav1.2 and Cav2 on the cytoplasmic I-II loop of Cav α 1. The inhibition imposed by the retention signal was observed to be reversed upon Cav β transient expression in COS cells. Besides, the genetic deletion of the retention signal was shown to facilitate Cav α 1 targeting to the membrane in the absence of Cav β (Bichet et al., 2000). However, some data are inconsistent with this hypothesis including Cav1.1 not being retained to the ER while sharing the same I-II loop with Cav1.2 and Cav2. Another hypothesis for the mechanism of the Cav β -related Cav α 1 trafficking to the plasma membrane would be indirect, through helping Cav α 1 to escape the degradation pathway by preventing its ubiquitination. Indeed, a treatment with an inhibitor of the proteasome was shown to induce the correct trafficking of Cav α 1 channel in absence of Cav β . This suggests that Cav β might interfere with the proteasome pathway, leading to the stabilization of Cav β (Altier et al., 2011).

b) HVA Ca²⁺ channel gating properties

Channel gating refers to the opening and closing of protein channels, and in this case of ion channels, regulating the passage of ions through the plasma membrane. Channel gating can be modulated by 1) electrophysiological features, due to the responsiveness of channels to the changes in electrical potential of the membrane; 2) ligand binding, this is the case for neurotransmitter receptors, 3) changes in pH, lipid molecules etc. (Jiang, 2019).

Channel gating is crucial for various cellular processes like the maintenance of resting membrane potential, the generation of AP in neurons or muscle cells, the regulation of muscle contraction, the control of hormone and neurotransmitter secretion (Excitation-Secretion Coupling). The modulation of channel gating features through the enhancement of Voltage-Dependent Activation (VDA) and/or Voltage-Dependent Inactivation (VDI). $Ca_v\beta$ proteins are able to modulate these channel gating properties.

Ca_vβ in Ca²⁺ channel activation:

The ion-channels display a voltage sensor function to open in response to membrane depolarization. All channels are not sensitive to the same changes in voltage: they display a threshold sensitivity, meaning that beyond a certain point, each channel undergoes a conformational change, causing it to open. All $Ca_v\beta$ have been demonstrated to shift this threshold to more hyperpolarized voltages, therefore facilitating $Ca_v\alpha 1$ opening (Gregg et al., 1996; Weissgerber et al., 2006). Indeed, when expressed in heterologous model, $Ca_v\alpha 1$ is able to induce Ca^{2+} influx into the cell but its co-expression with $Ca_v\beta$ subunit triggers major changes in its gating properties with increasing Ca^{2+} currents and an acceleration of channel activation and inactivation (Varadi et al., 1991). Similarly, $Ca_v\beta 2$ gene disruption in cardiomyocytes results in a reduced Ca^{2+} current (Weissgerber et al., 2006).

Ca_vβ in Ca²⁺ channel inactivation:

As VDA, $Ca_v\beta$ proteins trigger to VDI by contributing to a hyperpolarizing shift in the voltage dependence for inactivation. This means that at a specific voltage, $Ca_v\alpha 1$ will be more inactivated when $Ca_v\beta$ is present than when it is not: $Ca_v\beta$ lowers the threshold for inactivation. One exception is $Ca_v\beta 2a$, which actually shifts the voltage dependence for inactivation in a depolarizing direction. Besides, $Ca_v\beta$ accelerates the speed of how $Ca_v\alpha 1$ is inactivated after activation, therefore reducing the time during which Ca^{2+} can enter the cell (Buraei and Yang, 2013).

c) RGK inhibition of HVA Ca^{2+} channels

The RGK refers to a family of proteins named after its founding members: Rad, Rem, Rem2, and Gem/Kir. RGK proteins are small Ras-related GTP-binding proteins that belongs to the Ras superfamily. They are potent inhibitors of Voltage-Dependent Ca^{2+} Channels (VDCC), a group of channels including VGCC.

When co-expressed with $Ca_v\alpha 1$ and $Ca_v\beta$ VGCC subunits in heterologous systems, each RGK member ends up inhibiting Ca^{2+} currents while Ca^{2+} currents produced only by $Ca_v\alpha 1$ expression, in the absence of $Ca_v\beta$, are unaffected. This strongly indicates that RGKs impede VGCC through $Ca_v\beta$ (Rima et al., 2016). Several mechanisms have been proposed to explain RGK inhibition on VGCC function: 1)

competition between RGK proteins and $\text{Ca}_v\beta$ to interact with $\text{Ca}_v\alpha 1$ and therefore impeding the correct trafficking of $\text{Ca}_v\alpha 1$ to the plasma membrane and/or 2) inhibition of the $\text{Ca}_v\beta$ -related VGCC gating properties. Either ways, $\text{Ca}_v\beta$ are critical for the regulation of VGCC by RGK (Rima et al., 2016).

III- $\text{Ca}_v\beta 1$ & ECC

$\text{Ca}_v\beta$, and more specifically the skeletal muscle isoform $\text{Ca}_v\beta 1$, plays a critical role in ECC by assisting $\text{Ca}_v 1.1$ channel. When the $\text{Ca}_v\beta 1$ encoded gene (*Cacnb1*) is genetically inactivated, ECC is abolished (Gregg et al., 1996; Zhou et al., 2006), similarly to dysgenic mice (*Cacna1s^{-/-}*). As part of the HVA family, $\text{Ca}_v 1.1$ is regulated by $\text{Ca}_v\beta 1$, in the context of skeletal muscle ECC, accordingly to its properties described in the previous section: targeting $\text{Ca}_v\alpha 1$ to the sarcolemma, modulation of channel gating properties and inhibition by RGK proteins. This section reviews the additional mechanisms by which $\text{Ca}_v\beta 1$ regulates $\text{Ca}_v 1.1$ function to ensure proper skeletal muscle ECC mechanism.

a) Tetrad formation

As mentioned in Chapter 1, the skeletal muscle $\text{Ca}_v 1.1$ is specifically localized at the T-tubules (sarcolemma invagination) and organized in tetrads where they connect sarcolemma to the RS by interaction with RyR1 (**Fig. 9**). This structural conformation is required for ECC function. In a zebrafish *relaxed* homozygous mutant (*red^{ts25}*, which is a $\text{Ca}_v\beta 1$ -null mutant), the organization of $\text{Ca}_v 1.1$ opposing to RyR1 is disrupted. This defect is directly linked with a defective ECC, pointing $\text{Ca}_v\beta 1$ as the driver of tetrad formation, and tetrad formation as a prerequisite for ECC (Schredelseker et al., 2005). Re-expression of the cardiac/neural $\text{Ca}_v\beta 2a$ isoform (the phylogenetically closest to $\text{Ca}_v\beta 1$) in myotubes isolated from the *red^{ts25}* mutant shows a very limited recovery of tetrad formation. Indeed among all $\text{Ca}_v\beta$ isoforms, $\text{Ca}_v\beta 1$ and $\text{Ca}_v\beta 3$ are the only ones holding this specific function of allosteric modifier of $\text{Ca}_v 1.1$ conformation, allowing a complete restoration of Ca^{2+} current and zebrafish motility (Schredelseker et al., 2009).

Later, other studies expressed $\text{Ca}_v\beta 1/\text{Ca}_v\beta 4$ chimeras in the zebrafish *relaxed* strain to map the specific $\text{Ca}_v\beta 1$ domain responsible for tetrad formation. They observed that $\text{Ca}_v\beta 1/\text{Ca}_v\beta 4(\text{dist.C})$ (with $\text{Ca}_v\beta 4$ distal C-terminal domain) expression in *relaxed* zebrafish did not restore tetrad formation while the reverse chimera $\text{Ca}_v\beta 4/\text{Ca}_v\beta 1(\text{dist.C})$ did, therefore pointing this $\text{Ca}_v\beta 1$ -distal C-terminal domain as sufficient for driving tetrad formation, together with the restoration of Ca^{2+} current and zebrafish motility (Dayal et al., 2022).

b) Voltage sensing and charge movement

As mentioned before, the correct function of VGCC channels implies the sensing of membrane potential in order to adjust channel gating. Such sensing is translated in $\text{Ca}_v1.1$ (or $\text{Ca}_v\alpha1s$) charge movement. In the $\text{Ca}_v\beta1$ -null zebrafish model *relaxed*, not only $\text{Ca}_v1.1$ is not targeted to the triad and is unable to form tetrads, but it also lacks of its voltage-sensing function and therefore lacks charge movement, essential for the ECC mechanism. $\text{Ca}_v1.1$ alone cannot ensure voltage sensing and charge movement but needs $\text{Ca}_v\beta1$ subunit to support that role. Indeed, if Block and colleagues showed in 1988 structural evidences for a direct interaction between $\text{Ca}_v1.1$ and RyR1 (Block et al., 1988), $\beta1$ -null models showed that $\beta1$ subunit is a critical link between membrane depolarization sensed by the main $\alpha1s$ subunit and Ca^{2+} release from the RS by RyR1. If $\text{Ca}_v1.1$ charge movement allows its interaction (II-III loop) with RyR1 and Ca^{2+} release from SR, this coupling is allowed by the docking of Ca_v1 to RyR1 through $\text{Ca}_v\beta1$ subunit: without this docking, it might be difficult for $\text{Ca}_v1.1$ to transduce the signal to RyR1 (Hu et al., 2015).

All $\text{Ca}_v\beta$ isoforms can trigger charge movement with the exception of $\text{Ca}_v\beta3$. Dayal and colleagues published in 2013 a study in which they used artificially-generated $\text{Ca}_v\beta1/\text{Ca}_v\beta3$ chimeras to map the molecular domain important for such function. By measuring the resulting charge movement in *relaxed* myotubes, they identified a cooperation between $\text{Ca}_v\beta1$ -SH3 and C-terminus domains in promoting Ca_v1 voltage sensing. Interestingly, this study highlighted that specific residues of the SH3 domain, known as the PxxP motif is key for eliciting $\text{Ca}_v1.1$ voltage sensing function, $\text{Ca}_v\beta3$ being the only $\text{Ca}_v\beta$ isoform without this motif (Dayal et al., 2013).

c) Interaction with RyR1

$\text{Ca}_v1.1$ expression at the triads, tetrad formation and voltage sensing associated with charge movement are the three $\text{Ca}_v1.1$ -related prerequisites for a proper ECC Ca^{2+} transient. However, a missing component in this ECC has not been mentioned yet in this section: Ca^{2+} release goes through the opening of RyR1 channel at the SR membrane and this is primarily triggered by $\text{Ca}_v1.1$ charge movement which physically interacts with RyR1. However, $\text{Ca}_v\beta1$ displays an important role in the process.

The binding of $\text{Ca}_v\beta1$ subunit to RyR1 was evaluated and validated through affinity chromatography experiments. A group of positively charged amino acids $\text{K}^{3495}\text{KKRR}_-\text{R}^{3502}$ in RyR1 controls this interaction: when a RyR1 gene mutated on these residues is expressed in dyspedic myotubes, it results in the severe decrease of RyR1- Ca^{2+} current from the SR (Cheng et al., 2005). On $\text{Ca}_v\beta$ side, three different laboratories demonstrated the importance of a region of the $\text{Ca}_v\beta$ -distal C-terminal domain in the activation of RyR1 and its activity (Eltit et al., 2014; Hernández-Ochoa et al., 2014; Rebbeck et al., 2011). More specifically, three hydrophobic residues (L496, L500, W503) gather to bind RyR1 and, when mutated, it results in the disruption of RyR1 activation (Karunasekara et al., 2012). These results were however reconsidered by Dayal and colleagues in 2022 when they tested the effect of the three

hydrophobic residues mutated in vivo in relaxed zebrafishes and showed a correct Ca^{2+} transient restoration (Dayal et al., 2022).

Therefore, the physical interaction of not only $\text{Ca}_v\alpha 1$ s but also $\text{Ca}_v\beta 1$ with RyR1 is necessary for ECC.

IV- Ca_v -independent $\text{Ca}_v\beta$ function: Regulation of gene expression

Through their action in targeting VGCCs to the plasma membrane and in modulating their function, $\text{Ca}_v\beta$ proteins significantly regulate Ca^{2+} homeostasis. By consequence, they have role in numerous Ca^{2+} -mediated biological processes such as cell growth, division, differentiation, migration and death, but also muscle contraction through ECC, hormones secretion, etc. By controlling Ca^{2+} influx into the cell, VGCCs mediate such biological responses to stimuli through Excitation-Transcription Coupling. Indeed, Ca_v s-dependent Ca^{2+} signalling is required for the activation of CREB (Cyclic AMP Response Element Binding) which is involved in synaptic plasticity, memory and cell growth/survival, as well as the activation of Nuclear Factor of Activated T-cells (NFAT) which is involved in immune response regulation but also cardiac, skeletal muscle and nervous system development (Barbado et al., 2009).

However, it has become more and more evident that VGCCs also encompass additional functions, unrelated to their association with Ca_v s.

This section of the manuscript is entirely derived from a mini-review I wrote and published in 2022 (Vergnol et al., 2022), present in the additional documents of this manuscript.

a) Nuclear localization

After the initial cloning of $\text{Ca}_v\beta 1$ in skeletal muscle ($\text{Ca}_v\beta 1\text{D}$ formerly known as $\text{Ca}_v\beta 1\text{A}$ (Traoré et al., 2019)) (Ruth et al., 1989), several studies in various tissues have described $\text{Ca}_v\beta$ variants lacking the specific GK domain required for their interaction with $\text{Ca}_v\alpha 1$ subunit at the AID (Cohen et al., 2005; Harry et al., 2004). Other works have shown that $\text{Ca}_v\beta$ s can translocate to the nucleus, suggesting a role beyond its well-known function as a modulator of Ca_v channels. Under appropriate conditions, some isoforms of $\text{Ca}_v\beta 1$, $\text{Ca}_v\beta 2$, $\text{Ca}_v\beta 3$, and $\text{Ca}_v\beta 4$ exhibit nuclear localization (Buraei and Yang, 2010).

Role of electrical activity on $\text{Ca}_v\beta$ nuclear localization:

The nuclear localization of $\text{Ca}_v\beta 1$ in skeletal muscle (Traoré et al., 2019) and $\text{Ca}_v\beta 4$ in neurons (Etemad et al., 2014; Subramanyam et al., 2009) correlates with electrical activity. A study published by our team has demonstrated that after nerve damage, the embryonic $\text{Ca}_v\beta 1\text{E}$ isoform expression increased at the nuclei and near the Z-lines, while the constitutive adult muscle variant, $\text{Ca}_v\beta 1\text{D}$, remained associated with $\text{Ca}_v 1.1$ at the sarcolemma (Traoré et al., 2019). In neurons, $\text{Ca}_v\beta 4\text{A}$ and $\text{Ca}_v\beta 4\text{B}$ were found to translocate to the nuclei when electrical activity was stopped, while $\text{Ca}_v\beta 4\text{E}$ did not (Etemad

et al., 2014). Reduced expression and localization of Cav β 1E and Cav β 4 (isoforms A and B) at the nucleus correlates with increased electrical activity in muscle fibers and neurons during development (Etemad et al., 2014; Traoré et al., 2019). The proportion of Cav β 4 isoforms targeting nuclei correlates with their ability to regulate genes (Cav β 4B > Cav β 4A > Cav β 4E). Although the exact mechanism for nuclear localization of Cav β 2 and Cav β 3 is unknown, it is possible that they share a similar depolarization-sensitive mechanism.

Nuclear targeting related-Cav β domains:

As previously mentioned, some Cav β 1, Cav β 2, Cav β 3, and Cav β 4 splicing variants lack the ability to reach the nucleus. Small proteins can passively diffuse through the nuclear membrane, whereas larger proteins require a Nuclear Localization Sequence (NLS) to bind to Importins or associate with nuclear shuttle for targeting to the nucleus. The molecular mechanisms behind Cav β translocation to the nucleus is not fully understood. Subramanyam and colleagues showed that a specific double-arginine motif at the N-terminal is sufficient to recruit the Cav β 4B variant to nuclei in mouse brain, but this domain was subsequently demonstrated to be only partially involved in Cav β 4B nuclear docking. In skeletal muscle, Cav β 1E exhibits a putative NLS signal in its N-terminal domain, suggesting a potential nuclear targeting via Importin proteins (Taylor et al., 2014; Traoré et al., 2019).

Another proposed region implicated in the nuclear targeting of Cav β s is the SH3 domain for which Cav β 1 and Cav β 4 proteins have been showed to exhibit the functional features required the shuttling (Tadmouri et al., 2012; Taylor et al., 2014). The nuclear docking of Cav β s may also depend on their binding via the SH3-PxxP motif to proteins that themselves shuttle to the nucleus (Buraei and Yang, 2010). Cav β 4C nuclear localization, which relies on its interaction with HP1 γ , is prevented when a large part of its GK domain is truncated, suggesting the importance of SH3/GK interaction for this property (Hibino et al., 2003).

The molecular aspects of nuclear targeting for Cav β 2 and Cav β 3 are less studied. However, some studies suggest that their binding with chaperone proteins may support their targeting to the nucleus.

Such evidences of the nuclear localization/translocation of Cav β variants reveal an undeniable Cav β -independent function.

b) Ca²⁺ mediated modulation of gene expression

Cav β s were also reported to regulate intracellular Ca²⁺ levels independently of Cav α s by directly acting on Ca²⁺ stores. Cav β 3 has been shown to interfere with Inositol 3-Phosphate (IP3)-induced Ca²⁺ release from the ER in both pancreatic cells (Becker et al., 2021; Berggren et al., 2004) and fibroblasts (Belkacemi et al., 2018) by binding to the IP3 Receptor (IP3R), making cells less sensitive to low IP3

concentrations. Cav β 3 acts as a “brake” on Ca $^{2+}$ release, influencing glucose-induced insulin exocytosis in β -pancreatic cells (Becker et al., 2021; Berggren et al., 2004) and cellular mobility in fibroblasts (Belkacemi et al., 2018) (Fig. 15A). These studies showed that Cav β subunits regulate free cytosolic Ca $^{2+}$ concentration, which affects gene expression.

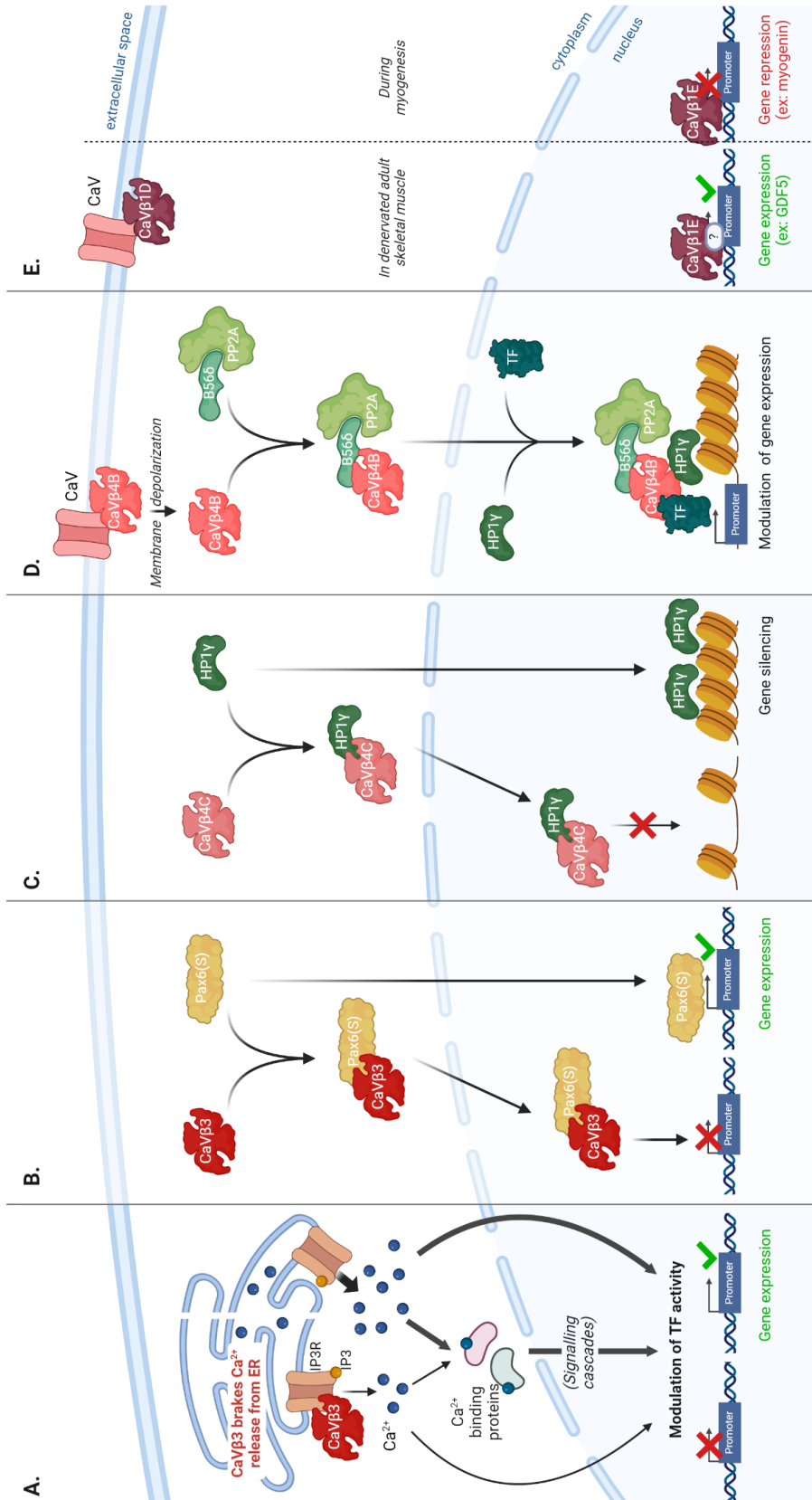


Figure 15. Cav-independent Cav β s functions in regulating gene expression.

A. Cav β 3 interacts with IP3R to desensitize cells to low IP3 concentration and brake Ca $^{2+}$ release, consequently interfering with the Ca $^{2+}$ -related modulation of gene expression and affecting glucose-triggered insulin secretion in β -pancreatic cells (Becker, et al 2021) and fibroblast mobility (Belkacemi et al., 2018). **B.** Cav β 3 translocates to the nucleus with Pax6(S), preventing its transcriptional activity (demonstrated in a reporter assay in HEK 293T cells) (Zhang et al. 2010). **C.** Cav β 4C translocates to the nucleus with HP1 γ , a factor known to silence the transcription of several genes by modulating heterochromatin conformation. Cav β 4C interaction with HP1 γ prevents its gene silencing activity in mammalian cells (Hibino et al. 2003, Xu et al. 2011). **D.** Cav β 4B stabilizes this protein complex, allowing its organizing platform for transcription-modulating factors including PP2A, HP1 γ and the transcription factor TR α . Cav β 4B acts directly or not on DNA regulatory sequences to modulate gene expression in hippocampal neurons in culture (Tadmouri et al. 2012). **E.** Cav β 1E acts directly or not on DNA regulatory sequences to modulate gene expression and influence myogenesis or skeletal muscle mass homeostasis after denervation (Taylor et al. 2014, Traoré et al. 2019) (created with BioRender.com).

c) Interaction with transcription factors

Ca_vβ3 prevents Pax6(S) transcriptional activity:

Zhang et al. found that Ca_vβ3 co-localize with Pax6(S) in the nucleus, resulting in a ≈50% decrease in Pax6(S) transcriptional activity (as demonstrated in *Xenopus oocytes* by an *in vitro* reporter system) while maintaining Ca_v channel properties (Zhang et al., 2010). In general, Pax6 proteins are made up of two DNA-binding domains: a Paired Domain (PD) and a HomeoDomain (HD) and a Proline/Serine/Threonine (PST)-rich C-terminal domain. PD and HD domains allow the binding to the cis-elements of target genes and regulate their transcription rate while PST-rich C-terminal domain has a trans-activation function. Zhang and colleagues found that Pax6(S) has intact PD and HD domains but a truncated C-terminal domain, resulting in a weaker Pax6(S) trans-activity. This isoform also differs from canonical Pax6 by having a distinct S-tail that facilitates the interaction with Ca_vβ3 (**Fig. 15B**). This work suggests a novel function of Ca_vβ3 in negatively regulating Pax6(S) protein activity, although the precise mechanism, supposed to occur either by Ca_vβ3 allosteric hindrance or by Pax6(S) removal from DNA binding sites, remains undefined. More importantly, this report showed for the first time a full-length Ca_vβ protein modulating gene transcription independently of VGCC channel (Zhang et al., 2010).

Ca_vβ4C prevents HP1γ gene silencing activity:

Hibino and colleagues discovered in 2003 the Ca_vβ4C variant in chicken cochlea. This truncated Ca_vβ4 isoform has been also found in the brain, eye, heart and lung, alongside full-length isoforms Ca_vβ4A and Ca_vβ4B. Ca_vβ4C, unlike the two other isoforms, lacks a large part of the GK domain required for association with Ca_vα1 (Chen et al., 2004). As a result, it has little effect on Ca²⁺ channel activity (Hibino et al., 2003). This -by then- newly identified variant interacts directly with the Chromo Shadow Domain (CSD) of the CHromo Box protein 2/Heterochromatin Protein 1γ (CHCB2/HP1γ), a nuclear protein that regulates heterochromatin conformation and therefore gene silencing. HP1γ binding to euchromatin DNA regions correlates with gene repression. Hibino's study reported that when co-expressed with HP1γ, Ca_vβ4C was recruited to the nucleus, significantly reduced CHCB2/HP1γ gene-silencing activity *in vitro* (Hibino et al., 2003).

A few years later, Xu and colleagues discovered Ca_vβ4C in the human brain and found it to interact with the CSD of HP1γ (Xu et al., 2011). This interaction was also showed to occur via a CSD binding motif, the PXVXL consensus sequence. Consistently with Hibino and colleagues' work, they found that binding of human Ca_vβ4C to HP1γ caused nuclear translocation and markedly reduced the gene-silencing activity of HP1γ *in vitro* (Xu et al., 2011). These studies illustrated a first manner for Ca_vβ subunits to indirectly modulate gene expression by affecting the activity DNA compaction proteins, like HP1γ (**Fig. 15C**).

Ca_vβ4B as an organizing platform for transcription-modulating factors:

The Ca_vβ4B full length isoform was found in neuron and muscle cell nuclei, with a negative correlation with electrical activity (Subramanyam et al., 2009). This protein's localization-related role was later discovered, with the demonstration that it acted as an organizing platform for a group of proteins that controlled transcription (Tadmouri et al., 2012). Among the complex-forming proteins, B56δ, a regulatory subunit of the PP2A phosphatase, induces histone dephosphorylation while HP1γ restructures heterochromatin. The last defined component of this complex is a transcription factor that binds to DNA at promoter regions, enabling B56δ and HP1γ activity (Tadmouri et al., 2012). Tyrosine hydroxylase (TH) is modulated by this mechanism, with thyroid hormone receptor α (TRα) serving as the corresponding transcription factor (Tadmouri et al., 2012). Unlike the previously described Ca_vβ4C effect on HP1γ activity, Ca_vβ4B enables the complex B56δ/HP1γ/TRα to access the activity site rather than modulating its function. Subramanyam and colleagues found a negative correlation between neuronal excitability and V5-tagged Ca_vβ4B positioning at the nucleus, while this report showed that endogenous Ca_vβ4B association with B56δ, originating their nucleus translocation, was consecutive to electrical activity (**Fig. 15D**). This suggests that the V5 tag may have hindered the pathways leading to Ca_vβ4B nuclear localization (Tadmouri et al., 2012).

Role of Ca_vβ4 as transcription factor: common function for other Ca_vβ?

Two studies found that while the nuclear Ca_vβ4 full-length inhibited cell proliferation, its epileptogenic mutant, lacking C-terminal domain, had no effect on cell-cycle related gene expression. Ca_vβ4 affects the cell cycle by interacting with B56δ or T-cell factor 4 (TCF4) transcription factors: in the first case, the recruitment of B56δ to nuclei by Ca_vβ4 is thought to repress genes involved in cell proliferation (Rima et al., 2017a). On the other hand, Ca_vβ4 binding to TCF4 prevents interaction with β-catenin, inhibiting Wnt-dependent gene expression and cell cycle (Rima et al., 2017b).

These studies established that a Ca_vβ isoform can regulate gene expression independently of Ca_v, either with or without electrical activity.

d) Interaction with regulatory DNA sequence

In muscle precursor cells (MPCs), Ca_vβ1 can translocate to the nuclei and bind at the promoter region of 952 genes (Taylor et al., 2014). Crucially, this demonstrates how the absence of Ca_vβ1 alters the expression of multiple genes, either misregulated positively or negatively, defining this subunit as having a transcription factor role (Taylor et al., 2014). The investigation of this role was particularly intriguing because it has been shown as affecting myogenin, which was up-regulated in a *Cacnb1*-null mouse model (Taylor et al., 2014), obstructing a proper myogenic development (Schuster-Gossler et al., 2007). The isoform identified as a transcription factor in this study was Ca_vβ1A. However, a study published by our team in 2019 revised this isoform identification by demonstrating that Ca_vβ1E, the

main $\text{Ca}_v\beta 1$ isoform in C2C12 myoblast cell line, actually carried the capacity to localize to the nucleus and to exert its function as a transcription factor (Traoré et al., 2019). Indeed, our research demonstrated that $\text{Ca}_v\beta 1E$ directly or indirectly regulated the transcriptional activity of the promoter triggering Growth Differentiation Factor 5 (GDF5) expression (Traoré et al., 2019), which in turn plays a critical role in maintaining adult muscle mass homeostasis, when electrical activity is impaired (Sartori et al., 2013) (**Fig. 15E**).

Based on all these studies, $\text{Ca}_v\beta$ s proteins have been identified as essential for controlling the expression of genes via Ca^{2+} signalling, DNA remodelling, modifying of transcription factors, or even functioning themselves as transcription factors. Multiple cellular functions are disrupted upon loss of these functions, involving $\text{Ca}_v\beta$ proteins in pathological conditions, separate and apart from Ca_v -related aspects.

V- $\text{Ca}_v\beta$ associated disorders

Mutations in *Cacnb1*, *Cacnb2*, *Cacnb3*, or *Cacnb4* genes can alter the expression of $\text{Ca}_v\beta$ proteins, which play a crucial role in biological processes that rely or not on HVA Ca^{2+} channel regulation. $\text{Ca}_v\beta$ s are both associated to disease-causing mutations and to disease-associated mutations.

a) $\text{Ca}_v\beta$ as Ca_v regulatory subunit

Brugada Syndrome is an inherited cardiac pathology, a channelopathy that manifests ST-segment elevation on an electrocardiogram. In humans, a mutation in the *CACNB2* gene, coding for $\text{Ca}_v\beta 2$ protein, has been associated with an abnormal HVA gating properties and more precisely an accelerated inactivation of Ca^{2+} current in the heart (Antzelevitch et al., 2007; Cordeiro et al., 2009). This mutation seems to be the causative variant for Brugada pathogenesis. Beside its role in Brugada Syndrome, $\text{Ca}_v\beta 2$ is also associated with Autism Spectrum Disorder (ASD). The role of VGCCs in the etiology of ASD has been reviewed by Liao and Li in 2020 (Liao and Li, 2020): they showed that mutations in $\text{Ca}_v\alpha 1$, $\text{Ca}_v\beta$ and even $\text{Ca}_v\alpha 2\delta$ subunits of HVA Ca^{2+} channels affected ASD pathogenesis, possibly by disturbing the function of Ca^{2+} signalling cascades (Liao and Li, 2020). Several mutations in the human *CACNB2* gene, related to a modulation of $\text{Ca}_v 1.2$ gating properties, have been highlighted.

$\text{Ca}_v\beta 4$ is primarily expressed in the nervous system and is referred in humans as carrying causative mutations to neuronal disorders such as Episodic Ataxia and Idiopathic Generalized Epilepsy (Escayg et al., 2000) as well as with Juvenile Myoclonic Epilepsy (Delgado-Escueta et al., 2013; Escayg et al., 2000). Inactivation of $\text{Ca}_v\beta 4$ in the mouse neurological mutant *lethargic* causes a complex neurological disorder characterized by absence epilepsy and ataxia. This is explained by a translational frameshift due to a mutation in a splice donor site, resulting in a truncated $\text{Ca}_v\beta 4$ protein lacking the Ca_v

interaction-domain AID (Burgess et al., 1997) and therefore an impairment in HVA function which has a central role in ataxia and epilepsy pathogenesis.

Considering $\text{Ca}_v\beta 3$, some neuronal diseases such as Developmental and Epileptic Encephalopathy or Lambert-Eaton Myastenic Syndrome are associated with this protein (Rosenfeld et al., 1993). Lambert-Eaton Myastenic Syndrome is an autoimmune disease caused by autoantibodies targeting $\text{Ca}_v\alpha 1$ extracellular loops. This disrupts VGCC modules at the NMJ regions, impairing neuromuscular transmission. Interestingly, antibodies against $\text{Ca}_v\beta 3$ are commonly found in patients sera, which may hinder the correct interaction between $\text{Ca}_v\alpha 1$ and $\text{Ca}_v\beta$ (Buraei and Yang, 2010).

Malignant Hyperthermia (MH) is a genetic disorder, associated with mutations in *RyR1* gene characterized by uncontrolled muscle metabolism. In 2018, Perez and colleagues have shown that the V156A variant in *Cacnb1* gene caused a reduction in the stability of SH3/GK $\text{Ca}_v\beta 1$ domains and therefore a dysregulation of Ca^{2+} handling. This study indicates that $\text{Ca}_v\beta 1$ -V156A can be a pathological variant for MH (Perez et al., 2018). $\text{Ca}_v\beta 1$ is also associated with Bailey-Bloch congenital myopathy, also known as STAC3 disorder. This neuromuscular condition is linked with mutations in various genes involved in ECC such as *STAC3* (causative mutation), *RYR1*, *CACNA1S*.

KO models exist for all $\text{Ca}_v\beta$: $\text{Ca}_v\beta 1$ -null mice is lethal at birth due to the absence of skeletal muscle $\text{Ca}_v\beta 1$ isoform, leading to a disrupted ECC and asphyxia. $\text{Ca}_v\beta 2$ -null mice die prenatally because of the lack of cardiac contractions. However, a KO of $\text{Ca}_v\beta 2$ gene in adult mouse cardiomyocytes is only associated with a $\approx 30\%$ reduction of Ca^{2+} currents, suggesting that $\text{Ca}_v\beta 2$ may be more important in developing that adult hearts. $\text{Ca}_v\beta 3$ -null mice are viable but show reduced inflammatory pain perception, high insulin secretion, elevated blood pressure on high salt diet, altered behaviour, impaired working memory, and immune system effect. $\text{Ca}_v\beta 4$ -null mice, also known as the previously mentioned *lethargic* mice, exhibit nervous system disorders like ataxia, epilepsy or seizures (Buraei and Yang, 2013).

b) Ca_v -independent disorders

Similarly to the IV- section of this Chapter, this sub-section is derived from the mini-review I wrote and published in 2022 (Vergnol et al., 2022), present in the additional documents of this manuscript.

When $\text{Ca}_v\beta$ proteins have been associated with pathological conditions, it was primarily linked with its Ca_v -associated role only. However, since the onset of $\text{Ca}_v\beta$ HVA-independent functions, additional molecular mechanisms have been identified.

The here-before mentioned role of $\text{Ca}_v\beta 4$ on epilepsy and ataxia was explained by an impairment in HVA function. However, it should be noted that in this context, $\text{Ca}_v\beta 4$ mutations were found to disrupt the interaction between the SH3 and GK domains, preventing the protein from reaching the nucleus

where mis-regulated $Ca_v\beta 4$ -dependent gene transcription may play a significant role in the pathogenesis of neurological disorders (Tadmouri et al., 2012).

In 2017, it was discovered that *CACNB2* gene was a genetic modifier of Hypertrophic Cardiomyopathy (HCM) which is caused by a *MYBPC3* (Myosin-Binding Protein C) variant (Zhang et al., 2017). The authors hypothesized that the attenuation of $Ca_v1.2$ - Ca^{2+} currents caused by *CACNB2* mutations was a possible mechanism for modifying disease phenotype. A subsequent study found that reduced cardiomyocyte hypertrophy was linked to a $Ca_v1.2$ -independent $Ca_v\beta 2$ function (Pickel et al., 2021). Accordingly, $Ca_v\beta 2$ localization and activity in cardiomyocyte nuclei significantly regulate Calpain activity and Calpastatin expression, which are pro-hypertrophic proteases and inhibitors, respectively (Pickel et al., 2021). Even though these events have not been explicitly linked to a reduction in cardiomyocyte hypertrophy, a relationship between the two could be hypothesized and would require further investigation.

A study published by our team in 2019 found that $Ca_v\beta 1E$ plays a major role in age-related muscle wasting. This research indicated that the $Ca_v\beta 1E$ -GDF5 pathway mitigated muscle mass loss after denervation. Noteworthy, this pathway was shown impaired in aged muscle fibers. Overexpressing $Ca_v\beta 1E$ in aged mouse muscle increased GDF5 expression and signalling, preventing muscle mass loss and force decline during aging (Traoré et al., 2019). The expression of an analogous of $Ca_v\beta 1E$ has been discovered in human muscle, decreasing in an age-related manner, suggesting that the defective h $Ca_v\beta 1E$ -GDF5 axis has a therapeutic potential in muscle aging and linked pathologies (Traoré et al., 2019).

To summarize, mutations in $Ca_v\beta$ encoding genes have been associated with disorders and although the pathological mechanisms have not always been fully characterized, both $Ca_v\beta$ roles linked or unlinked to HVA can be argued. Mutations in genes coding for $Ca_v\beta$ proteins and other HVA subunits (such as *CACNA2D1* and *CACNA1A*) contribute to Brugada Syndrome type 4 and Episodic ataxia type 5, indicating an HVA-linked involvement in pathological mechanisms. However, $Ca_v\beta$ can also cause and/or modify pathological features even independently of HVA, which is supposedly an underestimated situation.

CHAPTER 3: MuscleBlind Like (MBNL) proteins & Myotonic Dystrophy Type 1

MBNL proteins are key splicing factors contributing to the regulation of developmental transition from fetal to adult splice isoforms. They play a crucial role in muscle and brain development and function, and other cellular process by ensuring the correct splicing of pre-mRNA. MBNL proteins are extensively studied for their implication in Myotonic Dystrophy type 1 (DM1) and type 2 (DM2) where their sequestration by toxic nuclear aggregates leads to their functional inactivation. This results in widespread splicing defects that contribute to the clinical manifestations of DM1 and DM2.

I- Dystrophy Myotonic Type 1

Muscular dystrophy is a group of genetic disorders that causes progressive weakness and muscle mass loss. This group of disorder includes, not exhaustively, Duchenne/Becker Muscular Dystrophy, Facioscapulohumeral Dystrophy, Myotonic Dystrophy (DM) etc.

DM are complex disorders affecting multiple organ systems, with variable symptoms and patterns of disease progression. This pathology is divided into two subtypes: DM1 and DM2, both caused by genetic defects. Here, we will focus on DM1.

a) Generalities

DM1 is an autosomal, dominant inherited disorder that affects both men and women, also known as Steinert's disease, named after the person who described it in 1909. DM1 is the most prevalent form of muscular dystrophy in adults, affecting approximately 1 in 8 000 individuals worldwide. This disorder is characterized by multi-systemic syndromes that affects skeletal as well as smooth muscles but also heart, Central Nervous System (CNS), eyes and endocrine system. Symptoms are widespread, ranging from cataracts, cardiac arrhythmia and insulin resistance to more specific muscle-related issues as muscle weakness and myotonia, a hallmark of DM1 characterized by a delay in muscle relaxation after contraction. Symptoms can manifest at any age, but muscular damage typically first appears in adulthood (Machuca-Tzili et al., 2005).

Steinert's disease can present as asymptomatic with individuals carrying the genetic mutation but showing no signs of the disease even at advanced age, or can manifest very late in life. Conversely, there are severe forms with pathologic onset early from birth. The disease can be categorized into four distinct forms based on the age of symptom appearance, severity and progression: the congenital form begins in the neonatal period, the juvenile form appears during childhood or adolescence, the adult classic form typically manifests in adulthood and the late-onset form develops later in life.

b) Pathophysiology: DM1 as a toxic RNA disorder

The identification of the genetic cause was made in 1992 with the discovery of a mutation in the gene encoding DMPK (Myotonic Dystrophy Protein Kinase), located on chromosome 19. This mutation is a repeat expansion of CTG motif in the 3' Untranslated region (UTR) region of the DMPK gene. These CTG repeats are unstable and expand both at the somatic level during patient's lifetime, and across successive generations. The severity of the symptoms and the age of the disease onset increase with the expansion of CTG repeats, following an "anticipation" phenomenon (Ashizawa et al., 1992). This is characteristic of repeat expansion diseases where symptoms manifest at progressively earlier ages with each generation.

Two main studies have highlighted the role of mRNA poly(CUG) triplets in causing DM1 pathology. They used transgenic mouse models expressing CUG repeats, demonstrated that whether they are inserted into the human *DMPK* 3'-UTR gene to reproduce the genetic anomaly found in DM1 patients, or into the 3'-UTR of an unrelated mRNA, animals developed myotonia and myopathy (Mankodi et al., 2000; Seznec et al., 2001). Importantly, the model generated by Mankodi and published in 2000, is the widely used DM1 mouse model expressing the Human Skeletal alpha-Actin (*HSA*) gene carrying 250 CTG triplets in its 3'-UTR, known as HSA Long Repeats or *HSA^{LR}* model.

RNA transcripts containing expanded CUG repeats fold into stable double-stranded RNA hairpin structures, which results in nuclear aggregates that attract and trap RNA-binding proteins (RBP) (Tian et al., 2000), including those crucial for an appropriate muscle development, maturation and activity. Among the proteins sequestered in these RNA aggregates, MBNL proteins are largely involved in DM1 physiopathology (Miller et al., 2000). Indeed, MBNLs are RBPs, widely known as alternative splicing regulators but also involved in other mRNA processing mechanisms (mRNA polyadenylation, stability, localization etc.), these processes being dysregulated in DM1. CUG-BP, Elav-like Family (CELF) proteins are not trapped in DM1 RNA aggregates but are hyperphosphorylated by Protein Kinase C, which increases their stability and relocates them to nuclei. CELF proteins are therefore hyperactivated, which participates in the physiopathology of the disease (Kuyumcu-Martinez et al., 2007). Their sequestration leads to dysregulated alternative splicing, impaired mRNA translation, and mRNA instability (**Fig. 16**).

II- MBNL proteins

The *Muscleblind* gene (*Mbl*) was first identified in *Drosophila melanogaster*, in which it has been shown to be crucial for peripheral nervous system development (Kania et al., 1995), terminal differentiation of muscle cell Z-sarcomeric bands (Artero et al., 1998) and differentiation of photoreceptor cells (Begemann et al., 1997).

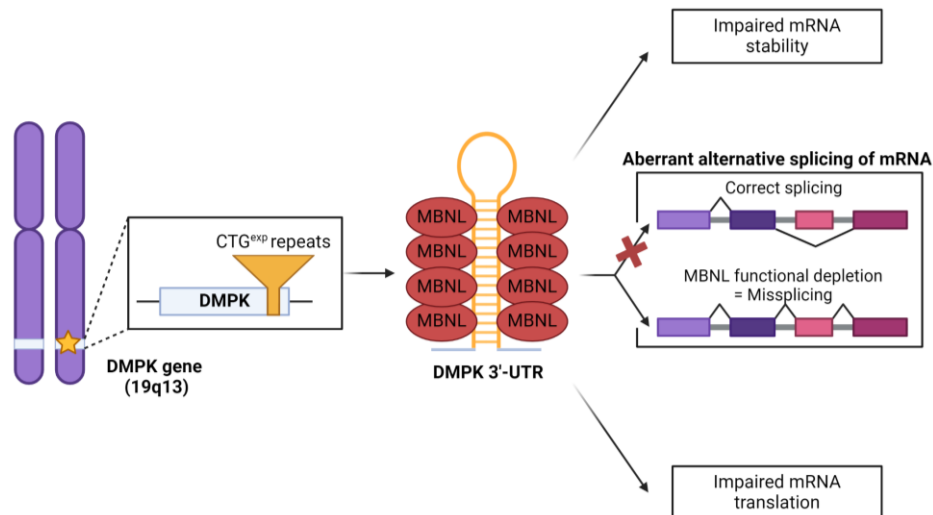


Figure 16. Molecular pathogenesis of DM1.

A triplet expansion in the 3'UTR of DMPK gene leads to the sequestration of MBNL proteins, resulting in impaired mRNA stability, aberrant alternative splicing and impaired mRNA translation (created with BioRender.com).

Mammal's MBNLs and *Drosophila* Mbl genes derive from speciation of a single ancestral copy, they are orthologs functionally exchangeable *in vivo*. However, the mammal's MBNL genes have a specific organization, distinct from the Mbl *Drosophila's* gene: both groups have evolved independently after the speciation event. The three mammalian MBNL genes have a very alike exon composition, indicating that they are paralogs resulting from a relatively recent duplication event and have subsequently acquired specialized functionality (Pascual et al., 2006). MuscleBlind-Like 1 (*Mbnl1*), MuscleBlind-Like 2 (*Mbnl2*) and MuscleBlind-Like 3 (*Mbnl3*) genes are present on three different chromosomes: chromosome 3, 13 and X respectively in mice. Although MBNL proteins act as splicing factors, their mRNAs are themselves subject to splicing. MBNL1 and MBNL2 isoforms mainly differ in the presence or not of exons 5, 7 and 8.

a) Generalities on MBNL proteins

Structure of MBNL proteins

MBNLs are specifically characterized by their CCCH-type zinc-finger (ZnF) domains consisting of about thirty amino acids, which stabilize protein folding using one or more Zn²⁺ ions. In mammals, MBNLs have two pairs of highly conserved ZnF motifs: ZnF1/2 and ZnF3/4, which include three cysteine and one histidine residues, giving rise to the "CCCH tandem ZnF" designation (Miller et al., 2000). ZnF1 and ZnF3, are structurally similar, as are ZnF2 and ZnF4. ZnF2 and ZnF4 are the ones responsible for MBNLs binding to RNA, enabling their functions. Between the two pairs of ZnF is a linker domain encoded by exon3, which is crucial for MBNL activity. Isoforms deriving from alternative splicing of this domain, or MBNLs genetically deleted of it (Tran et al., 2011) show a decreased affinity for their mRNA targets. Additionally, an NLS sequence, encoded in exon5 and the KRAEK motif in exon6, are present in MBNL1 and MBNL2 only, consistently with their primarily localization in the nucleus, while MBNL3 is mainly

cytoplasmic (Thomas et al., 2017). All three MBNL paralogs are able to interact each other through a portion of the C-terminal domain encoded by exon7, which allows MBNL proteins homodimerization. These different regions are central for MBNLs, affecting their localization, RNA binding, and mRNA processing functions (**Fig. 17**).

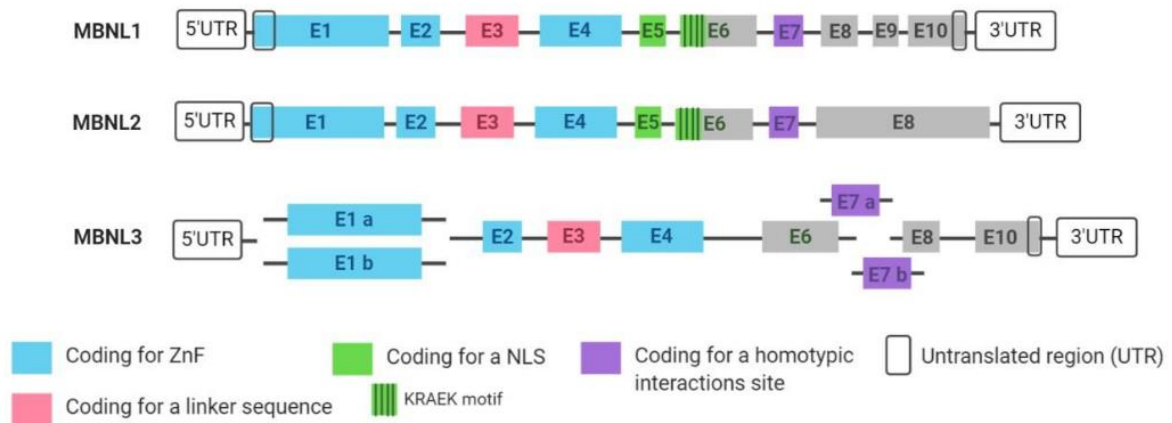


Figure 17. MBNL gene and protein domain structure.

MBNL1 MBNL2 and MBNL3 paralog structures, showing exons with corresponding functional domains, including those constitutively expressed in all transcripts and those undergoing alternative splicing (from López-Martínez et al. 2020).

MBNL's mechanism of action

A study published by Ho and colleagues in 2004 first demonstrated that MBNL1 binds to a common YGCY motif (where Y is a pyrimidine) on both chicken and human cardiac Troponin T (cTNT) transcripts, regulating their alternative splicing (Ho et al., 2004). Later, Teplova and Patel used crystallography to further elucidated this YGCY element recognition by the MBNLs CCCH ZnF motifs (Teplova and Patel, 2008) and importantly, the number and the arrangement of these YGCY motifs, along with the overall mRNA structure, influence binding affinity and splicing activity of MBNL proteins (Taylor et al., 2018). Several structural studies have proposed models of how CCCH ZnF motifs interact with YGCY motifs on either single- or double-stranded RNA targets, depending on the number of YGCY motifs and the number of nucleotides separating them (Konieczny et al., 2014) (**Fig. 18A**).

The CrossLinking ImmunoPrecipitation sequencing (CLIPseq) technology leads to the identification of mRNAs targeted by MBNL1 protein in a muscle-specific manner. Binding locations of MBNL1 on its targets were studied, leading to the identification of clusters enriched in YGCY consensus motifs, consistently with the previous demonstrations (Wang et al., 2012). The position of splicing factor binding sites is a key factor influencing the splicing activity. Indeed, it has been demonstrated that the binding of MBNL1 and MBNL2 proteins downstream or upstream the same exon was recognized to promote its inclusion or exclusion, respectively (Konieczny et al., 2014; Wang et al., 2012) (**Fig. 18B**). This YGCY consensus binding sequence was found to be associated with alternative splicing in the

nucleus but also in RNA targets present in the cytoplasm to carry their processing, trafficking (association of MBNLs with the cytoskeleton) and stability through a 3' UTR binding (Wang et al., 2012).

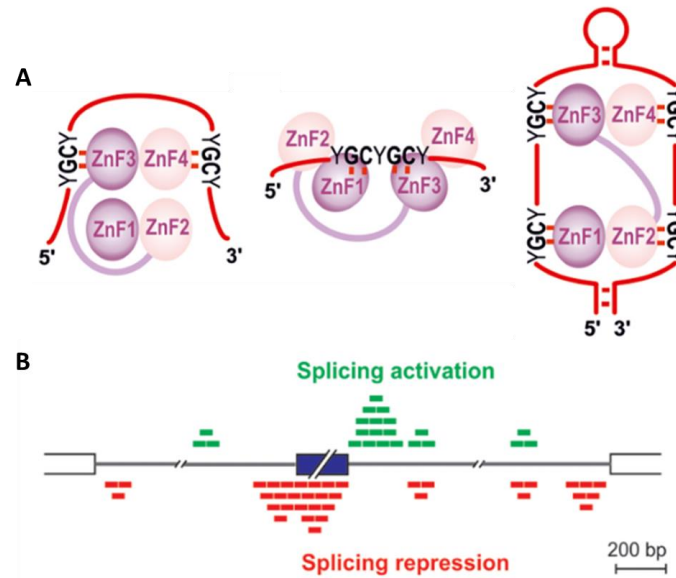


Figure 18. Binding of MBNL proteins to mRNA.

A. Models of various binding mode between ZnFs tandems and the single- or double-stranded target RNAs. **B.** MBNL1 binding upstream (red boxes) promotes exon exclusion, while binding downstream (green boxes) promotes exon inclusion. (modified from Konieczny et al. 2014)

b) MBNLs as key players in mRNA processing

Protein expression profiles

MBNL1, MBNL2 and MBNL3 proteins have distinct expression patterns across different tissues: MBNL1 is highly expressed in skeletal muscle, heart and brain, and at lower levels in other tissues. MBNL2 is predominantly found in the brain and heart, and at lower levels in other tissues. Both MBNL1 and MBNL2 show higher expressions in adult tissues, with an increased expression during tissue differentiation while, in contrast, MBNL3 is highly expressed during embryogenesis, with its expression significantly decreasing in most tissues after birth, except for continued expression in the placenta and certain reproductive tissues (Kanadia et al., 2003b). In skeletal muscle, MBNL3 is also transiently expressed following injury-induced muscle regeneration (Poulos et al., 2013). These patterns highlight the diverse tissue-specific and developmental stage-specific functions of MBNLs in mammals (Konieczny et al., 2014).

In C2C12 myoblasts MBNL3 inhibits muscle differentiation and its expression progressively decreases to be hardly detected in terminally differentiated myotubes (Lee et al., 2008) and adult skeletal muscle (Poulos et al., 2013). In C2C12, MBNL3 over-expression prevents muscle differentiation (Lee et al., 2008) while its depletion accelerates myogenesis (Poulos et al., 2013).

MBNLs as regulators of mRNA processing

As mentioned earlier, MBNLs are RBP, widely known as alternative splicing regulators but they are also involved in transcripts polyadenylation, stability and localization as well as miRNA biogenesis.

Alternative splicing is an RNA processing mechanism that generates protein diversity not only across cell types but also across various developmental stages. This mechanism is crucial for enhancing diversity and complexity of proteins, thereby controlling a wide array of biological processes. Mis-regulations of alternative splicing, including changes or imbalances in the expression, localization or function of splicing factors, disturb or disrupt cellular processes by altering or suppressing important protein physiological functions. Physiologically, MBNL3 carries embryonic splicing patterns, while MBNL1 supports adult muscle splicing events and MBNL2 performs this role in the brain (Charizanis et al., 2012). MBNL1 and MBNL2 present a highly interchangeable splicing factor function.

In the nucleus, MBNLs are also involved in the process of Alternative PolyAdenylation (APA). The 3' part of the last coding exon of the pre-mRNA generally contains polyadenylation sites that can be cleaved, followed by the addition of a poly-A tail. The presence of multiples APA sites allows for different polyadenylation configurations, generating alternative mRNA 3'UTR. These regions contain interaction sites for various factors, including RBP and microRNA, which can modulate RNA localization, translation and turnover (Tian and Manley, 2013). A study using fibroblasts from mice with inactivated *Mbnl* genes revealed that the absence of MBNLs led to a massive deregulation of APA events. The study demonstrated that MBNL proteins interact directly at polyadenylation sites, contributing to the transition of various APA profiles during postnatal development (Batra et al., 2014).

MBNL are also reported as regulating miRNA biogenesis. miRNA are small, single-stranded, non-coding RNA molecules containing 21 to 23 nucleotides, that negatively regulates gene expression through binding to complementary sites in their mRNA targets. The first description of MBNL implication in miRNA processes was by Rau and colleagues in 2011: they showed that MBNL1 interacts with pre-miRNA miR-1, promoting its processing into mature miR-1 through cleavage by the Dicer endonuclease (Rau et al., 2011). Recently, it was demonstrated in *Caenorhabditis elegans* that a short isoform of MBL-1 (*MBNL* orthologous gene) is generated specifically during development and is essential for normal lifespan. Interestingly, this short MBL-1 isoform acts on the regulation of miRNA expression to exert its developmental role (Verbeeren et al., 2023).

In parallel, several studies have explored the functions of MBNLs proteins related to their cytoplasmic localization. A study demonstrated that MBNL localizes the integrin $\alpha 3$ transcript from the nucleus to the plasma membrane for translation, thereby participating in its subcellular localization (Adereth et al., 2005). Consistent with the role of MBNL in regulating mRNA localization into different cellular compartments, MBNL1 cytoplasmic distribution is not uniform, localizing at the cell periphery or in structures that appear to anchor cellular projections (Wang et al., 2012). After MBNL1 and MBNL2 depletion in mouse myoblasts, the abundance of mRNA associated with membranes decreased and became enriched in the cytosolic compartment. The extent of this relocation correlated with the

binding density of MBNLs to their targets, evaluated by a transcriptomic analysis on different murine tissues (Wang et al., 2012). Therefore MBNLs have been shown to contribute to target hundreds of transcripts to membranes (either plasmatic or ER membranes) along with their role in participating in a set of mRNA efficient translation (Wang et al., 2012). One noteworthy point is that a common set of mRNAs that are targeted by MBNL proteins in the nucleus for splicing purpose are twice more likely to be also bound by MBNL proteins in the cytoplasm, thus suggesting the existence of a relationship between MBNLs function in the nucleus and in the cytoplasm (Wang et al., 2012). This MBNL role in regulating the localization of its targets was shown to be due to its binding to target 3'-UTR domains, as demonstrated by CrossLinking ImmunoPrecipitation (CLIP) analysis (Wang et al., 2012). This binding region was also found to be related to mRNA destabilization, in a study revealing that the binding of MBNL1 to its 3'UTR mRNA targets has a destabilization effect (Masuda et al., 2012).

c) MBNL and CELF proteins: antagonist role in RNA processing

MBNL and CELF are two families of protein that control developmental transition and their implication in several neuromuscular disorders, especially DM1, is today underlined (Brinegar and Cooper, 2016). While MBNL proteins, and particularly MBNL1 and MBNL2, increase during post-natal development to control fetal to adult alternative splicing shift of their mRNA targets, CELF proteins, and particularly CELF1 (or CUG-BP1), significantly decrease along skeletal muscle and brain development to reach a very low level of expression in adult.

In mice (and humans), 6 paralogues genes are contained in the CELF family (CELF1-6) with defined roles according to their localization: similarly to MBNLs, they control alternative splicing regulation in the nucleus and are mobilized in mRNA stability and translation in the cytoplasmic compartment. These proteins are preferentially binding G/U-rich sequences motifs (Brinegar and Cooper, 2016).

MBNL and CELF proteins target a common set of mRNAs on which they have independent activity (through a binding on distinct intronic sites), but antagonist effects (Poulos et al., 2013). Indeed, during post-natal stages MBNL1 relocalizes in the nuclear compartment and progressively replaces MBNL3 activity, promoting embryonic to adult splicing switch by skipping fetal and including adult exons (Lin et al., 2006), while CELF1 initially exerts the opposite splicing pattern (Brinegar and Cooper, 2016). Overall, mRNA transcripts follow a splicing arrangement with embryonic characteristics when CELF activity prevails and reversely they follow an adult splicing pattern when MBNL activity predominates (Pascual et al., 2006). Independently of CELF proteins, a previous study revealed that MBNL proteins are the most strongly associated with splicing patterns that differ between embryonic stem cells and cells already committed to specific lineages both in humans and in mice (Han et al., 2013).

III- Differential implication of MBNL proteins in DM1 physiopathology

Disruption in RBP proper functions during key periods, such as development or in a tissue specific manner, can lead to pathological conditions. As previously mentioned, the post-natal period involves a transition from embryonic to adult splicing pattern. This transition is physiologically regulated by a balance between MBNL3 and MBNL1 activities, along with CELF hyperactivation. However, in DM1, these splicing transitions are hindered due to the sequestration of MBNL proteins in nuclear foci and hyperactivation of CELF proteins, which together result in the persistence of embryonic splicing pattern in adult muscle (Brinegar and Cooper, 2016). This characterizes DM1 as a spliceopathy, the resulting aberrant mRNA leading to the diverse symptoms of the pathology.

The main genes concerned by a splicing alteration associated with DM1 symptoms, and mentioned in this section, are recapitulated in **Fig. 19**.

a) DM1 skeletal muscle defects

The mis-splicing observed as a result of the expression of poly(CUG) repeats in a transgenic mouse model is tightly reproduced by a *Mbnl1*^{ΔE3/ΔE3} KO model. Importantly, this model recapitulate skeletal muscle weakness and myotonia, two hallmarks of DM1 in skeletal muscle (Kanadia et al., 2003a). Reversely, MBNL1 over-expression in the *HSA^{LR}* model by Adeno-Associated Virus (AAV)-mediated delivery in the Tibialis Anterior (TA) muscle reverses myotonia and myopathy (Kanadia et al., 2006). MBNL1 controls a wide set of mRNA splicing in skeletal muscle, its functional inhibition leading to their mis-splicing, which originates many DM1 symptoms.

Myotonia has been linked to splicing defects in *Clc1*, which is controlled by MBNL1 (Kino et al., 2009). CLC1 is the most abundantly expressed Cl⁻ channel at the sarcolemma (Jentsch et al., 2002), these channels being crucial for membrane repolarization. In case of defects in repolarization, the membrane potential stays elevated triggering muscle hyperexcitability and myotonia (Brenes et al., 2023). Inclusion of *Clc1* exon7A is characteristic of the embryonic isoform, while it is absent in the adult *Clc1* transcript, leading to the production of a functional CLC1 Cl⁻ channel. The inclusion of *Clc1* exon7A is described in both *HSA^{LR}* and *Mbnl* KO mice (Kanadia et al., 2003a; Mankodi et al., 2000). A *Mbnl2* KO mouse model, mutated in intron 2, also showed a defect in *Clc1* expression, associated with a mild myotonia (Hao et al., 2008), while another model of *Mbnl2* KO caused by exon2 deletion (*Mbnl2*^{ΔE2/ΔE2} KO model), showed no muscular phenotype (Lin et al., 2006). Additionally, it was suggested that MBNL1 and MBNL3 compound depletion synergistically enhances myotonia by altering both *Clc1* mRNA splicing and its translation efficiency (Choi et al., 2015).

The characteristic muscle weakness in DM1 is associated with the mis-splicing of several transcripts, many of which are controlled by MBNL proteins. Among these targets, the exclusion of exon29 of *Cacna1s* (Ca_vα1s) (Tang et al., 2012), the exclusion of exon70 of *Ryr1* (Kimura et al., 2005) and the exclusion of exon11 of *Bin1* (Amphiphysin 2) (Fugier et al., 2011) lead to muscle weakness due to a

disturbed ECC mechanism. Indeed, as described in Chapter 1, ECC implies the cooperation of the skeletal muscle Ca_v1 Ca^{2+} channel (with $\text{Ca}_v\alpha1s$ as the pore channel subunit) and RyR1 to ensure a proper ECC. Amphiphysin 2 plays a crucial role in the proper formation of T-tubules, essential structures for an effective ECC. By altering ECC, the mis-splicing of these transcripts leads to muscle weakness. Other mRNA targets are mis-spliced in DM1, also contributing to muscle weakness, this is the case for *Capn3* (Calpain 3), *Dmd* (Dystrophin) or *Dtna* (Dystrobrevin- α , a protein of the DGC). *Mbnl1* itself is also mis-spliced in DM1 skeletal muscle (López-Martínez et al., 2020).

If the described splicing alterations are recapitulated in MBNL1 deficient model, a limitation of using a single *Mbnl* gene KO is the functional compensation by other MBNLs, particularly the increase in MBNL2 levels in response to MBNL1 depletion (Lee et al., 2013). To address this issue, Lee and colleagues proposed a model with combined MBNL1 and MBNL2 deficiency specifically in muscle fibers (*Mbnl1*^{-/-};*Mbnl2*^{C/C};*Myo-Cre*^{+/-} mice), which shows enhanced splicing defects and muscle pathology (Lee et al., 2013).

MBNL3 is also suggested to contribute to the poor muscle regeneration observed in DM1, leading to muscle dystrophy: the *Mbnl3* ^{$\Delta E2/\Delta E2$} model shows impaired muscle repair (Poulos et al., 2013) whereas MBNL1 and MBNL2 depletion have no impact on this process (Yadava et al., 2024).

Skeletal muscle is the primary tissue responding to insulin by taking up glucose from the bloodstream to lower blood sugar levels. It absorbs glucose and uses it for energy or stores it as glycogen. DM1 pathology is associated with an impaired glucose uptake in response to insulin, reflected by glucose intolerance and increased insulin levels in the blood. *Insr* gene, coding for the skeletal muscle insulin receptor is mis-spliced in DM1, triggering the glucose intolerance development (Savkur et al., 2001).

b) DM1 cognitive impairments

If MBNL2 deficiency (*Mbnl2* ^{$\Delta E2/\Delta E2$}) exhibits no muscular defects (Lin et al., 2006) it displayed features of DM1 at the neurological level, consistent with its pattern of expression. This demonstrates, at least partially, the involvement of MBNL2 in the symptoms at the level of CNS, including abnormally rapid eye movement during sleep and deficits in spatial memory, correlatively associated with hippocampal volume decrease (Charizanis et al., 2012; Sta Maria et al., 2021).

Microtubule-associated protein Tau (MAPT) and NMDA Receptor 1 (NMDAR1) are among the proteins affected by most of the described splicing defects observed in the DM1 brain (López-Martínez et al., 2020). Interestingly, similar to skeletal muscle, both *Mbnl1* and *Mbnl2* mRNA splicing events are affected in DM1 brain, contributing to the pathological splicing defects (López-Martínez et al., 2020).

c) DM1 cardiac defects

Cardiac conduction delay and arrhythmias are associated with DM1 pathology (Mahadevan et al., 2021). The molecular mechanisms causing conduction impairment involve the mis-splicing of ion channels that regulate cardiac ECC. Specifically, the abnormal inclusion of intron 19 in *Atp2a2* mRNA, which codes for SERCA2 Ca²⁺ ATPase channel, and the inclusion of exon6a in *Scn5a* mRNA, which codes for a subunit of the NaV1.5 Na⁺ channel, were proposed to contribute to these cardiac dysfunctions. These splicing abnormalities lead to the dysregulation of Ca²⁺ and an impaired NaV1.5 Na⁺ channel conductance in heart, ultimately resulting in conduction alterations (López-Martínez et al., 2020).

Other mRNAs mis-spliced in DM1 include *TNNT2* coding for the cardiac Troponin isoform, *TTN* coding for Titin, *MYOM1* coding for a sarcomeric protein, *ALPK3* coding for α -kinase 3. Importantly, *RBFOX2*, from the RNA binding Fox (RBFOX) family of proteins, is an important splicing factor in cardiac muscle and is abnormally spliced in DM1 cardiac tissues (López-Martínez et al., 2020).

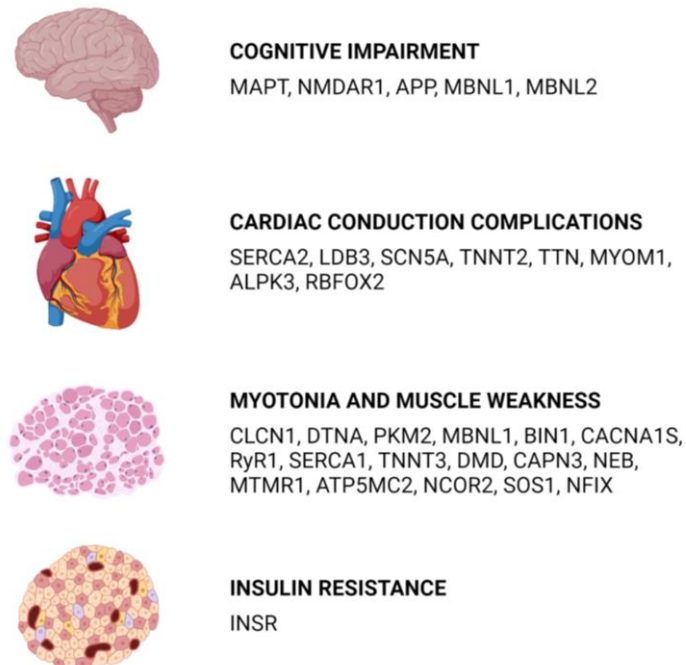


Figure 19. Different transcripts from different tissues are incorrectly spliced, causing most DM1 symptoms (modified from López-Martínez et al. 2020)

RATIONAL FOR THE CURRENT STUDY & THESIS OBJECTIVES

The neuromuscular system is a highly intricate network responsible for coordinating muscle movement, involving various molecular and cellular components. Within this system, $\text{Ca}_v\beta 1$ proteins are essential for regulating HVA Ca^{2+} channels and ECC. A previous research from our team has identified $\text{Ca}_v\beta 1D$ (and not $\text{Ca}_v\beta 1A$) as the adult constitutive isoform and $\text{Ca}_v\beta 1E$ as the embryonic variant, re-expressed following nerve damage (Traoré et al., 2019). Muscle tissues lacking $\text{Ca}_v\beta 1$ during development exhibited abnormal pre-patterning and aberrant innervation (Chen et al., 2011), pointing out a role of $\text{Ca}_v\beta 1$ proteins in NMJ formation.

The present study aims at further characterizing the different $\text{Ca}_v\beta 1$ isoforms, deciphering the mechanisms involved in their differential expression and finally better understanding their role in the physiology and pathophysiology of skeletal muscle. Indeed, we wondered which $\text{Ca}_v\beta 1$ isoform is critical for NMJ formation, and whether $\text{Ca}_v\beta 1$ proteins also affect its maintenance. Additionally, RNA sequencing (RNAseq) data from a previous study by our team revealed a significant correlation between MBNL and $\text{Ca}_v\beta 1$ protein expressions post-denervation (Traoré et al., 2019). This finding led us to explore the regulatory role of MBNL proteins on $\text{Ca}_v\beta 1$ isoforms. Given the involvement of MBNLs in the pathophysiology of DM1 where *Cacnb1* is mis-regulated (Arandel et al., 2017), we wondered about a potential connection between $\text{Ca}_v\beta 1$ isoforms and DM1 pathology.

To address these questions, the objectives of this thesis work are:

- Characterization of $\text{Ca}_v\beta 1$ isoforms
- Investigation of $\text{Ca}_v\beta 1$ involvement in NMJ pre-patterning, maturation and maintenance
- Exploration of $\text{Ca}_v\beta 1$ in DM1 pathophysiology
- Examination of the regulation of $\text{Ca}_v\beta 1$ isoforms by MBNL proteins

MATERIALS AND METHODS

Biological material

I- Plasmids

shMbn1 (target sequence GAAGTATGTAGAGAGTTTCAA) (Wang et al., 2012) was provided by Denis Furling lab and cloned in pSMD2 under CMV promoter. siMbn1 was generated with the same target sequence and siMbn3 (target sequence CCAAATGGTCCGGTTCTGATT) were generated by Eurogentec.

pCDNA3-Mbn1 and pCDNA3-Mbn3 have been generated by direct cloning of either Mbn1 or Mbn3 Open Reading Frame (ORF) (NM_020007.4 and NM_134163.5, respectively). Sequences synthesis and cloning has been performed using GeneArt technology (GeneArt string; ThermoFisher). Mbn1 ORF was flanked by NheI and BamHI while Mbn3 ORF was flanked by BamHI and KpnI for insertion in pCDNA3 vector backbone.

pCDNA3-Luciferase-3'UTR_Cacnb1A/D and pCDNA3-Luciferase-3'UTR_Cacnb1E plasmids were generated) as follow: cDNA corresponding to Cacnb1A/D and Cacnb1E respective sequences were amplified and EcoRV and FseI sites were inserted by Polymerase Chain Reaction (PCR). This cassette was subsequently sub-cloned into an HSVTK-Luc3' plasmid at EcoRV and FseI sites, downstream luciferase gene (GeneArt, ThermoFischer).

pSMD2-shEx2A was already generated (Traoré et al., 2019) and specifically targets Cacnb1 exon 2A (target sequence CCTCGGATACAACATCCAACA), therefore downregulating Cacnb1 embryonic isoforms specifically.

II- AAV production

pSMD2-shMbn1 and pSMD2-shEx2A vectors have been prepared in AAV1 serotype vectors by the AAV production facility of the Center of Research in Myology, by transfection in 293 cells as described previously (Traoré et al., 2019). The final viral preparations were kept in phosphate-buffered saline (PBS) solution at -80°C. The particle titer (number of viral genomes) was determined by quantitative PCR (qPCR). Transduction of these AAV1-containing plasmids will be referred as shMbn1 and shEx2A treatment.

Mouse experimental models

I- Animals and ethics

All animals were housed under specific-pathogen-free (SPF) conditions, with a 12 hours light cycle with access to rodent food and water *ad libitum*.

Embryos were from breeding housed directly in UMS28 animal facility or from gestating females from Janvier Lab. Embryos were staged, counting the appearance of the vaginal plug as day 0.5 post coitum

(pc) and collected at E12.5, E16 and P0. Newborn (7 days old) male and female mice were from breeding housed directly in UMS28 animal facility under SPF conditions. Adult (2 months old at the beginning of the procedures) C57/BL6 female mice were from Janvier Lab and accustomed to the facility for one week before inducing the experimental procedures.

In the end of the procedures, 7days old mice were euthanized by decapitation while adult mice were euthanized by cervical dislocation.

Animal experimental procedures were performed in accordance with national and European guidelines for animal experimentation, with the approval of the institutional ethics committee (MENESR: Project #29245 and Project #45606).

II- In vivo procedures

a) Injection procedures

For experiment on adult mice, female animals were injected 8 weeks old with either AAV1-shMbnl1, AAV1-shEx2A in TA only or in TA, GAS and SOL muscles. Anesthesia was achieved using isoflurane (3% induction, 2% maintenance), analgesia by buprenorphine (vetergesic 1mg/Kg, subcutaneous). One intramuscular (IM) injection (40 μ l/TA or 100 μ l/GAS+Sol) was performed at a final titer of 1.10⁹ vector genomes (vg)/mg of muscle. AAV1-scramble was injected as control under the same procedure. Mice were sacrificed 8 or 12 weeks after the injection.

For experiments on 7 days old pups (female and male), animals were injected at 7 days old with AAV1-shEx2A in TA and GAS/Sol muscles. Anesthesia was achieved using isoflurane (3% induction, 2% maintenance). One IM injection (10 μ l/TA or 15 μ l/GAS+Sol) was performed at a final titer of 1.10⁹ vg/mg of muscle. AAV1-scramble was injected as control under the same procedure. Mice were sacrificed 3 weeks after the injection.

Muscles were collected and either fixed in paraformaldehyde (PFA) 4% or frozen in isopentane precooled in liquid nitrogen and stored at -80 °C until histology or molecular analysis.

b) Denervation procedures

Right sciatic nerves were neuroectomized (ablation of a 5-mm segment of the sciatic nerve) under general anesthesia (Isoflurane, 3% induction, 2% maintenance) with Buprenorphine (vetergesic 1mg/Kg, subcutaneous). Mice were sacrificed 2, 3 or 14 days after denervation and muscles were collected and either fixed in PFA 4% or frozen in isopentane precooled in liquid nitrogen and stored at -80 °C until histology or molecular analysis.

c) Functional analyses

The force measurement of TA was evaluated by measuring *in vivo* muscle contraction in response to nerve stimulation, as previously described (Traoré et al., 2019). Mice were anesthetized with xylazine/ketamine (100mg/kg-20mg/kg), the knee and paw were fixed in place, and the distal tendon of the muscle was attached to the lever arm of a servomotor system (305B, Dual-Mode Lever, Aurora Scientific) using a silk ligature. Data were analyzed using the PowerLab system (4SP, ADInstruments) and software (Chart 4, ADInstruments). The sciatic nerve was stimulated using supramaximal square-wave pulses of 0.1ms in duration. Capacity for force generation was evaluated by measuring the absolute maximal force that was generated during isometric contractions in response to electrical stimulation (frequency of 75–150Hz; train of stimulation of 500ms). Maximal isometric force was determined at L0 (length at which maximal tension was obtained during the tetanus). Force was normalized by muscle mass as an estimate of specific force.

For Electroneuromyogram (ENMG), two monopolar reference and recording electrodes were inserted, one close to the patella tendon and the other in the middle of the TA muscle. A monopolar ground electrode was also inserted into the contralateral hindlimb muscle. The sciatic nerve was stimulated with series of 10 stimuli at 1, 5, 10, 20, 30, and 40Hz. Compound Muscle Activity Potentials (CMAPs) were amplified (BioAmp, ADInstruments), acquired with a sampling rate of 100kHz, and filtered with a 5kHz low-pass filter and a 1Hz high-pass filter (PowerLab 4/25, ADInstruments), and peak-to-peak amplitudes were analyzed with LabChart 8 software (ADInstruments).

During all experiments, mouse body temperature was maintained at 37°C with radiant heat.

In vitro procedures

I- C2C12 muscle cell line, transfection and luciferase assay

C2C12 muscle cell line was purchased from ATCC, seeded at 2500 cells/well in a black flat bottom 96-well plate (Sigma), and were cultured in IMDM medium (GibcoLife Technologies) supplemented with 20% Fetal Bovine Serum (FBS) and 0.1% gentamicin (Gibco–Life Technologies).

25ng of plasmid pCDNA3-Luciferase-3'UTR_Cacnb1A/D or pCDNA3-Luciferase-3'UTR_Cacnb1E was co-transfected in C2C12 cells with 25ng of unique plasmid or siRNA tools to modulate MBNL levels combined with 25ng of control backbone plasmid vector, to end up with a total of 75ng of plasmid/siRNA tools per well. In case of a combination of plasmid and siRNA tools, 25ng of each was used without control backbone plasmid vector addition, to end up with the same amount of 75ng of plasmid/siRNA tools per well. pCDNA3-Mbnl3, pCDNA3-Backbone, siMbnl1 or siMbnl3 were used for these experiments. The plasmid CMV-Renilla luciferase (1.5 ng) was also transfected in each condition as normalizer.

Cells were transfected using Lipofectamine 2000 (Life Technologies) according to the manufacturer's instructions. Briefly, Lipofectamine 2000 was diluted in Optimem reduced medium (GibcoLife Technologies). Six hours post-transfection, Optimem reduced-medium was replaced with IMDM supplemented with 20% FBS and 0.1% gentamicin. Cells were analyzed 24 hours after medium replacement. Firefly and Renilla luciferase luminescences were quantified with Dual-Glo Luciferase Assay System (Promega, according to manufacturer's instructions) on TECAN Spark™ 10M Microplate reader. Firefly luciferase activity was normalized on Renilla luciferase activity.

II- Primary cells, transduction and high differentiation induction

Primary myoblasts from Wild-Type (WT) newborn mice were prepared as described (Falcone et al., 2014). Briefly, after hind limb muscles isolation, muscles were minced and digested for 1.5h in PBS containing 0.5mg/ml collagenase (Sigma) and 3.5 mg/ml dispase (GibcoLife Technologies). Cell suspension was filtered through a 40µm cell strainer and preplated in IMEM + 10% FBS + 0.1% gentamycin for 4h, to discard the majority of fibroblasts and contaminating cells. Non-adherent myogenic cells were collected and plated in IMDM + 20% FBS + 1% Chick Embryo Extract (CEE) (MP Biomedical) + 0.1% gentamycin in 12-well plate or fluorodishes coated with IMDM 1:100 Matrigel Reduced Factor (BD Bioscience). Differentiation was triggered by medium switch in IMDM + 2% horse serum + 0.1% gentamycin. A thick layer of Matrigel Reduced Factor (1:3 in IMDM) was added 24h after differentiation medium addition. Myotubes were treated with 100µg/ml of agrin, and the medium was changed every 2 days, for 8 days of differentiation (Falcone et al., 2014). Downregulation of embryonic Ca_vβ1 isoforms was achieved concurrently with the induction of differentiation through transduction of AAV1-shEx2A.

Gene expression analyses

I- RNA isolation and gene expression analyses

Total RNA was extracted from muscle cryosections using Trizol (TermoFisher Scientific) /Direct-zol RNA MiniPrep w/ Zymo-Spin IIC Columns (Ozyme) and from cells using NucleoSpin RNA Columns (Macherey-Nagel). 200ng of total RNA were subjected to Reverse Transcription (RT) using Superscript II Reverse transcriptase kit (18064022, TermoFisher Scientific) or 1µg of total RNA using Maxima H Minus Reverse Transcriptase (EP0753, TermoFisher Scientific), with a mix of random primers (48190011, TermoFisher Scientific) and oligo(dT) (18418020, TermoFisher Scientific), to generate complementary DNA (cDNA). 2µL of cDNA was amplified in 20µL reactions in PCR Master Mix (M7505, Promega), Phusion High-Fidelity PCR Master Mix with GC Buffer (F532L, TermoFisher Scientific) or Q5 Hot Start High-Fidelity 2X Master Mix (M0494S, New England Biolabs) for RT-PCR and RT-PCR triplex. 2µL of 1:5 diluted cDNA was amplified in 10µL reactions in Power SYBR Green PCR MasterMix (TermoFisher Scientific) to performed qPCR on StepOne Plus Real-Time PCR System (Applied Biosystems). Data were analyzed using $\Delta\Delta CT$ method and normalized to RPLPO (Ribosomal protein

lateral stalk subunit PO) mRNA expression. The sample reference to calculate mRNA fold change is indicated in each panel. Primers are listed in **Table S1**.

II- Nanopore sequencing

600ng of total RNA were subjected to RT with an anchored poly-dT primer (12577011, ThermoFisher Scientific) and Maxima H Minus Reverse Transcriptase. The amplification of the *Cacnb1* transcriptome was independently processed in each sample through two PCR steps, using 2 μ L of diluted RT reactions (12-fold dilution). First, a pre-amplification was performed for 20 cycles using specific primers fused with universal sequences U1 and U2 (referenced in **Table S2**). These primers are specifically base paired with the first and last exons of *Cacnb1* transcripts. The PCR reactions were treated with exonuclease I to remove primer excess and purified with the NucleoMag[®] NGS Clean-up and Size Select (Macherey-Nagel). Next, a second amplification of 18 cycles was performed to incorporate barcodes associated with individual samples. All samples were combined to create a stoichiometric multiplexed library, which was prepared using the Oxford Nanopore SQK-LSK109 kit. The library was subsequently sequenced using a MinION Flow Cell (R9.4.1). The Oxford Nanopore data were analyzed as previously described (Dos Reis et al., 2022) and Fastq files generated in this study have been deposited in the ENA database (<https://www.ebi.ac.uk/ena/browser>) under accession code XXXX.

III- ChIP experiments

TA and GAS muscles were harvested from 8-weeks old female mice, innervated or 2 days after denervation. Tissues were finely minced with a scalpel in PBS, incubated for 10min in PBS containing 1% formaldehyde, then 5min in PBS containing 125mM Glycine. Aliquots used for RNAPII immunoprecipitation were fixed a second time with Disuccinimidyl glutarate (DSG) diluted to 2mM in PBS for 40min at room temperature, as previously described (Tian et al., 2012). Tissues were then dissociated with a MACS dissociator using the muscle-specific program.

Resuspended material was incubated on ice 5min in 1mL of chilled buffer A (0.25% TRITON, 10 mM TRIS pH8, 10mM EDTA, 0.5mM EGTA), 30min in 1mL of buffer B (250mM NaCl, 50mM TRIS pH8, 1mM EDTA, 0.5mM EGTA), and then resuspended in 100 to 200 μ L of buffer C (1% SDS, 10mM TRIS pH8, 1mM EDTA, 0.5mM EGTA) at room temperature. All buffers were extemporately supplemented by Complete protease and PhosSTOP phosphatase inhibitors (Roche). Cell suspensions in 0.6mL μ tube were sonicated in water bath at 4°C during 15min (15sec. ON, 15sec. OFF) with a Bioruptor apparatus (Diagenode) setted on high power and then clarified by 10min centrifugation at 10 000rpm, 4°C. Shearing of the DNA was checked after reversing the crosslinking on agarose gel electrophoresis to be around 300-500bp. Sheared chromatin was quantified by optical density (260nm) and diluted 10-fold in IP buffer to final concentrations: 1% TRITON, 0.1% NaDeoxycholate, 0.1% SDS, 150mM NaCl, 10mM TRIS pH8, 1mM EDTA, 0.5mM EGTA, 1X protease and phosphatase inhibitors). 15 μ g of chromatin and 2 μ g of antibodies (listed in **Table S3**), in a final volume of 500 μ L, were incubated at 4°C for 16h on a

wheel. 25µL of saturated magnetic beads coupled to protein G (Dynabeads) were used to recover the immuno-complexes. After 2h of incubation the bound complexes were washed extensively 5min at room temperature on a wheel in the following wash buffers: WBI (1% TRITON, 0.1% NaDOC, 150mM NaCl, 10mM TRIS pH8), WBII (1% TRITON, 1% NaDOC, 150mM KCl, 10mM TRIS pH8), WBIII (0.5% TRITON, 0.1% NaDOC, 100mM NaCl, 10mM TRIS pH8), WBIV (0.5% Igepal CA630 (Sigma), 0.5% NaDOC, 250mM LiCl, 10mM TRIS pH8, 1mM EDTA), WBV (0.1% Igepal, 150mM NaCl, 20mM TRIS pH8, 1mM EDTA), WBVI (0.001% Igepal, 10mM TRIS pH8). 20µg of sheared chromatin used as input and ChIP beads were then boiled 10min in 100µL H₂O containing 10% (V/W) chelex resin (BioRad), followed by Proteinase K (0.5mg/mL)-digestion for 30min at 55°C, and then finally incubated 10min at 100°C. 1µL of ChIP eluate was used for qPCR assays in 10µL reactions with Brilliant III Ultra Fast SYBR-Green Mix (Agilent) using a Stratagene MX3005p system. The analysis of qPCR was performed using the MxPro software. Primers are listed in **Table S1**.

Protein analyses

I- Immunoblotting

Approximately 500µm of muscle cryosections from frozen muscle were homogenized with a Dounce homogenizer protein extraction buffer. For MBNL immunoblotting, proteins were extracted in RIPA buffer (89900, ThermoFisher Scientific) with Halt Protease and Phosphatase inhibitor cocktail (78440, ThermoFisher Scientific). Samples were sonicated in water bath at 4°C during 10min (30sec. ON, 30sec. OFF) with a Bioruptor apparatus (Diagenode). For all the other proteins immunoblotting, proteins were extracted in a lysis buffer containing 50mM Tris-HCl, pH 7.4, 100mM NaCl, 0,5% NP40, with Halt Protease and Phosphatase inhibitor cocktail (78440, ThermoFisher Scientific). Samples were then centrifuged for 10min at 1500g at 4°C and supernatants were collected. Protein concentration was determined by Bradford assay (ThermoFisher Scientific).

For MBNL proteins immunoblotting, samples were denatured at 70°C for 10min with NuPAGE LDS Sample Buffer (NP0007, ThermoFisher Scientific). For Ca_vβ1 proteins and all other proteins immunoblotting, samples were denatured at room temperature for 30 min, or at 95°C for 5min, respectively, with Laemmli buffer with 5% βmercaptoethanol.

Proteins were separated by electrophoresis (Nu-PAGE 4–12% Bis-Tris gel; Life Technologies) and then transferred to nitrocellulose membranes (GE Healthcare). Membranes were blocked with 5% BSA (Ca_vβ1 proteins) or 5% milk (all other proteins) and incubated overnight at 4°C with primary antibodies (listed in **Table S3**) diluted in the blocking buffer. Membranes were then labelled with fluorescent secondary antibodies (listed in **Table S4**) diluted in blocking buffer for 1h in the dark.

Images were acquired with camera LAS4000 (GE Healthcare). Western blot image analysis was performed with the public domain software ImageJ (analyze gel tool).

II- Immunofluorescence (IF) and image acquisition

a) Muscle cryosections

IF procedures were performed on 10µm muscles cryosections fixed on glass slides and stored at -80°C. Slides were rehydrated in PBS, fixed with PFA 4% for 10 min, permeabilized with 0.5% Triton X-100 (Sigma-Aldrich) and blocked in PBS with 4% bovine serum albumin, 0.1% Triton X-100 for 1h. Sections were incubated in PBS with 2% BSA, 0.1% Triton X-100 with primary antibodies (listed in **Table S3**) overnight at 4°C. Aspecific sites were blocked with BSA 5% 1h and slides were incubated for 1h with secondary antibodies (listed in **Table S4**) and incubated 5min with 4',6'-diamidino-2-phenylindole (DAPI) for nuclear staining and mounted in Fluoromount (Southern Biotech).

b) Isolated fibers

TA muscles were collected, rinsed once in PBS and fixed in a PBS 4% PFA solution at room temperature for 1 hour. Groups of approximately 10 muscle fibers were gently dissected and incubated overnight in PBS with 0.1M glycine at 4°C with mild shaking. The next day, after a day of washing in PBS 0.5% Triton X-100, fibers were incubated in permeabilized and blocked for 6 hours in PBS 3% BSA 5% goat serum 1% Triton X-100 at room temperature. Fibers were incubated with primary antibodies (listed in **Table S3**) at 4°C over weekend in blocking solution. Fibers were then rinsed for several hours at room temperature, in PBS 0.5% Triton X-100 and incubated overnight at 4°C with secondary antibodies (**Table S4**) and α -Bungarotoxin-Alexa Fluor conjugated-594 (**Table S3**) in blocking solution. Finally, after a day of washing in PBS 0.5% Triton X-100, fibers were mounted on slides in non-hardening Vectashield mounting medium (H-1000, Vector Laboratories).

NMJ images were acquired with Zeiss Axio Observer microscope coupled with apotome module (63x objective) and edited with Zeiss Zen Lite 3.7 software. The same laser power and setting of parameters were used throughout to ensure comparability. The images presented were single projected images obtained by overlaying sets of collected z-stacks. NMJ morphometric analysis was performed on confocal z-stack projections of individual NMJs by using ImageJ-based workflow adapted from NMJ-morph1. At least 100 NMJs have been analyzed per condition. NMJ morphometric analysis was performed in a blinded manner by the same investigator.

c) Primary myotubes

For IF analyses, primary myotubes were seeded and cultured in fluorodishes (Dutscher). Cells were fixed in 4% PFA for 10 min, permeabilized with PBS 5% Triton X-100. Aspecific sites were blocked with BSA 1% and goat serum 10% for 30 min. Cells were incubated with primary antibodies (listed in **Table S3**) overnight at 4°C in PBS 0.1% saponin 1% BSA. Cells were washed three times and then incubated with secondary antibodies (listed in **Table S4**) and DAPI (1:10 000) for 1h in the dark.

Fluorescence images of myotubes were acquired Spinning Disk confocal scanner unit (CSU-W1 YOKOGAWA) with a 40x oil-immersion objective (plan fluor 40x/1.3 oil OFN25 DIC N2 cyan), coupled with a Photometrics PRIM 95B Camera. Software used was MetaMorph 7.10.2. Image analyses and quantification of AChR clusters size and distribution were performed with the public domain software ImageJ by using a macro developed in the lab by MyoImage facility.

Statistical analyses

Comparison between two groups was tested for normality using Shapiro-Wilk test followed by parametric (two-tailed paired, unpaired Student's t-tests) or non-parametric test (Mann-Whitney) to calculate p-values. For comparison of more than two groups, ordinary one or two-ways ANOVA tests followed by appropriated post hoc tests were performed. All statistical analyses were performed with GraphPad Prism 8 or 9 software and statistical significance was set at $p < 0.05$.

RESULTS

CHAPTER 1 - Identification and characterization of $\text{Ca}_v\beta 1$ embryonic isoforms in skeletal muscle: Implication for neuromuscular junction (NMJ) formation, maturation and maintenance

I- Chapter abstract

$\text{Ca}_v\beta 1$ proteins have been originally described as subunits of the skeletal muscle Ca_v1 Ca^{2+} channel, essential for ECC (Buraei and Yang, 2013). Later, they have been reported as modulator of gene expression independently of Ca_v1 channel, notably in muscle precursor cells and in adult skeletal muscle after nerve damage (Taylor et al., 2014; Traoré et al., 2019). $\text{Ca}_v\beta 1$ proteins exist as several variants, $\text{Ca}_v\beta 1D$ is the constitutive adult isoform and $\text{Ca}_v\beta 1E$ being identified as an embryonic isoform, described to be re-expressed in adult skeletal muscle after nerve damage to limit muscle atrophy (Traoré et al., 2019). Interestingly, $\text{Ca}_v\beta 1$ have been demonstrated as essential for NMJ development, independently of ECC (Chen et al., 2011), although the isoform(s) responsible for such function was not identified.

In this Chapter 1, we added insights in the understanding of the diversity of $\text{Ca}_v\beta 1$ isoforms expressed in skeletal muscle by identifying $\text{Ca}_v\beta 1A$ as a second embryonic/perinatal isoform and by bringing evidences suggesting the existence of an additional variant that we named $\text{Ca}_v\beta 1\text{early}$. This potential new isoform is expressed at early stages of embryogenesis and originates from the use of a premature STOP codon in exon8, in frame in *Cacnb1* transcripts lacking exon7A. We found that the expression of the different isoforms is regulated by the use of two differential promoters: Prom1 driving the expression of embryonic $\text{Ca}_v\beta 1s$ isoforms during embryogenesis and re-activated after nerve damage in adult skeletal muscle, and Prom2 constitutively driving $\text{Ca}_v\beta 1D$ adult isoform expression in adult skeletal muscle. We found that the embryonic $\text{Ca}_v\beta 1s$ isoforms are involved in the proper NMJ formation in an *in vitro* agrin-induced AChR clustering system on primary myotubes, and that their postnatal expression is required for NMJ maturation and maintenance.

II- Results

a) Article in preparation

Identification and characterization of $Ca_v\beta 1$ embryonic isoforms in skeletal muscle: involvement in neuromuscular junction formation

Vergnol Amélie¹, Bourguiba Aly¹, Bauché Stephanie¹, Gentil Christel¹, Pezet Sonia¹, Traoré Massiré¹, Saillard Lucile¹, Gelin Maxime¹, Benkhelifa-Ziyyat Sofia¹, Meunier Pierre¹, Lemaitre Mégane², Perronnet Julianne², Cadot Bruno¹, Guesmia Zoheir¹, Tores Frederic³, Gautier Candice⁴, Allemand Eric⁴, Batsché Eric⁵, Pietri-Rouxel France^{1†}, Falcone Sestina^{1†*}

¹ Centre de Recherche en Myologie – U974 INSERM, Sorbonne Université, Paris, 75013, France

² Phénotypage du petit animal – UM28 INSERM, Sorbonne Université, Paris, 75013, France

³ Institut Imagine – BIP-D Plateforme de Bioinformatique, Université Paris Cité, Paris, 75015, France

⁴ Institut Imagine – U1163 INSERM, Université Paris Cité, Paris, 75015, France

⁵ Institut de Biologie Paris-Seine (IBPS) – UMR 8256 CNRS, Sorbonne Université, Paris, 75005, France

* Corresponding author. s.falcone@institut-myologie.org

† These authors contributed equally to this work

ABSTRACT

Four $\text{Ca}_v\beta$ proteins ($\text{Ca}_v\beta 1$ to $\text{Ca}_v\beta 4$) are described as regulatory subunit of Voltage-gated Ca^{2+} channel (VGCC), each exhibiting expression patterns in excitable cells based on their function. While primarily recognized for their role in VGCC regulation, $\text{Ca}_v\beta$ s have channel-independent activity and regulate gene expression. Among these, $\text{Ca}_v\beta 1$ is expressed in skeletal muscle as different isoforms. The adult constitutive isoform, $\text{Ca}_v\beta 1D$, is located at the triad, where it modulates Ca_v1 function in the Excitation-Contraction Coupling (ECC). Here, we further explored the less characterized $\text{Ca}_v\beta 1$ isoforms, focusing on embryonic/perinatal variants, and their specific role in the neuromuscular systems at different stages of NMJ formation, maturation and maintenance. Our findings revealed that $\text{Ca}_v\beta 1$ isoforms expression is regulated by differential activation of promoters during development. First, we identified $\text{Ca}_v\beta 1A$, in addition to the known $\text{Ca}_v\beta 1E$ variant, as embryogenic variant re-expressed after denervation in adult mouse skeletal muscle. Interestingly, the re-expression of these embryonic/perinatal $\text{Ca}_v\beta 1$ isoforms after nerve damage in adult muscle is due to a shift of promoter activation. In addition, we found that these embryonic/perinatal isoforms are involved in NMJ formation in a neural agrin-induced AChR clustering system on primary myotubes *in vitro* and that their postnatal expression is crucial for NMJ maturation/stability. Altogether, these data provide new insights on knowledge of neuromuscular system homeostasis.

INTRODUCTION

Ca_vβ1 proteins, encoded by *Cacnb1* gene from exon1 to exon14, exist as several variants in multiple tissues. In skeletal muscle, *Cacnb1D* transcript, which spans exon1 to exon13end, gives Ca_vβ1D, the constitutive adult isoform. *Cacnb1E* transcript, ranging from exon2B to exon14, encodes Ca_vβ1E, an embryonic isoform that is re-expressed in adult skeletal muscle after nerve damage (Traoré et al., 2019). Ca_vβ1 proteins have been originally described as key regulators of the skeletal muscle voltage-gated Ca²⁺ channel (VGCC) Ca_v1 (Buraei and Yang, 2013) and showed to be required for a proper Excitation Contraction Coupling (ECC). In particular, Ca_vβ1D holds the regulatory function for this process in adult skeletal muscle, modulating the interaction between two calcium (Ca²⁺) channels: Ca_v1.1, and Ryanodine Receptor 1 (RyR1) at the triad (Traoré et al., 2019). In addition, Ca_vβ1 proteins have been reported as modulators of gene expression independently of Ca_v1 channel, notably in muscle precursor cells regulating myogenesis, and in adult skeletal muscle after nerve damage, contributing to limit muscle mass loss (Taylor et al., 2014; Traoré et al., 2019). These roles have been described to be accomplished by the embryonic Ca_vβ1E isoform. In addition to Ca_vβ1D role in regulating ECC at the triad and Ca_vβ1E role in modulating gene expression, another study highlighted the relevance of Ca_vβ1 proteins in skeletal muscle, by showing its crucial implication in the nerve-muscle connection in during embryogenesis (Chen et al., 2011).

During mammalian development and into early post-natal life, the formation, maturation and stabilization of neuromuscular junction (NMJ) are complex processes that require multiple cues for the establishment of functional nerve-muscle synapses. At early embryogenic stages, before the initiation of muscle innervation, aneural acetylcholine receptor (AChR) clusters are formed in a broad middle region of myotubes in a muscle-intrinsic manner and independently of innervation (Arber et al., 2002; Yang et al., 2001). This phenomenon, known as muscle pre-patterning, represents the first initiating event of the NMJ formation (Li et al., 2018). Alterations of aneural AChR pre-patterning give rise to abnormal growth and spreading of innervating neurites along the muscle fibers (Chen et al., 2011). Between E14 and E18, innervation begins, and agrin, released by the nerve, triggers the clustering of AChR under the nerve ending through the agrin/Low-density lipoprotein receptor-related protein 4 (Lrp4)/Muscle Specific Kinase (MuSK) signalling. Later, in adult muscles, depolarization induces the release of acetylcholine (ACh) from the nerve ending, which activates the postsynaptic AChR. This activation leads to various signalling cascades, essential for NMJ maturation. Besides being essential for NMJ formation and maturation, these actors are also critical for NMJ maintenance and function throughout life. Docking protein 7 (Dok7) and rapsyn are other key players in maintaining NMJ integrity. Dok7 activates the tyrosine kinase domain of MuSK, independently of agrin/Lrp4 pathway

(Eguchi et al., 2016), while rapsyn acts as a chaperone protein to stabilize AChR clusters in muscle post-synaptic membrane (Moransard et al., 2003; Oury et al., 2019).

Ca²⁺ influx and release through Cav1.1 and RyR1, rather than the ECC mechanism itself, are crucial for AChRs aggregation during NMJ formation. This concept was introduced by using mouse embryo models with disruption either in the ECC mechanism and/or in Ca²⁺ influx/release. Dysgenic (Cav1.1^{-/-}) (Rieger et al., 1984) mouse embryos exhibit abnormal AChR distribution while dyspedic (RyR1^{-/-}) mouse embryos show normal AChR distribution (Kaplan et al., 2018), despite both having disrupted ECC processes. The importance of Ca²⁺ influx/release rather than ECC itself, was further demonstrated using a genetically modified model of Cav1.1 (Cav1.1^{nc/nc}), where Cav1.1 functions as a voltage sensor but not as a Ca²⁺ channel. This model displayed normal AChR pre-patterning, while the double RyR1^{-/-}; Cav1.1^{nc/nc} KO model, which lacks both Ca²⁺ influx from Cav1.1 and release from RyR1, show an abnormal AChR distribution (Kaplan et al., 2018). Similarly to these models, *Cacnb1*^{-/-} mice show severely affected NMJ pre-patterning, independently of ECC (Chen et al., 2011). However, the role of Cavβ1 proteins in modulating various other aspects and mechanisms of NMJ formation, maturation and stability may have been underestimated.

In the present study, we aimed at identifying the major representative *Cacnb1* transcripts in embryonic pre- and post-innervated muscles in order to characterize their function in the formation and maturation of NMJ, as well as for NMJ maintenance implication in adult innervated and denervated muscles. We confirmed the expression of *Cacnb1D* in adult innervated muscle and found that *Cacnb1A*, in addition to *Cacnb1E*, is expressed in embryonic and denervated adult mouse skeletal muscle. We demonstrated that the expression of the different *Cacnb1* isoforms is driven by the activation of specific promoters on embryonic and adult muscles, and that denervation is associated with the restoration of the embryonic epigenetic program. Analysis of the formation and maturation of NMJs after ablation of the embryonic Cavβ1 isoforms revealed a precocious differentiation of primary myotubes *in vitro*, associated with an increase in the size of neural agrin-induced AChRs, while it induced a decrease in the size of endplates in postnatal myofibers. In adult innervated muscle, Cavβ1 embryonic isoforms ablation induces NMJ destabilization, accompanied by denervation-like signs, accordingly to what observed in the early phases of muscle aging (Massiré et al., 2024).

Overall, our findings demonstrate the crucial relevance of Cavβ1 embryonic isoforms in all the processes needed for the establishment and maturation of functional NMJ, shedding light on novel fundamental players involved in development, growth and maintenance of the neuromuscular system.

MATERIAL AND METHODS

Plasmids & Adeno Associated Virus (AAV) production

pSMD2-shEx2A was already described (Traoré et al., 2019) to specifically targets *Cacnb1* exon 2A (target sequence CCTCGGATACAACATCCAACA), therefore downregulating *Cacnb1* embryonic isoforms specifically. pSMD2-shEx2A has been prepared in AAV1 serotype vector by the AAV production facility of the Center of Research in Myology, by transfection in 293 cells as described previously (Traoré et al., 2019). The final viral preparations were kept in phosphate-buffered saline (PBS) solution at -80°C. The particle titer (number of viral genomes) was determined by quantitative PCR. Transduction of this AAV1-containing plasmid will be referred shEx2A treatment.

Animals and ethics

All animals were housed under specific-pathogen-free (SPF) conditions, with a 12 hours light cycle with access to rodent food and water *ab libitum*. Embryos were from breeding housed directly in UMS28 animal facility or from gestating females from Janvier Lab. Newborn (7 days old) male and female mice were from breeding housed directly in UMS28 animal facility. Adult (2 months old at the beginning of the procedures) C57/BL6 female mice were from Janvier Lab and accustomed to the animal facility for one week before inducing the experimental procedures. In the end of the procedures, 7days old mice were euthanized by decapitation while adult mice were euthanized by cervical dislocation. Animal experimental procedures were performed in accordance with national and European guidelines for animal experimentation, with the approval of the institutional ethics committee (MENESR: Project #17975 and Project #45606).

Injection procedures

For experiment on adult mice, female animals were injected 8 weeks old with AAV1-shEx2A or AAV1-scramble in Tibialis Anterior (TA) muscles. Anesthesia was achieved using isoflurane (3% induction, 2% maintenance), analgesia by buprenorphine (vetergesic 1mg/Kg, subcutaneous). One intramuscular injection (40µl/TA or 100µl/gastrocnemius (GAS) + Soleus (Sol)) was performed at a final titer of 1.10^9 vector genomes (vg)/mg of muscle. Mice were sacrificed 8 weeks after the injection. For experiments on 7 days old pups (female and male), animals were injected at 7 days old with AAV1-shEx2A or AAV1-scramble in TA and GAS/Sol muscles. Anesthesia was achieved using isoflurane (3% induction, 2% maintenance). One intramuscular injection (10 µl/TA or 15µL/GAS+Sol) was performed at a final titer of 1.10^9 vg/mg of muscle. Mice were sacrificed 3 weeks after the injection. Muscles were collected and either fixed in paraformaldehyde (PFA) 4% or frozen in isopentane precooled in liquid nitrogen and stored at -80 °C until histology or molecular analysis.

Denervation procedures

Right sciatic nerves were neuroectomized (ablation of a 5-mm segment of the sciatic nerve) under general anesthesia (Isoflurane, 3% induction, 2% maintenance) with Buprenorphine (vetergesic 1mg/Kg, subcutaneous). Mice were sacrificed 2, 3 or 14 days after denervation and muscles were collected and either fixed in PFA 4% or frozen in isopentane precooled in liquid nitrogen and stored at -80 °C until histology or molecular analysis.

Functional analyses

The force measurement of TA was evaluated by measuring *in vivo* muscle contraction in response to nerve stimulation, as previously described (Traoré et al., 2019). Mice were anesthetized with xylazine/ketamine (100mg/kg-20mg/kg), the knee and paw were fixed in place, and the distal tendon of the muscle was attached to the lever arm of a servomotor system (305B, Dual-Mode Lever, Aurora Scientific) using a silk ligature. Data were analyzed using the PowerLab system (4SP, ADInstruments) and software (Chart 4, ADInstruments). The sciatic nerve was stimulated using supramaximal square-wave pulses of 0.1ms in duration. Capacity for force generation was evaluated by measuring the absolute maximal force that was generated during isometric contractions in response to electrical stimulation (frequency of 75–150Hz; train of stimulation of 500ms). Maximal isometric force was determined at L0 (length at which maximal tension was obtained during the tetanus). Force was normalized by muscle mass as an estimate of specific force.

For electroneuromyogram (ENMG), two monopolar reference and recording electrodes were inserted, one close to the patella tendon and the other in the middle of the TA muscle. A monopolar ground electrode was also inserted into the contralateral hindlimb muscle. The sciatic nerve was stimulated with series of 10 stimuli at 1, 5, 10, 20, 30, and 40Hz. Compound muscle activity potential (CMAP) was amplified (BioAmp, ADInstruments), acquired with a sampling rate of 100kHz, and filtered with a 5kHz low-pass filter and a 1Hz high-pass filter (PowerLab 4/25, ADInstruments), and peak-to-peak amplitudes were analyzed with LabChart 8 software (ADInstruments).

During all experiments, mouse body temperature was maintained at 37°C with radiant heat.

Primary cells, transduction and high differentiation induction

Primary myoblasts from WT newborn mice were prepared as described (Falcone et al., 2014). Briefly, after hind limb muscles isolation, muscles were minced and digested for 1.5h in PBS containing 0.5mg/ml collagenase (Sigma) and 3.5 mg/ml dispase (GibcoLife Technologies). Cell suspension was filtered through a 40µm cell strainer and preplated in IMEM + 10% FBS + 0.1% gentamycin for 4h, to discard the majority of fibroblasts and contaminating cells. Non-adherent myogenic cells were

collected and plated in IMDM + 20% FBS + 1% Chick Embryo Extract (MP Biomedical) + 0.1% gentamycin in 12-well plate or fluorodishes coated with IMDM 1:100 Matrigel Reduced Factor (BD Bioscience). Differentiation was triggered by medium switch in IMDM + 2% horse serum + 0.1% gentamycin. A thick layer of Matrigel Reduced Factor (1:3 in IMDM) was added 24h after differentiation medium addition. Myotubes were treated with 100µg/ml of agrin, and the medium was changed every 2 days, for 8 days of differentiation (Falcone et al., 2014). Downregulation of embryonic Cavβ1 isoforms was achieved concurrently with the induction of differentiation through transduction of AAV1-shEx2A.

RNA isolation and gene expression analyses

Total RNA was extracted from muscle cryosections using Trizol (TermoFisher Scientific) /Direct-zol RNA MiniPrep w/ Zymo-Spin IIC Columns (Ozyme) and from cells using NucleoSpin RNA Columns (Macherey-Nagel). 200ng of total RNA were subjected to Reverse transcription (RT) using Superscript II Reverse transcriptase kit (18064022, TermoFisher Scientific) or 1µg of total RNA using Maxima H Minus Reverse Transcriptase (EP0753, TermoFisher Scientific), with a mix of random primers (48190011, TermoFisher Scientific) and oligo(dT) (18418020, TermoFisher Scientific), to generate complementary DNA (cDNA). 2µL of cDNA was amplified in 20µL reactions in PCR Master Mix (M7505, Promega), Phusion High-Fidelity PCR Master Mix with GC Buffer (F532L, TermoFisher Scientific) or Q5 Hot Start High-Fidelity 2X Master Mix (M0494S, New England Biolabs) for RT-PCR and RT-PCR triplex. 2µL of 1:5 diluted cDNA was amplified in 10µL reactions in Power SYBR Green PCR MasterMix (TermoFisher Scientific) to performed quantitative real-time PCR (qPCR) on StepOne Plus Real-Time PCR System (Applied Biosystems). Data were analyzed using $\Delta\Delta\text{CT}$ method and normalized to RPLP0 (Ribosomal protein lateral stalk subunit P0) mRNA expression. The sample reference to calculate mRNA fold change is indicated in each panel. Primers are listed in **Table S1**.

Nanopore sequencing

600ng of total RNA were subjected to RT with an anchored poly-dT primer (12577011, TermoFisher Scientific) and Maxima H Minus Reverse Transcriptase. The amplification of the *Cacnb1* transcriptome was independently processed in each sample through two PCR steps, using 2µL of diluted RT reactions (12-fold dilution). First, a pre-amplification was performed for 20 cycles using specific primers fused with universal sequences U1 and U2 (referenced in **Table S2**). These primers are specifically base paired with the first and last exons of *Cacnb1* transcripts. The PCR reactions were treated with exonuclease I to remove primer excess and purified with the NucleoMag® NGS Clean-up and Size Select (Macherey-Nagel). Next, a second amplification of 18 cycles was performed to incorporate barcodes associated with individual samples. All samples were combined to create a stoichiometric multiplexed library, which was prepared using the Oxford Nanopore SQK-LSK109 kit. The library was subsequently

sequenced using a MinION Flow Cell (R9.4.1). The Oxford Nanopore data were analyzed as previously described (Dos Reis et al., 2022) and Fastq files generated in this study have been deposited in the ENA database (<https://www.ebi.ac.uk/ena/browser>) under accession code XXXX.

ChIP experiments

TA and GAS muscles were harvested from 8-weeks old female mice, innervated or 2 days after denervation. Tissues were finely minced with a scalpel in PBS, incubated for 10min in PBS containing 1% formaldehyde, then 5min in PBS containing 125mM Glycine. Aliquots used for RNAPII immunoprecipitation were fixed a second time with Disuccinimidyl glutarate (DSG) diluted to 2mM in PBS for 40min at room temperature, as previously described (Tian et al., 2012). Tissues were then dissociated with a MACS dissociator using the muscle-specific program.

Resuspended material was incubated on ice 5min in 1mL of chilled buffer A (0.25% TRITON, 10 mM TRIS pH8, 10mM EDTA, 0.5mM EGTA), 30min in 1mL of buffer B (250mM NaCl, 50mM TRIS pH8, 1mM EDTA, 0.5mM EGTA), and then resuspended in 100 to 200 μ L of buffer C (1% SDS, 10mM TRIS pH8, 1mM EDTA, 0.5mM EGTA) at room temperature. All buffers were extemporately supplemented by Complete protease and PhosSTOP phosphatase inhibitors (Roche). Cell suspensions in 0.6mL μ tube were sonicated in water bath at 4°C during 15min (15sec. ON, 15sec. OFF) with a Bioruptor apparatus (Diagenode) setted on high power and then clarified by 10min centrifugation at 10 000rpm, 4°C. Shearing of the DNA was checked after reversing the crosslinking on agarose gel electrophoresis to be around 300-500bp. Sheared chromatin was quantified by optical density (260nm) and diluted 10-fold in IP buffer to final concentrations: 1% TRITON, 0.1% NaDeoxycholate, 0.1% SDS, 150mM NaCl, 10mM TRIS pH8, 1mM EDTA, 0.5mM EGTA, 1X protease and phosphatase inhibitors). 15 μ g of chromatin and 2 μ g of antibodies, in a final volume of 500 μ L, were incubated at 4°C for 16h on a wheel. 25 μ L of saturated magnetic beads coupled to protein G (Dynabeads) were used to recover the immunocomplexes. After 2h of incubation the bound complexes were washed extensively 5min at room temperature on a wheel in the following wash buffers: WBI (1% TRITON, 0.1% NaDOC, 150mM NaCl, 10mM TRIS pH8), WBII (1% TRITON, 1% NaDOC, 150mM KCl, 10mM TRIS pH8), WBIII (0.5% TRITON, 0.1% NaDOC, 100mM NaCl, 10mM TRIS pH8), WBIV (0.5% Igepal CA630 (Sigma), 0.5% NaDOC, 250mM LiCl, 10mM TRIS pH8, 1mM EDTA), WBV (0.1% Igepal, 150mM NaCl, 20mM TRIS pH8, 1mM EDTA), WBVI (0.001% Igepal, 10mM TRIS pH8). 20 μ g of sheared chromatin used as input and ChIP beads were then boiled 10min in 100 μ L H₂O containing 10% (V/W) chelex resin (BioRad), followed by Proteinase K (0.5mg/mL)-digestion for 30min at 55°C, and then finally incubated 10min at 100°C. 1 μ L of ChIP eluate was used for qPCR assays in 10 μ L reactions with Brilliant III Ultra Fast SYBR-Green Mix (Agilent) using a

Stratagene MX3005p system. The analysis of qPCR was performed using the MxPro software. Primers are listed in **Table S1**.

Immunoblotting

Approximately 500µm of muscle cryosections from frozen muscle were homogenized with a Dounce homogenizer protein extraction buffer containing 50mM Tris-HCl, pH 7.4, 100mM NaCl, 0,5% NP40, with Halt Protease and Phosphatase inhibitor cocktail (78440, ThermoFisher Scientific). Samples were then centrifuged for 10min at 1500g at 4°C and supernatants were collected. Protein concentration was determined by Bradford assay (ThermoFisher Scientific). Samples were denatured at room temperature for 30 min (Ca_vβ1 proteins), or at 95°C for 5min (all other proteins), with Laemmli buffer with 5% βmercaptoethanol. Proteins were separated by electrophoresis (Nu-PAGE 4–12% Bis-Tris gel; Life Technologies) and then transferred to nitrocellulose membranes (GE Healthcare). Membranes were blocked with 5% BSA (Ca_vβ1 proteins) or 5% milk (all other proteins) and incubated overnight at 4°C with primary antibodies (listed in **Table S3**) diluted in the blocking buffer. Membranes were then labelled with fluorescent secondary antibodies (listed in **Table S4**) diluted in blocking buffer for 1h in the dark. Images were acquired with camera LAS4000 (GE Healthcare). Western blot image analysis was performed with the public domain software ImageJ (analyze gel tool).

Immunofluorescence and image acquisition – muscle cryosections

Immunofluorescence procedures were performed on 10µm muscles cryosections fixed on glass slides and stored at -80°C. Slides were rehydrated in PBS, fixed with PFA 4% for 10 min, permeabilized with 0.5% Triton X-100 (Sigma-Aldrich) and blocked in PBS with 4% bovine serum albumin, 0.1% Triton X-100 for 1h. Sections were incubated in PBS with 2% BSA, 0.1% Triton X-100 with primary antibodies (listed in **Table S3**) overnight at 4°C. Aspecific sites were blocked with BSA 5% 1h and slides were incubated for 1h with secondary antibodies (listed in **Table S4**) and incubated 5min with 4',6'-diamidino-2-phenylindole (DAPI) for nuclear staining and mounted in Fluoromount (Southern Biotech).

Immunofluorescence and image acquisition – muscle fibers

TA muscles were collected, rinsed once in PBS and fixed in a PBS 4% PFA solution at room temperature for 1 hour. Groups of approximately 10 muscle fibers were gently dissected and incubated overnight in PBS with 0.1M glycine at 4°C with mild shaking. The next day, after a day of washing in PBS 0.5% Triton X-100, fibers were incubated in permeabilized and blocked for 6 hours in PBS 3% BSA 5% goat serum 1% Triton X-100 at room temperature. Fibers were incubated with primary antibodies (**Table S3**) at 4°C over weekend in blocking solution. Fibers were then rinsed for several hours at room temperature, in PBS 0.5% Triton X-100 and incubated overnight at 4°C with secondary antibodies (**Table S4**) and α-Bungarotoxin-Alexa Fluor conjugated-594 (**Table S3**) in blocking solution. Finally, after

a day of washing in PBS 0.5% Triton X-100, fibers were mounted on slides in non-hardening Vectashield mounting medium (H-1000, Vector Laboratories).

NMJ images were acquired with Zeiss Axio Observer microscope coupled with apotome module (63x objective) and edited with Zeiss Zen Lite 3.7 software. The same laser power and setting of parameters were used throughout to ensure comparability. The images presented were single projected images obtained by overlaying sets of collected z-stacks. NMJ morphometric analysis was performed on confocal z-stack projections of individual NMJs by using ImageJ-based workflow adapted from NMJ-morph1. At least 100 NMJs have been analyzed per condition. NMJ morphometric analysis was performed in a blinded manner by the same investigator.

Immunofluorescence and image acquisition – primary myotubes

For immunofluorescence analyses, primary myotubes were seeded and cultured in fluorodishes (Dutscher). Cells were fixed in 4% PFA for 10 min, permeabilized with PBS 5% Triton X-100. Aspecific sites were blocked with BSA 1% and goat serum 10% for 30 min. Cells were incubated with primary antibodies (listed in **Table S3**) overnight at 4°C in PBS 0.1% saponin 1% BSA. Cells were washed three times and then incubated with secondary antibodies (listed in **Table S4**) and DAPI (1:10 000) for 1h in the dark.

Fluorescence images of myotubes were acquired Spinning Disk confocal scanner unit (CSU-W1 YOKOGAWA) with a 40x oil-immersion objective (plan fluor 40x/1.3 oil OFN25 DIC N2 cyan), coupled with a Photometrics PRIM 95B Camera. Software used was MetaMorph 7.10.2. Image analyses and quantification of AChR clusters size and distribution were performed with the public domain software ImageJ by using a macro developed in the lab by MyoImage facility.

Statistical analyses

Comparison between two groups was tested for normality using Shapiro-Wilk test followed by parametric (two-tailed paired, unpaired Student's t-tests) or non-parametric test (Mann-Whitney) to calculate p-values. For comparison of more than two groups, ordinary one or two-ways ANOVA tests followed by appropriated post hoc tests were performed. All statistical analyses were performed with GraphPad Prism 8 or 9 software and statistical significance was set at $p < 0.05$.

RESULTS

Identification of a new Ca_vβ1 isoform in adult denervated and in embryonic skeletal muscles

The first description of the *Cacnb1E* embryonic isoform emerged from RT-PCR and genome-wide transcriptomic analysis (Traoré et al., 2019). This research revealed modulation of *Cacnb1* expression at the exon level. However, the existence of several unidentified isoforms sharing the same exons, adds complexity to the interpretation of the results. To address this issue, we used Nanopore sequencing (Mulroney, 2020) in adult muscle to delineate the full-length *Cacnb1* transcripts. The visualization of the high-quality aligned nanopore reads revealed the vast diversity of *Cacnb1* transcript variants, but with one major isoform per transcription unit (TU) (**Fig 1A**): more than 94% of the transcripts of the TU#1, ranging from exon1 to exon14 corresponds to *Cacnb1E* isoform and more than 83% of the transcripts of the TU#2, ranging from exon2B to exon13end corresponds to *Cacnb1D* isoform. The examination of the TU#3, ranging from exon1 to exon13end revealed that more than 93% of the transcripts of this TU corresponds to *Cacnb1A* (**Fig 1A**). It should be noted that these percentages represent the predominance of each isoform within their respective transcriptional units, not their overall abundance in the muscle. We validated these data by performing RT-PCR analyses of full-length transcripts and confirmed that these three transcripts were expressed in adult mouse muscle and that the expression of both *Cacnb1A* and *Cacnb1E* significantly increased in denervated muscle (*Cacnb1A*: P=0.0041; *Cacnb1E*: P=0.0001), while *Cacnb1D* decreased (**Fig 1B**). When we analyzed Ca_vβ1 proteins expression by western blot, using a custom antibody specific to Ca_vβD and A variants (exon 13end epitope). We found increased expression of a 58kDa band, corresponding to Ca_vβ1A, in denervated muscle, while the 53kDa band, corresponding to the Ca_vβ1D, did not change in the different conditions (**Fig 1C**). We could not assess Ca_vβ1E expression at protein levels due to technical limitations.

Given the same expression profile of *Cacnb1A* and *Cacnb1E* transcripts in denervated adult muscle, we wondered whether the newly identified *Cacnb1A* might be an embryonic isoform, similarly to *Cacnb1E* (Traoré et al., 2019). By amplifying full-length transcripts of *Cacnb1A*, *E* and *D* and assessing Ca_vβ1 protein levels by western blot, in embryonic muscles, we observed the appearance of *Cacnb1D* transcript and Ca_vβ1D protein during the later stages of embryogenesis to be fully expressed in adult as expected (**Fig 1D,E**). Additionally, both *Cacnb1A* and *E* transcripts are present during embryogenesis (**Fig 1D**) with Ca_vβ1A protein also being expressed, yet mainly at P0 (**Fig 1E**).

Overall, our results revealed that *Cacnb1A*, and not only *Cacnb1E* transcript are expressed in mouse skeletal muscle during embryogenesis and increased after nerve damage, with Ca_vβ1A protein

following this pattern. Taken together, this underlines the complexity of Cav β 1 isoforms and intrigued about the specific role of each of these Cav β 1 proteins in skeletal muscle physiology.

Molecular mechanisms implicated in the expression of *Cacnb1* isoforms in embryonic and adult muscles

To further investigate the transition of embryonic versus adult Cav β 1 isoforms, we performed triplex RT-PCR analyses to investigate the kinetic of exon2B inclusion characterizing the adult *Cacnb1D* isoform versus exon2A, identifying the embryonic *Cacnb1A/E* variants. As expected, we observed that exon2A was present from E12.5, while exon2B expression increased perinatally and was highly expressed in adult muscle (**Fig 2A**). We wondered if *Cacnb1D* and *Cacnb1A/E* expressions might be orchestrated by the activation of distinct promoters in embryonic and in adult muscles. Nanopore sequencing revealed that the mRNAs starting at exon1 were never associated with exon2B (**Fig S1**). This suggests that the expression of exon2B may be exclusively triggered by a promoter located within this exon. To validate this hypothesis, we performed an *in silico* analysis (ENCODE project, UCSC Genome browser) of ChIPseq signals of methylation marks and RNA-Polymerase II occupancy on mouse *Cacnb1* gene in embryonic muscles compared to adult hind limb muscles. We found that methylation marks H3K4me3, H3K9ac and H3K27ac, characteristic of active promoters (Igolkina et al., 2019), were mostly located at exon1 in E12.5 mouse muscle, while H3K27ac was mainly located at exon2B in three different adult mouse hind limb muscles (**Fig 2B**). In addition, RNA-Polymerase II was strongly recruited at *Cacnb1* exon1 in E12.5 mouse muscle and at exon2B in adult mouse muscle (**Fig 2B**), suggesting a transcription initiation site (Wang et al., 1992). Together, these data strongly suggest that distinct promoters are used for the expression of embryonic (Prom1) versus adult (Prom2) *Cacnb1* isoforms.

We wondered if the innervation status in adult muscle could affect the activity of *Cacnb1* promoters, therefore modulating the expression of *Cacnb1* isoforms. We found that the percentage of exon2B inclusion was higher in innervated and decreased in denervated muscles whereas exon1 inclusion was very low in innervated and increased significantly in denervated muscle RNA extracts (**Fig 2C**). To evaluate the activity of the putative specific promoters, we performed a ChIP-PCR analysis on *Cacnb1* gene. We observed a reduction in epigenetic marks of active promoters (H3K4me3 and H3K9ac) at Prom2 site, while these marks were enriched around Prom1 following denervation. Accordingly, the quantification of RNA-Polymerase II recruitment displayed increased enzyme's occupancy around

Prom1 and decreased enzyme's occupancy at Prom2 site in denervated compared to innervated muscles (**Fig 2D**).

Overall, our results show that *Cacnb1* isoform transition from embryonic to adult isoforms is regulated by the activation of two distinct promoters. Furthermore, we demonstrate that adult skeletal muscle restores the embryonic epigenetic program in *Cacnb1* gene after nerve damage, suggesting a role for *Cacnb1* in the compensatory mechanisms aiming at recovering a proper innervation status and potentially in other event associated to neuromuscular physiology.

Role of embryonic Ca_vβ1 isoforms in AChR clustering

The adaptation of *Cacnb1* isoforms expression to the innervation state of the muscle, in embryonic and in adult stages, raised the question on the specific role of the different variants in the formation, maturation and maintenance of NMJ.

We investigated the role of embryonic *Cacnb1* isoforms in agrin-mediated AChR clustering in highly differentiated primary myotubes (Pęziński et al., 2020) by downregulating these isoforms using shRNA tool, referred to as shEx2A (**Fig 3A**). After validating Ca_vβ1 embryonic isoforms downregulation (**Fig 3A, Fig S2A**), we observed that their absence had no effect on AChR aggregation capacity, showed by a similar number of AChR clusters per myofiber surface compared to the control condition (**Fig 3B,C**). However, it did induce a significant increase in AChR cluster size, with a mean fold increase of 2.93 (**Fig 3B,C**). Additionally, we observed an increased distance between AChR aggregates and the nearest nuclei, suggesting that embryonic Ca_vβ1 isoforms may play a role in positioning the future sub-synaptic nuclei (**Fig 3B,C**). To identify the mechanisms responsible for these *in vitro* AChR clustering abnormalities, we measured protein expression of AChR subunits as well as key players in AChR formation including MuSK, Dok7 and Rapsyn. Although we did not observe a significant increase in AChRα1 protein, we did find an elevated MuSK expression in shEx2A myotubes compared to controls (**Fig 3D**), suggesting a possible enhancement of the molecular pathway associated with AChR aggregation. Lrp4, Dok7 and Rapsyn protein levels were unchanged under shEx2A treatment, indicating that these proteins were not implicated in the observed alteration of AChR clustering (**Fig S2B**).

Then, we investigated the potential role of embryonic *Cacnb1* isoforms on the myogenic differentiation process. Despite increased myogenin expression (**Fig S2C**), we measured a significantly increase in MyHC3, MyHC8 and MCK mRNA expressions ($p=0.0318$, $p=0.027$ and $p=0.0203$ respectively) (**Fig 3E**),

as well as an elevated MF20 protein expression levels in shEx2A myotubes compared to controls (**Fig 3E**). In addition, adult *Cacnb1D* expression was also increased (**Fig S2D**), suggesting that myogenic maturation was aberrantly accelerated in the absence of embryonic *Cacnb1* isoforms, corroborated by the increased width of shEx2A treated myotubes compared to controls (**Fig S2E**). These results suggest that embryonic $\text{Ca}_v\beta 1$ isoforms are needed not only to modulate the first phases of myogenesis, as previously shown (Taylor et al., 2014), but also to ensure the coordinated terminal muscle cell differentiation and AChR aggregation.

Embryonic $\text{Ca}_v\beta 1$ isoforms in post-natal NMJ maturation and maintenance

The presence of embryonic $\text{Ca}_v\beta 1A$ isoform expressed post-natally until at least P14 (**Fig 4A**), suggests a possible involvement in NMJ postnatal maturation. To investigate embryonic $\text{Ca}_v\beta 1$ s role in this process, we downregulated their expression using the same shEx2A treatment in the lower limbs of 7 days-old pups (**Fig 4B**), and analysed NMJ morphology 21 days later, in 1 month old mice, when endplates are usually mature (Tintignac et al., 2015). We quantified NMJ morphological parameters and found that the perimeter and area of both pre- and post-synaptic regions were significantly reduced upon embryonic *Cacnb1* depletion compared to controls (**Fig 4C,D,E**). Additionally, the size of synaptic contact and the overlap between nerve terminals and post-synaptic apparatus were reduced (**Fig 4C,F**). Furthermore, a significant NMJ fragmentation was observed (**Fig 4G**) upon embryonic $\text{Ca}_v\beta 1$ downregulation. Although NMJ morphology appeared strikingly altered, we did not measure changes in *AChRa1* or *Dok7* transcripts (**Fig S3A**) nor protein levels (**Fig S3B**) but we observed an increase in MuSK protein (**Fig 4H**). Overall, these observations suggest that compensatory mechanisms aiming at counteract the NMJ alterations, are just being initiated like indicated by MuSK increased levels, a key player in agrin/Lrp4/MuSK signalling required for the transcription of NMJ player genes in sub-synaptic nuclei.

To better understand if embryonic $\text{Ca}_v\beta 1$ isoforms may play a role in the stabilization of nerve-muscle synapses once they are completely formed and mature, we disrupted their expression in the Tibialis Anterior (TA) of adult mice via the same AAV-shEx2A tool (**Fig 5A**). We then analysed functional and molecular readouts of NMJ features 12 weeks post-injection. Force generation, whether by direct (muscle) indirect (nerve) stimulation, was not affected by the ablation of embryonic $\text{Ca}_v\beta 1$ proteins (**Fig 5B**). The neuromuscular connectivity, as measured by compound muscle activity potential (CMAP) decrement in electroneuromyogram (ENMG) analysis, remained unchanged as well (**Fig 5B**). However, while *Lrp4* and *Rapsyn* expressions remains unmodulated (**Fig 5C**), there was a significant increase in

AChRa1, *AChR γ* subunits, and *Musk* expressions (**Fig 5D**). This suggests an alteration in the signalling pathways involved in the maintenance of AChR below the nerve terminal (Li et al., 2018).

Altogether, these data suggest that embryonic Ca ν β 1 isoforms are involved in NMJ formation, the maturation of the post-synaptic apparatus at early developmental stages and in NMJ maintenance in adult muscles.

DISCUSSION

Neuromuscular system plays a vital role for all vertebrates. Its proper development, maturation and maintenance are strictly regulated processes requiring a multitude of mechanisms not yet completely elucidated. In this context, it has been described some years ago, that a component of ECC machinery, $\text{Ca}_v\beta 1$, the regulatory subunit of muscle Voltage-gated Ca^{2+} channel encoded by the *Cacnb1* gene, was essential in the formation of nerve-muscle patterning during embryonic development (Chen et al., 2011). In a further study this protein has been demonstrated as having transcription factor properties in muscle precursor cells (Taylor et al., 2014). More recently, two $\text{Ca}_v\beta 1$ skeletal muscle isoforms have been identified by our team: $\text{Ca}_v\beta 1\text{D}$, defined as the adult constitutive isoform, and $\text{Ca}_v\beta 1\text{E}$, defined as an embryonic isoform with a role in limiting muscle mass loss after denervation and during aging (Traoré et al., 2019).

Here, we aimed to further characterize $\text{Ca}_v\beta 1$ variants, investigate the mechanisms behind the regulation of their expression, and understand their role in the formation, maturation and stability of neuromuscular system.

Using Nanopore sequencing as innovative and powerful exploring technology, we have identified $\text{Ca}_v\beta 1\text{A}$ as an additional embryonic isoform, rising further questions about the role of multiple $\text{Ca}_v\beta 1$ variants during development and for skeletal muscle homeostasis.

Investigating the mechanisms regulating the differential expression of $\text{Ca}_v\beta 1$ proteins, we have discovered that adult and embryonic isoforms are expressed through the activation of two promoters located in exon1 (Prom1) and exon2B (Prom2), which are regulated differently during development. We have demonstrated that Prom1 is active during embryogenesis, while Prom2 is active in mature adult muscle, perinatal stages marking a period of transition between the activation of these two promoters. In addition, we have shown that, in adult muscle, nerve damage leads to the restoration of the embryonic epigenetic program of *Cacnb1* promoters. These evidences shed light on the molecular events behind $\text{Ca}_v\beta 1$ modulation and open new hypotheses on other upstream factors potentially implicated in the fine tuning of their epigenetic program.

To gain insights into transcription factors binding at these promoter regions and potentially regulating them, we used the UCSC Genome Browser, an online software allowing comprehensive visualization and analysis of genomic data, including features like transcription factors binding sites. Among the wide range of transcription factors potentially binding to Prom1 and Prom2 regions, some could be relevant to skeletal muscle tissue. Indeed, myogenin presents binding sites in both Prom1 and Prom2

regions, this muscle-specific transcription factor is known to promote transcription of muscle-specific target genes and especially in genes important for myogenesis and AChR clustering (Tang et al., 2006; Tang and Goldman, 2006). The factor BRD4, potentially binding Prom2 region, is known to act as a regulator of catabolic genes in skeletal muscle, and regulating myogenesis by impairing myogenic differentiation (Segatto et al., 2017; Yang et al., 2022). KDM1A (or LSD1), potentially binding Prom1, also presents beneficial effect on muscle regeneration and recovery after injury by regulating key myogenic transcription factor genes (Tosic et al., 2018). And lastly, MEF2A, potentially binding Prom2, belongs to MEF2 transcription factor family, working in concert with MyoD to regulate muscle gene transcription. More investigations are needed to decipher the factors involved in such promoter activity regulation.

Together with these analyses we also investigated on the role of $Ca_v\beta 1$ on the different stages on NMJ formation, maturation and stability. As mentioned, previous study demonstrated that genetically ablated *Cacnb1* mice exhibited muscle patterning defects and aberrant innervation at E14.5 and E18.5 in mice. However, to really conclude with pre-patterning defects, it would have been more accurate to look at the aspect of AChR clustering before axonal growth cone arrival around E14.5. By working on aneural myotubes *in vitro*, we found increased AChR clusters sizes and precocious myotube maturation, which align with Chen and colleagues' post-innervation results, which showed increased endplate areas and more perforated clusters, indicative of a precocious maturation. Our results suggest that the defects observed in their study originate from abnormalities occurring before innervation begins. However, it cannot be excluded that the observed defects are modified or amplified by nerve-derived factors.

We can connect the increase in MuSK levels with the increase in AChR clusters size that we observed, through a possible effect on LRP4 or through an independent pathway (Mazhar and Herbst, 2012). This increased MuSK level could result from a transcriptional effect of myogenin (Tang and Goldman, 2006), which has been shown as negatively regulated by $Ca_v\beta 1$ proteins (Taylor et al., 2014).

Furthermore, the size of AChR clusters could be modulated by the level of myotube maturation independently of a MuSK effect. We observed precocious maturation of myotubes and one possibility is that AChR clusters enlarged due to increased myotube width, perhaps through a mechanical effect.

In this study, we observed alterations in NMJ morphology of 1-month old pups in which $Ca_v\beta 1A/E$ were ablated. The observed defects could be due to alterations in maturation, maintenance, or a combination of both and distinguishing between these two processes is very challenging.

Given the increased muscle maturation observed under ablation of embryonic/perinatal $\text{Ca}_v\beta 1$ isoforms in our model, NMJ fragmentation might be a mechanism to extend as the muscle matures precociously. Indeed, the link between NMJ fragmentation and degeneration should not be systematic and some studies suggest that endplate fragmentation could also be a sign of regeneration, as a process of synaptic plasticity aimed at extending synaptic area (Haddix et al., 2018; Li et al., 2011; Slater, 2020).

Alterations of NMJ are also observed in other conditions as in aging muscles, where $\text{Ca}_v\beta 1A/E$ expressions are defective (Traoré et al., 2019). Indeed, postsynaptic fragmentation, reduced AChR density and synaptic decoupling are reported during aging (Valdez et al., 2012), but these age-related NMJ morphological abnormalities precedes changes in NMJ molecular markers expression (Massiré et al., 2024). Therefore, the fact that we do not observe a global alteration in NMJ actors despite NMJ morphological alteration is not necessarily surprising. Moreover, the increased MuSK protein, which activation is known to induce transcription of key NMJ genes in sub-synaptic nuclei might be the mark of the initiation of such process and we may observe a wider modulation of NMJ actors after longer periods of treatment. This adult model would require further deep analyses to study NMJ molecular actors and morphological aspect, that we suppose to align with the natural aging progression in mice, like the post-natal *in vivo* shEx2A model do. Globally, we can presume that downregulating $\text{Ca}_v\beta 1A/E$ isoforms in skeletal muscle reproduce neuromuscular aging features.

As remaining consideration, in this study, we examined the effects of downregulating both $\text{Ca}_v\beta 1A$ and $\text{Ca}_v\beta 1E$ isoforms on distinct NMJ specific stages. It would be of high relevance to give precision on which of $\text{Ca}_v\beta 1A$ or $\text{Ca}_v\beta 1E$ isoform is responsible for the observed effects.

Overall, in this study we highlighted molecular and functional aspects of $\text{Ca}_v\beta 1s$ as molecular players involved in the neuromuscular system formation, maturation and maintenance. Further investigations are needed to give additional insights on their relevance for skeletal muscle physiology and pathophysiology.

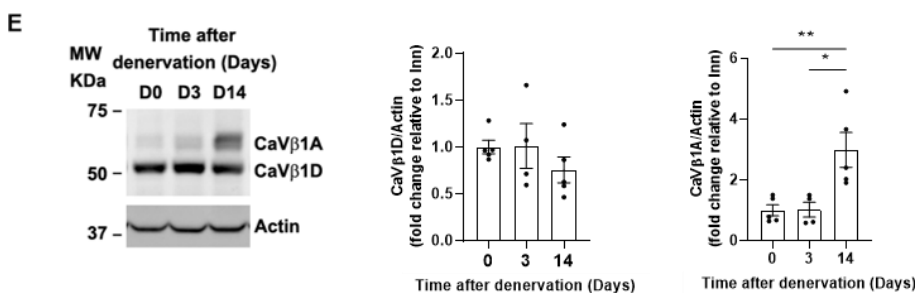
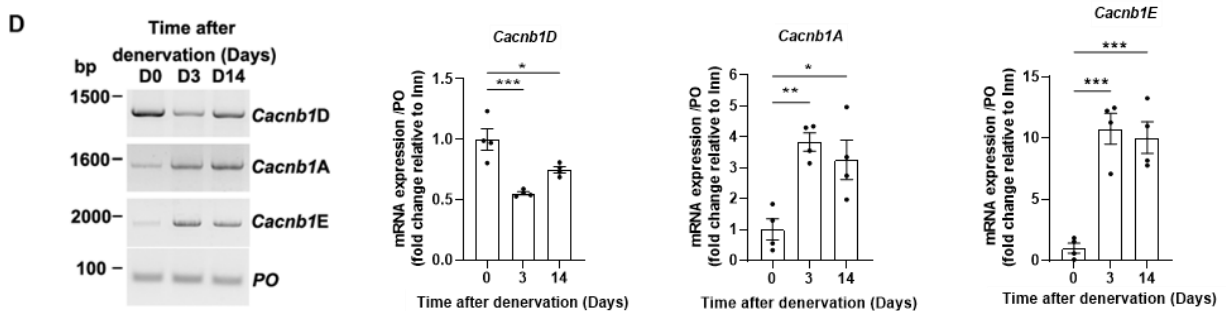
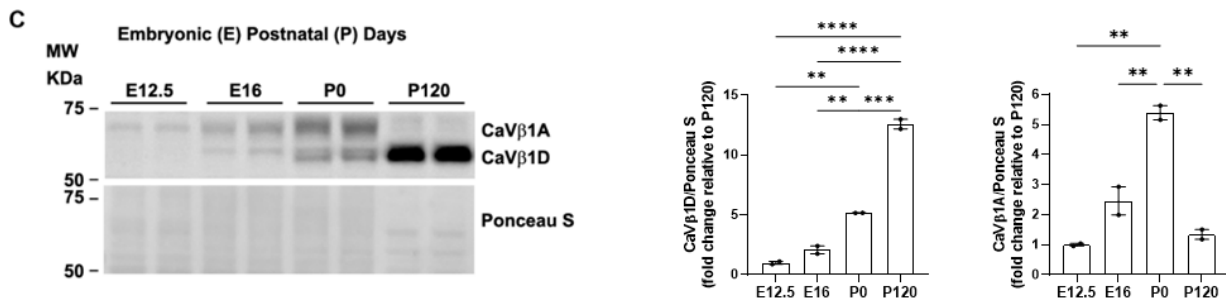
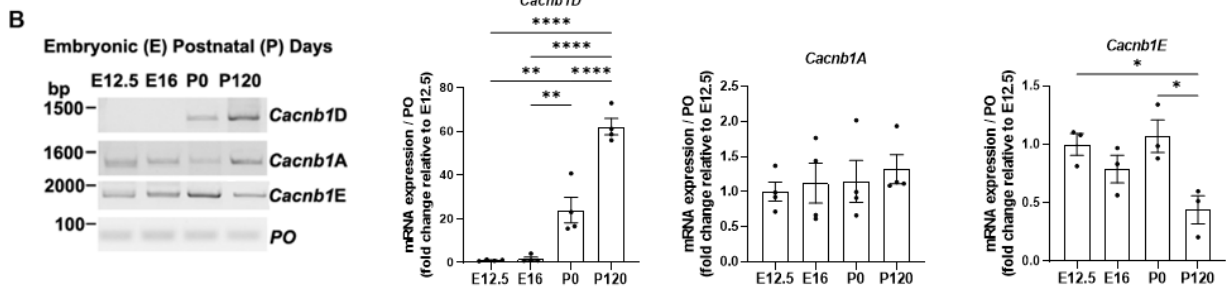
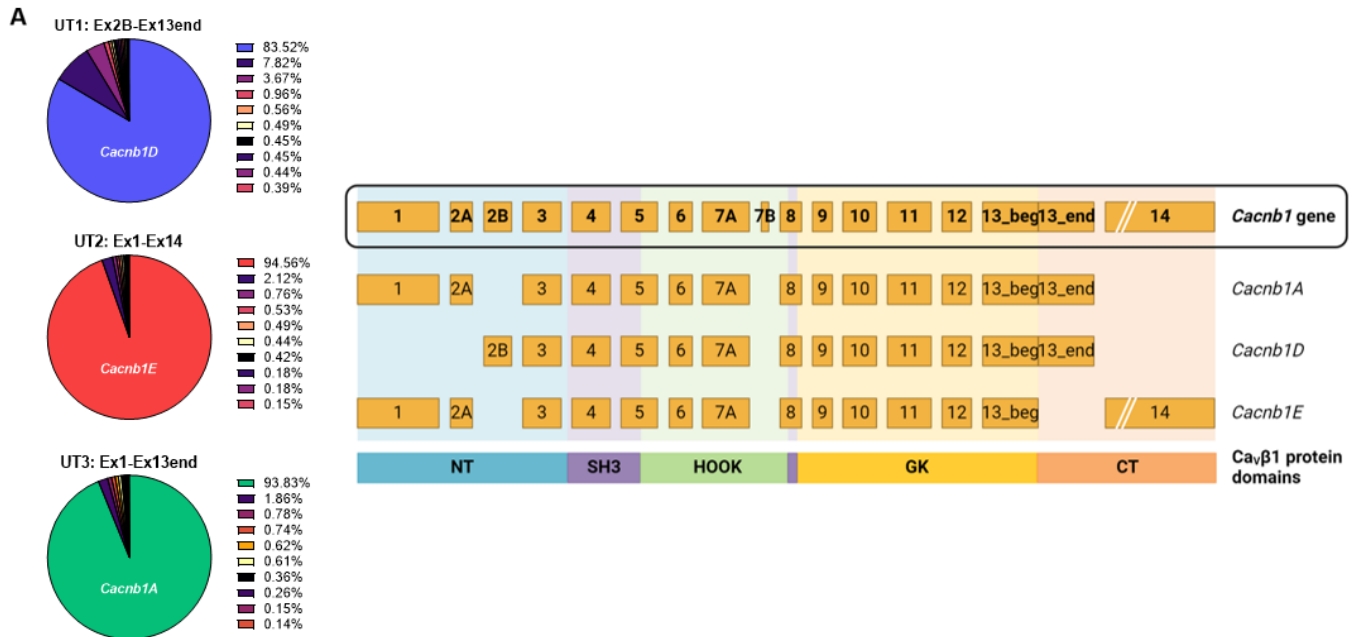
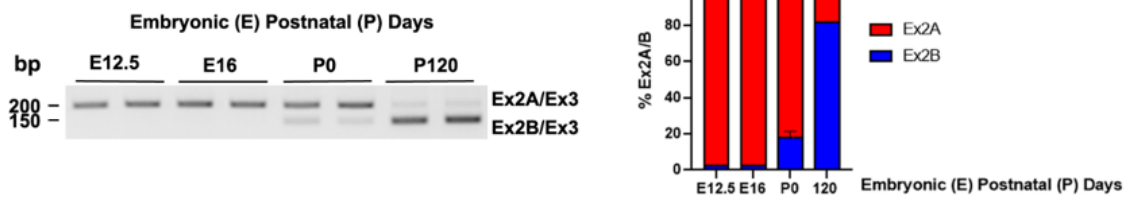
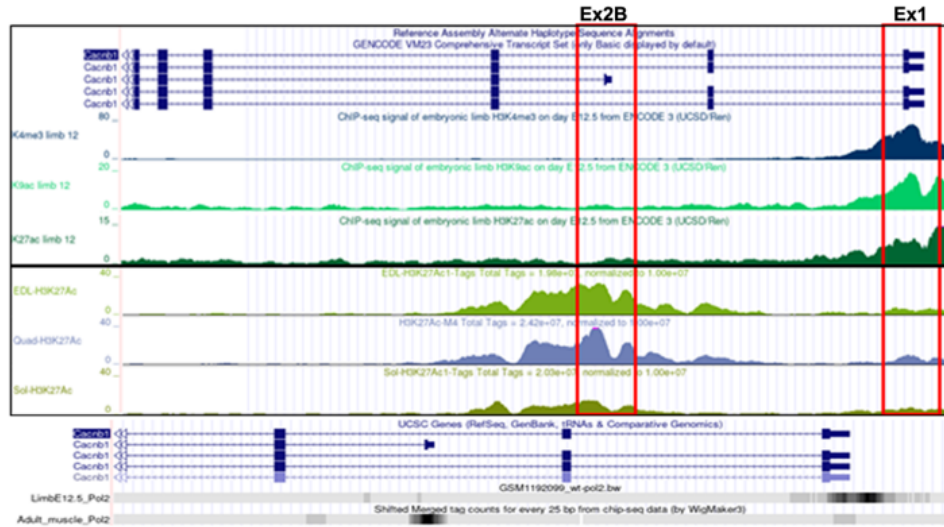


Figure 1. Identification of a new Cavβ1 isoform in embryonic muscles. **A.** Full-length sequencing of *Cacnb1* transcript through Nanopore technology led to the identification of one major isoform per TU: *Cacnb1D*, *Cacnb1E* and *Cacnb1A*. *Cacnb1* gene and skeletal muscle transcript variants as well as the corresponding protein domains are represented. **B.** RT-PCR and quantification of the three full-length *Cacnb1* variants in innervated (D0) TA muscles or after the indicated number of days of denervation. PO was the loading control. **C.** Western Blot and quantification of Cavβ1A and Cavβ1D in innervated (D0) or after the indicated number of days of denervation. Actin was the loading control. **D.** RT-PCR and quantification of the three full-length *Cacnb1* variants in embryonic muscles and adult TA muscles. PO was the loading control. **E.** Western Blot and quantification of Cavβ1A and Cavβ1D in embryonic muscles and adult TA muscles. Actin was the loading control. All data are mean ± SEM (* $P < 0.05$, ** $P < 0.01$, *** $P < 0.001$). P values were calculated by ordinary one-way ANOVA followed by Tukey's multiple comparison test.

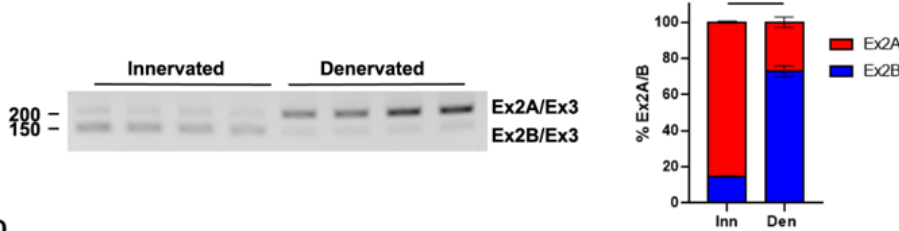
A



B



C



D

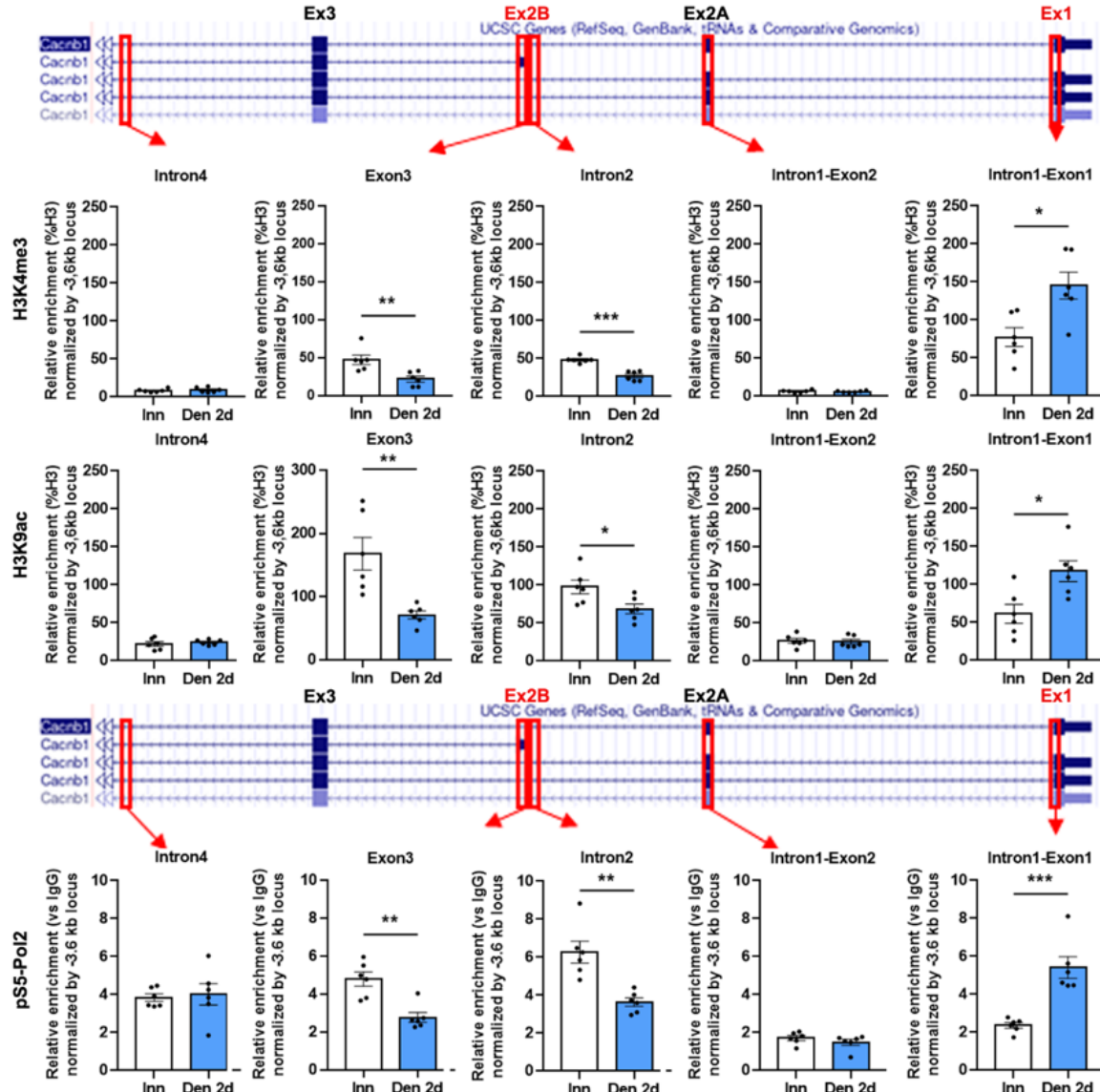


Figure 2. Two distinct promoters drive the expression of *Cacnb1* isoforms in skeletal muscle. A. Triplex RT-PCR and quantification of the percentage of exon2A versus exon2B inclusion in embryonic and adult TA muscles. **B.** Visualization of epigenetic marks and RNA Polymerase II at *Cacnb1* promoters using UCSC Genome Browser. Image displaying the location of activating epigenetic marks (H3K3me3, H3K9ac and H3K27ac) and RNA Polymerase II occupancy at Prom1 and Prom2 in either embryonic (E12.5) muscles (ENCODE project) or adult muscles (Extensor digitorum longus (EDL), Quadriceps and Soleus). **C.** Triplex RT-PCR and quantification of the percentage of exon2A versus exon2B inclusion in innervated and 3-days denervated adult TA muscles. **D.** Chromatin immunoprecipitation (ChIP) followed by PCR analysis showing the presence of activating epigenetic marks (H3K3me3, H3K9ac and H3K27ac) and RNA Polymerase II occupancy at Prom1 and Prom2 in in innervated and 2-days denervated adult TA/Gas muscles. All data are mean \pm SEM (* $P < 0.05$, ** $P < 0.01$, *** $P < 0.001$). P values were calculated by ordinary one-way ANOVA followed by Tukey's multiple comparison test (**A**) or unpaired t-test (**C,D**).

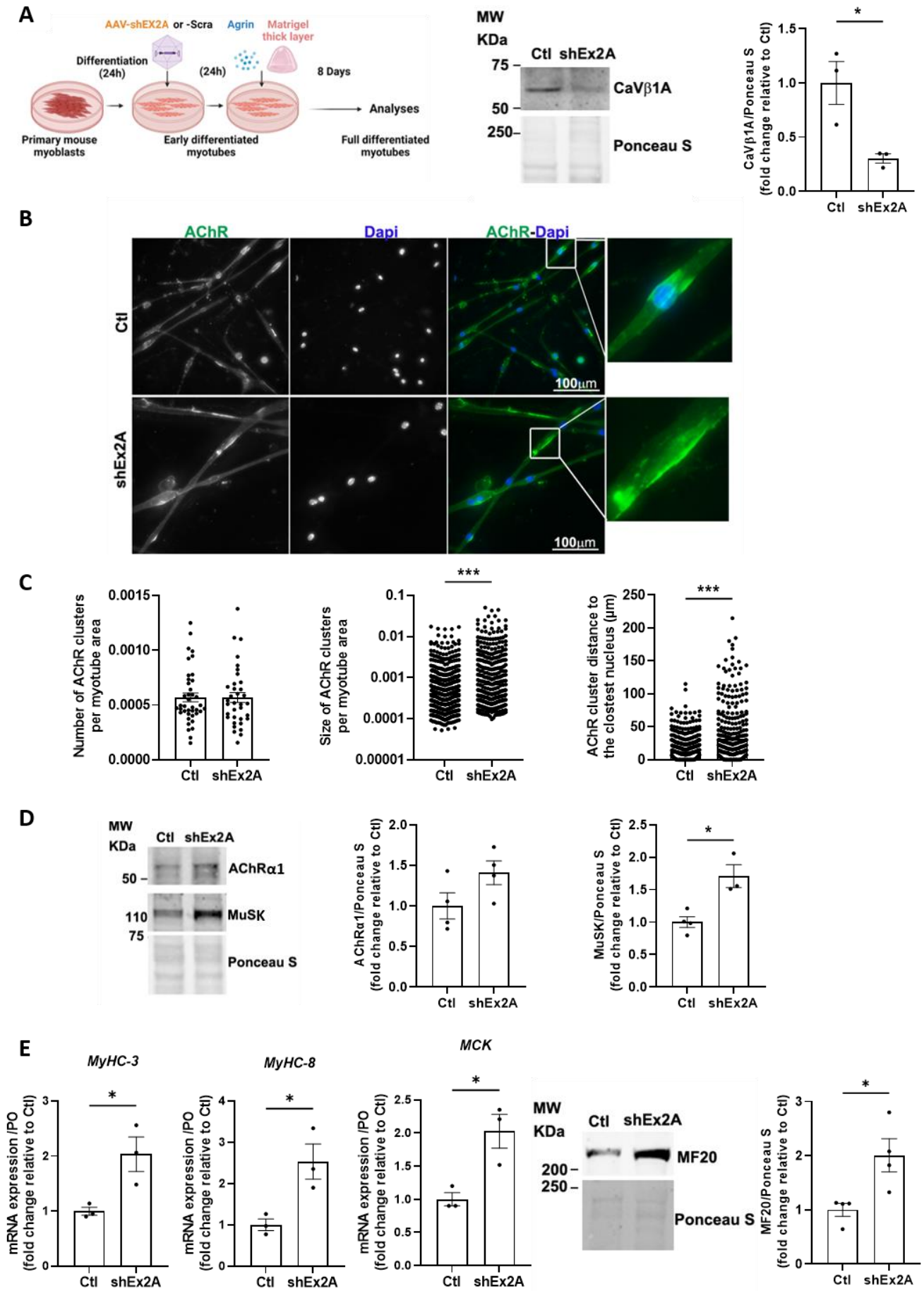


Figure 3. Downregulation of embryonic $\text{Ca}_v\beta 1$ isoforms induces bigger AChR aggregates and myotube precocious maturation in an *in vitro* model of highly differentiated myotubes. **A.** Schematic representation of the experimental protocol. Western Blot and quantification of $\text{Ca}_v\beta 1\text{A}$ in control and shEx2A treated myotubes. **B.** Immunofluorescence (IF) images of control or shEx2A treated myotubes stained with AChRa1 (green) and DAPI (blue). **C.** Quantification of AChR clusters number and size per myotube area and distance between AChR clusters and the nearest nuclei. **D.** Western Blot and quantification of AChRa1 and MuSK in control and shEx2A treated myotubes. **E.** RT-qPCR of *MyHC3*, *MyHC8* and *MCK* in control and shEx2A treated myotubes. Western Blot and quantification of MF20 in control and shEx2A treated myotubes. All data are mean \pm SEM (* $P < 0.05$, ** $P < 0.01$, *** $P < 0.001$). P values were calculated by unpaired t-test (**C,D**).

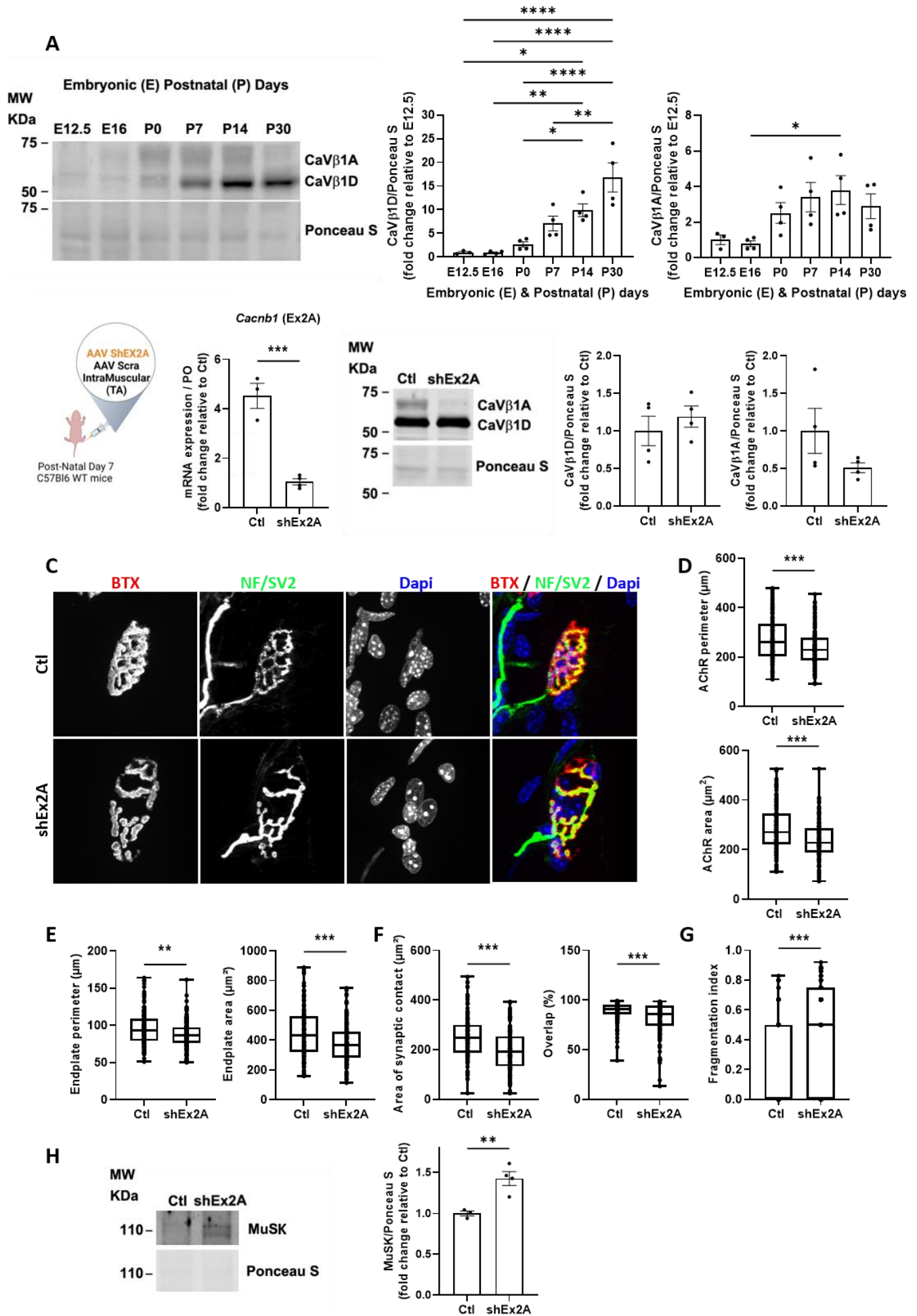


Figure 4. NMJ structural and molecular defects upon downregulation of embryonic $\text{Ca}_v\beta 1$ isoforms in TA muscles at postnatal stages. **A.** Western Blot and quantification of $\text{Ca}_v\beta 1\text{A}$ and $\text{Ca}_v\beta 1\text{D}$ in muscles at indicated embryonic and postnatal stages. **B.** Schematic representation of the experimental protocol. RT-qPCR of embryonic *Cacnb1* variants using primer in exon2A in control and shEx2A treated TA muscles, 3-weeks post-injection. Western Blot and quantification of $\text{Ca}_v\beta 1\text{A}$ and $\text{Ca}_v\beta 1\text{D}$ in control and shEx2A treated TA muscles, 3-weeks post-injection. **C.** Immunofluorescence (IF) images of control and shEx2A treated TA muscles, 3-weeks post-injection, stained with α -bungarotoxin (BTX) for AChR (red), neurofilaments and synaptophysin (green) and DAPI (blue). **D-G.** Quantification of NMJ morphology with perimeter and area of AChR (**D**) and endplate (**E**), area of synaptic contact and overlap between nerve terminals and post-synaptic apparatus (**F**) and fragmentation index (**G**). **H.** Western Blot and quantification of MuSK in control and shEx2A treated TA muscles, 3-weeks post-injection. All data are mean \pm SEM (* $P < 0.05$, ** $P < 0.01$, *** $P < 0.001$). P values were calculated by ordinary one-way ANOVA followed by Tukey's multiple comparison test (**A**) or unpaired t-test (**B,D-H**).

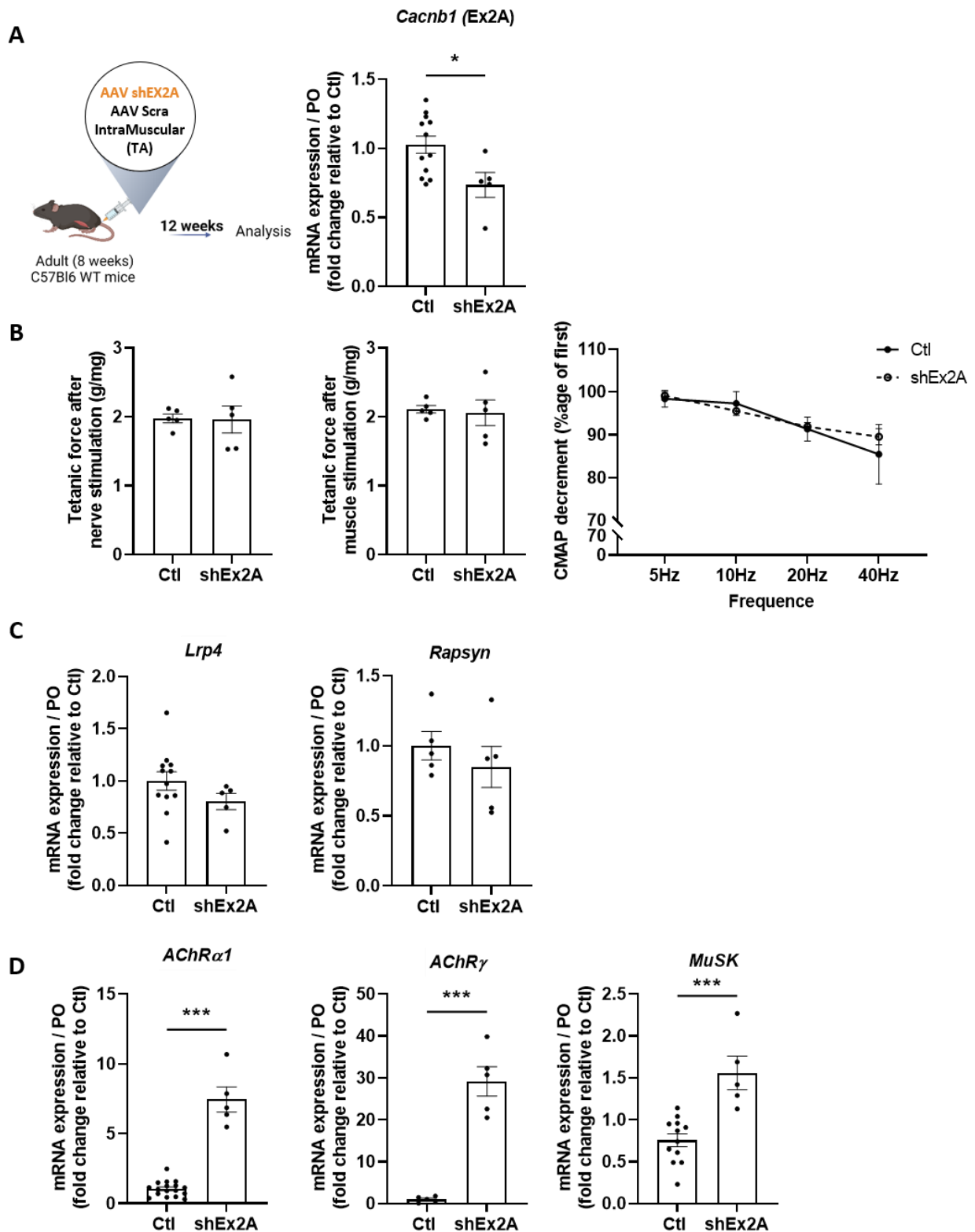
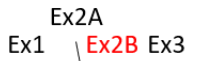


Figure 5. NMJ transcriptional and functional defects upon downregulation of embryonic $Ca_v\beta 1$ isoforms in adult TA muscles. **A.** Schematic representation of the experimental protocol. RT-qPCR of embryonic *Cacnb1* variants using primer in exon2A in control and shEx2A treated TA adult muscles, 12-weeks post-injection. **B.** Indirect (nerve) or direct (muscle) tetanic force measured in control and shEx2A treated TA adult muscles, 12-weeks post-injection. CMAP decrement measured by ENMG in

control and shEx2A treated TA adult muscles, 12-weeks post-injection. **C-D**. RT-qPCR of *Lrp4* and *Rapsyn* (**C**), and of *AChRa1*, *AChRg* and *MuSK* (**D**) in control and shEx2A treated TA adult muscles, 12-weeks post-injection. All data are mean \pm SEM (* $P < 0.05$, ** $P < 0.01$, *** $P < 0.001$). P values were calculated by unpaired t-test.



	TA inn	TA den	GAS inn	GAS den	Somme
	100,00	100,00	100,00	100,00	100,00
11000111111111111111	93,84	90,44	71,13	88,05	85,86
110001100000000001	0,00	0,00	10,43	0,10	2,63
110001111110111111	1,86	1,92	1,59	1,82	1,80
110000000000000011	0,00	0,01	6,72	0,06	1,70
110001100000001111	0,00	2,01	4,59	0,01	1,65
110001111011111111	0,78	1,26	0,62	0,97	0,91
110001000000000001	0,01	0,00	0,49	2,81	0,83
110001111101111111	0,61	0,78	0,68	0,85	0,73
110001110111111111	0,74	0,66	0,57	0,74	0,68
100001111111111111	0,62	0,43	0,49	0,49	0,51
110001111111111011	0,36	0,25	0,28	0,43	0,33
100000000000000001	0,26	0,54	0,35	0,11	0,31
110001000000000011	0,00	0,00	0,01	1,11	0,28
100000000000000011	0,00	0,00	0,69	0,02	0,18
110001111100000011	0,00	0,00	0,00	0,66	0,16
110000111111111111	0,14	0,16	0,15	0,19	0,16
110001100000000011	0,00	0,02	0,04	0,55	0,15
110001000111111111	0,00	0,01	0,52	0,01	0,14
110001111100111111	0,15	0,11	0,08	0,14	0,12
100000000000011111	0,00	0,41	0,01	0,00	0,10
110001111111011111	0,11	0,10	0,08	0,11	0,10
110001011111111111	0,09	0,12	0,09	0,11	0,10
110001101111111111	0,06	0,05	0,06	0,08	0,06
110001000000001111	0,00	0,22	0,01	0,00	0,06
110001100111111111	0,05	0,05	0,01	0,08	0,05
100001111110111111	0,05	0,06	0,03	0,02	0,04
110001111110011111	0,06	0,03	0,03	0,03	0,04
110001110110111111	0,04	0,03	0,02	0,04	0,03
110001111001111111	0,04	0,02	0,05	0,02	0,03
110001111111101111	0,02	0,04	0,03	0,04	0,03

0 = Exon absent / 1 = Exon present

Figure S1. *Cacnb1* exon2B is systematically excluded when exon1 is expressed. Long-read Nanopore sequencing data depicting exon presence and absence for each *Cacnb1* variant (only the first 30 are showed). Each row represents an individual transcript, with “1” indicating the presence and “0” indicating the absence of specific exons. This binary representation allows the observation that none of the transcripts starting at exon1 include exon2B, suggesting that alternative splicing is not the mechanism regulating exon2B inclusion but rather indicates the existence of an alternative promoter at exon 2B.

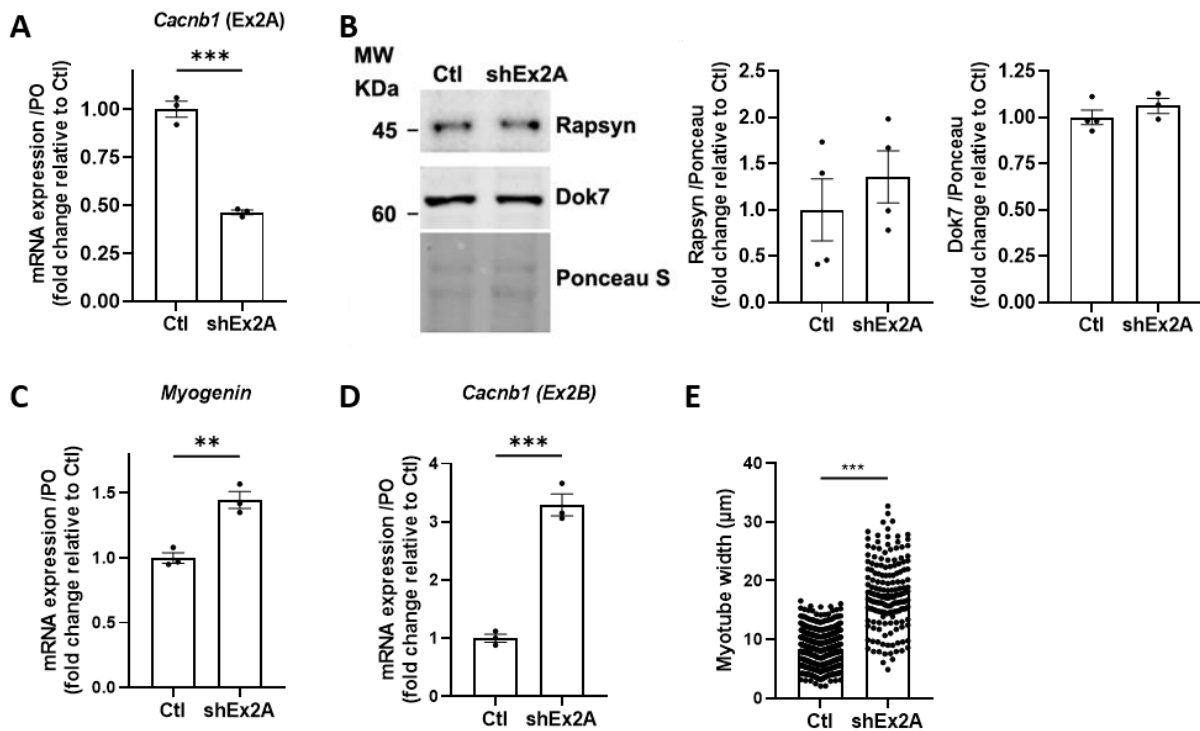


Figure S2. Additional data from Figure 3. **A.** RT-qPCR of embryonic *Cacnb1* variants using primer in exon2A in control and shEx2A treated myotubes. **B.** Western Blot and quantification of rapsyn and Dok7 in control and shEx2A treated myotubes. **C.** Immunofluorescence (IF) images of control or shEx2A treated myotubes stained with AChRa1 (green) and DAPI (blue). **C-D.** RT-qPCR of *Myogenin* (**C**) and *Cacnb1D* (**D**) in control and shEx2A treated myotubes. **E.** Quantification of myotube width in control and shEx2A treated myotubes. All data are mean \pm SEM (* P < 0.05, ** P < 0.01, *** P < 0.001). P values were calculated by unpaired t-test.

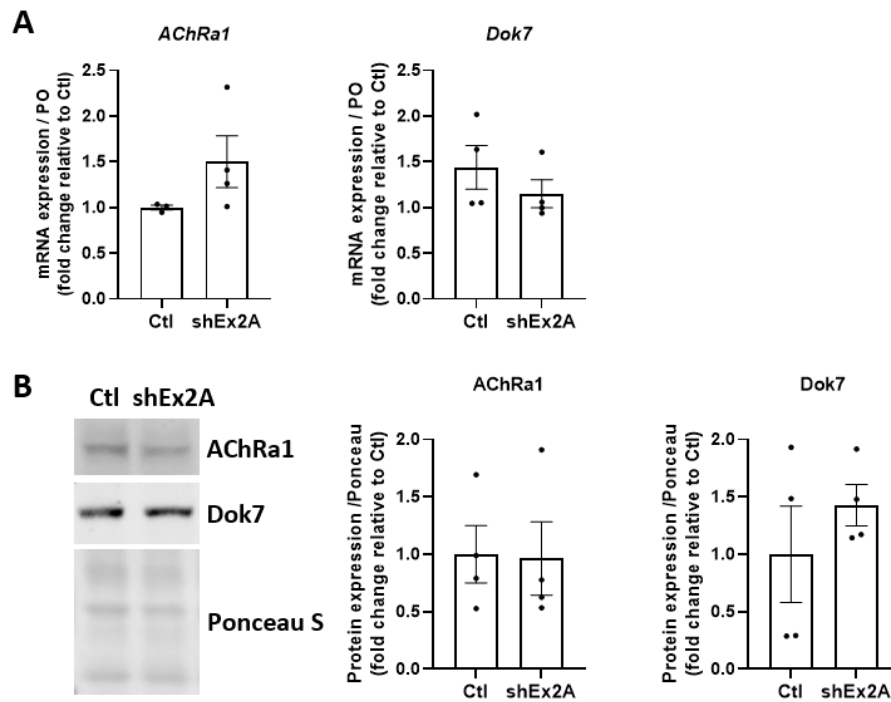


Figure S3. Additional data from Figure 4. A. RT-qPCR of *AChRa1* and *Dok7* in control and shEx2A treated TA muscles, 3-weeks post-injection. **B.** Western Blot and quantification of AChRa1 and Dok7 in control and shEx2A treated TA muscles, 3-weeks post-injection. All data are mean \pm SEM (* $P < 0.05$, ** $P < 0.01$, *** $P < 0.001$). P values were calculated by unpaired t-test.

Name	Forward	Reverse	Application
Cacnb1 (Ex2A-Ex3)	GGAAGTACAGCAAGAGG	GTTGGTCTTGGCTTTCTCG	
Cacnb1 (Ex2B-Ex3)	CAGCCGGACCCTGGTAGTG	GTTGGTCTTGGCTTTCTCG	
Cacnb1 (all isoforms)	GACAGCCTTCGCTCTGCTGCAG	CATGTCTGTACCTCATAGCC	
Myogenin	ACGATGGACGTAAAGGGAGTG	AGTGAATGCAACTCCCAGAG	
MCK	AGACAAGCATAAGACCCGACCT	AGGCAGAGTGTAAACCCCTTGAT	
Myhc3	AAGGCCAAAAAGGCCATC	CATCCAGACGGTTGCTGCAG	RT-qPCR
Myhc8	CTGTTAAAGGGTTAAGGAAGC	CGCCTGTAATTTGTCCACCA	
Lrp4	AGTCACCCGCAAGGCTGTCATTA	GTTGGCACTATTGATGCTCTTGG	
Rapsyn	CTGGATGAAGGTCGTGGAGAAG	CCGAGCAGTATCAATCTGGACC	
Achra1	AAGCTACTGTGAGATCATCGTCAC	TGACGAAGTGGTAGGTGATGTCCA	
Achrg	GCTCAGCTGCAAGTTGATCTC	CCTCCTGCTCCATCTCTGTC	
Musk	TTCAGCGGACTGAGAAACT	TGCTTCCACGCTCAGAATG	
PO	CTCCAAGCAGATGCAGCAGA	ATAGCCTTGGCCATCATGGT	RT-qPCR + RT-PCR
Cacnb1 (Ex2A-Ex2B-Ex3)	GGAAGTACAGCAAGAGG	GTTGGTCTTGGCTTTCTCG	Triplex RT-PCR
Cacnb1 (Ex6-Ex8)	GACAGCCTTCGCTCTGCTGCAG	CATGTCTGTACCTCATAGCC	RT-PCR
Cacnb1 (-3,6kb)	CTCCAGCCTCCTTGTTCA TTC	CTTTGCCCACTGAAAATCTTGG	
Cacnb1 (Ex1-Int1)	ACCTTCCCAAGAGATCCCTATG	GGCATATAACCCCTTCCCTCCC	
Cacnb1 (Int1-Ex2A)	CTGGTAGGAGCTGAACTAGGAA	ATGTTGTATCCGAGGACGTACT	
Cacnb1 (Int2)	CATGTGCAAACTGCTAGGGTAT	ATAGCATGCTTCTGTGGTTGAG	ChIP qPCR
Cacnb1 (Ex2B-Int3)	GAAGAGATGAGCTGGGAGAAAAG	GCAGTTGCACATGTAGCAATT	
Cacnb1 (Int4)	TTACAATACAAAAGCGACGGGT	GGCAGAGGATGCCTGTATAAAG	

Table S1. Primer list for RT-PCR, RT-qPCR, Triplex RT-PCR and ChIP-qPCR.

Name	Sequence
U1-Ex1-Cacnb1-fw	GCAGTCGAAACATGTAGCTGACTCAGGTACCCGGACCCGGAGGATCCTCTC
U1-Ex2B Int-Cacnb1-fw	GCAGTCGAAACATGTAGCTGACTCAGGTACCGCAAATTCTGCTTGTAACTGAGCTC
U1-Ex2B-Cacnb1-fw	GCAGTCGAAACATGTAGCTGACTCAGGTACCCAGCCGGACCCCTGGTAGTG
U2-Ex13 end-Cacnb1-rv	TGGATCACTTGTGCAAGCATCACATCGTAGGCTACATGGCCGTGCTCCTGAG
U2-Ex14-Cacnb1-rv	TGGATCACTTGTGCAAGCATCACATCGTAGCCTCTCAGCCGGATGTAGACCGC

Table S2. Primer list for Nanopore sequencing.

Name/Target	Source	Reference	Species	Application	Dilution
Cacnb1-66:84	ThermoFisher Scientific	Custom antibody	Rabbit		1:1000
Cacnb1-506:524	ThermoFisher Scientific	Custom antibody	Rabbit		1:500
AChRa1	Invitrogen	11565752	Mouse	WB	1:100
MuSK	Sigma Aldrich	ABS549	Rabbit		1:100
Actin	Merck Millipore	A4700	Mouse		1:5000
Rapsyn			Mouse		1:100
Dok7	Santa Cruz	sc-50463 (H-284)	Rabbit		1:100
Nefm	DSHB	2H3	Mouse		1:500
SV2A	DSHB	SV2	Mouse		1:500
α -Bungarotoxin-Alexa Fluor™ conjugated 594	ThermoFisher Scientific	B13423	Bungarus multicinctus	IF	1:500
AChRa1	Covance	MRT-609R-506	Rat		
Histone H3	Abcam	Ab1791	Rabbit		0.3 μ g
H3K9ac	Abcam	Ab113674 (no longer on the market)	Mouse	ChIP	1 μ g
RNAPII pS5 (4H8)	Abcam	Ab5408	Mouse		2 μ g
H3K4me3	ThermoFisher Scientific	PA5-27029	Rabbit		1.2 μ g
IgG mouse	Sigma Aldrich	I-5381	Mouse		2 μ g

Table S3. Primary antibodies.

Name/Target	Source	Reference	Species	Application	Dilution
StarBright Blue 700 Goat Anti-Mouse IgG	BioRad	12004159	Mouse	WB	1:10 000
StarBright Blue 700 Goat Anti-Rabbit IgG		12004162	Rabbit		
StarBright Blue 520 Goat Anti-Mouse IgG		12005867	Mouse		
StarBright Blue 520 Goat Anti-Rabbit IgG		12005870	Rabbit		
Goat anti-Mouse IgG (H+L) Highly Cross-Adsorbed Secondary Antibody, Alexa Fluor™ 488	ThermoFisher Scientific	A-11029	Mouse	IF	1:400

Table S4. Secondary antibodies.

REFERENCES

- Arber, Silvia, Steven J. Burden, and A. John Harris, 'Patterning of Skeletal Muscle', *Current Opinion in Neurobiology*, 12.1 (2002), pp. 100–103, doi:10.1016/s0959-4388(02)00296-9
- Buraei, Zafir, and Jian Yang, 'Structure and Function of the β Subunit of Voltage-Gated Ca^{2+} Channels', *Biochimica Et Biophysica Acta*, 1828.7 (2013), pp. 1530–40, doi:10.1016/j.bbamem.2012.08.028
- Chen, Fujun, Yun Liu, Yoshie Sugiura, Paul D Allen, Ronald G Gregg, and Weichun Lin, 'Neuromuscular Synaptic Patterning Requires the Function of Skeletal Muscle Dihydropyridine Receptors', *Nature Neuroscience*, 14.5 (2011), pp. 570–77, doi:10.1038/nn.2792
- Dos Reis, Raphaël, Etienne Kornobis, Alyssa Pereira, Frederic Tores, Judit Carrasco, Candice Gautier, and others, 'Complex Regulation of Gephyrin Splicing Is a Determinant of Inhibitory Postsynaptic Diversity', *Nature Communications*, 13.1 (2022), p. 3507, doi:10.1038/s41467-022-31264-w
- Eguchi, Takahiro, Tohru Tezuka, Sadanori Miyoshi, and Yuji Yamanashi, 'Postnatal Knockdown of Dok-7 Gene Expression in Mice Causes Structural Defects in Neuromuscular Synapses and Myasthenic Pathology', *Genes to Cells: Devoted to Molecular & Cellular Mechanisms*, 21.6 (2016), pp. 670–76, doi:10.1111/gtc.12370
- Falcone, Sestina, William Roman, Karim Hnia, Vincent Gache, Nathalie Didier, Jeanne Lainé, and others, 'N-WASP Is Required for Amphiphysin-2/BIN1-Dependent Nuclear Positioning and Triad Organization in Skeletal Muscle and Is Involved in the Pathophysiology of Centronuclear Myopathy', *EMBO Molecular Medicine*, 6.11 (2014), pp. 1455–75, doi:10.15252/emmm.201404436
- Haddix, Seth G., Young il Lee, Joe N. Kornegay, and Wesley J. Thompson, 'Cycles of Myofiber Degeneration and Regeneration Lead to Remodeling of the Neuromuscular Junction in Two Mammalian Models of Duchenne Muscular Dystrophy', *PLoS ONE*, 13.10 (2018), p. e0205926, doi:10.1371/journal.pone.0205926
- Igolkina, Anna A., Arsenii Zinkevich, Kristina O. Karandasheva, Aleksey A. Popov, Maria V. Selifanova, Daria Nikolaeva, and others, 'H3K4me3, H3K9ac, H3K27ac, H3K27me3 and H3K9me3 Histone Tags Suggest Distinct Regulatory Evolution of Open and Condensed Chromatin Landmarks', *Cells*, 8.9 (2019), p. 1034, doi:10.3390/cells8091034
- Kaplan, Mehmet Mahsum, Nasreen Sultana, Ariane Benedetti, Gerald J. Obermair, Nina F. Linde, Symeon Papadopoulos, and others, 'Calcium Influx and Release Cooperatively Regulate AChR Patterning and Motor Axon Outgrowth during Neuromuscular Junction Formation', *Cell Reports*, 23.13 (2018), pp. 3891–3904, doi:10.1016/j.celrep.2018.05.085
- Li, Lei, Wen-Cheng Xiong, and Lin Mei, 'Neuromuscular Junction Formation, Aging, and Disorders', *Annual Review of Physiology*, 80.1 (2018), pp. 159–88, doi:10.1146/annurev-physiol-022516-034255
- Li, Yue, Young il Lee, and Wesley J. Thompson, 'Changes in Aging Mouse Neuromuscular Junctions Are Explained by Degeneration and Regeneration of Muscle Fiber Segments at the Synapse', *The Journal of Neuroscience: The Official Journal of the Society for Neuroscience*, 31.42 (2011), pp. 14910–19, doi:10.1523/JNEUROSCI.3590-11.2011

Massiré, Traoré, Noviello Chiara, Vergnol Amélie, Gentil Christel, Halliez Marius, Saillard Lucile, and others, 'GDF5 as a Rejuvenating Treatment for Age-Related Neuromuscular Failure', *Brain: A Journal of Neurology*, 2024, p. awae107, doi:10.1093/brain/awae107

Mazhar, Sania, and Ruth Herbst, 'The Formation of Complex Acetylcholine Receptor Clusters Requires MuSK Kinase Activity and Structural Information from the MuSK Extracellular Domain', *Molecular and Cellular Neuroscience*, 49.4 (2012), pp. 475–86, doi:10.1016/j.mcn.2011.12.007

Moransard, Martijn, Lucia S. Borges, Raffaella Willmann, P. Angelo Marangi, Hans Rudolf Brenner, Michael J. Ferns, and others, 'Agrin Regulates Rapsyn Interaction with Surface Acetylcholine Receptors, and This Underlies Cytoskeletal Anchoring and Clustering', *The Journal of Biological Chemistry*, 278.9 (2003), pp. 7350–59, doi:10.1074/jbc.M210865200

Mulroney, Logan Moran, 'Identification of Full-Length Transcript Isoforms Using Nanopore Sequencing of Individual RNA Strands' (UC Santa Cruz, 2020) <<https://escholarship.org/uc/item/36j135qg>> [accessed 27 July 2024]

Oury, Julien, Yun Liu, Ana Töpf, Slobodanka Todorovic, Esthelle Hoedt, Veeramani Preethish-Kumar, and others, 'MACF1 Links Rapsyn to Microtubule- and Actin-Binding Proteins to Maintain Neuromuscular Synapses', *The Journal of Cell Biology*, 218.5 (2019), pp. 1686–1705, doi:10.1083/jcb.201810023

Pęziński, Marcin, Patrycja Daszczuk, Bhola Shankar Pradhan, Hanns Lochmüller, and Tomasz J. Prószyński, 'An Improved Method for Culturing Myotubes on Laminins for the Robust Clustering of Postsynaptic Machinery', *Scientific Reports*, 10.1 (2020), p. 4524, doi:10.1038/s41598-020-61347-x

Segatto, Marco, Raffaella Fittipaldi, Fabrizio Pin, Roberta Sartori, Kyung Dae Ko, Hossein Zare, and others, 'Epigenetic Targeting of Bromodomain Protein BRD4 Counteracts Cancer Cachexia and Prolongs Survival', *Nature Communications*, 8.1 (2017), p. 1707, doi:10.1038/s41467-017-01645-7

Slater, Clarke R., "'Fragmentation" of NMJs: A Sign of Degeneration or Regeneration? A Long Journey with Many Junctions', *Neuroscience*, 439 (2020), pp. 28–40, doi:10.1016/j.neuroscience.2019.05.017

Tang, Huibin, and Daniel Goldman, 'Activity-Dependent Gene Regulation in Skeletal Muscle Is Mediated by a Histone Deacetylase (HDAC)-Dach2-Myogenin Signal Transduction Cascade', *Proceedings of the National Academy of Sciences of the United States of America*, 103.45 (2006), pp. 16977–82, doi:10.1073/pnas.0601565103

Tang, Huibin, Matthew B. Veldman, and Daniel Goldman, 'Characterization of a Muscle-Specific Enhancer in Human MuSK Promoter Reveals the Essential Role of Myogenin in Controlling Activity-Dependent Gene Regulation', *The Journal of Biological Chemistry*, 281.7 (2006), pp. 3943–53, doi:10.1074/jbc.M511317200

Taylor, Jackson, Andrea Pereyra, Tan Zhang, Maria Laura Messi, Zhong-Min Wang, Claudia Hereñú, and others, 'The Cav β 1a Subunit Regulates Gene Expression and Suppresses Myogenin in Muscle Progenitor Cells', *The Journal of Cell Biology*, 205.6 (2014), pp. 829–46, doi:10.1083/jcb.201403021

Tian, Bing, Jun Yang, and Allan R. Brasier, 'Two-Step Cross-Linking for Analysis of Protein-Chromatin Interactions', *Methods in Molecular Biology (Clifton, N.J.)*, 809 (2012), pp. 105–20, doi:10.1007/978-1-61779-376-9_7

Tintignac, Lionel A., Hans-Rudolf Brenner, and Markus A. Rüegg, 'Mechanisms Regulating Neuromuscular Junction Development and Function and Causes of Muscle Wasting', *Physiological Reviews*, 95.3 (2015), pp. 809–52, doi:10.1152/physrev.00033.2014

Tosic, Milica, Anita Allen, Dominica Willmann, Christoph Lepper, Johnny Kim, Delphine Duteil, and others, 'Lsd1 Regulates Skeletal Muscle Regeneration and Directs the Fate of Satellite Cells', *Nature Communications*, 9.1 (2018), p. 366, doi:10.1038/s41467-017-02740-5

Traoré, Massiré, Christel Gentil, Chiara Benedetto, Jean-Yves Hogrel, Pierre De la Grange, Bruno Cadot, and others, 'An Embryonic CaV β 1 Isoform Promotes Muscle Mass Maintenance via GDF5 Signaling in Adult Mouse', *Science Translational Medicine*, 11.517 (2019), p. eaaw1131, doi:10.1126/scitranslmed.aaw1131

Valdez, Gregorio, Juan C. Tapia, Jeff W. Lichtman, Michael A. Fox, and Joshua R. Sanes, 'Shared Resistance to Aging and ALS in Neuromuscular Junctions of Specific Muscles', *PLOS ONE*, 7.4 (2012), p. e34640, doi:10.1371/journal.pone.0034640

Wang, Weidong, Michael Carey, and Jay D. Gralla, 'Polymerase II Promoter Activation: Closed Complex Formation and ATP-Driven Start Site Opening', *Science*, 255.5043 (1992), pp. 450–53, doi:10.1126/science.1310361

Yang, Naidi, Dipanwita Das, Shilpa Rani Shankar, Pierre-Alexis Goy, Ernesto Guccione, and Reshma Taneja, 'An Interplay between BRD4 and G9a Regulates Skeletal Myogenesis', *Frontiers in Cell and Developmental Biology*, 10 (2022), doi:10.3389/fcell.2022.978931

Yang, Xia, Silvia Arber, Christopher William, Li Li, Yasuto Tanabe, Thomas M. Jessell, and others, 'Patterning of Muscle Acetylcholine Receptor Gene Expression in the Absence of Motor Innervation', *Neuron*, 30.2 (2001), pp. 399–410, doi:10.1016/S0896-6273(01)00287-2

b) Additional results

As described in the article in preparation presented above, this thesis work allowed a clarification of the diversity of $Ca_v\beta 1$ isoforms in skeletal muscle with $Ca_v\beta 1A$ and $Ca_v\beta 1E$ being two embryonic/perinatal isoforms while $Ca_v\beta 1D$ is the adult constitutive isoform.

Intriguingly, Nanopore sequencing analysis revealed that at E12.5, the most abundant isoform of both Ex1-Ex13end and Ex1-Ex14 Transcriptional Units (TU) are transcripts lacking exon7A and not *Cacnb1A* and *Cacnb1E*. The abundance of *Cacnb1A_Δ7A* and *Cacnb1E_Δ7A* within their respective TU drops from 54,85% to 2,36% and 61,55% to 4,12% respectively, between E12.5 and P0, to be replaced by *Cacnb1A* and *Cacnb1E* (Fig. 20A). We validated *Cacnb1A/E_Δ7A* variants by RT-PCR with the observation of a shift in the size of the full-length *Cacnb1A* and *Cacnb1E* transcripts at E12.5 (Fig. 20B), Sanger analysis of this lower band confirming the absence of Ex7A (data not showed). A RT-PCR using primers flanking exon7A (without *Cacnb1* isoform specificity) allowed the observation of a clear

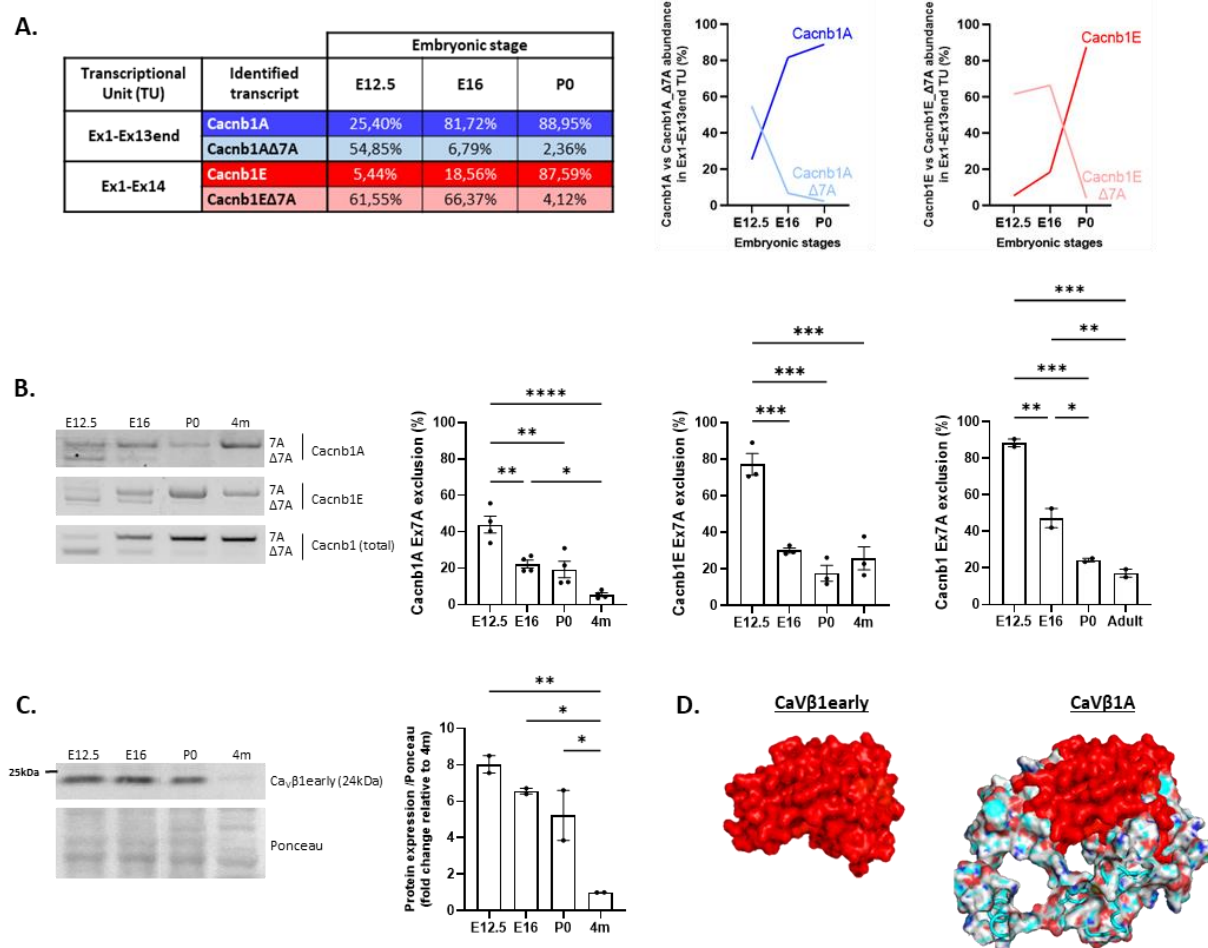


Figure 20. Identification of a putative new $Ca_v\beta 1$ isoform: $Ca_v\beta 1$ early.

A. Nanopore sequencing results showing the relative abundance of *Cacnb1* transcripts lacking exon7A within *Cacnb1* Ex1-Ex13end and Ex1-Ex14 transcriptional unit (TU). **B.** RT-PCR and quantification of the embryonic full-length *Cacnb1* isoforms, and of exon6-exon8 *Cacnb1* total variants, in embryonic and adult muscles, showing a shift in band size corresponding to the transcripts lacking exon7A. **C.** Western Blot and quantification of a band corresponding to the size of the putative $Ca_v\beta 1$ early isoform in embryonic and adult muscles. **D.** In silico 3D modelling of $Ca_v\beta 1$ early isoform and $Ca_v\beta 1A$ isoform, demonstrating a similar folding of the exon1-exon8 encoded domains in both $Ca_v\beta 1$ early $Ca_v\beta 1A$ isoforms. All data are mean \pm SEM (* $P < 0.05$, ** $P < 0.01$, *** $P < 0.001$). P values were calculated by ordinary one-way ANOVA followed by Tukey's multiple comparison test (B-C).

progressive inclusion of exon7A in *Cacnb1* global variants from embryonic to adult skeletal muscle stage (**Fig. 20B**). Interestingly, this induces a shift in the ORF, which leads to the use of a premature STOP codon in exon8. At protein level, western blot analysis showed the expression of an approximately 24kDa protein, the putative molecular weight of this identified isoform coded by *Cacnb1A/E_Δ7A* transcripts. Interestingly, this protein was expressed in embryonic muscle and decreased until almost undetectable levels in adult innervated mouse muscle (**Fig. 20C**).

The structural folding of a protein is crucial for its function. Here, we investigated whether the potential newly identified $\text{Ca}_v\beta 1$ early isoform might share the same structural characteristics as the full-length isoforms in their common domains or if the amino acidic sequence encoded after exon8 could affect the folding of the preceding domains. To do so, we performed an *ab initio* modelling of the putative $\text{Ca}_v\beta 1$ early and homology modelling of the embryonic $\text{Ca}_v\beta 1A$ isoform using the online Robetta server. After free energy optimization, we used the “align” algorithm to achieve a structural superposition alignment. We observed that the 3D structure of $\text{Ca}_v\beta 1$ early matches that of $\text{Ca}_v\beta 1A$ on the domains encoded by the corresponding sequences (**Fig. 20D**), meaning that the full-length protein is not necessary to ensure to correct folding of exon1 to exon8 $\text{Ca}_v\beta 1$ domains. To quantify this, we use the Root Mean Square Deviation (RMSD) calculation, indicating the average deviation between the positions of atoms in $\text{Ca}_v\beta 1$ early structure compared to the corresponding domains in $\text{Ca}_v\beta 1A$ structure. We found a RMSD at 1.37 Å, meaning that the two structures are similar (this is the case of RMSD below 2 Å). This suggests that their conformations are closely aligned and that any structural differences are relatively minor. Therefore, we can speculate that a function attributed to the NT, SH3 and HOOK domains of $\text{Ca}_v\beta 1$, independently of the GK and CT domains, can be hold by $\text{Ca}_v\beta 1$ early isoform (**Fig. 14** - introduction of this manuscript).

CHAPTER 2 - Regulation of $\text{Ca}_v\beta 1$ isoforms expression by MBNLs and involvement in Myotonic Dystrophy Type 1

I- Introduction

MBNL proteins are essential splicing factors regulating the transition from fetal to adult protein splice isoforms. They are crucial during development and for the function of muscle and brain tissues. They are key players in a wide range of cellular processes, by ensuring a proper mRNA processing, by regulating alternative splicing but also mRNA stability, localization and translation. MBNL1 is expressed in adult skeletal muscle, while MBNL3 is mainly expressed during development as well as in adult muscle after denervation (Traoré et al., 2019). While mainly associated with neuronal tissue, MBNL2 expression increases upon MBNL1 loss in skeletal muscle in which these proteins show functional interchangeability. MBNL1 and MBNL2 display nuclear localization, in accordance with regulation of alternative splicing events, whereas MBNL3 predominantly localizes in the cytoplasm where it preferentially binds 3'-UTR sequences, thereby influencing mRNA expression levels and/or localization of specific transcripts, as well as their translation efficiency (Wang et al., 2012).

Extensive research has focused on MBNL proteins due to their involvement in DM1, a disease characterized by the sequestration and inactivation of these proteins, among others, by CTG toxic nuclear aggregates. The skeletal muscle-related symptoms are highly associated with misregulation of MBNL targets, in particular *Clc1* exon7A inclusion has been associated with myotonia, a hallmark symptom of DM1. In adult muscle, CLC1 protein is mainly localized at the sarcolemma, and at the T-tubules, to allow proper Cl^- ions flows across the membrane. Cl^- conductance plays a crucial role in ensuring a stable resting membrane potential at rest and in membrane repolarization and after contraction, therefore regulating muscle excitability (Lueck et al., 2007). In DM1, not only *Clc1* mis-splicing but also independent CLC1 protein translation issues are responsible for myotonia (Choi et al., 2015). In parallel, muscle fiber type profile in DM1 muscles exhibits an aberrant shift from glycolytic (type 2X and 2B) to oxidative (type 1 and type 2A) fibers, that is a parameter influenced by the altered *Clc1* splicing and associated with myotonia (Hu et al., 2023).

Given that *Cacnb1* is misregulated in human immortalized DM1 muscle cells (Arandel et al., 2017) and that MBNLs and $\text{Ca}_v\beta 1$ isoforms expressions are correlated after nerve damage (Traoré et al., 2019), we wondered about a potential connection between MBNL proteins and $\text{Ca}_v\beta 1$ expression. Besides, $\text{Ca}_v\beta 1\text{E}$ has been demonstrated as a key player in regulating muscle mass homeostasis after nerve damage, which led us to investigate the role of $\text{Ca}_v\beta 1$ isoforms in DM1 pathophysiology.

To study how MBNL modulation affects $\text{Ca}_v\beta 1$ isoform expression we initially planned to use different mouse models with both upregulated and downregulated MBNL proteins. Given the crucial role of MBNL1 in mRNA processing in skeletal muscle, we first induced MBNL1 overexpression. However, this approach led to muscle damage and degeneration causing a progressive loss of the non-integrative

AAV vector, weakening the effect of the transgene (data not showed). Consequently, we redirected our attention to a mouse model in which MBNL1 was down-regulated. In these mice, we demonstrated DM1 features with splicing alteration of key transcripts associated with pathological relevance, loss of muscle force and myotonia. Importantly, we showed that the embryonic $Ca_v\beta 1s$ isoform levels were increased upon MBNL1 downregulation and that MBNL3 expression was subsequently enhanced, which is involved in $Ca_v\beta 1$ variant expression regulation via their 3'UTR. Additionally, we observed that $Ca_v\beta 1$ embryonic isoforms depletion in our shMbnl1 model led to an exacerbation of myotonia, associated with an intensified loss of CLC1 protein membrane correct localization. Altogether, this study demonstrates that MBNL proteins are involved in regulating the expression of $Ca_v\beta 1$ isoforms, whose embryonic variants play a role in mitigating myotonia, a major feature of DM1.

II- Results

a) shMbnl1, a DM1 model?

To locally downregulate MBNL1, we injected an AAV1 carrying shMbnl1 in TA muscles (referred as shMbnl1 model – **Fig. 21A**). We validated its efficacy by assessing the decreased expression of *Mbnl1* transcripts by RT-qPCR (**Fig. 21B**) and the decreased number of MBNL1-positive nuclei in shMbnl1 treated muscle fibers by IF analysis (**Fig. 21C**). We observed no change in *Mbnl2* transcript level (**Fig. 21D**) but an increase in MBNL2 protein level (**Fig. 21E**), consistent with studies reporting a compensatory MBNL2 upregulation in response to MBNL1 loss (Lee et al., 2013; Nitschke et al., 2023).

To assess the effect of MBNL1 downregulation, we examined various transcript targets of MBNL1, among which we observed significant mis-splicing events, including an increase in *Nfix* exon7 inclusion, *ATP2a1* exon22 exclusion, *Clc1* exon7A inclusion, *Cacna1s* exon29 exclusion, *ArfGap2* exon8 exclusion, *Zasp* exon11 inclusion, *Bin1* exon11 exclusion and *Camk2b* exon13 exclusion (**Fig. 21F**). These readouts validated the functional effect of MBNL1 deficiency, despite the compensatory increase in MBNL2 protein levels.

To determine if these splicing impairments were accompanied by muscle function deficits in our shMbnl1 model, we performed functional analyses. Force measurements revealed a decreased force generation upon both direct (muscle) and indirect (nerve) stimulation (**Fig. 21G**), as well as the appearance of myotonia (**Fig. 21H**) in shMbnl1-treated muscles compared to controls. Additionally, we evaluated neurotransmission by ENMG, finding altered Compound Muscle Activity Potential (CMAP) (**Fig. 21I**). These results suggest that MBNL1 depletion is sufficient to induce DM1 features despite MBNL2 compensation, affecting both mRNA processing and muscle function.

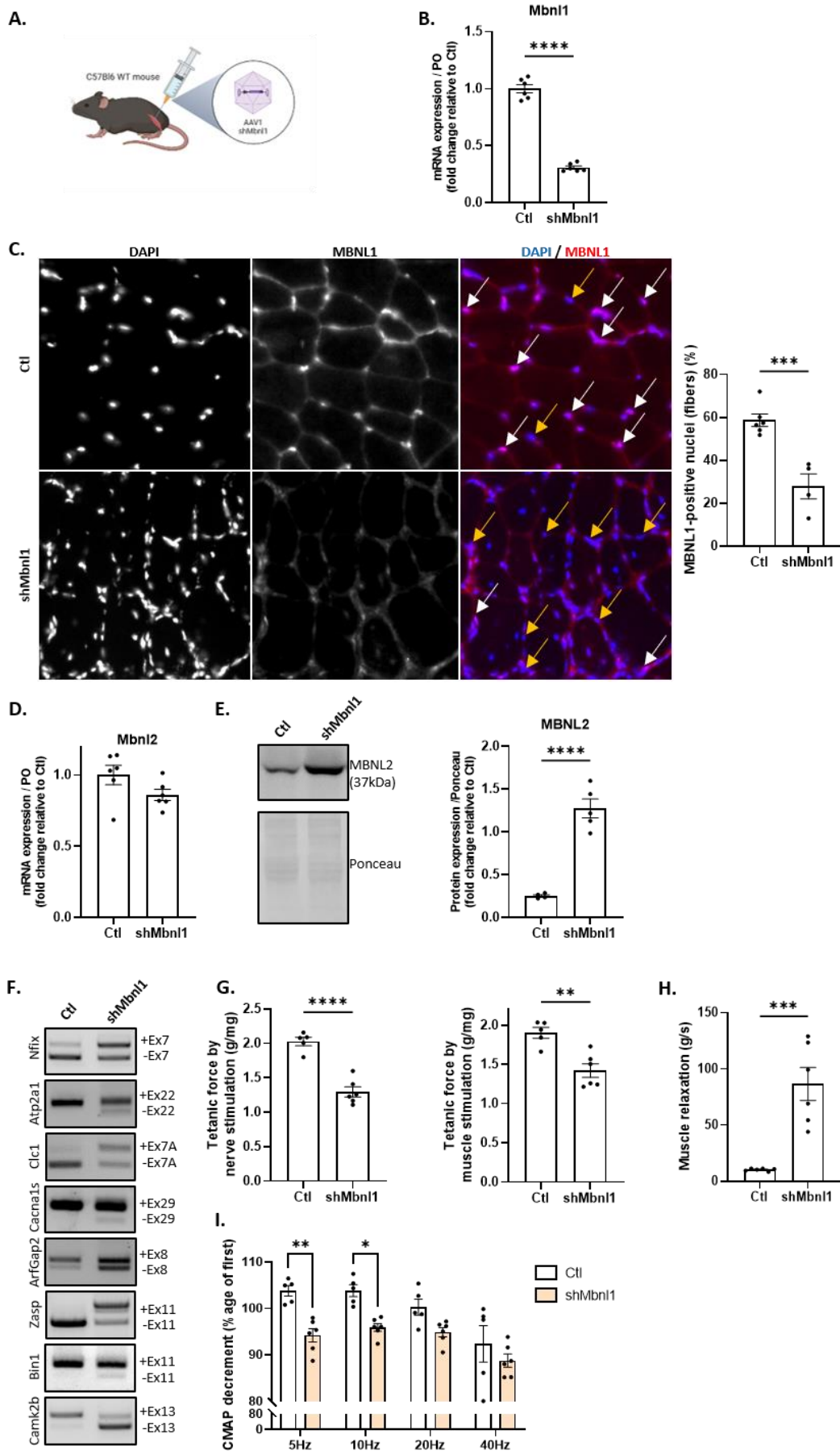


Figure 21. shMbn1 model recapitulating DM1 features.

A. Schematic representation of the experimental protocol. **B.** RT-qPCR of *Mbn1* in control and shMbn1 treated muscles, 12-weeks after injection. **C.** Immunofluorescence (IF) images and quantification of control and shMbn1 treated TA muscles, 12-weeks post-injection, stained with MBNL1 (red) and DAPI (blue). White arrows show MBNL1 positive nuclei while yellow arrows show MBNL1 negative nuclei. **D.** RT-qPCR of *Mbnl2* in control and shMbn1 treated muscles, 12-weeks after injection. **E.** Western Blot and quantification of MBNL2 in control and shMbn1 treated TA muscles, 12-weeks post-injection. **F.** RT-PCR of *Nfix*, *Atp2a1*, *Clc1*, *Cacna1s*, *ArfGap2*, *Zasp*, *Bin1* and *Camk2b* in control and shMbn1 treated TA muscles, 12-weeks post-injection, showing the inclusion or exclusion of the indicated exons, characteristic of DM1 mis-splicing. **G-I.** Indirect (nerve) or direct (muscle) tetanic force (**G**), measure of muscle relaxation (**H**), and CMAP decrement measured by ENMG (**I**), measured in control and shMbn1 treated TA adult muscles, 12-weeks post-injection. All data are mean \pm SEM (* $P < 0.05$, ** $P < 0.01$, *** $P < 0.001$). *P* values were calculated by unpaired t-test.

To investigate the possible role of $Ca_v\beta 1$ proteins in DM1, we analysed the expression of the different $Ca_v\beta 1$ isoforms in our shMbn1 model. At transcriptional level, we observed a global increase in *Cacnb1* transcripts (Fig. 22A). By looking more specifically to the different isoforms, we observed an increase in the expression of the embryonic isoforms (evaluated through RT-qPCR using primer in exon2A), while the adult *Cacnb1D* transcript (evaluated through RT-qPCR using primer in exon2B) was decreased (Fig. 22A). $Ca_v\beta 1A$ protein levels were increased in shMbn1 treated compared to control muscles while $Ca_v\beta 1D$ protein remained unaffected (Fig. 22B). We could not assess $Ca_v\beta 1E$ expression at protein levels due to technical limitations.

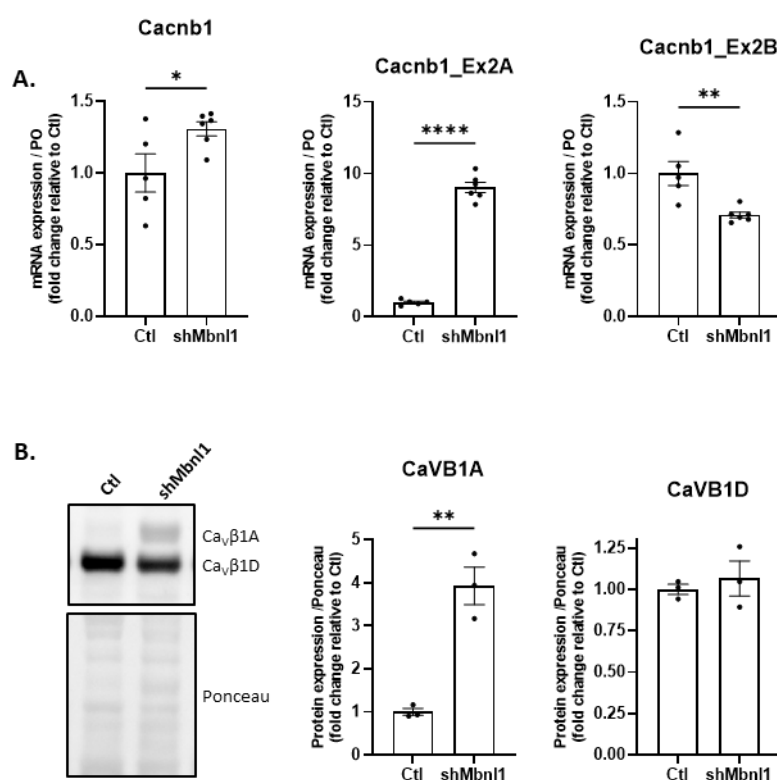


Figure 22. MBNL1 regulates embryonic $Ca_v\beta 1$ isoforms expression.

A. RT-qPCR of total *Cacnb1* transcripts, of embryonic *Cacnb1* variants using primers in exon2A and of adult *Cacnb1D* isoform using primers in exon2B, in control and shMbn1 treated muscles, 12-weeks after injection. **B.** Western Blot and quantification of $Ca_v\beta 1A$ and $Ca_v\beta 1D$ in control and shMbn1 treated TA muscles, 12-weeks post-injection. All data are mean \pm SEM (* $P < 0.05$, ** $P < 0.01$, *** $P < 0.001$). P values were calculated by unpaired t-test.

b) Role of $Ca_v\beta 1$ in DM1 features

Based on a previous study conducted by our team demonstrating that increased expression of the embryonic $Ca_v\beta 1E$ isoform contributes to limit muscle mass loss following denervation (Traoré et al., 2019), and given that we demonstrated the existence of an additional embryonic isoform $Ca_v\beta 1A$, we sought to investigate the role of these isoforms in the pathophysiology of DM1 by injecting an AAV1 carrying an shRNA specifically targeting $Ca_v\beta 1$ embryonic variants (referred as shEx2A model) in our

shMbnl1 model (**Fig. 23A**). The efficiency of their downregulation was validated by RT-qPCR and WB analysis by comparing shMbnl1 with shMbnl1+shEx2A muscles (**Fig. 23B,C**).

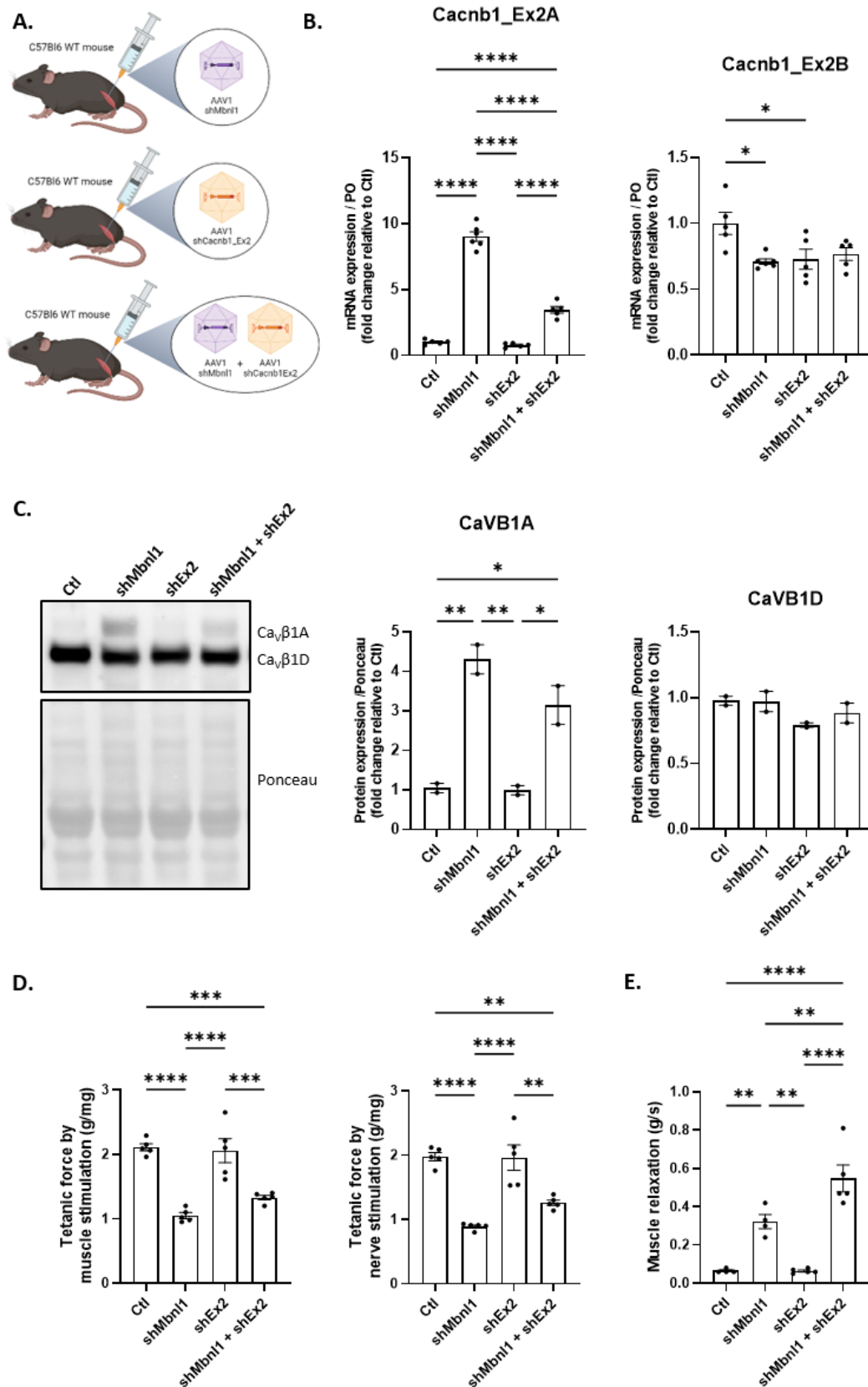


Figure 23. Downregulating embryonic $Ca_v\beta 1$ isoforms in *shMbnl1* model exacerbates myotonia.

A. Schematic representation of the experimental protocol. **B.** RT-qPCR of embryonic *Cacnb1* variants, as described in Fig 22, in control, *shMbnl1*, *shEx2A* and *shMbnl1+shEx2A* treated muscles, 12-weeks after injection. **C.** Western Blot and quantification of $Ca_v\beta 1A$ and $Ca_v\beta 1D$ in control, *shMbnl1*, *shEx2A* and *shMbnl1+shEx2A* treated muscles, 12-weeks after injection. **D-E.** Direct (muscle) or indirect (nerve) tetanic force (**D**) and measure of muscle relaxation (**E**) in control, *shMbnl1*, *shEx2A* and *shMbnl1+shEx2A* treated muscles, 12-weeks after injection. All data are mean \pm SEM (* $P < 0.05$, ** $P < 0.01$, *** $P < 0.001$). P values were calculated by ordinary one-way ANOVA followed by Tukey's multiple comparison test.

We wondered about the impact of the ablation of $\text{Ca}_v\beta 1$ embryonic isoforms on key muscle functionalities. We observed no modulation of direct nor indirect muscle force (**Fig. 23D**) but revealed that myotonia was exacerbated upon downregulation of $\text{Ca}_v\beta 1$ embryonic isoforms in shMbnl1 models compared to muscles treated solely with shMbnl1 (**Fig. 23E**). These results indicate that embryonic $\text{Ca}_v\beta 1$ s may play a role in mitigating myotonia, a hallmark feature of DM1.

To explore myotonia-related molecular defects, we investigated *Clc1* splicing but we did not find exon7A inclusion exacerbation after shEx2A treatment, on the contrary we surprisingly observed that *Clc1* was less severely mis-spliced (**Fig. 24A**). We also found that the pattern of CLC1 protein following a fiber-type specificity was lost under both shMbnl1 and shMbnl1+shEx2A treatment compared to control muscles, while unchanged in shEx2A alone treated muscles (**Fig. 24B**). This change in fiber-type pattern being shared with or without embryonic $\text{Ca}_v\beta 1$ s isoforms ablation, it did not explain the myotonia worsening under shEx2A and was rather probably related to a global decrease in CLC1 protein expression levels. However, CLC1 protein localization at the membrane was lost in shMbnl1+shEx2A treated muscles while preserved in both shMbnl1 and shEx2A individually treated muscles compared to control muscles (**Fig. 24B**). Additionally, we observed an increase in the percentage of type 2A oxidative fibers together with a decrease in the percentage of type 2X and 2B glycolytic fibers under shMbnl1 single treatment, featuring DM1 characteristics, but not worsened by shMbnl1+shEx2A double treatment (**Fig. 24C,D**).

Altogether, these results suggest that the exacerbation of myotonia induced upon downregulation of $\text{Ca}_v\beta 1$ embryonic isoforms in shMbnl1 treated muscles could be attributed to CLC1 protein mis-localization at the sarcolemma.

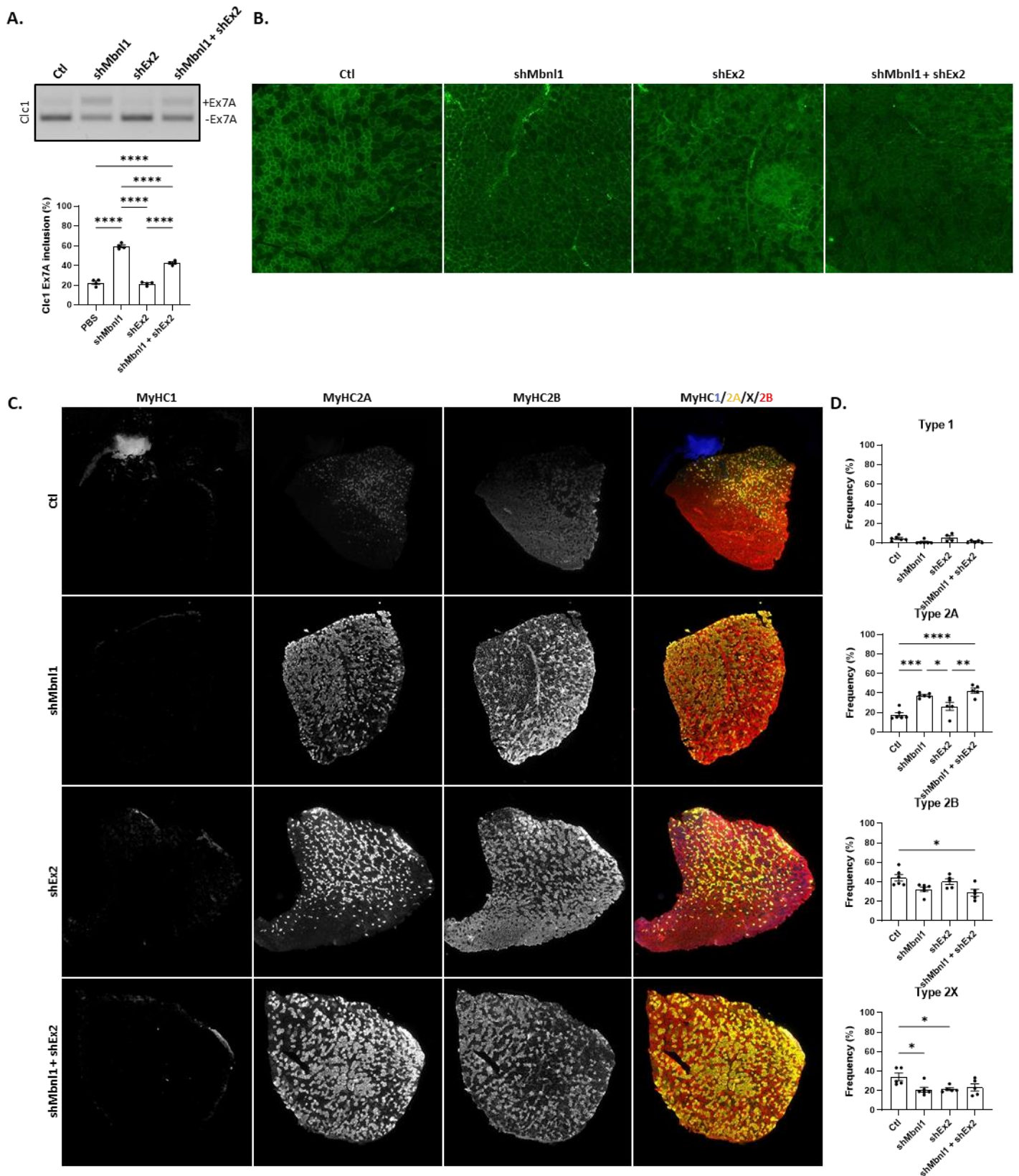


Figure 24. Effect of embryonic *Ca ν 1* isoforms downregulation on myotonia-related molecular defects.

A. RT-PCR and quantification of *Clc1* exon7A inclusion in control, *shMbn1*, *shEx2A* and *shMbn1+shEx2A* treated muscles, 12-weeks after injection. **B.** Immunofluorescence (IF) images of control and *shMbn1* treated TA muscles, 12-weeks post-injection, stained with CLC1 (green). **C-D.** Immunofluorescence (IF) images (C) and quantification (D) of control and *shMbn1* treated TA muscles, 12-weeks post-injection, stained with MyHC1 (blue), MyHC2A (yellow), and MyHC2B (red). All data are mean \pm SEM (* P < 0.05, ** P < 0.01, *** P < 0.001). P values were calculated by ordinary one-way ANOVA followed by Tukey's multiple comparison test.

c) MBNL3 involvement in Ca_vβ1 isoform regulation

In our previous study, RNAseq analysis comparing innervated vs denervated skeletal muscle revealed MBNL3 as the most significantly upregulated splicing factor after denervation (Traoré et al., 2019), which led us to investigate its role in regulating Ca_vβ1 isoforms in adult muscle. Intriguingly, we observed a similar upregulation of *Mbnl3* in our shMbnl1 model (**Fig. 25A**), suggesting a potential repressive effect of *Mbnl1* on *Mbnl3*, or a compensatory response of *Mbnl3* in response to decreased *Mbnl1*. To explore *Mbnl3* involvement in Ca_vβ1 isoform regulation, we triggered *Mbnl3* expression via nerve damage, modulated or not via its downregulation by injecting AAV carrying *Mbnl3*-targetted shRNA (referred as shMbnl3 treatment - **Fig. 25B**). Comparing denervated muscles with shMbnl3 denervated muscles confirmed the decreased *Mbnl3* expression (**Fig. 25C**). We established that *Mbnl3* was required to enable the effective upregulation of *Cacnb1* embryonic isoforms following denervation, by showing the decreased *Cacnb1* exon2A level in shMbnl3 denervated muscles compared to control denervated muscles (**Fig. 25D**). In contrast, Mbnl3 modulation did not affect adult *Cacnb1D*, as revealed by the non-modulated *Cacnb1* exon2B levels (**Fig. 25D**). Consequently, the increased expression of embryonic Ca_vβ1s isoforms observed under shMbnl1 treatment (**Fig. 22A,B**) could be attributed either directly to the depletion of *Mbnl1*, to the subsequent increase in *Mbnl3* levels or to a combination of both events. A model combining shMbnl1 and shMbnl3 treatment would allow to decipher the impact of MBNL proteins on Ca_vβ1 isoforms regulation.

d) Mechanistic of the regulation of Ca_vβ1 expression by MBNLs

We next investigated *in vitro*, the role of MBNL3 in the regulation of Ca_vβ1 isoforms expression, and more specifically we wondered if MBNL3 could impact *Cacnb1* mRNAs processing through their 3'UTR. *Cacnb1A* and *Cacnb1D* end with exon13end while *Cacnb1E* ends with exon14 (**Fig. 1** – article in preparation), therefore displaying two different 3'UTRs. We used two distinct plasmid reporter systems, each carrying one *Cacnb1* 3'-UTRs downstream of luciferase. We used these reporter systems in C2C12 myoblasts, where we manipulated MBNL proteins by increasing *Mbnl3* levels (referred as OE_Mbnl3), and reducing *Mbnl1* or *Mbnl3* by siRNA tools (**Fig. 25E**).

Given that the *in vivo* downregulation of MBNL1 positively regulated *Mbnl3* levels (**Fig. 25A**), we chose to combine OE_Mbnl3 and siMbnl1 *in vitro* to enhance Mbnl3 expression. After assessing the efficacy of the different MBNLs OE and siRNA plasmid transfections (**Fig. 25F**), we validated Mbnl3 as a regulator of 3'UTR mRNA stability by quantifying *S100a4* transcript expression, a described target of MBNL3 (Poulos et al., 2013) (**Fig. 25G**). We found that the combined OE_Mbnl3+siMbnl1 transfection led to a reduction in *Cacnb1A/D* 3'-UTR related-luciferase activity. Interestingly, neither OE_Mbnl3 alone nor siMbnl1 alone had a significant impact, suggesting the existence of a threshold of MBNL3 level necessary to affect *Cacnb1A/D* via their 3'UTR. Conversely, transfection with siMbnl3 resulted in increased *Cacnb1A/D* 3'-UTR related-luciferase activity (**Fig. 25H**). In contrast, we did not observe any change in *Cacnb1E* 3'-UTR related-luciferase activity under MBNLs modulation (**Fig. 25I**). Collectively,

these results suggest that MBNL3 acts on *Cacnb1A/D* 3'-UTR sequence but has no impact on *Cacnb1E* 3'UTR.

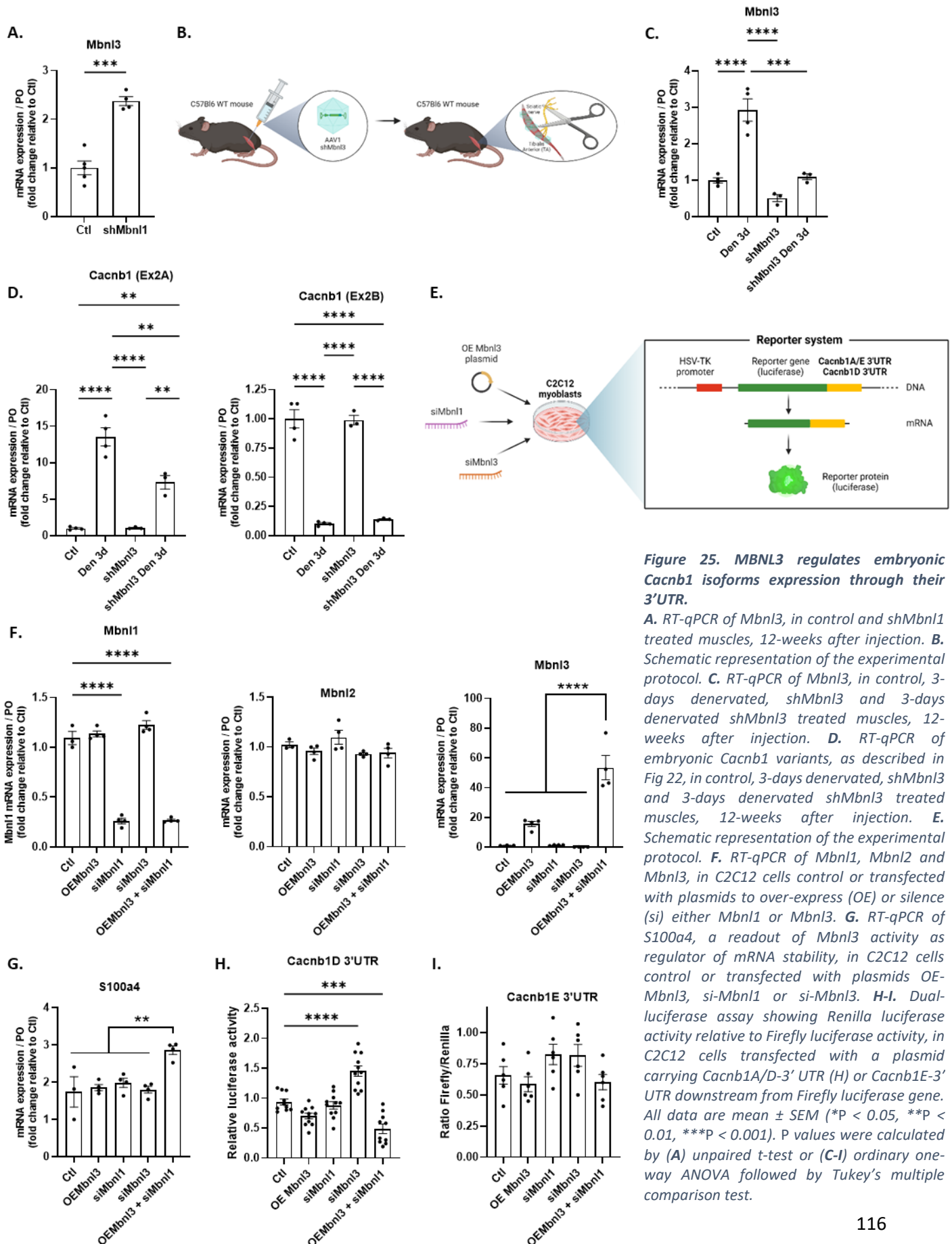


Figure 25. MBNL3 regulates embryonic *Cacnb1* isoforms expression through their 3'UTR.

A. RT-qPCR of *Mbnl3*, in control and *shMbnl1* treated muscles, 12-weeks after injection. **B.** Schematic representation of the experimental protocol. **C.** RT-qPCR of *Mbnl3*, in control, 3-days denervated, *shMbnl3* and 3-days denervated *shMbnl3* treated muscles, 12-weeks after injection. **D.** RT-qPCR of embryonic *Cacnb1* variants, as described in Fig 22, in control, 3-days denervated, *shMbnl3* and 3-days denervated *shMbnl3* treated muscles, 12-weeks after injection. **E.** Schematic representation of the experimental protocol. **F.** RT-qPCR of *Mbnl1*, *Mbnl2* and *Mbnl3*, in C2C12 cells control or transfected with plasmids to over-express (OE) or silence (si) either *Mbnl1* or *Mbnl3*. **G.** RT-qPCR of *S100a4*, a readout of *Mbnl3* activity as regulator of mRNA stability, in C2C12 cells control or transfected with plasmids OE-*Mbnl3*, si-*Mbnl1* or si-*Mbnl3*. **H-I.** Dual-luciferase assay showing Renilla luciferase activity relative to Firefly luciferase activity, in C2C12 cells transfected with a plasmid carrying *Cacnb1A/D*-3' UTR (H) or *Cacnb1E*-3' UTR downstream from Firefly luciferase gene. All data are mean \pm SEM (* $P < 0.05$, ** $P < 0.01$, *** $P < 0.001$). P values were calculated by (A) unpaired t-test or (C-I) ordinary one-way ANOVA followed by Tukey's multiple comparison test.

GENERAL DISCUSSION

Overall, this thesis provided insights into $\text{Ca}_v\beta 1$ isoforms knowledge: while $\text{Ca}_v\beta 1D$ was already known as the adult constitutive isoform and $\text{Ca}_v\beta 1E$ as an embryonic isoform (Traoré et al., 2019), we identified $\text{Ca}_v\beta 1A$ as an embryonic/perinatal isoform, also re-expressed after denervation in skeletal muscle. We demonstrated that $\text{Ca}_v\beta 1$ isoforms are regulated through the use of two distinct promoters regulated differently during development, perinatal stages marking a period of transition between the activation of these two promoters and nerve damage in adult muscle leading to the restoration of their embryonic epigenetic program. Additionally, MBNL proteins are involved in $\text{Ca}_v\beta 1$ regulation of expression, at least through *Cacnb1* mRNA processing via 3'UTR modulation. Importantly, we provided insights into $\text{Ca}_v\beta 1$ isoform roles in NMJ pre-patterning and post-natal maturation/maintenance as well as in myotonia DM1 feature.

$\text{Ca}_v\beta 1$ isoforms characterization

I- Deciphering $\text{Ca}_v\beta 1$ isoforms: identification/characterization

The skeletal muscle $\text{Ca}_v\beta 1$, encoded by *Cacnb1* gene was the first $\text{Ca}_v\beta$ protein to be discovered and cloned in the 90' (Pragnell et al., 1991; Ruth et al., 1989), and in 1992 it was demonstrated that several $\text{Ca}_v\beta 1$ isoform, encoded by the same *Cacnb1* gene, existed (Powers et al., 1992). $\text{Ca}_v\beta 1A$ has long be considered as the adult isoform (Gregg et al., 1996; Taylor et al., 2014, 2009) but in 2019, the study of Traoré and colleagues demonstrated that $\text{Ca}_v\beta 1D$ and not $\text{Ca}_v\beta 1A$ was the adult constitutive isoform, these proteins sharing 97% of sequence homology (Traoré et al., 2019). This same study revealed the existence of $\text{Ca}_v\beta 1E$, encoded by *Cacnb1E*, as an embryonic isoform, re-expressed in adult muscle after nerve damage (Traoré et al., 2019). The characterization of both of these isoform mRNA transcripts was made via RNA seq technology and validated by RT-PCR of transcripts fragments. However, before RNA sequencing, mRNA must be fragmented, converted to cDNA and amplified. The subsequent reads reassembling often leads to multi-mapping alignment challenges. In our 2019 study, we dealt with the challenge of multiple isoforms of *Cacnb1* gene and identified *Cacnb1E* based on mRNA fragment scale reassembly. In this new study, Nanopore sequencing technology, which sequences mRNAs from end to end, allowed the identification of *Cacnb1A* as another embryonic isoform in skeletal muscle. One limitation of our Nanopore study is that it does not allow the evaluation of transcript abundance sequenced from different TUs, meaning that we do not have access to a notion of quantity of *Cacnb1A* vs *Cacnb1D* vs *Cacnb1E* transcripts in skeletal muscle during embryogenesis and in adult muscle. To overcome this issue, the next step would be the use of Nanopore sequencing with oligo(dT) priming, providing quantitative data on transcript abundance thus allowing the measurement of gene expression levels, without specific priming amplification biases.

Another challenge we need to address is the precise validation of the corresponding $\text{Ca}_v\beta 1$ proteins by mass spectrometry proteomic. This technology identifies proteins by returning multiple peptide identifications. However, just as RNAseq requires dealing with multi-mapping reads, mass spectrometry proteomic encounters peptides that are shared by various protein isoforms. We have

not been able to validate the different $\text{Ca}_v\beta 1$ protein isoforms by mass spectrometry, despite their separation by molecular weight, because no peptide is unique to a single isoform. To overcome this issue, long-read proteogenomic analysis would be necessary.

II- $\text{Ca}_v\beta 1$ early isoform

In *Cacnb1* transcripts, exon7 exists as two mutually exclusive forms: exon7A, present in *Cacnb1A*, *Cacnb1D* and *Cacnb1E* isoforms (in other words, in skeletal muscle isoforms), and exon7B found in *Cacnb1B*, *Cacnb1C* and *Cacnb1F* isoforms. In this study, we have shown that during early embryogenesis, exon7 (both A and B) is completely excluded in skeletal muscle. To our knowledge, this is the first report of a *Cacnb1* transcript lacking exon7, this exclusion resulting in a frameshift and the appearance of a STOP codon in exon8. Given the role of MBNL proteins in regulating a wide range of mRNA transcript splicing events, and more specifically MBNL3 during embryogenesis, we wonder if exon7A exclusion may be associated with MBNL3 splicing factor activity.

A major question concerns this potential new $\text{Ca}_v\beta 1$ early isoform since the presence of a premature STOP codon usually triggers the Non-sense Mediated Decay (NMD) mechanism, a translation-coupled process that eliminates aberrant mRNA to prevent potential molecular errors. The distinction between normal and premature STOP codon depends on the mRNA context: the translation machinery moves across the transcript, and Release Factors like the eukaryotic Translation Termination Factor 1 (eRF1) that recognize STOP codons. Normal Termination Codons (NTC) are reinforced by the presence of termination-enhancing factors, while Premature Termination Codons (PTC) are not. During the first round of translation, the ribosome displaces the Exon Junction Complex (EJC), a process incomplete if the ribosomes stopes at a PTC. The mechanisms triggering NMD are complex but generally leads to the degradation of transcripts with a PTC, ensuring the elimination of truncated proteins that might be toxic (Celik et al., 2015; Chu et al., 2021). Consequently, this PTC in *Cacnb1* exon8 could results in two different outcomes:

- Degradation by NMD: In this case, the exclusion of exon7A might be a way to prevent the precocious expression of $\text{Ca}_v\beta 1$ protein isoforms.
- Escape from NMD: It has been reported that 5 to 30% of transcript are resistant to NMD (Hoek et al., 2019). Additionally, Zetoune and colleagues demonstrated that NMD efficiency varies according to the tissue, leading to differential expression of truncated protein (Zetoune et al., 2008), meaning that even when NMD is efficient for one tissue, it is not a rule for another tissue. In this case, it would be of great interest to decipher the function of this new $\text{Ca}_v\beta 1$ early isoform.

To validate the existence of $\text{Ca}_v\beta 1$ early isoform, preliminary experiments are ongoing to use mass spectrometry proteomic analyses. The absence of exon7A results in the formation of peptides at the beginning of exon8, which are not present in any other $\text{Ca}_v\beta 1$ isoform and can be detected through mass spectrometry proteomic analysis.

Regulation of Ca_vβ1 isoforms expression

I- Promoter regulation

The mechanisms underlying the regulation of Ca_vβ1 protein isoform expressions are currently unknown. Our study shed light on the use of two differential promoters, located in exon1 (Prom1) and exon2B (Prom2) to drive the independent expression of the embryonic/perinatal isoforms Ca_vβ1A/E and the adult isoform Ca_vβ1D, respectively. However, the factors responsible for the differential regulation of these promoters during development and after nerve damage, are still to be investigated. To gain insights into transcription factors binding at these promoter regions and potentially regulating them, we used the UCSC Genome Browser, an online software allowing comprehensive visualization and analysis of genomic data, including features like transcription factors binding sites. Among the wide range of transcription factors potentially binding to Prom1 and Prom2 regions, we selected a few that could be relevant to skeletal muscle tissue:

- Myogenin presents binding sites in both Prom1 and Prom2 regions, this muscle-specific transcription factor is known to promote transcription of muscle-specific target genes and especially in genes important for muscle differentiation and myogenesis.
- BRD4, potentially binding Prom2 region, is known to act as a regulator of catabolic genes in skeletal muscle, and regulating myogenesis by impairing myogenic differentiation (Segatto et al., 2017; Yang et al., 2022).
- KDM1A (or LSD1), potentially binding Prom1, presents beneficial effect on muscle regeneration and recovery after injury by regulating key myogenic transcription factor genes (Tosic et al., 2018).
- MEF2A, potentially binding Prom2, is possibly one very interesting transcription factor for the regulation of *Cacnb1* promoters since MBNL proteins have been shown to regulated their activity. MEF2A belongs to MEF2 transcription factor family, working in concert with MyoD to regulate muscle gene transcription (Potthoff and Olson, 2007). Each MEF2 gene has a highly conserved β-exon between exon6 and exon7, subject to alternative splicing which, when included, results in enhancing MEF2 activity on their targeted promoters (Zhu et al., 2005). Interestingly, MBNL3 has been showed to promote MEF2 β-exon exclusion (Lee et al., 2010). One hypothesis is that in adult muscle, MEF2A β-exon inclusion activates Prom2. Conversely, during embryogenesis, when MBNL3 expression is high, and after nerve damage, when MBNL3 is re-expressed, this splicing factor excludes MEF2A β-exon, making the protein a less effective transcription factor, leading to reduced activation of Prom2. Moreover, MEF2A is mis-spliced in immortalized muscle cells derived from patients affected by DM1 (Arandel et al., 2017).

We investigated potential enhancer regions located upstream or downstream of *Cacnb1* promoters to understand how they are modulated. Using the UCSC Genome Browser, which also provides information about DNA chromatin interactions based on referenced Hi-C (Chromosome conformation capture technique), ChIA-PET (Chromatin Interaction Analysis with Paired-End Tag) or Capture-C

(Capture chromatin conformation) data, we looked after visual indicators of physical interactions between Prom1 or Prom2 regions and potential enhancer regions that could regulate them. We identified e6289 and e6307 as two enhancer regions physically linked with *Cacnb1* promoters, located approximately 55kb upstream and 327kb downstream respectively (**Fig. 26**). However, neither of these enhancer regions display the activating epigenetic marks presented here, contrasting with the active epigenetic landscape observed at Prom1 in embryonic (E12) muscles and at Prom2 in adult EDL, Quadriceps and SOL muscles (**Fig 27, Fig. 28**). This suggests that these enhancers regions, despite being physically linked, are not regulating the *Cacnb1* promoters.

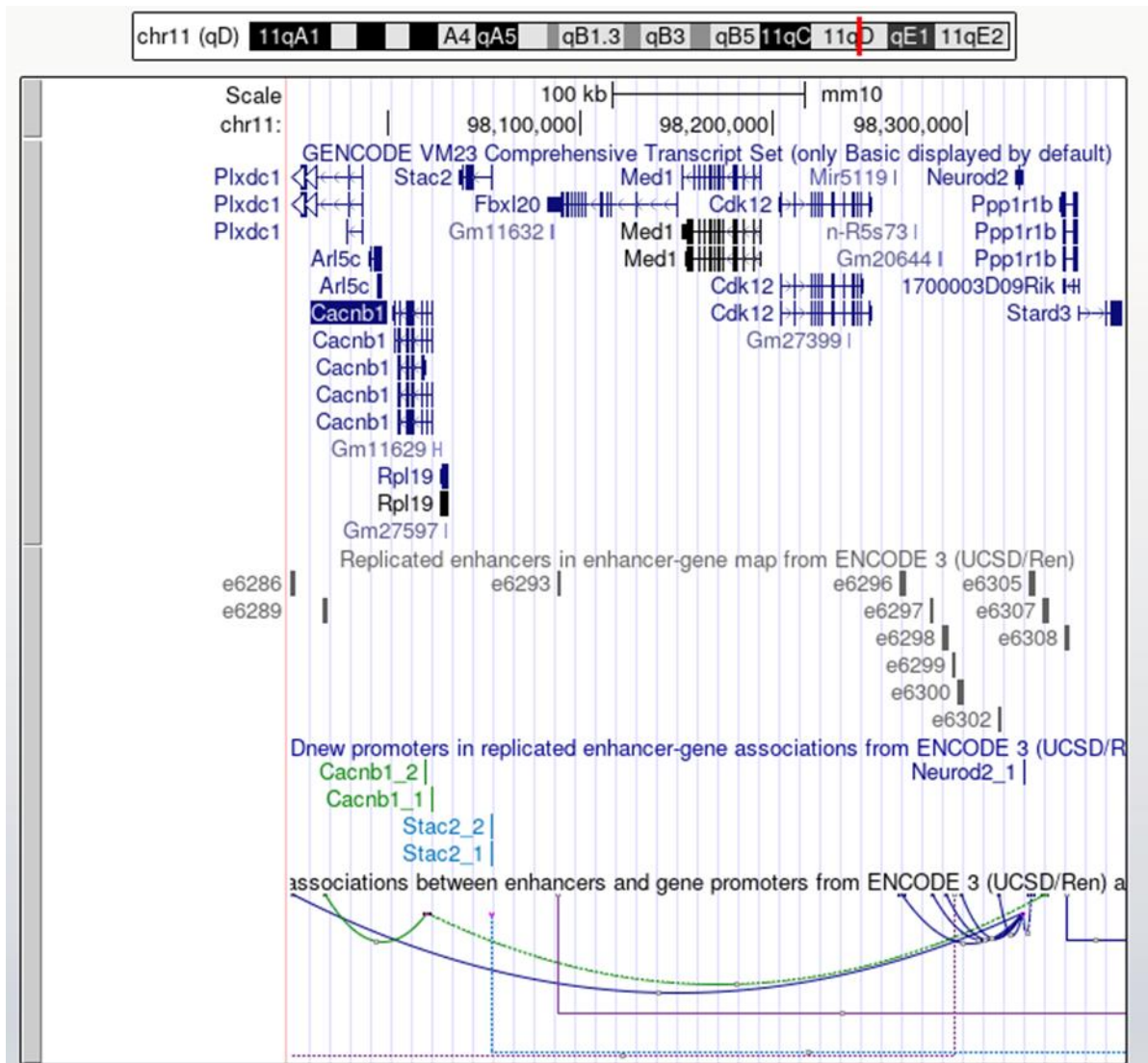


Figure 26. *Cacnb1* promoters display physical interaction with two enhancer domains.

Image from UCSC Genome Browser showing the genomic region surrounding *Cacnb1* Prom1 and Prom2 (highlighted in blue). Annotated enhancer regions are visible along the sequence. Physical interactions between these enhancers and *Cacnb1* promoters are indicated by green connectors. Two distinct enhancer regions (e6289 and e6307, highlighted in red), are shown to interact with *Cacnb1* promoters.

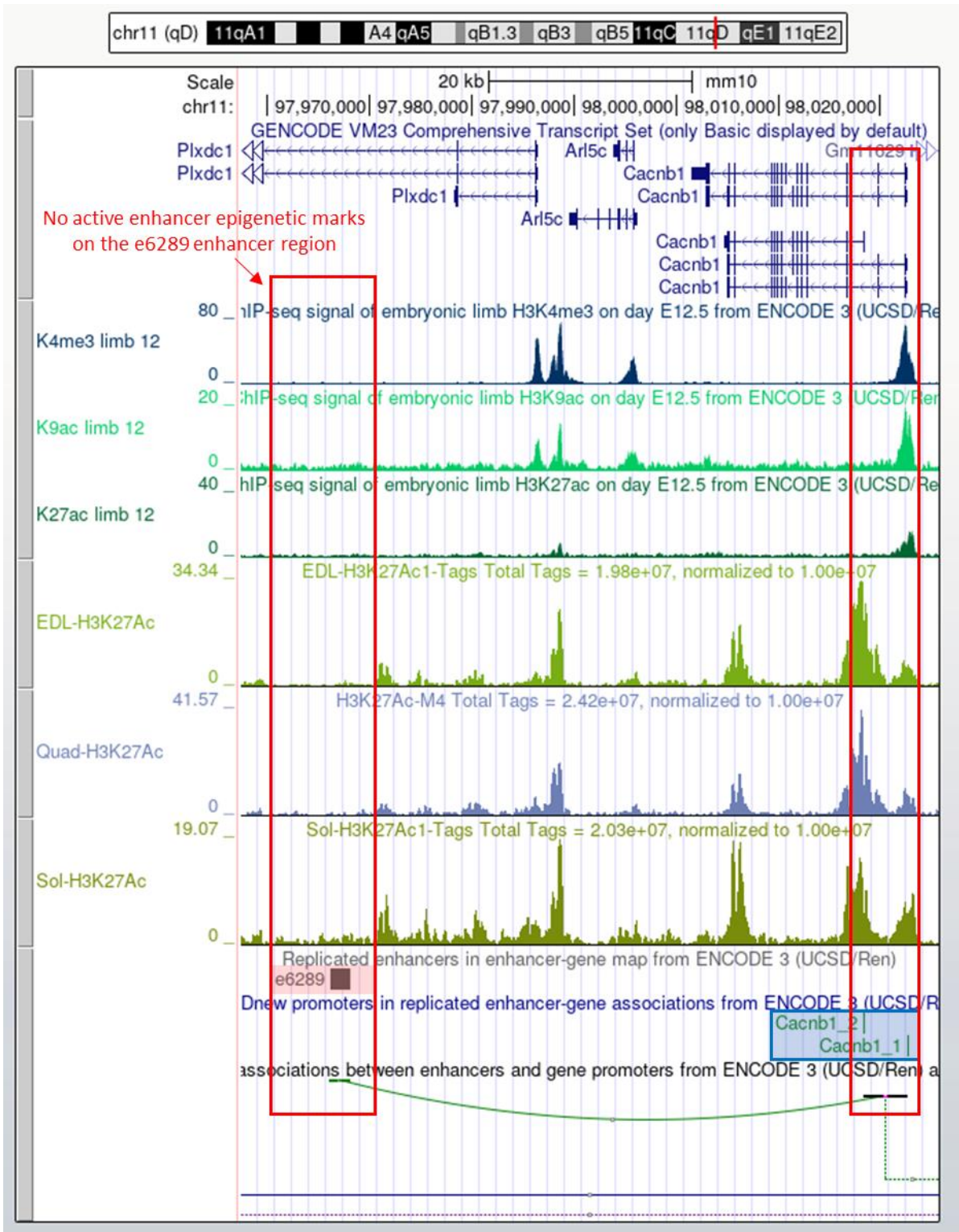


Figure 27. Lack of activating epigenetic marks at the e6289 enhancer region.

Screenshot from UCSC Genome Browser showing the relative abundance of activating epigenetic marks (H3K3me3, H3K9ac and H3K27ac) at Cacnb1 promoters and e6289 enhancer region in embryonic (E12) muscles (ENCODE project) or adult muscles (Extensor digitorum longus (EDL), Quadriceps and Soleus).

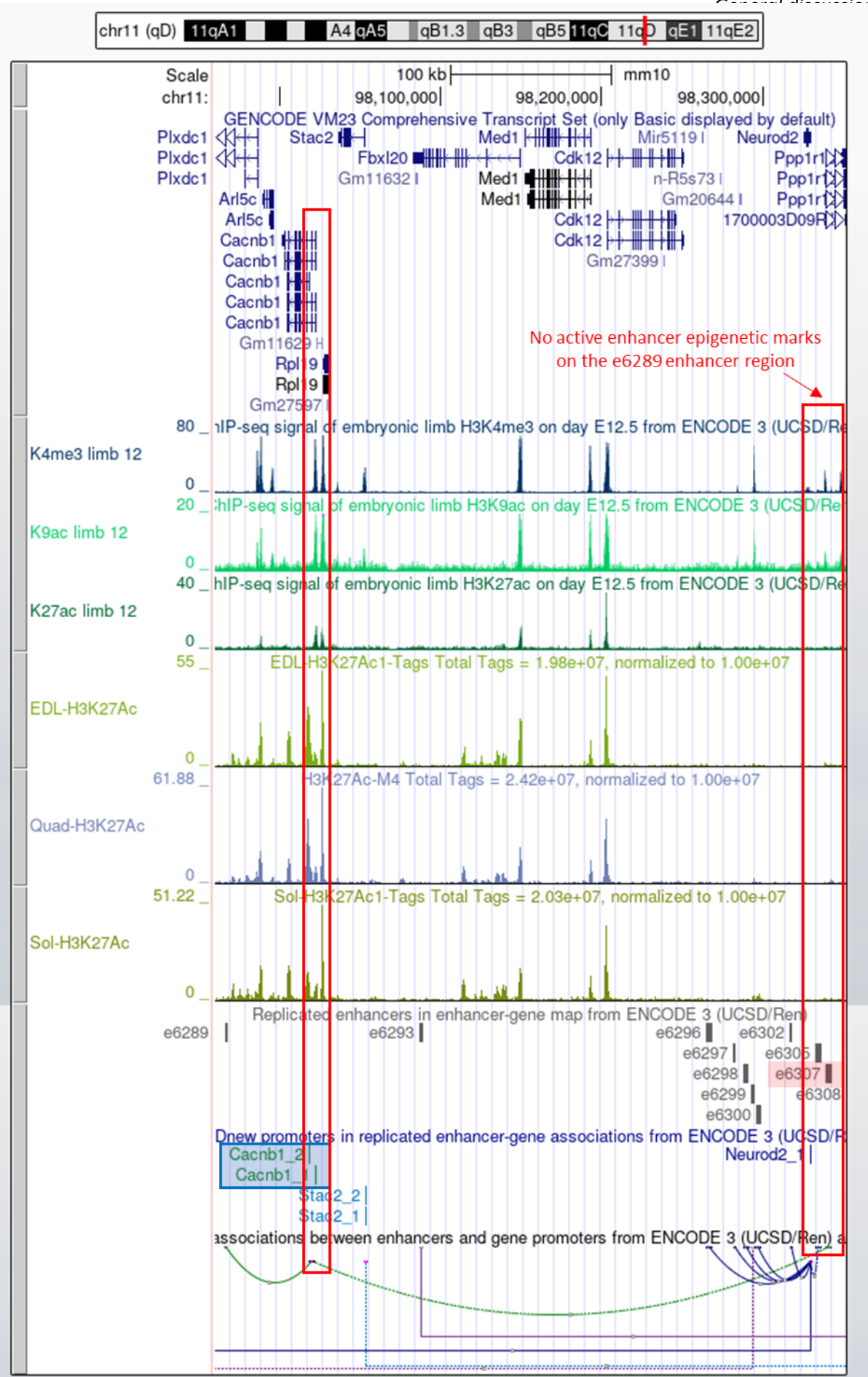


Figure 28. Lack of activating epigenetic marks at the e6307 enhancer region.
 Screenshot from UCSC Genome Browser showing the relative abundance of activating epigenetic marks (H3K3me3, H3K9ac and H3K27ac) at Cacnb1 promoters and e6307 enhancer region in embryonic (E12) muscles (ENCODE project) or adult muscles (Extensor digitorum longus (EDL), Quadriceps and Soleus).

II- 3'-UTR regulation

The 3'-UTR of transcript plays a crucial role in post-transcriptional regulation of gene expression by influencing mRNA stability, localization, translation efficiency, and interaction with regulatory actors like RBP (Hong and Jeong, 2023). In this study we demonstrated MBNL-related post-transcriptional regulation of *Cacnb1* gene through their 3'-UTR. Indeed, the different $Ca_v\beta 1$ isoforms display distinct 3'-UTRs: $Ca_v\beta 1A$ and $Ca_v\beta 1D$ end with exon13end while $Ca_v\beta 1E$ ends with exon14 (**Fig. 1A** – article in preparation). In C2C12 cells, enhanced MBNL3 expression results in decreased Luciferase activity when upstream of $Ca_v\beta 1A/D$ 3'-UTR, whereas MBNLs have no impact on Luciferase activity when upstream of $Ca_v\beta 1E$ 3'-UTR. This suggests that the exon13end-related 3'-UTR contains MBNL binding site(s), while exon14-related 3'-UTR does not. These data are corroborated with CLIP experiments showing a direct interaction between MBNL3 and *Cacnb1* 3'UTR (Wang et al., 2012). However, since MBNL proteins influence myoblast proliferation and differentiation, and *Cacnb1* levels fluctuate during these myogenic stages, we cannot rule out the possibility that the observed effect is indirect. It may occur through MBNL proteins' impact on myogenesis, which in turn could affect *Cacnb1* processing. The observed post-transcriptional regulation of *Cacnb1* expression via its 3'-UTR can be related to either mRNA reduced stability or decreased translation efficiency.

$Ca_v\beta 1$ role in NMJ processes

I- $Ca_v\beta 1$ effect on AChR aggregation

a) Hypothesis on the regulation of upstream molecular players

While there was no defect in the aggregation process (same number of AChR clusters), we did observe an increase in the size of AChR clusters in our highly differentiated myotube model upon shEx2A treatment, together with elevated MuSK protein level. Different hypothesis can be raised:

1) In this study, the evaluation of Lrp4 protein is missing, we cannot exclude that the increase of MuSK is combined with Lrp4 protein increase, which in turn would explain the increase in AChR cluster size by modulating its phosphorylation state.

2) Additionally, myogenin, which is positively regulated in *Cacnb1* KO proliferative myoblasts (Taylor et al., 2014), is similarly increased in our highly differentiated myotube system upon ablation of $Ca_v\beta 1$ embryonic isoforms. Myogenin has been described to positively regulate MuSK transcription (Tang and Goldman, 2006), which could explain the increase in MuSK expression and the related effects mentioned in point 1). Another possible explanation could be the action of Myogenin in a MuSK-independent manner. Indeed a myogenin-dependent AChR clustering in aneural myotubes has been demonstrated, and neither MuSK, rapsyn or AChRs overexpression in *Myogenin* Knock Down (KD) myotubes was associated with a rescue of the AChR clustering defects (Macpherson et al., 2006). This suggest that Myogenin controls crucial actors of AChR clustering, this would need to be further explored.

3) Furthermore, the size of AChR clusters could be modulated by the level of myotube maturation also independently of a MuSK effect. We observed precocious maturation of myotubes and one possibility is that AChR clusters enlarged due to increased myotube width, perhaps through a mechanical effect.

b) A Ca^{2+} related process?

A previous study demonstrated that genetically ablated *Cacnb1* mice exhibited muscle patterning defects and aberrant innervation at E14.5 and E18.5 in mice (Chen et al., 2011). However, to really conclude with pre-patterning defects, it would have been more accurate to look at the aspect of AChR clustering before axonal growth cone arrival around E14.5. Here it cannot be excluded that the observed defects are modified or amplified by nerve-derived factors. By working on non-innervated myotubes *in vitro*, we focused on the role of $Ca_v\beta 1$ isoforms during nerve-independent stages (although *in vitro* studies are not fully transposable to *in vivo* processes) and found increased AChR clusters size and enhanced myotube maturation. These findings align with Chen and colleagues' post-innervation results, which showed increased endplate areas and more perforated clusters, indicated a precocious maturation. Our data suggest that the defects observed in their study originate from abnormalities occurring before innervation begins.

Their study (Chen et al., 2011) concluded on the role of $Ca_v\beta 1$ isoforms in regulating pre-patterning through Ca^{2+} flux, independently of ECC. This is supported by other studies showing an impairment in pre-patterning in models in which calcium influx/release is disrupted, no matter the ECC status (Kaplan et al., 2018; Kaplan and Flucher, 2019). Our study add insight in the $Ca_v\beta 1$ role in AChR aggregation by suggesting an effect that might be independent of Ca^{2+} . Indeed, their interpretation only considered $Ca_v\beta 1$ as a regulator of the Ca_v1 channel ($Ca_v\beta 1D$) and neglected the role of others $Ca_v\beta 1$ isoforms in gene expression regulation (Vergnol et al., 2022). In skeletal muscle, the $Ca_v\beta 1$ -related gene regulation role was suggested to be linked to its translocation to the nucleus via an NLS sequence in exon1, which is shared by the two embryonic isoforms that we downregulated. We obtained results consistent with Chen and colleagues *in vivo* findings, but we suggest that $Ca_v\beta 1$ embryonic isoforms, in addition to $Ca_v\beta 1D$ (the isoform associated with Ca_v1 at the triad), are involved in the pre-patterning of the NMJ at very early stages before innervation is established, in a Ca^{2+} independent manner.

II- $Ca_v\beta 1$ effect on NMJ maturation/maintenance

NMJ formation, maturation and maintenance depends on signals from both pre- and post-synaptic compartments. At birth the NMJ already features neurotransmission but still needs to mature to ensure its optimal functionality. This maturation is complete approximately 3 weeks after birth with the increased size of AChR clusters, the morphological development of NMJ in pretzel-like shape and the development of deeper neural folds. Distinguishing between defects originating from such maturation features and those from maintenance defects in post-natal stages is very challenging. Therefore, in this study, the defects observed in NMJ morphology of 1-month old pups injected at 7

days with shEx2A, could be due to alterations in maturation, maintenance, or a combination of both. Given the increased muscle maturation observed under ablation of embryonic/perinatal $\text{Ca}_v\beta 1$ isoforms in our model, NMJ fragmentation might be a mechanism to extend as the muscle matures precociously. Indeed, the link between NMJ fragmentation and degeneration should not be systematic and some studies suggest that endplate fragmentation could also be a sign of regeneration, as a process of synaptic plasticity aimed at extending synaptic area (Haddix et al., 2018; Li et al., 2011; Slater, 2020).

In aging muscles, where $\text{Ca}_v\beta 1A/E$ expressions are defective (Traoré et al., 2019), NMJ morphological defects including postsynaptic fragmentation, reduced AChR density and synaptic decoupling are reported (Valdez et al., 2012), but these aging-related NMJ morphological abnormalities precedes changes in NMJ molecular markers expression (Massiré et al., 2024). Therefore, the fact that we do not observe a global alteration in NMJ actors despite NMJ morphological alteration is not necessarily surprising. Moreover, increased protein expression of MuSK, whose tyrosine kinase domain activation is known to induce transcription of key NMJ genes in sub-synaptic nuclei could be the hallmark of the initiation of such process and we could observe greater modulation of NMJ players after a longer period of treatment. In parallel, our adult *in vivo* shEx2A model shows transcriptional signs of NMJ remodeling with increased *AChRa1*, *AChRg* and *Musk* expressions after 2 months of treatment, supporting this timeframe-related hypothesis. Nevertheless, this adult model would require further deep analyses to study NMJ molecular actors at the protein level, and morphological NMJ aspect, that we suppose to align with the natural aging progression in mice, like the post-natal *in vivo* shEx2A model do. Globally, we can presume downregulating $\text{Ca}_v\beta 1A/E$ isoforms in skeletal muscle reproduce neuromuscular aging features.

One aspect that remains to be explored is the effect of $\text{Ca}_v\beta 1$ on NMJ stability following nerve damage, specifically regarding muscle re-innervation. Indeed, $\text{Ca}_v\beta 1E$ has been shown to trigger GDF5 pathway after nerve injury to prevent muscle mass loss (Traoré et al., 2019), and GDF5 is known to help preserving NMJ morphology during aging and stimulates re-innervation related genes (Massiré et al., 2024). Studying how $\text{Ca}_v\beta 1$ influences these innervation-dependent processes could provide the scientific community with important information for understanding these neuromuscular mechanisms.

III- Limitations of the highly-differentiated myotube model

Overall, while the results obtained from these highly differentiated myotubes cannot be fully extrapolated to *in vivo* conditions, they do suggest the mechanism in play in the muscles of developing embryos. Moreover, given that the satellite cells we differentiate are isolated from 7 days old pups, therefore coming from an environment with already pre-patterned and innervated fibers, it cannot be excluded that they have an intrinsic specialization to form AChR clusters, which would be absent in

satellite cells before innervation begins at E14.5. Therefore, this system is not representative of *in vivo* pre-patterning, but it uses agrin to study the aggregation capacity of AChR.

Fully translating our *in vitro* AChR aggregation results to *in vivo* models strictly before innervation is challenging. Intra-placental injections imply a very narrow time frame between the earliest possible injection at E9.5 and the onset of innervation at E14.5.

Ca_vβ1s & DM1 pathophysiology

I- The shMbnl1 model

In this study, we used the shMbnl1 model to study the effect of MBNL modulation on Ca_vβ1 isoforms expression. The downregulation of MBNL1 protein alone, led to the increase in MBNL2 protein levels, described as having a compensatory effect since these proteins share a wide range of target genes. In our study, MBNL2 compensatory increase did not prevent the MBNL1-related molecular defects since we did observe the mis-splicing of all the target genes tested, characteristic of DM1 as well as myotonia. However, that these effects would probably have been exacerbated upon MBNL1 and MBNL2 combined depletion.

One unexpected observation was the increase in *Mbnl3* expression upon downregulation of *Mbnl1 in vivo*, which, to our knowledge, has never been described. We suggest the existence of a negative regulation driven by MBNL1 protein on *Mbnl3* expression. MBNL3 is known to be important for a proper muscle regeneration (Poulos et al., 2013). Given that our model presents an increase in centrally nucleated fibers (data not showed), we cannot exclude that the upregulation of *Mbnl3* expression is linked with muscle regeneration, and not directly related with the downregulation of *Mbnl1*. However, several arguments did not align with this hypothesis: upon nerve damage in adult muscle, *Mbnl3* expression is increased while no regeneration is observed and no satellite cell activation is described, suggesting that the two processes are not always linked. Moreover, in C2C12 cells, the induced *Mbnl3* OE is enhanced by the downregulation of *Mbnl1*, in favor of the MBNL1 induced modulation of MBNL3 expression hypothesis.

An issue we encountered was the evaluation of MBNL3 at the protein level, as both WB and IF analysis were unsuccessful. Consequently, we had to base our conclusions on transcript modulation only.

II- Ca_vβ1 protective effect on myotonia?

Under shMbnl1, myotonia was observed, in relation with an impaired *Clc1* splicing, an impaired CLC1 protein expression and localization, and a change in fiber-type toward oxidative fibers. To further understand the mechanisms explaining the exacerbated myotonia under the additional Ca_vβ1 embryonic isoform depletion in the shMbnl1 model, a deeper study on the molecular mechanisms behind CLC1 localization at the membrane and behind CLC1 function would be needed. To begin with,

CLC1 localization depends on different cell signalling pathways (Conte et al., 2020; Papponen et al., 2005) that could be altered by embryonic $\text{Ca}_v\beta 1$ isoforms. Besides, our study allowed the visualization of CLC1 protein at the membrane but not specifically at T-tubules. IF analyses on transverse muscle sections or isolated muscles fibers under shMbnl1 vs shMbnl1+shEx2A treatment would allow visualization of CLC1 protein in T-tubule compared to sarcolemma, which might help understanding the origin of the exacerbated myotonia under $\text{Ca}_v\beta 1$ embryonic isoforms. In addition to its expression and localization defects, the biophysical behaviour of the Cl^- channel might also be altered. Investigating pathways regulating its function, like protein kinase C (PKC) isoforms (Conte et al., 2020), might be investigated.

III- MBNL1

Several studies report NMJ defects in models with impaired MBNL proteins. For instance, abnormalities in NMJ were described in the diaphragm of a poly(CUG) transgenic mouse model for DM1, showing decreased endplate size and AChR density on the post-synaptic membrane (Panaite et al., 2008). More severe defects, including NMJ fragmentation, were reported in TA muscles in *Mbnl1^{-/-};Mbnl2^{+/-}* mice (Lee et al., 2013). Corroborating these results, preliminary data from our *in vivo* shMbnl1 mouse model shows increased expression of several molecular components involved in NMJ remodeling, such as *AChRa1*, *AChRg*, *Musk*, and *Ncam*, at transcriptional level. Moreover, we observed an increased tetanic fade, suggesting either NMJ instability or an imbalance between the amount of ACh released from the pre-synaptic compartment and the number of AChR at the post-synaptic surface (Nagashima et al., 2013). These preliminary data suggest an altered NMJ stability under *Mbnl1* downregulation and would need to be enriched with the study of both morphological features and biochemical actors of the NMJ, to better understand these phenomena.

IV- MBNL3

Upon nerve damage, pre- and post- synaptic systems undergo changes, exhibiting plasticity that support repair and reinnervation. In skeletal muscle, denervation induces changes in synaptic gene expression, leading to re-expression of embryonic AChR γ subunit and other proteins involved in the maintenance and repair of these peripheral synapses. In addition to NMJ-related genes, a wide range of factors also revert to their embryonic form, including MBNL3 and $\text{Ca}_v\beta 1\text{A/E}$ (Traoré et al., 2019). Our preliminary data show that downregulating *Mbnl3* after nerve damage exacerbates the modulation of NMJ-related genes (data not showed), similarly to $\text{Ca}_v\beta 1\text{A/E}$ downregulation. This suggest that MBNL3 may influence NMJ regeneration after nerve injury, either through its modulatory effect on $\text{Ca}_v\beta 1$ isoforms, via a yet unknown independent pathway, or a combination of both. Given that $\text{Ca}_v\beta 1\text{E}$ has been shown to trigger the GDF5 pathway, which helps in preserving NMJ morphology during aging (Massiré et al., 2024), it would be interesting to investigate whether MBNLs, $\text{Ca}_v\beta 1$ s and GDF5 are part of a common pathway that regulates NMJ function and morphology.

A study by Poulos and colleagues in 2013 shed light on the role of MBNL3 in DM1 pathophysiological features by showing that its inhibition leads to impaired muscle functions and impaired adult muscle regeneration capacities, normally associated with age. They proposed their *Mbnl3^{ΔE3}* mouse model as a novel model for studying the DM1 age-associated muscle defects. They did not study the morphological, molecular or functional aspect of NMJ but it might be an interesting aspect to investigate, especially since MBNL3, expressed at a very low basal level in adult muscle, decreases during aging (data not showed).

Which of the embryonic Ca_vβ1 isoform is involved in the different described processes?

I- In NMJ formation, maturation and maintenance

In this study, we examined the effects of downregulating both Ca_vβ1A and Ca_vβ1E isoforms at distinct developmental stages of the NMJ, firstly on the *in vitro* pre-patterning, and secondly on its maturation/maintenance during the first weeks of life in mice with normal innervation. A limitation of our study is the lack of precision on which of Ca_vβ1A or Ca_vβ1E embryonic/perinatal isoforms is responsible for the observed effects. The use of downregulation tools targeting exon14 would allow the specific depletion of Ca_vβ1E, but depleting specifically Ca_vβ1A is impossible since it does not have a unique sequence that distinguishes it from Ca_vβ1D and Ca_vβ1E. Using *Cacnb1^{-/-}* mouse model (Gregg et al., 1996) would help address this issue by allowing to test phenotypes through the use of either Ca_vβ1A or Ca_vβ1E transgenes in different contexts:

- These mice are lethal at birth due to impaired ECC causing respiratory failure. However, satellite cells can be isolated from late embryogenic stages (around E19-E20), and used for *in vitro* AChR aggregation studies. The addition of either Ca_vβ1A or/and Ca_vβ1E transgenes, would allow to look after their individual and combined effect on *in vitro* AChR aggregation.
- Intra-placental injection of the adult Ca_vβ1D before birth might allow for mice survival and it would be possible to play with either Ca_vβ1A, Ca_vβ1E or a combination of both transgenes to see their effect in NMJ maturation and maintenance in post-natal stages.

II- In DM1 pathophysiology

Similarly, we downregulating simultaneously both Ca_vβ1A and Ca_vβ1E isoforms in our shMbnl1 model to study their combinatory effect on DM1 features. However, the same limitation is true here, we do not know which of Ca_vβ1A or/and Ca_vβ1E is responsible for the observed modulations. Similarly, Ca_vβ1E can be individually depleted through exon14 targeted shRNA, but it cannot be done for Ca_vβ1A, as explained in the previous section. Instead of downregulating their expression, increasing specifically their levels by transgenic tools can be done to investigate if their individual or combinatory expression can improve DM1 molecular and functional parameters.

III- In ECC during embryogenesis

As mentioned in introduction of this manuscript, three prerequisites are needed to ensure a proper ECC mechanism: 1) $\text{Ca}_v1.1$ and RyR1 have to be correctly expressed and localized at the triad, 2) $\text{Ca}_v1.1$ needs to be able to ensure the charge movement and 3) $\text{Ca}_v1.1$ must be organized in tetrads. $\text{Ca}_v\beta1$ protein regulates $\text{Ca}_v1.1$ protein in a way to fulfil, or at least participate, to these prerequisites by being essential for $\text{Ca}_v1.1$ docking at the sarcolemma and at the triad (Brice et al., 1997), triggering its organization in tetrads and ensuring charge movement facilitation. However, while these roles have been associated with the $\text{Ca}_v\beta1$ proteins, there is no indication on which isoform holds them during the different skeletal muscle stages of life. $\text{Ca}_v\beta1D$ is the one located at the triad while $\text{Ca}_v\beta1E$ has been described at Z lines and in nuclei (Taylor et al., 2014; Traoré et al., 2019), it is therefore fair to think that $\text{Ca}_v\beta1D$ is the one holding such $\text{Ca}_v1.1$ -related properties critical for ECC. However, $\text{Ca}_v\beta1D$ protein is detectable only at perinatal stages whereas triadic proteins are already located at the triad earlier, suggesting that other $\text{Ca}_v\beta1$ isoforms might hold this role during embryogenesis. Supporting this hypothesis, the key region for $\text{Ca}_v\beta1$ - $\text{Ca}_v1.1$ interaction is in the GK domain, a region shared by all isoforms. Therefore, it is reasonable to think that one or several embryonic $\text{Ca}_v\beta1$ isoforms is able to fill this function during embryogenesis. In this context, the loss of ECC efficacy described in $\text{Ca}_v\beta1^{-/-}$ at E16 (Gregg et al., 1996) might be the result of the absence of either $\text{Ca}_v\beta1A$, $\text{Ca}_v\beta1E$, $\text{Ca}_v\beta1\text{early}$ or a combination of them.

Supplementary data

Name	Forward	Reverse	Application
Mbnl1	GTTGCAGCCCGTGCCAATGTT	TTGGGAAACAGGCCCCAGGTAA	RT-qPCR
Mbnl2	GAGTAATTGCTGCTTTGATTCCCTCAA	GGAGCGGCGTTCCTGGAAACATA	
Mbnl3	GAGTAATTGCTGCTTTGATTCCCTCAA	GAACCTCTGGCAGTGCAAGA	
Cacnb1 (Ex2A-Ex3)	GGCAAGTACAGCAAGAGG	GTTTGGTCTTGGCTTTCTCG	
Cacnb1 (Ex2B-Ex3)	CAGCCGGACCTGGTAGTG	GTTTGGTCTTGGCTTTCTCG	
Cacnb1 (all isoforms)	GACAGCCTTCGTCTGCTGCAG	CATGTCTGTCACCTCATAGCC	
Myogenin	ACGATGGACGTAAGGGAGTG	AGTGAATGCAACTCCCAGAG	
MCK	AGACAAGCATAAGACCGACCT	AGGCAGAGTGTAACCCTTGAT	
S100a4	GGCAAGACCCTTGGAGGAGGC	GAACCTGTCAACCTCTTGCCTGAG	
Myhc3	AAGGCCAAAAAGGCCATC	CATTCCAGACGGTTGCTGCAG	
Myhc8	CTGTAAAGGGTTAAGGAAGC	CGCCTGTAATTTGTCCACCA	
Lrp4	AGTCAACGCAAGGCTGTCATTA	GTTGGCACTATTGATGCTCTTGG	
Rapsyn	CTGGATGAAGTCTGTTGAGAAG	CCGAGCAGTATCAATCTGGACC	
Achra1	AAGCTACTGTGAGATCATCGTCAC	TGACGAAGTGGTAGGTGATGTCCA	
Achrg	GCTCAGCTGCAAGTTGATCTC	CCTCCTGCTCCATCTCTGTC	
Musk	TTCAGCGGGACTGAGAACT	TGTCTTCCACGCTCAGAATG	
PO	CTCCAAGCAGATGCAGCAGA	ATAGCCTTGCGCATCATGGT	RT-qPCR + RT-PCR
Cacnb1 (Ex2A-Ex2B-Ex3)	GGCAAGTACAGCAAGAGG	GTTTGGTCTTGGCTTTCTCG	Triplex RT-PCR
	CAGCCGGACCTGGTAGTG		
Cacnb1 (Ex6-Ex8)	GACAGCCTTCGTCTGCTGCAG	CATGTCTGTCACCTCATAGCC	RT-PCR
Nfix	GAGTCCAGTAGATGATGTGTTCTA	CTGCACAACTCCTTCAGCGAGTC	
Atp2a	ATCTTCAAGCTCCGGGCCCT	CAGCTTTGGCTGAAGATGCA	
Clc1	GCTGCTGTCCTCAGCAAGTT	CTGAATGTGGCTGCAAAGAA	
Cacna1s	GCTATTTTGGAGATCCTTGGAA	AGCAGGGTGCGCACACCCTC	
ArfGap2	GACTCTGATTTCTTACAGAACAT	TGCTCTCGGAGCTTCTCTGCCA	
Zasp	GGAAGATGAGGCTGATGAGTGG	TGCTGACAGTGGTAGTGCTCTTC	
Bin1	CTCAATCAGAACCTCAATGATGTCCTG	CTCTGGCTCATGGTTCACTCTGATC	
Camk2b	AGGAGACTGTGGAATGTCTG	GGCATCTTCATCCTCTATGGTTG	
Cacnb1 (-3,6kb)	CTCCAGCCTCCTGTTTCATTC	CTTTGCCCACTGAAATTCTTGG	
Cacnb1 (Ex1-Int1)	ACCTTCCAAGAGATCCCTATG	GGCATATAACCCTTTCCTTCCC	
Cacnb1 (Int1-Ex2A)	CTGGTAGGAGCTGAACTAGGAA	ATGTTGTATCCGAGGACGTA	
Cacnb1 (Int2)	CATGTGCAAACTGCTAGGGTAT	ATAGCATGCTTCTGTGGTTGAG	
Cacnb1 (Ex2B-Int3)	GAAGAGATGAGCTGGGAGAAAG	GCAGTTTGACATGTAGCAATT	
Cacnb1 (Int4)	TTACAATACAAAAGCGACGGGT	GGCAGAGGATGCTGTATAAAG	

Table S1. Primer list for RT-PCR, RT-qPCR, Triplex RT-PCR and ChIP-qPCR.

Name	Sequence
U1-Ex1-Cacnb1-fw	GCAGTCGAACATGTAGCTGACTCAGGTACCCGGACCCGGAGGATCCTCTC
U1-Ex2BInt-Cacnb1-fw	GCAGTCGAACATGTAGCTGACTCAGGTACCCGGACCCGGAGGATCCTCTC
U1-Ex2B-Cacnb1-fw	GCAGTCGAACATGTAGCTGACTCAGGTACCCGGACCCGGAGGATCCTCTC
U2-Ex13end-Cacnb1-rv	TGGATCACTTGTGCAAGCATCACATCGTAGGCTACATGGCGTGCTCCTGAG
U2-Ex14-Cacnb1-rv	TGGATCACTTGTGCAAGCATCACATCGTAGGCTCAGCGGATGTAGAGGC

Table S2. Primer list for Nanopore.

Name/Target	Source	Reference	Species	Application	Dilution
Cacnb1-66:84	ThermoFisher Scientific	Custom antibody	Rabbit		1:1000
Cacnb1-506:524	ThermoFisher Scientific	Custom antibody	Rabbit		1:500
MBNL2	Glenn Morris (CIND)	MB2a - 3B4	Mouse		1:100
AChRa1	Invitrogen	11565752	Mouse		1:100
MyHC	DSHB	MF20	Mouse	WB	1:10
MuSK	Sigma Aldrich	ABS549	Rabbit		1:100
Actin	Merck Millipore	A4700	Mouse		1:5000
Rapsyn			Mouse		1:100
Dok7	Santa Cruz	sc-50463 (H-284)	Rabbit		1:100
Nefm	DSHB	2H3	Mouse		1:500
SV2A	DSHB	SV2	Mouse		1:500
α -Bungarotoxin-Alexa Fluor™ conjugated 594	ThermoFisher Scientific	B13423	Bungarus multicinctus		1:500
MBNL1	Glenn Morris (CIND)	MB1a - 4A8	Mouse		1:100
CLC1	Alpha Diagnostic International	CLC11-A	Rat	IF	1:50
MyHC-I	DSHB	BA-D5-s	Mouse		1:5
MyHC-IIA	DSHB	SC-71-s	Mouse		1:10
MyHC-IIB	DSHB	BF-F3-s	Mouse		1:10
Laminin	Merck Millipore	L9393	Rabbit		1:200
AChRa1	Covance	MRT-609R-506	Rat		
Histone H3	Abcam	Ab1791	Rabbit		0.3µg
H3K9ac	Abcam	Ab113674 (no longer on the market)	Mouse	ChIP	per 10µg of chromatin
RNAPII pS5 (4H8)	Abcam	Ab5408	Mouse		1µg
H3K4me3	ThermoFisher Scientific	PA5-27029	Rabbit		2µg
IgG mouse	Sigma Aldrich	I-5381	Mouse		1.2µg
					2µg

Table S3. Primary antibodies.

Name/Target	Source	Reference	Species	Application	Dilution
StarBright Blue 700 Goat Anti-Mouse IgG	BioRad	12004159	Mouse	WB	1:10 000
StarBright Blue 700 Goat Anti-Rabbit IgG		12004162	Rabbit		
StarBright Blue 520 Goat Anti-Mouse IgG		12005867	Mouse		
StarBright Blue 520 Goat Anti-Rabbit IgG		12005870	Rabbit		
Goat anti-Mouse IgG (H+L) Highly Cross-Adsorbed Secondary Antibody, Alexa Fluor™ 555	ThermoFisher Scientific	A-21424	Mouse	IF	1:1 000
Goat anti-Rabbit IgG (H+L) Highly Cross-Adsorbed Secondary Antibody, Alexa Fluor™ 555		A-21429	Rabbit		
Goat anti-Mouse IgG (H+L) Highly Cross-Adsorbed Secondary Antibody, Alexa Fluor™ 488		A-11029	Mouse		
Goat anti-Rabbit IgG (H+L) Highly Cross-Adsorbed Secondary Antibody, Alexa Fluor™ 488		A-11034	Rabbit		
Goat anti-Mouse IgG (H+L) Highly Cross-Adsorbed Secondary Antibody, Alexa Fluor™ 488		A-11029	Mouse	IF fibres	1:400

Table S4. Secondary antibodies.

REFERENCES

- Adereth, Y., Dammai, V., Kose, N., Li, R., Hsu, T., 2005. RNA-dependent integrin alpha3 protein localization regulated by the Muscleblind-like protein MLP1. *Nat. Cell Biol.* 7, 1240–1247. <https://doi.org/10.1038/ncb1335>
- Ahern, C.A., Arikath, J., Vallejo, P., Gurnett, C.A., Powers, P.A., Campbell, K.P., Coronado, R., 2001. Intramembrane charge movements and excitation- contraction coupling expressed by two-domain fragments of the Ca²⁺ channel. *Proc Natl Acad Sci U S A* 98, 6935–6940. <https://doi.org/10.1073/pnas.111001898>
- Altier, C., Garcia-Caballero, A., Simms, B., You, H., Chen, L., Walcher, J., Tedford, H.W., Hermosilla, T., Zamponi, G.W., 2011. The Cav β subunit prevents RFP2-mediated ubiquitination and proteasomal degradation of L-type channels. *Nat Neurosci* 14, 173–180. <https://doi.org/10.1038/nn.2712>
- Anderson, M.J., Cohen, M.W., 1977. Nerve-induced and spontaneous redistribution of acetylcholine receptors on cultured muscle cells. *J Physiol* 268, 757–773. <https://doi.org/10.1113/jphysiol.1977.sp011880>
- Andersson-Cedergren, E., 1959. Ultrastructure of motor end plate and sarcoplasmic components of mouse skeletal muscle fiber as revealed by three-dimensional reconstructions from serial sections. *Journal of Ultrastructure Research* 2, 5–191. [https://doi.org/10.1016/S0889-1605\(59\)80002-1](https://doi.org/10.1016/S0889-1605(59)80002-1)
- Antzelevitch, C., Pollevick, G.D., Cordeiro, J.M., Casis, O., Sanguinetti, M.C., Aizawa, Y., Guerchicoff, A., Pfeiffer, R., Oliva, A., Wollnik, B., Gelber, P., Bonaros, E.P., Burashnikov, E., Wu, Y., Sargent, J.D., Schickel, S., Oberheiden, R., Bhatia, A., Hsu, L.-F., Haïssaguerre, M., Schimpf, R., Borggrefe, M., Wolpert, C., 2007. Loss-of-function mutations in the cardiac calcium channel underlie a new clinical entity characterized by ST-segment elevation, short QT intervals, and sudden cardiac death. *Circulation* 115, 442–449. <https://doi.org/10.1161/CIRCULATIONAHA.106.668392>
- Arandel, L., Polay Espinoza, M., Matloka, M., Bazinet, A., De Dea Diniz, D., Naouar, N., Rau, F., Jollet, A., Edom-Vovard, F., Mamchaoui, K., Tarnopolsky, M., Puymirat, J., Battail, C., Boland, A., Deleuze, J.-F., Mouly, V., Klein, A.F., Furling, D., 2017. Immortalized human myotonic dystrophy muscle cell lines to assess therapeutic compounds. *Dis Model Mech* 10, 487–497. <https://doi.org/10.1242/dmm.027367>
- Arber, S., Burden, S.J., Harris, A.J., 2002. Patterning of skeletal muscle. *Curr Opin Neurobiol* 12, 100–103. [https://doi.org/10.1016/s0959-4388\(02\)00296-9](https://doi.org/10.1016/s0959-4388(02)00296-9)
- Armstrong, C.M., Bezanilla, F.M., Horowicz, P., 1972. Twitches in the presence of ethylene glycol bis(- aminoethyl ether)-N,N'-tetracetic acid. *Biochim Biophys Acta* 267, 605–608. [https://doi.org/10.1016/0005-2728\(72\)90194-6](https://doi.org/10.1016/0005-2728(72)90194-6)
- Artero, R., Prokop, A., Paricio, N., Begemann, G., Pueyo, I., Mlodzik, M., Perez-Alonso, M., Baylies, M.K., 1998. The muscleblind gene participates in the organization of Z-bands and epidermal attachments of *Drosophila* muscles and is regulated by Dmef2. *Dev Biol* 195, 131–143. <https://doi.org/10.1006/dbio.1997.8833>
- Ashizawa, T., Dubel, J.R., Dunne, P.W., Dunne, C.J., Fu, Y.H., Pizzuti, A., Caskey, C.T., Boerwinkle, E., Perryman, M.B., Epstein, H.F., 1992. Anticipation in myotonic dystrophy. II. Complex relationships between clinical findings and structure of the GCT repeat. *Neurology* 42, 1877–1883. <https://doi.org/10.1212/wnl.42.10.1877>

- Atchley, W.R., Fitch, W.M., Bronner-Fraser, M., 1994. Molecular evolution of the MyoD family of transcription factors. *Proc Natl Acad Sci U S A* 91, 11522–11526.
- Au, Y., 2004. The muscle ultrastructure: a structural perspective of the sarcomere. *Cell Mol Life Sci* 61, 3016–3033. <https://doi.org/10.1007/s00018-004-4282-x>
- Barbado, M., Fablet, K., Ronjat, M., De Waard, M., 2009. Gene regulation by voltage-dependent calcium channels. *Biochimica et Biophysica Acta (BBA) - Molecular Cell Research*, 10th European Symposium on Calcium 1793, 1096–1104. <https://doi.org/10.1016/j.bbamcr.2009.02.004>
- Barik, A., Lu, Y., Sathyamurthy, A., Bowman, A., Shen, C., Li, L., Xiong, W., Mei, L., 2014. LRP4 Is Critical for Neuromuscular Junction Maintenance. *J Neurosci* 34, 13892–13905. <https://doi.org/10.1523/JNEUROSCI.1733-14.2014>
- Batra, R., Charizanis, K., Manchanda, M., Mohan, A., Li, M., Finn, D.J., Goodwin, M., Zhang, C., Sobczak, K., Thornton, C.A., Swanson, M.S., 2014. Loss of MBNL Leads to Disruption of Developmentally Regulated Alternative Polyadenylation in RNA-Mediated Disease. *Mol Cell* 56, 311–322. <https://doi.org/10.1016/j.molcel.2014.08.027>
- Beam, K.G., Knudson, C.M., Powell, J.A., 1986. A lethal mutation in mice eliminates the slow calcium current in skeletal muscle cells. *Nature* 320, 168–170. <https://doi.org/10.1038/320168a0>
- Becker, A., Wardas, B., Salah, H., Amini, M., Fecher-Trost, C., Sen, Q., Martus, D., Beck, A., Philipp, S.E., Flockerzi, V., Belkacemi, A., 2021. Cav β 3 Regulates Ca $^{2+}$ Signaling and Insulin Expression in Pancreatic β -Cells in a Cell-Autonomous Manner. *Diabetes* 70, 2532–2544. <https://doi.org/10.2337/db21-0078>
- Begemann, G., Paricio, N., Artero, R., Kiss, I., Pérez-Alonso, M., Mlodzik, M., 1997. muscleblind, a gene required for photoreceptor differentiation in Drosophila, encodes novel nuclear Cys 3 His-type zinc-finger-containing proteins. *Development* 124, 4321–4331. <https://doi.org/10.1242/dev.124.21.4321>
- Belkacemi, A., Hui, X., Wardas, B., Laschke, M.W., Wissenbach, U., Menger, M.D., Lipp, P., Beck, A., Flockerzi, V., 2018. IP $_3$ Receptor-Dependent Cytoplasmic Ca $^{2+}$ Signals Are Tightly Controlled by Cav β 3. *Cell Rep* 22, 1339–1349. <https://doi.org/10.1016/j.celrep.2018.01.010>
- Belotti, E., Schaeffer, L., 2020. Regulation of Gene expression at the neuromuscular Junction. *Neuroscience Letters* 735, 135163. <https://doi.org/10.1016/j.neulet.2020.135163>
- Benavides Damm, T., Egli, M., 2014. Calcium's Role in Mechanotransduction during Muscle Development. *Cellular Physiology and Biochemistry* 33, 249–272. <https://doi.org/10.1159/000356667>
- Benedetti, B., Tuluc, P., Mastrolia, V., Dlaska, C., Flucher, B.E., 2015. Physiological and pharmacological modulation of the embryonic skeletal muscle calcium channel splice variant CaV1.1e. *Biophys J* 108, 1072–1080. <https://doi.org/10.1016/j.bpj.2015.01.026>
- Bergamin, E., Hallock, P.T., Burden, S.J., Hubbard, S.R., 2010. The cytoplasmic adaptor protein Dok7 activates the receptor tyrosine kinase MuSK via dimerization. *Mol Cell* 39, 100–109. <https://doi.org/10.1016/j.molcel.2010.06.007>
- Berggren, P.-O., Yang, S.-N., Murakami, M., Efanov, A.M., Uhles, S., Köhler, M., Moede, T., Fernström, A., Appelskog, I.B., Aspinwall, C.A., Zaitsev, S.V., Larsson, O., de Vargas, L.M., Fecher-Trost, C.,

- Weissgerber, P., Ludwig, A., Leibiger, B., Juntti-Berggren, L., Barker, C.J., Gromada, J., Freichel, M., Leibiger, I.B., Flockerzi, V., 2004. Removal of Ca²⁺ channel beta3 subunit enhances Ca²⁺ oscillation frequency and insulin exocytosis. *Cell* 119, 273–284. <https://doi.org/10.1016/j.cell.2004.09.033>
- Berkes, C.A., Tapscott, S.J., 2005. MyoD and the transcriptional control of myogenesis. *Seminars in Cell & Developmental Biology, Biology of Hypoxia and Myogenesis and Muscle Disease* 16, 585–595. <https://doi.org/10.1016/j.semcdb.2005.07.006>
- Bezakova, G., Ruegg, M.A., 2003. New insights into the roles of agrin. *Nat Rev Mol Cell Biol* 4, 295–308. <https://doi.org/10.1038/nrm1074>
- Bichet, D., Cornet, V., Geib, S., Carlier, E., Volsen, S., Hoshi, T., Mori, Y., De Waard, M., 2000. The I-II loop of the Ca²⁺ channel alpha1 subunit contains an endoplasmic reticulum retention signal antagonized by the beta subunit. *Neuron* 25, 177–190. [https://doi.org/10.1016/s0896-6273\(00\)80881-8](https://doi.org/10.1016/s0896-6273(00)80881-8)
- Blaauw, B., Schiaffino, S., Reggiani, C., 2013. Mechanisms Modulating Skeletal Muscle Phenotype. *Comprehensive Physiology* 3, 1645–1687. <https://doi.org/10.1002/cphy.c130009>
- Block, B.A., Imagawa, T., Campbell, K.P., Franzini-Armstrong, C., 1988. Structural evidence for direct interaction between the molecular components of the transverse tubule/sarcoplasmic reticulum junction in skeletal muscle. *Journal of Cell Biology* 107, 2587–2600. <https://doi.org/10.1083/jcb.107.6.2587>
- Bober, E., Franz, T., Arnold, H.H., Gruss, P., Tremblay, P., 1994. Pax-3 is required for the development of limb muscles: a possible role for the migration of dermomyotomal muscle progenitor cells. *Development* 120, 603–612. <https://doi.org/10.1242/dev.120.3.603>
- Braun, T., Rudnicki, M.A., Arnold, H.H., Jaenisch, R., 1992. Targeted inactivation of the muscle regulatory gene Myf-5 results in abnormal rib development and perinatal death. *Cell* 71, 369–382. [https://doi.org/10.1016/0092-8674\(92\)90507-9](https://doi.org/10.1016/0092-8674(92)90507-9)
- Brenes, O., Pusch, M., Morales, F., 2023. ClC-1 Chloride Channel: Inputs on the Structure–Function Relationship of Myotonia Congenita-Causing Mutations. *Biomedicines* 11, 2622. <https://doi.org/10.3390/biomedicines11102622>
- Brice, N.L., Berrow, N.S., Campbell, V., Page, K.M., Brickley, K., Tedder, I., Dolphin, A.C., 1997. Importance of the Different β Subunits in the Membrane Expression of the α 1A and α 2 Calcium Channel Subunits: Studies Using a Depolarization-sensitive α 1A Antibody. *European Journal of Neuroscience* 9, 749–759. <https://doi.org/10.1111/j.1460-9568.1997.tb01423.x>
- Brinegar, A.E., Cooper, T.A., 2016. Roles for RNA-binding proteins in development and disease. *Brain Res* 1647, 1–8. <https://doi.org/10.1016/j.brainres.2016.02.050>
- Buckingham, M., Bajard, L., Chang, T., Daubas, P., Hadchouel, J., Meilhac, S., Montarras, D., Rocancourt, D., Relaix, F., 2003. The formation of skeletal muscle: from somite to limb. *J Anat* 202, 59–68. <https://doi.org/10.1046/j.1469-7580.2003.00139.x>
- Buraei, Z., Yang, J., 2013. Structure and function of the β subunit of voltage-gated Ca²⁺ channels. *Biochim Biophys Acta* 1828, 1530–1540. <https://doi.org/10.1016/j.bbamem.2012.08.028>

- Buraei, Z., Yang, J., 2010. The β Subunit of Voltage-Gated Ca^{2+} Channels. *Physiol Rev* 90, 1461–1506. <https://doi.org/10.1152/physrev.00057.2009>
- Burgess, D.L., Jones, J.M., Meisler, M.H., Noebels, J.L., 1997. Mutation of the Ca^{2+} channel beta subunit gene *Cchb4* is associated with ataxia and seizures in the lethargic (lh) mouse. *Cell* 88, 385–392. [https://doi.org/10.1016/s0092-8674\(00\)81877-2](https://doi.org/10.1016/s0092-8674(00)81877-2)
- Calderón, J.C., Bolaños, P., Caputo, C., 2014. The excitation–contraction coupling mechanism in skeletal muscle. *Biophys Rev* 6, 133–160. <https://doi.org/10.1007/s12551-013-0135-x>
- Campiglio, M., Di Biase, V., Tuluc, P., Flucher, B.E., 2013. Stable incorporation versus dynamic exchange of β subunits in a native Ca^{2+} channel complex. *J Cell Sci* 126, 2092–2101. <https://doi.org/10.1242/jcs.jcs124537>
- Catterall, W.A., 2011. Voltage-gated calcium channels. *Cold Spring Harb Perspect Biol* 3, a003947. <https://doi.org/10.1101/cshperspect.a003947>
- Celik, A., Kervestin, S., Jacobson, A., 2015. NMD: at the crossroads between translation termination and ribosome recycling. *Biochimie* 114, 2–9. <https://doi.org/10.1016/j.biochi.2014.10.027>
- Cetin, H., Beeson, D., Vincent, A., Webster, R., 2020. The Structure, Function, and Physiology of the Fetal and Adult Acetylcholine Receptor in Muscle. *Front Mol Neurosci* 13, 581097. <https://doi.org/10.3389/fnmol.2020.581097>
- Chargé, S.B.P., Rudnicki, M.A., 2004. Cellular and molecular regulation of muscle regeneration. *Physiol Rev* 84, 209–238. <https://doi.org/10.1152/physrev.00019.2003>
- Charizanis, K., Lee, K.-Y., Batra, R., Goodwin, M., Zhang, C., Yuan, Y., Shiue, L., Cline, M., Scotti, M.M., Xia, G., Kumar, A., Ashizawa, T., Clark, H.B., Kimura, T., Takahashi, M.P., Fujimura, H., Jinnai, K., Yoshikawa, H., Gomes-Pereira, M., Gourdon, G., Sakai, N., Nishino, S., Foster, T.C., Ares, M., Darnell, R.B., Swanson, M.S., 2012. Muscleblind-like 2-mediated alternative splicing in the developing brain and dysregulation in myotonic dystrophy. *Neuron* 75, 437–450. <https://doi.org/10.1016/j.neuron.2012.05.029>
- Chen, F., Liu, Y., Sugiura, Y., Allen, P.D., Gregg, R.G., Lin, W., 2011. Neuromuscular synaptic patterning requires the function of skeletal muscle dihydropyridine receptors. *Nat Neurosci* 14, 570–577. <https://doi.org/10.1038/nn.2792>
- Chen, Y.-H., Li, M.-H., Zhang, Y., He, L.-L., Yamada, Y., Fitzmaurice, A., Shen, Y., Zhang, H., Tong, L., Yang, J., 2004. Structural basis of the alpha1-beta subunit interaction of voltage-gated Ca^{2+} channels. *Nature* 429, 675–680. <https://doi.org/10.1038/nature02641>
- Cheng, W., Altafaj, X., Ronjat, M., Coronado, R., 2005. Interaction between the dihydropyridine receptor Ca^{2+} channel beta-subunit and ryanodine receptor type 1 strengthens excitation-contraction coupling. *Proc Natl Acad Sci U S A* 102, 19225–19230. <https://doi.org/10.1073/pnas.0504334102>
- Choi, J., Personius, K.E., DiFranco, M., Dansithong, W., Yu, C., Srivastava, S., Dixon, D.M., Bhatt, D.B., Comai, L., Vergara, J.L., Reddy, S., 2015. Muscleblind-Like 1 and Muscleblind-Like 3 Depletion Synergistically Enhances Myotonia by Altering Clc-1 RNA Translation. *EBioMedicine* 2, 1034–1047. <https://doi.org/10.1016/j.ebiom.2015.07.028>

- Chu, G.C., Moscoso, L.M., Sliwkowski, M.X., Merlie, J.P., 1995. Regulation of the acetylcholine receptor ϵ subunit gene by recombinant ARIA: An in vitro model for transynaptic gene regulation. *Neuron* 14, 329–339. [https://doi.org/10.1016/0896-6273\(95\)90289-9](https://doi.org/10.1016/0896-6273(95)90289-9)
- Chu, V., Feng, Q., Lim, Y., Shao, S., 2021. Selective destabilization of polypeptides synthesized from NMD-targeted transcripts. *Mol Biol Cell* 32, ar38. <https://doi.org/10.1091/mbc.E21-08-0382>
- Clark, K.A., McElhinny, A.S., Beckerle, M.C., Gregorio, C.C., 2002. Striated muscle cytoarchitecture: an intricate web of form and function. *Annu Rev Cell Dev Biol* 18, 637–706. <https://doi.org/10.1146/annurev.cellbio.18.012502.105840>
- Cohen, R.M., Foell, J.D., Balijepalli, R.C., Shah, V., Hell, J.W., Kamp, T.J., 2005. Unique modulation of L-type Ca^{2+} channels by short auxiliary beta1d subunit present in cardiac muscle. *Am J Physiol Heart Circ Physiol* 288, H2363-2374. <https://doi.org/10.1152/ajpheart.00348.2004>
- Cohen, S.A., Fischbach, G.D., 1973. Regulation of muscle acetylcholine sensitivity by muscle activity in cell culture. *Science* 181, 76–78. <https://doi.org/10.1126/science.181.4094.76>
- Conte, E., Fonzino, A., Cibelli, A., De Benedictis, V., Imbrici, P., Nicchia, G.P., Pierno, S., Camerino, G.M., 2020. Changes in Expression and Cellular Localization of Rat Skeletal Muscle ClC-1 Chloride Channel in Relation to Age, Myofiber Phenotype and PKC Modulation. *Front Pharmacol* 11, 714. <https://doi.org/10.3389/fphar.2020.00714>
- Cordeiro, J.M., Marieb, M., Pfeiffer, R., Calloe, K., Burashnikov, E., Antzelevitch, C., 2009. Accelerated inactivation of the L-type calcium current due to a mutation in CACNB2b underlies Brugada syndrome. *J Mol Cell Cardiol* 46, 695–703. <https://doi.org/10.1016/j.yjmcc.2009.01.014>
- Davis, R.L., Weintraub, H., Lassar, A.B., 1987. Expression of a single transfected cDNA converts fibroblasts to myoblasts. *Cell* 51, 987–1000. [https://doi.org/10.1016/0092-8674\(87\)90585-X](https://doi.org/10.1016/0092-8674(87)90585-X)
- Dayal, A., Bhat, V., Franzini-Armstrong, C., Grabner, M., 2013. Domain cooperativity in the β_{1a} subunit is essential for dihydropyridine receptor voltage sensing in skeletal muscle. *Proc. Natl. Acad. Sci. U.S.A.* 110, 7488–7493. <https://doi.org/10.1073/pnas.1301087110>
- Dayal, A., Perni, S., Franzini-Armstrong, C., Beam, K.G., Grabner, M., 2022. The distal C terminus of the dihydropyridine receptor β_{1a} subunit is essential for tetrad formation in skeletal muscle. *Proc Natl Acad Sci U S A* 119, e2201136119. <https://doi.org/10.1073/pnas.2201136119>
- Delgado-Escueta, A.V., Koeleman, B.P.C., Bailey, J.N., Medina, M.T., Durón, R.M., 2013. The quest for juvenile myoclonic epilepsy genes. *Epilepsy Behav* 28 Suppl 1, S52-57. <https://doi.org/10.1016/j.yebeh.2012.06.033>
- Dolphin, A.C., 2021. Functions of Presynaptic Voltage-gated Calcium Channels. *Function (Oxf)* 2, zqaa027. <https://doi.org/10.1093/function/zqaa027>
- Dos Reis, R., Kornobis, E., Pereira, A., Tores, F., Carrasco, J., Gautier, C., Jahannault-Talignani, C., Nitschké, P., Muchardt, C., Schlosser, A., Maric, H.M., Ango, F., Allemand, E., 2022. Complex regulation of Gephyrin splicing is a determinant of inhibitory postsynaptic diversity. *Nat Commun* 13, 3507. <https://doi.org/10.1038/s41467-022-31264-w>

- Dulhunty, A., 2006. EXCITATION–CONTRACTION COUPLING FROM THE 1950s INTO THE NEW MILLENNIUM. *Clinical and Experimental Pharmacology and Physiology* 33, 763–772. <https://doi.org/10.1111/j.1440-1681.2006.04441.x>
- Dum, R.P., Strick, P.L., 2002. Motor areas in the frontal lobe of the primate. *Physiol Behav* 77, 677–682. [https://doi.org/10.1016/s0031-9384\(02\)00929-0](https://doi.org/10.1016/s0031-9384(02)00929-0)
- Ebashi, S., Ebashi, F., 1964. A NEW PROTEIN FACTOR PROMOTING CONTRACTION OF ACTOMYOSIN. *Nature* 203, 645–646. <https://doi.org/10.1038/203645a0>
- Ebashi, S., Ebashi, F., Kodama, A., 1967. Troponin as the Ca⁺⁺-receptive protein in the contractile system. *J Biochem* 62, 137–138. <https://doi.org/10.1093/oxfordjournals.jbchem.a128628>
- Eftimie, R., Brenner, H.R., Buonanno, A., 1991. Myogenin and MyoD join a family of skeletal muscle genes regulated by electrical activity. *Proc Natl Acad Sci U S A* 88, 1349–1353.
- Eguchi, T., Tezuka, T., Miyoshi, S., Yamanashi, Y., 2016. Postnatal knockdown of dok-7 gene expression in mice causes structural defects in neuromuscular synapses and myasthenic pathology. *Genes Cells* 21, 670–676. <https://doi.org/10.1111/gtc.12370>
- Eltit, J.M., Franzini-Armstrong, C., Perez, C.F., 2014. Amino Acid Residues 489–503 of Dihydropyridine Receptor (DHPR) β 1a Subunit Are Critical for Structural Communication between the Skeletal Muscle DHPR Complex and Type 1 Ryanodine Receptor. *J Biol Chem* 289, 36116–36124. <https://doi.org/10.1074/jbc.M114.615526>
- Ertel, E.A., Campbell, K.P., Harpold, M.M., Hofmann, F., Mori, Y., Perez-Reyes, E., Schwartz, A., Snutch, T.P., Tanabe, T., Birnbaumer, L., Tsien, R.W., Catterall, W.A., 2000. Nomenclature of voltage-gated calcium channels. *Neuron* 25, 533–535. [https://doi.org/10.1016/s0896-6273\(00\)81057-0](https://doi.org/10.1016/s0896-6273(00)81057-0)
- Escayg, A., De Waard, M., Lee, D.D., Bichet, D., Wolf, P., Mayer, T., Johnston, J., Baloh, R., Sander, T., Meisler, M.H., 2000. Coding and noncoding variation of the human calcium-channel beta4-subunit gene CACNB4 in patients with idiopathic generalized epilepsy and episodic ataxia. *Am J Hum Genet* 66, 1531–1539. <https://doi.org/10.1086/302909>
- Etemad, S., Obermair, G.J., Bindreither, D., Benedetti, A., Stanika, R., Di Biase, V., Burtscher, V., Koschak, A., Kofler, R., Geley, S., Wille, A., Lusser, A., Flockerzi, V., Flucher, B.E., 2014. Differential neuronal targeting of a new and two known calcium channel β 4 subunit splice variants correlates with their regulation of gene expression. *J Neurosci* 34, 1446–1461. <https://doi.org/10.1523/JNEUROSCI.3935-13.2014>
- Falcone, S., Roman, W., Hnia, K., Gache, V., Didier, N., Lainé, J., Auradé, F., Marty, I., Nishino, I., Charlet-Berguerand, N., Romero, N.B., Marazzi, G., Sassoon, D., Laporte, J., Gomes, E.R., 2014. N-WASP is required for Amphiphysin-2/BIN1-dependent nuclear positioning and triad organization in skeletal muscle and is involved in the pathophysiology of centronuclear myopathy. *EMBO Molecular Medicine* 6, 1455–1475. <https://doi.org/10.15252/emmm.201404436>
- Felder, E., Protasi, F., Hirsch, R., Franzini-Armstrong, C., Allen, P.D., 2002. Morphology and Molecular Composition of Sarcoplasmic Reticulum Surface Junctions in the Absence of DHPR and RyR in Mouse Skeletal Muscle. *Biophysical Journal* 82, 3144–3149. [https://doi.org/10.1016/S0006-3495\(02\)75656-7](https://doi.org/10.1016/S0006-3495(02)75656-7)

- Flucher, B.E., Andrews, S.B., Daniels, M.P., 1994. Molecular organization of transverse tubule/sarcoplasmic reticulum junctions during development of excitation-contraction coupling in skeletal muscle. *MBoC* 5, 1105–1118. <https://doi.org/10.1091/mbc.5.10.1105>
- Frank, E., Fischbach, G.D., 1979. Early events in neuromuscular junction formation in vitro: induction of acetylcholine receptor clusters in the postsynaptic membrane and morphology of newly formed synapses. *Journal of Cell Biology* 83, 143–158. <https://doi.org/10.1083/jcb.83.1.143>
- Franzini-Armstrong, C., 1991. Simultaneous maturation of transverse tubules and sarcoplasmic reticulum during muscle differentiation in the mouse. *Dev Biol* 146, 353–363. [https://doi.org/10.1016/0012-1606\(91\)90237-w](https://doi.org/10.1016/0012-1606(91)90237-w)
- Franzini-Armstrong, C., Pincon-Raymond, M., Rieger, F., 1991. Muscle fibers from dysgenic mouse in vivo lack a surface component of peripheral couplings. *Dev Biol* 146, 364–376. [https://doi.org/10.1016/0012-1606\(91\)90238-x](https://doi.org/10.1016/0012-1606(91)90238-x)
- Fugier, C., Klein, A.F., Hammer, C., Vassilopoulos, S., Ivarsson, Y., Toussaint, A., Tosch, V., Vignaud, A., Ferry, A., Messaddeq, N., Kokunai, Y., Tsuburaya, R., de la Grange, P., Dembele, D., Francois, V., Precigout, G., Boulade-Ladame, C., Hummel, M.-C., de Munain, A.L., Sergeant, N., Laquerrière, A., Thibault, C., Deryckere, F., Auboeuf, D., Garcia, L., Zimmermann, P., Udd, B., Schoser, B., Takahashi, M.P., Nishino, I., Bassez, G., Laporte, J., Furling, D., Charlet-Berguerand, N., 2011. Misregulated alternative splicing of BIN1 is associated with T tubule alterations and muscle weakness in myotonic dystrophy. *Nat Med* 17, 720–725. <https://doi.org/10.1038/nm.2374>
- Galvani, L., Volta, A., Zambelli, J., Burndy Library, donor D., 1791. Aloysii Galvani De viribus electricitatis in motu musculari commentarius. Bononiae : Ex Typographia Institutii Scientiarium.
- Gattenlöhner, S., Schneider, C., Thamer, C., Klein, R., Roggendorf, W., Gohlke, F., Niethammer, C., Czub, S., Vincent, A., Müller-Hermelink, H., Marx, A., 2002. Expression of foetal type acetylcholine receptor is restricted to type 1 muscle fibres in human neuromuscular disorders. *Brain* 125, 1309–1319. <https://doi.org/10.1093/brain/awf136>
- Gautam, M., DeChiara, T.M., Glass, D.J., Yancopoulos, G.D., Sanes, J.R., 1999. Distinct phenotypes of mutant mice lacking agrin, MuSK, or rapsyn. *Brain Res Dev Brain Res* 114, 171–178. [https://doi.org/10.1016/s0165-3806\(99\)00013-9](https://doi.org/10.1016/s0165-3806(99)00013-9)
- Grady, R.M., Zhou, H., Cunningham, J.M., Henry, M.D., Campbell, K.P., Sanes, J.R., 2000. Maturation and Maintenance of the Neuromuscular Synapse: Genetic Evidence for Roles of the Dystrophin–Glycoprotein Complex. *Neuron* 25, 279–293. [https://doi.org/10.1016/S0896-6273\(00\)80894-6](https://doi.org/10.1016/S0896-6273(00)80894-6)
- Gregg, R.G., Messing, A., Strube, C., Beurg, M., Moss, R., Behan, M., Sukhareva, M., Haynes, S., Powell, J.A., Coronado, R., Powers, P.A., 1996. Absence of the α subunit (cchb1) of the skeletal muscle dihydropyridine receptor alters expression of the β 1 subunit and eliminates excitation-contraction coupling. *Proc. Natl. Acad. Sci. USA*.
- Grouselle, M., Koenig, J., Lascombe, M.L., Chapron, J., Méléard, P., Georgescauld, D., 1991. Fura-2 imaging of spontaneous and electrically induced oscillations of intracellular free Ca²⁺ in rat myotubes. *Pflugers Arch* 418, 40–50. <https://doi.org/10.1007/BF00370450>

- Haddix, S.G., Lee, Y. il, Kornegay, J.N., Thompson, W.J., 2018. Cycles of myofiber degeneration and regeneration lead to remodeling of the neuromuscular junction in two mammalian models of Duchenne muscular dystrophy. *PLoS One* 13, e0205926. <https://doi.org/10.1371/journal.pone.0205926>
- Han, H., Irimia, M., Ross, P.J., Sung, H.-K., Alipanahi, B., David, L., Golipour, A., Gabut, M., Michael, I.P., Nachman, E.N., Wang, E., Trcka, D., Thompson, T., O'Hanlon, D., Slobodeniuc, V., Barbosa-Morais, N.L., Burge, C.B., Moffat, J., Frey, B.J., Nagy, A., Ellis, J., Wrana, J.L., Blencowe, B.J., 2013. MBNL proteins repress ES-cell-specific alternative splicing and reprogramming. *Nature* 498, 241–245. <https://doi.org/10.1038/nature12270>
- Hao, M., Akrami, K., Wei, K., De Diego, C., Che, N., Ku, J.-H., Tidball, J., Graves, M.C., Shieh, P.B., Chen, F., 2008. Muscleblind-like 2 (Mbnl2)-deficient mice as a model for myotonic dystrophy. *Developmental Dynamics* 237, 403–410. <https://doi.org/10.1002/dvdy.21428>
- Harry, J.B., Kobrinsky, E., Abernethy, D.R., Soldatov, N.M., 2004. New Short Splice Variants of the Human Cardiac Cav β 2 Subunit. *Journal of Biological Chemistry* 279, 46367–46372. <https://doi.org/10.1074/jbc.M409523200>
- Hasty, P., Bradley, A., Morris, J.H., Edmondson, D.G., Venuti, J.M., Olson, E.N., Klein, W.H., 1993. Muscle deficiency and neonatal death in mice with a targeted mutation in the myogenin gene. *Nature* 364, 501–506. <https://doi.org/10.1038/364501a0>
- He, L.-L., Zhang, Y., Chen, Y.-H., Yamada, Y., Yang, J., 2007. Functional modularity of the beta-subunit of voltage-gated Ca $^{2+}$ channels. *Biophys J* 93, 834–845. <https://doi.org/10.1529/biophysj.106.101691>
- Hernández-Ochoa, E.O., Olojo, R.O., Rebbeck, R.T., Dulhunty, A.F., Schneider, M.F., 2014. β 1a490–508, a 19-Residue Peptide from C-Terminal Tail of Cav1.1 β 1a Subunit, Potentiates Voltage-Dependent Calcium Release in Adult Skeletal Muscle Fibers. *Biophys J* 106, 535–547. <https://doi.org/10.1016/j.bpj.2013.11.4503>
- Hernández-Ochoa, E.O., Pratt, S.J.P., Lovering, R.M., Schneider, M.F., 2016. Critical Role of Intracellular RyR1 Calcium Release Channels in Skeletal Muscle Function and Disease. *Front Physiol* 6, 420. <https://doi.org/10.3389/fphys.2015.00420>
- Hesser, B.A., Henschel, O., Witzemann, V., 2006. Synapse disassembly and formation of new synapses in postnatal muscle upon conditional inactivation of MuSK. *Mol Cell Neurosci* 31, 470–480. <https://doi.org/10.1016/j.mcn.2005.10.020>
- Hibino, H., Pironkova, R., Onwumere, O., Rousset, M., Charnet, P., Hudspeth, A.J., Lesage, F., 2003. Direct interaction with a nuclear protein and regulation of gene silencing by a variant of the Ca $^{2+}$ -channel beta 4 subunit. *Proc Natl Acad Sci U S A* 100, 307–312. <https://doi.org/10.1073/pnas.0136791100>
- Ho, T.H., Charlet-B, N., Poulos, M.G., Singh, G., Swanson, M.S., Cooper, T.A., 2004. Muscleblind proteins regulate alternative splicing. *EMBO J* 23, 3103–3112. <https://doi.org/10.1038/sj.emboj.7600300>
- Hodgkin, A.L., Horowicz, P., 1960. The effect of sudden changes in ionic concentrations on the membrane potential of single muscle fibres. *J Physiol* 153, 370–385. <https://doi.org/10.1113/jphysiol.1960.sp006540>

- Hoek, T.A., Khuperkar, D., Lindeboom, R.G.H., Sonneveld, S., Verhagen, B.M.P., Boersma, S., Vermeulen, M., Tanenbaum, M.E., 2019. Single-Molecule Imaging Uncovers Rules Governing Nonsense-Mediated mRNA Decay. *Mol Cell* 75, 324-339.e11. <https://doi.org/10.1016/j.molcel.2019.05.008>
- Hong, D., Jeong, S., 2023. 3'UTR Diversity: Expanding Repertoire of RNA Alterations in Human mRNAs. *Mol Cells* 46, 48–56. <https://doi.org/10.14348/molcells.2023.0003>
- Horstick, E.J., Linsley, J.W., Dowling, J.J., Hauser, M.A., McDonald, K.K., Ashley-Koch, A., Saint-Amant, L., Satish, A., Cui, W.W., Zhou, W., Sprague, S.M., Stamm, D.S., Powell, C.M., Speer, M.C., Franzini-Armstrong, C., Hirata, H., Kuwada, J.Y., 2013. Stac3 is a component of the excitation-contraction coupling machinery and mutated in Native American myopathy. *Nat Commun* 4, 1952. <https://doi.org/10.1038/ncomms2952>
- Hu, H., Wang, Z., Wei, R., Fan, G., Wang, Q., Zhang, K., Yin, C.-C., 2015. The molecular architecture of dihydropyridine receptor/L-type Ca²⁺ channel complex. *Sci Rep* 5, 8370. <https://doi.org/10.1038/srep08370>
- Hu, N., Kim, E., Antoury, L., Wheeler, T.M., 2023. Correction of Clcn1 alternative splicing reverses muscle fiber type transition in mice with myotonic dystrophy. *Nat Commun* 14, 1956. <https://doi.org/10.1038/s41467-023-37619-1>
- Igolkina, A.A., Zinkevich, A., Karandasheva, K.O., Popov, A.A., Selifanova, M.V., Nikolaeva, D., Tkachev, V., Penzar, D., Nikitin, D.M., Buzdin, A., 2019. H3K4me3, H3K9ac, H3K27ac, H3K27me3 and H3K9me3 Histone Tags Suggest Distinct Regulatory Evolution of Open and Condensed Chromatin Landmarks. *Cells* 8, 1034. <https://doi.org/10.3390/cells8091034>
- Inoue, A., Setoguchi, K., Matsubara, Y., Okada, K., Sato, N., Iwakura, Y., Higuchi, O., Yamanashi, Y., 2009. Dok-7 activates the muscle receptor kinase MuSK and shapes synapse formation. *Sci Signal* 2, ra7. <https://doi.org/10.1126/scisignal.2000113>
- Inui, M., Saito, A., Fleischer, S., 1987. Purification of the ryanodine receptor and identity with feet structures of junctional terminal cisternae of sarcoplasmic reticulum from fast skeletal muscle. *J Biol Chem* 262, 1740–1747.
- Jentsch, T.J., Stein, V., Weinreich, F., Zdebik, A.A., 2002. Molecular Structure and Physiological Function of Chloride Channels. *Physiological Reviews* 82, 503–568. <https://doi.org/10.1152/physrev.00029.2001>
- Jiang, Q.-X., 2019. Cholesterol-dependent gating effects on ion channels. *Adv Exp Med Biol* 1115, 167–190. https://doi.org/10.1007/978-3-030-04278-3_8
- Johnston, J.R., Chase, P.B., Pinto, J.R., 2018. Troponin through the looking-glass: emerging roles beyond regulation of striated muscle contraction. *Oncotarget* 9, 1461–1482. <https://doi.org/10.18632/oncotarget.22879>
- Jorgensen, A.O., Shen, A.C., Arnold, W., Leung, A.T., Campbell, K.P., 1989. Subcellular distribution of the 1,4-dihydropyridine receptor in rabbit skeletal muscle in situ: an immunofluorescence and immunocolloidal gold-labeling study. *J Cell Biol* 109, 135–147. <https://doi.org/10.1083/jcb.109.1.135>

- Kanadia, R.N., Johnstone, K.A., Mankodi, A., Lungu, C., Thornton, C.A., Esson, D., Timmers, A.M., Hauswirth, W.W., Swanson, M.S., 2003a. A Muscleblind Knockout Model for Myotonic Dystrophy. *Science* 302, 1978–1980. <https://doi.org/10.1126/science.1088583>
- Kanadia, R.N., Shin, J., Yuan, Y., Beattie, S.G., Wheeler, T.M., Thornton, C.A., Swanson, M.S., 2006. Reversal of RNA missplicing and myotonia after muscleblind overexpression in a mouse poly(CUG) model for myotonic dystrophy. *Proc Natl Acad Sci U S A* 103, 11748–11753. <https://doi.org/10.1073/pnas.0604970103>
- Kanadia, R.N., Urbinati, C.R., Crusselle, V.J., Luo, D., Lee, Y.-J., Harrison, J.K., Oh, S.P., Swanson, M.S., 2003b. Developmental expression of mouse muscleblind genes Mbnl1, Mbnl2 and Mbnl3. *Gene Expr Patterns* 3, 459–462. [https://doi.org/10.1016/s1567-133x\(03\)00064-4](https://doi.org/10.1016/s1567-133x(03)00064-4)
- Kania, A., Salzberg, A., Bhat, M., D'Evelyn, D., He, Y., Kiss, I., Bellen, H.J., 1995. P-Element Mutations Affecting Embryonic Peripheral Nervous System Development in *Drosophila Melanogaster*. *Genetics* 139, 1663–1678.
- Kaplan, M.M., Flucher, B.E., 2019. Postsynaptic CaV1.1-driven calcium signaling coordinates presynaptic differentiation at the developing neuromuscular junction. *Sci Rep* 9, 18450. <https://doi.org/10.1038/s41598-019-54900-w>
- Kaplan, M.M., Sultana, N., Benedetti, A., Obermair, G.J., Linde, N.F., Papadopoulos, S., Dayal, A., Grabner, M., Flucher, B.E., 2018. Calcium Influx and Release Cooperatively Regulate AChR Patterning and Motor Axon Outgrowth during Neuromuscular Junction Formation. *Cell Reports* 23, 3891–3904. <https://doi.org/10.1016/j.celrep.2018.05.085>
- Karunasekara, Y., Rebbeck, R.T., Weaver, L.M., Board, P.G., Dulhunty, A.F., Casarotto, M.G., 2012. An α -helical C-terminal tail segment of the skeletal L-type Ca²⁺ channel β 1a subunit activates ryanodine receptor type 1 via a hydrophobic surface. *FASEB J* 26, 5049–5059. <https://doi.org/10.1096/fj.12-211334>
- Kassar-Duchossoy, L., Gayraud-Morel, B., Gomès, D., Rocancourt, D., Buckingham, M., Shinin, V., Tajbakhsh, S., 2004. Mrf4 determines skeletal muscle identity in Myf5:Myod double-mutant mice. *Nature* 431, 466–471. <https://doi.org/10.1038/nature02876>
- Kilarski, W., Jakubowska, M., 1979. An electron microscope study of myofibril formation in embryonic rabbit skeletal muscle. *Z Mikrosk Anat Forsch* 93, 1159–1181.
- Kimura, T., Nakamori, M., Lueck, J.D., Pouliquin, P., Aoike, F., Fujimura, H., Dirksen, R.T., Takahashi, M.P., Dulhunty, A.F., Sakoda, S., 2005. Altered mRNA splicing of the skeletal muscle ryanodine receptor and sarcoplasmic/endoplasmic reticulum Ca²⁺-ATPase in myotonic dystrophy type 1. *Hum Mol Genet* 14, 2189–2200. <https://doi.org/10.1093/hmg/ddi223>
- Kino, Y., Washizu, C., Oma, Y., Onishi, H., Nezu, Y., Sasagawa, N., Nukina, N., Ishiura, S., 2009. MBNL and CELF proteins regulate alternative splicing of the skeletal muscle chloride channel CLCN1. *Nucleic acids research* 37, 6477–90. <https://doi.org/10.1093/nar/gkp681>
- Knudson, C.M., Chaudhari, N., Sharp, A.H., Powell, J.A., Beam, K.G., Campbell, K.P., 1989. Specific absence of the alpha 1 subunit of the dihydropyridine receptor in mice with muscular dysgenesis. *J Biol Chem* 264, 1345–1348.

- Ko, C.-P., Robitaille, R., 2015. Perisynaptic Schwann Cells at the Neuromuscular Synapse: Adaptable, Multitasking Glial Cells. *Cold Spring Harb Perspect Biol* 7, a020503. <https://doi.org/10.1101/cshperspect.a020503>
- Kodama, N., Sekiguchi, S., 1984. The development of spontaneous body movement in prenatal and perinatal mice. *Dev Psychobiol* 17, 139–150. <https://doi.org/10.1002/dev.420170205>
- Kong, X.C., Barzaghi, P., Ruegg, M.A., 2004. Inhibition of synapse assembly in mammalian muscle in vivo by RNA interference. *EMBO Rep* 5, 183–188. <https://doi.org/10.1038/sj.embor.7400065>
- Konieczny, P., Stepniak-Konieczna, E., Sobczak, K., 2014. MBNL proteins and their target RNAs, interaction and splicing regulation. *Nucleic Acids Research* 42, 10873–10887. <https://doi.org/10.1093/nar/gku767>
- Kopta, C., Steinbach, J.H., 1994. Comparison of mammalian adult and fetal nicotinic acetylcholine receptors stably expressed in fibroblasts. *J Neurosci* 14, 3922–3933. <https://doi.org/10.1523/JNEUROSCI.14-06-03922.1994>
- Kummer, T.T., Misgeld, T., Lichtman, J.W., Sanes, J.R., 2004. Nerve-independent formation of a topologically complex postsynaptic apparatus. *J Cell Biol* 164, 1077–1087. <https://doi.org/10.1083/jcb.200401115>
- Kummer, T.T., Misgeld, T., Sanes, J.R., 2006. Assembly of the postsynaptic membrane at the neuromuscular junction: paradigm lost. *Curr Opin Neurobiol* 16, 74–82. <https://doi.org/10.1016/j.conb.2005.12.003>
- Kuyumcu-Martinez, N.M., Wang, G.-S., Cooper, T.A., 2007. Increased Steady-State Levels of CUGBP1 in Myotonic Dystrophy 1 Are Due to PKC-Mediated Hyperphosphorylation. *Molecular Cell* 28, 68–78. <https://doi.org/10.1016/j.molcel.2007.07.027>
- Lacerda, A.E., Kim, H.S., Ruth, P., Perez-Reyes, E., Flockerzi, V., Hofmann, F., Birnbaumer, L., Brown, A.M., 1991. Normalization of current kinetics by interaction between the alpha 1 and beta subunits of the skeletal muscle dihydropyridine-sensitive Ca²⁺ channel. *Nature* 352, 527–530. <https://doi.org/10.1038/352527a0>
- Larson, L., Liroy, J., Johnson, J., Medler, S., 2019. Transitional Hybrid Skeletal Muscle Fibers in Rat Soleus Development. *J Histochem Cytochem.* 67, 891–900. <https://doi.org/10.1369/0022155419876421>
- Lee, K.-S., Cao, Y., Witwicka, H.E., Tom, S., Tapscott, S.J., Wang, E.H., 2010. RNA-binding Protein Muscleblind-like 3 (MBNL3) Disrupts Myocyte Enhancer Factor 2 (Mef2) β-Exon Splicing. *J Biol Chem* 285, 33779–33787. <https://doi.org/10.1074/jbc.M110.124255>
- Lee, K.-S., Smith, K., Amieux, P.S., Wang, E.H., 2008. MBNL3/CHCR prevents myogenic differentiation by inhibiting MyoD-dependent gene transcription. *Differentiation* 76, 299–309. <https://doi.org/10.1111/j.1432-0436.2007.00209.x>
- Lee, K.-Y., Li, M., Manchanda, M., Batra, R., Charizanis, K., Mohan, A., Warren, S.A., Chamberlain, C.M., Finn, D., Hong, H., Ashraf, H., Kasahara, H., Ranum, L.P.W., Swanson, M.S., 2013. Compound loss of muscleblind-like function in myotonic dystrophy. *EMBO Mol Med* 5, 1887–1900. <https://doi.org/10.1002/emmm.201303275>

- Lemerle, E., Lainé, J., Benoist, M., Moulay, G., Bigot, A., Labasse, C., Madelaine, A., Canette, A., Aubin, P., Vallat, J.-M., Romero, N.B., Bitoun, M., Mouly, V., Marty, I., Cadot, B., Picas, L., Vassilopoulos, S., 2023. Caveolae and Bin1 form ring-shaped platforms for T-tubule initiation. *Elife* 12, e84139. <https://doi.org/10.7554/eLife.84139>
- Li, L., Xiong, W.-C., Mei, L., 2018. Neuromuscular Junction Formation, Aging, and Disorders. *Annual Review of Physiology* 80, 159–188. <https://doi.org/10.1146/annurev-physiol-022516-034255>
- Li, Y., Lee, Y. il, Thompson, W.J., 2011. Changes in aging mouse neuromuscular junctions are explained by degeneration and regeneration of muscle fiber segments at the synapse. *J Neurosci* 31, 14910–14919. <https://doi.org/10.1523/JNEUROSCI.3590-11.2011>
- Liao, X., Li, Y., 2020. Genetic associations between voltage-gated calcium channels and autism spectrum disorder: a systematic review. *Molecular Brain* 13, 96. <https://doi.org/10.1186/s13041-020-00634-0>
- Lin, S., Landmann, L., Ruegg, M.A., Brenner, H.R., 2008. The Role of Nerve- versus Muscle-Derived Factors in Mammalian Neuromuscular Junction Formation. *J Neurosci* 28, 3333–3340. <https://doi.org/10.1523/JNEUROSCI.5590-07.2008>
- Lin, X., Miller, J.W., Mankodi, A., Kanadia, R.N., Yuan, Y., Moxley, R.T., Swanson, M.S., Thornton, C.A., 2006. Failure of MBNL1-dependent post-natal splicing transitions in myotonic dystrophy. *Hum Mol Genet* 15, 2087–2097. <https://doi.org/10.1093/hmg/ddl132>
- Liu, D., Westerfield, M., 1992. Clustering of muscle acetylcholine receptors requires motoneurons in live embryos, but not in cell culture. *J Neurosci* 12, 1859–1866. <https://doi.org/10.1523/JNEUROSCI.12-05-01859.1992>
- Liu, Y., Padgett, D., Takahashi, M., Li, H., Sayeed, A., Teichert, R.W., Olivera, B.M., McArdle, J.J., Green, W.N., Lin, W., 2008. Essential roles of the acetylcholine receptor gamma-subunit in neuromuscular synaptic patterning. *Development* 135, 1957–1967. <https://doi.org/10.1242/dev.018119>
- Lo, H.P., Lim, Y.-W., Xiong, Z., Martel, N., Ferguson, C., Ariotti, N., Giacomotto, J., Rae, J., Floetenmeyer, M., Moradi, S.V., Gao, Y., Tillu, V.A., Xia, D., Wang, H., Rahnama, S., Nixon, S.J., Bastiani, M., Day, R.D., Smith, K.A., Palpant, N.J., Johnston, W.A., Alexandrov, K., Collins, B.M., Hall, T.E., Parton, R.G., 2021. Cavin4 interacts with Bin1 to promote T-tubule formation and stability in developing skeletal muscle. *J Cell Biol* 220, e201905065. <https://doi.org/10.1083/jcb.201905065>
- López-Martínez, A., Soblechero-Martín, P., de-la-Puente-Ovejero, L., Nogales-Gadea, G., Arechavala-Gomez, V., 2020. An Overview of Alternative Splicing Defects Implicated in Myotonic Dystrophy Type I. *Genes* 11, 1109. <https://doi.org/10.3390/genes11091109>
- Lorenzon, P., Bernareggi, A., Degasperis, V., Nurowska, E., Wernig, A., Ruzzier, F., 2002. Properties of primary mouse myoblasts expanded in culture. *Exp Cell Res* 278, 84–91. <https://doi.org/10.1006/excr.2002.5562>
- Lueck, J.D., Mankodi, A., Swanson, M.S., Thornton, C.A., Dirksen, R.T., 2007. Muscle chloride channel dysfunction in two mouse models of myotonic dystrophy. *J Gen Physiol* 129, 79–94. <https://doi.org/10.1085/jgp.200609635>

- Luff, A.R., Atwood, H.L., 1971. Changes in the sarcoplasmic reticulum and transverse tubular system of fast and slow skeletal muscles of the mouse during postnatal development. *J Cell Biol* 51, 369–383. <https://doi.org/10.1083/jcb.51.2.369>
- Machuca-Tzili, L., Brook, D., Hilton-Jones, D., 2005. Clinical and molecular aspects of the myotonic dystrophies: a review. *Muscle Nerve* 32, 1–18. <https://doi.org/10.1002/mus.20301>
- Macpherson, P.C.D., Cieslak, D., Goldman, D., 2006. Myogenin-dependent nAChR clustering in aneural myotubes. *Mol Cell Neurosci* 31, 649–660. <https://doi.org/10.1016/j.mcn.2005.12.005>
- Mahadevan, M.S., Yadava, R.S., Mandal, M., 2021. Cardiac Pathology in Myotonic Dystrophy Type 1. *Int J Mol Sci* 22, 11874. <https://doi.org/10.3390/ijms222111874>
- Mankodi, A., Logigian, E., Callahan, L., McClain, C., White, R., Henderson, D., Krym, M., Thornton, C.A., 2000. Myotonic dystrophy in transgenic mice expressing an expanded CUG repeat. *Science* 289, 1769–1773. <https://doi.org/10.1126/science.289.5485.1769>
- Massiré, T., Chiara, N., Amélie, V., Christel, G., Marius, H., Lucile, S., Maxime, G., Anne, F., Mégane, L., Zoheir, G., Bruno, C., Eriky, C., Benjamin, M., Nathalie, M., Julien, M., Laure, S., Jeremy, S., Lofti, S., Ariane, J., Pierre, D. la G., Jean-Yves, H., France, P.-R., Sestina, F., 2024. GDF5 as a rejuvenating treatment for age-related neuromuscular failure. *Brain* awae107. <https://doi.org/10.1093/brain/awae107>
- Masuda, A., Andersen, H.S., Doktor, T.K., Okamoto, T., Ito, M., Andresen, B.S., Ohno, K., 2012. CUGBP1 and MBNL1 preferentially bind to 3' UTRs and facilitate mRNA decay. *Sci Rep* 2, 209. <https://doi.org/10.1038/srep00209>
- Mazhar, S., Herbst, R., 2012. The formation of complex acetylcholine receptor clusters requires MuSK kinase activity and structural information from the MuSK extracellular domain. *Molecular and Cellular Neuroscience* 49, 475–486. <https://doi.org/10.1016/j.mcn.2011.12.007>
- Medler, S., 2019. Mixing it up: the biological significance of hybrid skeletal muscle fibers. *J Exp Biol* 222, jeb200832. <https://doi.org/10.1242/jeb.200832>
- Meissner, G., 1986. Ryanodine activation and inhibition of the Ca²⁺ release channel of sarcoplasmic reticulum. *J Biol Chem* 261, 6300–6306.
- Messéant, J., Ezan, J., Delers, P., Glebov, K., Marchiol, C., Lager, F., Renault, G., Tissir, F., Montcouquiol, M., Sans, N., Legay, C., Strohlic, L., 2017. Wnt proteins contribute to neuromuscular junction formation through distinct signaling pathways. *Development* 144, 1712–1724. <https://doi.org/10.1242/dev.146167>
- Miller, J.W., Urbinati, C.R., Teng-umnuay, P., Stenberg, M.G., Byrne, B.J., Thornton, C.A., Swanson, M.S., 2000. Recruitment of human muscleblind proteins to (CUG)_n expansions associated with myotonic dystrophy. *The EMBO Journal* 19, 4439–4448. <https://doi.org/10.1093/emboj/19.17.4439>
- Misgeld, T., Burgess, R.W., Lewis, R.M., Cunningham, J.M., Lichtman, J.W., Sanes, J.R., 2002. Roles of neurotransmitter in synapse formation: development of neuromuscular junctions lacking choline acetyltransferase. *Neuron* 36, 635–648. [https://doi.org/10.1016/s0896-6273\(02\)01020-6](https://doi.org/10.1016/s0896-6273(02)01020-6)

- Misgeld, T., Kummer, T.T., Lichtman, J.W., Sanes, J.R., 2005. Agrin promotes synaptic differentiation by counteracting an inhibitory effect of neurotransmitter. *Proc Natl Acad Sci U S A* 102, 11088–11093. <https://doi.org/10.1073/pnas.0504806102>
- Mishina, M., Takai, T., Imoto, K., Noda, M., Takahashi, T., Numa, S., Methfessel, C., Sakmann, B., 1986. Molecular distinction between fetal and adult forms of muscle acetylcholine receptor. *Nature* 321, 406–411. <https://doi.org/10.1038/321406a0>
- Missias, A.C., Chu, G.C., Klocke, B.J., Sanes, J.R., Merlie, J.P., 1996. Maturation of the acetylcholine receptor in skeletal muscle: regulation of the AChR gamma-to-epsilon switch. *Dev Biol* 179, 223–238. <https://doi.org/10.1006/dbio.1996.0253>
- Moransard, M., Borges, L.S., Willmann, R., Marangi, P.A., Brenner, H.R., Ferns, M.J., Fuhrer, C., 2003. Agrin regulates rapsyn interaction with surface acetylcholine receptors, and this underlies cytoskeletal anchoring and clustering. *J Biol Chem* 278, 7350–7359. <https://doi.org/10.1074/jbc.M210865200>
- Moretti, I., Ciciliot, S., Dyar, K.A., Abraham, R., Murgia, M., Agatea, L., Akimoto, T., Biciato, S., Forcato, M., Pierre, P., Uhlénhaut, N.H., Rigby, P.W.J., Carvajal, J.J., Blaauw, B., Calabria, E., Schiaffino, S., 2016. MRF4 negatively regulates adult skeletal muscle growth by repressing MEF2 activity. *Nat Commun* 7, 12397. <https://doi.org/10.1038/ncomms12397>
- Mulroney, L.M., 2020. Identification of full-length transcript isoforms using nanopore sequencing of individual RNA strands. UC Santa Cruz.
- Nabeshima, Y., Hanaoka, K., Hayasaka, M., Esumi, E., Li, S., Nonaka, I., Nabeshima, Y., 1993. Myogenin gene disruption results in perinatal lethality because of severe muscle defect. *Nature* 364, 532–535. <https://doi.org/10.1038/364532a0>
- Nagashima, M., Yasuhara, S., Martyn, J.A.J., 2013. Train-of-Four and Tetanic Fade are not Always a Prejunctional Phenomenon as Evaluated by Toxins Having Highly Specific Pre- and Postjunctional Actions. *Anesth Analg* 116, 994–1000. <https://doi.org/10.1213/ANE.0b013e31828841e3>
- Nayak, T.K., Bruhova, I., Chakraborty, S., Gupta, S., Zheng, W., Auerbach, A., 2014. Functional differences between neurotransmitter binding sites of muscle acetylcholine receptors. *Proceedings of the National Academy of Sciences* 111, 17660–17665. <https://doi.org/10.1073/pnas.1414378111>
- Nelson, B.R., Wu, F., Liu, Y., Anderson, D.M., McAnally, J., Lin, W., Cannon, S.C., Bassel-Duby, R., Olson, E.N., 2013. Skeletal muscle-specific T-tubule protein STAC3 mediates voltage-induced Ca²⁺ release and contractility. *Proceedings of the National Academy of Sciences* 110, 11881–11886. <https://doi.org/10.1073/pnas.1310571110>
- Ngo, S.T., Noakes, P.G., Phillips, W.D., 2007. Neural agrin: a synaptic stabiliser. *Int J Biochem Cell Biol* 39, 863–867. <https://doi.org/10.1016/j.biocel.2006.10.012>
- Nicot, A.-S., Toussaint, A., Tosch, V., Kretz, C., Wallgren-Pettersson, C., Iwarsson, E., Kingston, H., Garnier, J.-M., Biancalana, V., Oldfors, A., Mandel, J.-L., Laporte, J., 2007. Mutations in amphiphysin 2 (BIN1) disrupt interaction with dynamin 2 and cause autosomal recessive centronuclear myopathy. *Nat Genet* 39, 1134–1139. <https://doi.org/10.1038/ng2086>

- Nitschke, L., Hu, R.-C., Miller, A.N., Lucas, L., Cooper, T.A., 2023. Alternative splicing mediates the compensatory upregulation of MBNL2 upon MBNL1 loss-of-function. *Nucleic Acids Res* 51, 1245–1259. <https://doi.org/10.1093/nar/gkac1219>
- Obermair, G.J., Kugler, G., Baumgartner, S., Tuluc, P., Grabner, M., Flucher, B.E., 2005. The Ca²⁺ channel alpha2delta-1 subunit determines Ca²⁺ current kinetics in skeletal muscle but not targeting of alpha1S or excitation-contraction coupling. *J Biol Chem* 280, 2229–2237. <https://doi.org/10.1074/jbc.M411501200>
- Obermair, G.J., Schlick, B., Di Biase, V., Subramanyam, P., Gebhart, M., Baumgartner, S., Flucher, B.E., 2010. Reciprocal interactions regulate targeting of calcium channel beta subunits and membrane expression of alpha1 subunits in cultured hippocampal neurons. *J Biol Chem* 285, 5776–5791. <https://doi.org/10.1074/jbc.M109.044271>
- Okada, K., Inoue, A., Okada, M., Murata, Y., Kakuta, S., Jigami, T., Kubo, S., Shiraishi, H., Eguchi, K., Motomura, M., Akiyama, T., Iwakura, Y., Higuchi, O., Yamanashi, Y., 2006. The muscle protein Dok-7 is essential for neuromuscular synaptogenesis. *Science* 312, 1802–1805. <https://doi.org/10.1126/science.1127142>
- Oury, J., Liu, Y., Töpf, A., Todorovic, S., Hoedt, E., Preethish-Kumar, V., Neubert, T.A., Lin, W., Lochmüller, H., Burden, S.J., 2019. MACF1 links Rapsyn to microtubule- and actin-binding proteins to maintain neuromuscular synapses. *J Cell Biol* 218, 1686–1705. <https://doi.org/10.1083/jcb.201810023>
- Pacifici, P.G., Peter, C., Yampolsky, P., Koenen, M., McArdle, J.J., Witzemann, V., 2011. Novel mouse model reveals distinct activity-dependent and -independent contributions to synapse development. *PLoS One* 6, e16469. <https://doi.org/10.1371/journal.pone.0016469>
- Panaite, P.-A., Gantelet, E., Kraftsik, R., Gourdon, G., Kuntzer, T., Barakat-Walter, I., 2008. Myotonic dystrophy transgenic mice exhibit pathologic abnormalities in diaphragm neuromuscular junctions and phrenic nerves. *J Neuropathol Exp Neurol* 67, 763–772. <https://doi.org/10.1097/NEN.0b013e318180ec64>
- Papponen, H., Kaisto, T., Myllylä, V.V., Myllylä, R., Metsikkö, K., 2005. Regulated sarcolemmal localization of the muscle-specific ClC-1 chloride channel. *Exp Neurol* 191, 163–173. <https://doi.org/10.1016/j.expneurol.2004.07.018>
- Parton, R.G., Way, M., Zorzi, N., Stang, E., 1997. Caveolin-3 Associates with Developing T-tubules during Muscle Differentiation. *J Cell Biol* 136, 137–154.
- Pascual, M., Vicente, M., Monferrer, L., Artero, R., 2006. The Muscleblind family of proteins: an emerging class of regulators of developmentally programmed alternative splicing. *Differentiation* 74, 65–80. <https://doi.org/10.1111/j.1432-0436.2006.00060.x>
- Perez, C.F., Eltit, J.M., Lopez, J.R., Bodnár, D., Dulhunty, A.F., Aditya, S., Casarotto, M.G., 2018. Functional and structural characterization of a novel malignant hyperthermia-susceptible variant of DHPR-β1a subunit (CACNB1). *Am J Physiol Cell Physiol* 314, C323–C333. <https://doi.org/10.1152/ajpcell.00187.2017>

- Pette, D., Staron, R.S., 2000. Myosin isoforms, muscle fiber types, and transitions. *Microscopy Research and Technique* 50, 500–509. [https://doi.org/10.1002/1097-0029\(20000915\)50:6<500::AID-JEMT7>3.0.CO;2-7](https://doi.org/10.1002/1097-0029(20000915)50:6<500::AID-JEMT7>3.0.CO;2-7)
- Pęziński, M., Daszczuk, P., Pradhan, B.S., Lochmüller, H., Prószyński, T.J., 2020. An improved method for culturing myotubes on laminins for the robust clustering of postsynaptic machinery. *Sci Rep* 10, 4524. <https://doi.org/10.1038/s41598-020-61347-x>
- Pickel, S., Cruz-Garcia, Y., Bandleon, S., Barkovits, K., Heindl, C., Völker, K., Abeßer, M., Pfeiffer, K., Schaaf, A., Marcus, K., Eder-Negrin, P., Kuhn, M., Miranda-Laferte, E., 2021. The β 2-Subunit of Voltage-Gated Calcium Channels Regulates Cardiomyocyte Hypertrophy. *Front Cardiovasc Med* 8, 704657. <https://doi.org/10.3389/fcvm.2021.704657>
- Piétri-Rouxel, F., Gentil, C., Vassilopoulos, S., Baas, D., Mouisel, E., Ferry, A., Vignaud, A., Hourdé, C., Marty, I., Schaeffer, L., Voit, T., Garcia, L., 2010. DHPR α 1S subunit controls skeletal muscle mass and morphogenesis. *EMBO J* 29, 643–654. <https://doi.org/10.1038/emboj.2009.366>
- Podolsky, R.J., Costantin, L.L., 1964. REGULATION BY CALCIUM OF THE CONTRACTION AND RELAXATION OF MUSCLE FIBERS. *Fed Proc* 23, 933–939.
- Porter, K.R., Palade, G.E., 1957. Studies on the endoplasmic reticulum. III. Its form and distribution in striated muscle cells. *J Biophys Biochem Cytol* 3, 269–300. <https://doi.org/10.1083/jcb.3.2.269>
- Potthoff, M.J., Olson, E.N., 2007. MEF2: a central regulator of diverse developmental programs. *Development* 134, 4131–4140. <https://doi.org/10.1242/dev.008367>
- Poulos, M.G., Batra, R., Li, M., Yuan, Y., Zhang, C., Darnell, R.B., Swanson, M.S., 2013. Progressive impairment of muscle regeneration in muscleblind-like 3 isoform knockout mice. *Hum Mol Genet* 22, 3547–3558. <https://doi.org/10.1093/hmg/ddt209>
- Powell, J.A., Fambrough, D.M., 1973. Electrical properties of normal and dysgenic mouse skeletal muscle in culture. *J Cell Physiol* 82, 21–38. <https://doi.org/10.1002/jcp.1040820104>
- Powers, P.A., Liu, S., Hogan, K., Gregg, R.G., 1992. Skeletal muscle and brain isoforms of a beta-subunit of human voltage-dependent calcium channels are encoded by a single gene. *Journal of Biological Chemistry* 267, 22967–22972. [https://doi.org/10.1016/S0021-9258\(18\)50042-9](https://doi.org/10.1016/S0021-9258(18)50042-9)
- Pragnell, M., Sakamoto, J., Jay, S.D., Campbell, K.P., 1991. Cloning and tissue-specific expression of the brain calcium channel beta-subunit. *FEBS Lett* 291, 253–258. [https://doi.org/10.1016/0014-5793\(91\)81296-k](https://doi.org/10.1016/0014-5793(91)81296-k)
- Rau, F., Freyermuth, F., Fugier, C., Villemin, J.-P., Fischer, M.-C., Jost, B., Dembele, D., Gourdon, G., Nicole, A., Duboc, D., Wahbi, K., Day, J.W., Fujimura, H., Takahashi, M.P., Auboeuf, D., Dreumont, N., Furling, D., Charlet-Berguerand, N., 2011. Misregulation of miR-1 processing is associated with heart defects in myotonic dystrophy. *Nat Struct Mol Biol* 18, 840–845. <https://doi.org/10.1038/nsmb.2067>
- Rebeck, R.T., Karunasekara, Y., Gallant, E.M., Board, P.G., Beard, N.A., Casarotto, M.G., Dulhunty, A.F., 2011. The β 1a Subunit of the Skeletal DHPR Binds to Skeletal RyR1 and Activates the Channel via Its 35-Residue C-Terminal Tail. *Biophys J* 100, 922–930. <https://doi.org/10.1016/j.bpj.2011.01.022>

- Reggiani, C., Bottinelli, R., Stienen, G.J.M., 2000. Sarcomeric Myosin Isoforms: Fine Tuning of a Molecular Motor. *Physiology* 15, 26–33. <https://doi.org/10.1152/physiologyonline.2000.15.1.26>
- Rieger, F., Powell, J.A., Pinçon-Raymond, M., 1984. Extensive nerve overgrowth and paucity of the tailed asymmetric form (16 S) of acetylcholinesterase in the developing skeletal neuromuscular system of the dysgenic (mdg/mdg) mouse. *Dev Biol* 101, 181–191. [https://doi.org/10.1016/0012-1606\(84\)90128-3](https://doi.org/10.1016/0012-1606(84)90128-3)
- Rima, M., Daghsni, M., De Waard, S., Gaborit, N., Fajloun, Z., Ronjat, M., Mori, Y., Brusés, J.L., De Waard, M., 2017a. The $\beta 4$ subunit of the voltage-gated calcium channel (Cacnb4) regulates the rate of cell proliferation in Chinese Hamster Ovary cells. *Int J Biochem Cell Biol* 89, 57–70. <https://doi.org/10.1016/j.biocel.2017.05.032>
- Rima, M., Daghsni, M., Fajloun, Z., M'rad, R., Brusés, J.L., Ronjat, M., De Waard, M., 2016. Protein partners of the calcium channel β subunit highlight new cellular functions. *Biochem J* 473, 1831–1844. <https://doi.org/10.1042/BCJ20160125>
- Rima, M., Daghsni, M., Lopez, A., Fajloun, Z., Lefrancois, L., Dunach, M., Mori, Y., Merle, P., Brusés, J.L., De Waard, M., Ronjat, M., 2017b. Down-regulation of the Wnt/ β -catenin signaling pathway by Cacnb4. *Mol Biol Cell* 28, 3699–3708. <https://doi.org/10.1091/mbc.E17-01-0076>
- Romey, G., Garcia, L., Dimitriadou, V., Pincon-Raymond, M., Rieger, F., Lazdunski, M., 1989. Ontogenesis and localization of Ca^{2+} channels in mammalian skeletal muscle in culture and role in excitation-contraction coupling. *Proc Natl Acad Sci U S A* 86, 2933–2937. <https://doi.org/10.1073/pnas.86.8.2933>
- Rosenfeld, M.R., Wong, E., Dalmau, J., Manley, G., Ponser, J.B., Sher, E., Furneaux, H.M., 1993. Cloning and characterization of a lambert-eaton myasthenic syndrome antigen. *Annals of Neurology* 33, 113–120. <https://doi.org/10.1002/ana.410330126>
- Rudnicki, M.A., Braun, T., Hinuma, S., Jaenisch, R., 1992. Inactivation of *MyoD* in mice leads to up-regulation of the myogenic HLH gene *Myf-5* and results in apparently normal muscle development. *Cell* 71, 383–390. [https://doi.org/10.1016/0092-8674\(92\)90508-A](https://doi.org/10.1016/0092-8674(92)90508-A)
- Rudnicki, M.A., Schnegelsberg, P.N.J., Stead, R.H., Braun, T., Arnold, H.-H., Jaenisch, R., 1993. MyoD or Myf-5 is required for the formation of skeletal muscle. *Cell* 75, 1351–1359. [https://doi.org/10.1016/0092-8674\(93\)90621-V](https://doi.org/10.1016/0092-8674(93)90621-V)
- Ruth, P., Röhrkasten, A., Biel, M., Bosse, E., Regulla, S., Meyer, H.E., Flockerzi, V., Hofmann, F., 1989. Primary structure of the beta subunit of the DHP-sensitive calcium channel from skeletal muscle. *Science* 245, 1115–1118. <https://doi.org/10.1126/science.2549640>
- Sandow, A., 1952. Excitation-Contraction Coupling in Muscular Response. *Yale J Biol Med* 25, 176–201.
- Sanes, J.R., Lichtman, J.W., 2001. Induction, assembly, maturation and maintenance of a postsynaptic apparatus. *Nat Rev Neurosci* 2, 791–805. <https://doi.org/10.1038/35097557>
- Sartori, R., Schirwis, E., Blaauw, B., Bortolanza, S., Zhao, J., Enzo, E., Stantzou, A., Mouisel, E., Toniolo, L., Ferry, A., Stricker, S., Goldberg, A.L., Dupont, S., Piccolo, S., Amthor, H., Sandri, M., 2013. BMP signaling controls muscle mass. *Nat Genet* 45, 1309–1318. <https://doi.org/10.1038/ng.2772>

- Savkur, R.S., Philips, A.V., Cooper, T.A., 2001. Aberrant regulation of insulin receptor alternative splicing is associated with insulin resistance in myotonic dystrophy. *Nat Genet* 29, 40–47. <https://doi.org/10.1038/ng704>
- Schredelseker, J., Dayal, A., Schwerte, T., Franzini-Armstrong, C., Grabner, M., 2009. Proper Restoration of Excitation-Contraction Coupling in the Dihydropyridine Receptor β 1-null Zebrafish Relaxed Is an Exclusive Function of the β 1a Subunit*. *Journal of Biological Chemistry* 284, 1242–1251. <https://doi.org/10.1074/jbc.M807767200>
- Schredelseker, J., Di Biase, V., Obermair, G.J., Felder, E.T., Flucher, B.E., Franzini-Armstrong, C., Grabner, M., 2005. The β 1a subunit is essential for the assembly of dihydropyridine-receptor arrays in skeletal muscle. *Proc Natl Acad Sci U S A* 102, 17219–17224. <https://doi.org/10.1073/pnas.0508710102>
- Schuster-Gossler, K., Cordes, R., Gossler, A., 2007. Premature myogenic differentiation and depletion of progenitor cells cause severe muscle hypotrophy in Delta1 mutants. *Proceedings of the National Academy of Sciences* 104, 537–542. <https://doi.org/10.1073/pnas.0608281104>
- Segatto, M., Fittipaldi, R., Pin, F., Sartori, R., Dae Ko, K., Zare, H., Fenizia, C., Zanchettin, G., Pierobon, E.S., Hatakeyama, S., Sperti, C., Merigliano, S., Sandri, M., Filippakopoulos, P., Costelli, P., Sartorelli, V., Caretti, G., 2017. Epigenetic targeting of bromodomain protein BRD4 counteracts cancer cachexia and prolongs survival. *Nat Commun* 8, 1707. <https://doi.org/10.1038/s41467-017-01645-7>
- Seznec, H., Agbulut, O., Sergeant, N., Savouret, C., Ghestem, A., Tabti, N., Willer, J.C., Ourth, L., Duros, C., Brisson, E., Fouquet, C., Butler-Browne, G., Delacourte, A., Junien, C., Gourdon, G., 2001. Mice transgenic for the human myotonic dystrophy region with expanded CTG repeats display muscular and brain abnormalities. *Hum Mol Genet* 10, 2717–2726. <https://doi.org/10.1093/hmg/10.23.2717>
- Shen, C., Lu, Y., Zhang, B., Figueiredo, D., Bean, J., Jung, J., Wu, H., Barik, A., Yin, D.-M., Xiong, W.-C., Mei, L., 2013. Antibodies against low-density lipoprotein receptor-related protein 4 induce myasthenia gravis. *J Clin Invest* 123, 5190–5202. <https://doi.org/10.1172/JCI66039>
- Slater, C.R., 2020. “Fragmentation” of NMJs: a sign of degeneration or regeneration? A long journey with many junctions. *Neuroscience* 439, 28–40. <https://doi.org/10.1016/j.neuroscience.2019.05.017>
- Sta Maria, N.S., Zhou, C., Lee, S.J., Valiulahi, P., Li, X., Choi, J., Liu, X., Jacobs, R., Comai, L., Reddy, S., 2021. Mbnl1 and Mbnl2 regulate brain structural integrity in mice. *Commun Biol* 4, 1342. <https://doi.org/10.1038/s42003-021-02845-0>
- Subramanyam, P., Obermair, G.J., Baumgartner, S., Gebhart, M., Striessnig, J., Kaufmann, W.A., Geley, S., Flucher, B.E., 2009. Activity and calcium regulate nuclear targeting of the calcium channel beta4b subunit in nerve and muscle cells. *Channels (Austin)* 3, 343–355. <https://doi.org/10.4161/chan.3.5.9696>
- Tadmouri, A., Kiyonaka, S., Barbado, M., Rousset, M., Fablet, K., Sawamura, S., Bahembera, E., Pernet-Gallay, K., Arnoult, C., Miki, T., Sadoul, K., Gory-Faure, S., Lambrecht, C., Lesage, F., Akiyama, S., Khochbin, S., Baulande, S., Janssens, V., Andrieux, A., Dolmetsch, R., Ronjat, M., Mori, Y., De Waard, M., 2012. Cacnb4 directly couples electrical activity to gene expression, a process defective in juvenile epilepsy. *EMBO J* 31, 3730–3744. <https://doi.org/10.1038/emboj.2012.226>

- Takekura, H., Flucher, B.E., Franzini-Armstrong, C., 2001. Sequential Docking, Molecular Differentiation, and Positioning of T-Tubule/SR Junctions in Developing Mouse Skeletal Muscle. *Developmental Biology* 239, 204–214. <https://doi.org/10.1006/dbio.2001.0437>
- Takekura, H., Nishi, M., Noda, T., Takeshima, H., Franzini-Armstrong, C., 1995. Abnormal junctions between surface membrane and sarcoplasmic reticulum in skeletal muscle with a mutation targeted to the ryanodine receptor. *Proc Natl Acad Sci U S A* 92, 3381–3385. <https://doi.org/10.1073/pnas.92.8.3381>
- Takeshima, H., Iino, M., Takekura, H., Nishi, M., Kuno, J., Minowa, O., Takano, H., Noda, T., 1994. Excitation-contraction uncoupling and muscular degeneration in mice lacking functional skeletal muscle ryanodine-receptor gene. *Nature* 369, 556–559. <https://doi.org/10.1038/369556a0>
- Talbot, J., Maves, L., 2016. Skeletal muscle fiber type: using insights from muscle developmental biology to dissect targets for susceptibility and resistance to muscle disease. *Wiley Interdiscip Rev Dev Biol* 5, 518–534. <https://doi.org/10.1002/wdev.230>
- Tanabe, T., Takeshima, H., Mikami, A., Flockerzi, V., Takahashi, H., Kangawa, K., Kojima, M., Matsuo, H., Hirose, T., Numa, S., 1987. Primary structure of the receptor for calcium channel blockers from skeletal muscle. *Nature* 328, 313–318. <https://doi.org/10.1038/328313a0>
- Tang, H., Goldman, D., 2006. Activity-dependent gene regulation in skeletal muscle is mediated by a histone deacetylase (HDAC)-Dach2-myogenin signal transduction cascade. *Proc Natl Acad Sci U S A* 103, 16977–16982. <https://doi.org/10.1073/pnas.0601565103>
- Tang, H., Macpherson, P., Argetsinger, L.S., Cieslak, D., Suhr, S.T., Carter-Su, C., Goldman, D., 2004. CaM kinase II-dependent phosphorylation of myogenin contributes to activity-dependent suppression of nAChR gene expression in developing rat myotubes. *Cell Signal* 16, 551–563. <https://doi.org/10.1016/j.cellsig.2003.09.006>
- Tang, H., Veldman, M.B., Goldman, D., 2006. Characterization of a muscle-specific enhancer in human MuSK promoter reveals the essential role of myogenin in controlling activity-dependent gene regulation. *J Biol Chem* 281, 3943–3953. <https://doi.org/10.1074/jbc.M511317200>
- Tang, Z.Z., Yarotsky, V., Wei, L., Sobczak, K., Nakamori, M., Eichinger, K., Moxley, R.T., Dirksen, R.T., Thornton, C.A., 2012. Muscle weakness in myotonic dystrophy associated with misregulated splicing and altered gating of Ca(V)1.1 calcium channel. *Hum Mol Genet* 21, 1312–1324. <https://doi.org/10.1093/hmg/ddr568>
- Taylor, J., Pereyra, A., Zhang, T., Messi, M.L., Wang, Z.-M., Hereñú, C., Kuan, P.-F., Delbono, O., 2014. The Cavβ1a subunit regulates gene expression and suppresses myogenin in muscle progenitor cells. *J Cell Biol* 205, 829–846. <https://doi.org/10.1083/jcb.201403021>
- Taylor, J.R., Zheng, Z., Wang, Z.-M., Payne, A.M., Messi, M.L., Delbono, O., 2009. Increased Cavβ1A expression with aging contributes to skeletal muscle weakness. *Aging Cell* 8, 584–594. <https://doi.org/10.1111/j.1474-9726.2009.00507.x>
- Taylor, K., Sznajder, Ł.J., Cywoniuk, P., Thomas, J.D., Swanson, M.S., Sobczak, K., 2018. MBNL splicing activity depends on RNA binding site structural context. *Nucleic Acids Res* 46, 9119–9133. <https://doi.org/10.1093/nar/gky565>

- Teplova, M., Patel, D.J., 2008. Structural insights into RNA recognition by the alternative-splicing regulator muscleblind-like MBNL1. *Nat Struct Mol Biol* 15, 1343–1351. <https://doi.org/10.1038/nsmb.1519>
- Thomas, J.D., Sznajder, Ł.J., Bardhi, O., Aslam, F.N., Anastasiadis, Z.P., Scotti, M.M., Nishino, I., Nakamori, M., Wang, E.T., Swanson, M.S., 2017. Disrupted prenatal RNA processing and myogenesis in congenital myotonic dystrophy. *Genes Dev* 31, 1122–1133. <https://doi.org/10.1101/gad.300590.117>
- Tian, B., Manley, J.L., 2013. Alternative cleavage and polyadenylation: the long and short of it. *Trends Biochem Sci* 38, 312–320. <https://doi.org/10.1016/j.tibs.2013.03.005>
- Tian, B., White, R.J., Xia, T., Welle, S., Turner, D.H., Mathews, M.B., Thornton, C.A., 2000. Expanded CUG repeat RNAs form hairpins that activate the double-stranded RNA-dependent protein kinase PKR. *RNA* 6, 79–87. <https://doi.org/10.1017/s1355838200991544>
- Tian, B., Yang, J., Brasier, A.R., 2012. Two-step cross-linking for analysis of protein-chromatin interactions. *Methods Mol Biol* 809, 105–120. https://doi.org/10.1007/978-1-61779-376-9_7
- Tintignac, L.A., Brenner, H.-R., Rüegg, M.A., 2015. Mechanisms Regulating Neuromuscular Junction Development and Function and Causes of Muscle Wasting. *Physiol Rev* 95, 809–852. <https://doi.org/10.1152/physrev.00033.2014>
- Tosic, M., Allen, A., Willmann, D., Lepper, C., Kim, J., Duteil, D., Schüle, R., 2018. Lsd1 regulates skeletal muscle regeneration and directs the fate of satellite cells. *Nat Commun* 9, 366. <https://doi.org/10.1038/s41467-017-02740-5>
- Tran, H., Gourrier, N., Lemercier-Neuillet, C., Dhaenens, C.-M., Vautrin, A., Fernandez-Gomez, F.J., Arandel, L., Carpentier, C., Obriot, H., Eddarkaoui, S., Delattre, L., Brussels, E.V., Holt, I., Morris, G.E., Sablonnière, B., Buée, L., Charlet-Berguerand, N., Schraen-Maschke, S., Furling, D., Behm-Ansmant, I., Branlant, C., Caillet-Boudin, M.-L., Sergeant, N., 2011. Analysis of Exonic Regions Involved in Nuclear Localization, Splicing Activity, and Dimerization of Muscleblind-like-1 Isoforms *. *Journal of Biological Chemistry* 286, 16435–16446. <https://doi.org/10.1074/jbc.M110.194928>
- Traoré, M., Gentil, C., Benedetto, C., Hogrel, J.-Y., De la Grange, P., Cadot, B., Benkhelifa-Ziyyat, S., Julien, L., Lemaitre, M., Ferry, A., Piétri-Rouxel, F., Falcone, S., 2019. An embryonic CaVβ1 isoform promotes muscle mass maintenance via GDF5 signaling in adult mouse. *Sci Transl Med* 11, eaaw1131. <https://doi.org/10.1126/scitranslmed.aaw1131>
- Tsien, R.W., Lipscombe, D., Madison, D.V., Bley, K.R., Fox, A.P., 1988. Multiple types of neuronal calcium channels and their selective modulation. *Trends in Neurosciences* 11, 431–438. [https://doi.org/10.1016/0166-2236\(88\)90194-4](https://doi.org/10.1016/0166-2236(88)90194-4)
- Tuluc, P., Molenda, N., Schlick, B., Obermair, G.J., Flucher, B.E., Jurkat-Rott, K., 2009. A CaV1.1 Ca²⁺ channel splice variant with high conductance and voltage-sensitivity alters EC coupling in developing skeletal muscle. *Biophys J* 96, 35–44. <https://doi.org/10.1016/j.bpj.2008.09.027>
- Valdez, G., Tapia, J.C., Lichtman, J.W., Fox, M.A., Sanes, J.R., 2012. Shared Resistance to Aging and ALS in Neuromuscular Junctions of Specific Muscles. *PLOS ONE* 7, e34640. <https://doi.org/10.1371/journal.pone.0034640>

- Varadi, G., Lory, P., Schultz, D., Varadi, M., Schwartz, A., 1991. Acceleration of activation and inactivation by the beta subunit of the skeletal muscle calcium channel. *Nature* 352, 159–162. <https://doi.org/10.1038/352159a0>
- Venuti, J.M., Morris, J.H., Vivian, J.L., Olson, E.N., Klein, W.H., 1995. Myogenin is required for late but not early aspects of myogenesis during mouse development. *J Cell Biol* 128, 563–576. <https://doi.org/10.1083/jcb.128.4.563>
- Verbeeren, J., Teixeira, J., Garcia, S.M.D.A., 2023. The Muscleblind-like protein MBL-1 regulates microRNA expression in *Caenorhabditis elegans* through an evolutionarily conserved autoregulatory mechanism. *PLoS Genet* 19, e1011109. <https://doi.org/10.1371/journal.pgen.1011109>
- Vergnol, A., Traoré, M., Pietri-Rouxel, F., Falcone, S., 2022. New Insights in CaV β Subunits: Role in the Regulation of Gene Expression and Cellular Homeostasis. *Front Cell Dev Biol* 10, 880441. <https://doi.org/10.3389/fcell.2022.880441>
- Viegas, S., Jacobson, L., Waters, P., Cossins, J., Jacob, S., Leite, M.I., Webster, R., Vincent, A., 2012. Passive and active immunization models of MuSK-Ab positive myasthenia: electrophysiological evidence for pre and postsynaptic defects. *Exp Neurol* 234, 506–512. <https://doi.org/10.1016/j.expneurol.2012.01.025>
- Wang, E.T., Cody, N.A.L., Jog, S., Biancolella, M., Wang, T.T., Treacy, D.J., Luo, S., Schroth, G.P., Housman, D.E., Reddy, S., Lécuyer, E., Burge, C.B., 2012. Transcriptome-wide regulation of pre-mRNA splicing and mRNA localization by muscleblind proteins. *Cell* 150, 710–724. <https://doi.org/10.1016/j.cell.2012.06.041>
- Wang, W., Carey, M., Gralla, J.D., 1992. Polymerase II Promoter Activation: Closed Complex Formation and ATP-Driven Start Site Opening. *Science* 255, 450–453. <https://doi.org/10.1126/science.1310361>
- Wang, Z.-Z., Washabaugh, C.H., Yao, Y., Wang, J.-M., Zhang, L., Ontell, M.P., Watkins, S.C., Rudnicki, M.A., Ontell, M., 2003. Aberrant Development of Motor Axons and Neuromuscular Synapses in MyoD-Null Mice. *J. Neurosci.* 23, 5161–5169. <https://doi.org/10.1523/JNEUROSCI.23-12-05161.2003>
- Weber, A., 1959. On the role of calcium in the activity of adenosine 5'-triphosphate hydrolysis by actomyosin. *J Biol Chem* 234, 2764–2769.
- Weis, J., 1994. Jun, Fos, MyoD1, and Myogenin proteins are increased in skeletal muscle fiber nuclei after denervation. *Acta Neuropathol* 87, 63–70. <https://doi.org/10.1007/BF00386255>
- Weissgerber, P., Held, B., Bloch, W., Kaestner, L., Chien, K.R., Fleischmann, B.K., Lipp, P., Flockerzi, V., Freichel, M., 2006. Reduced cardiac L-type Ca²⁺ current in Ca(V)beta2^{-/-} embryos impairs cardiac development and contraction with secondary defects in vascular maturation. *Circ Res* 99, 749–757. <https://doi.org/10.1161/01.RES.0000243978.15182.c1>
- Weston, C., Yee, B., Hod, E., Prives, J., 2000. Agrin-Induced Acetylcholine Receptor Clustering Is Mediated by the Small Guanosine Triphosphatases Rac and Cdc42. *J Cell Biol* 150, 205–212.
- Wu, H., Xiong, W.C., Mei, L., 2010. To build a synapse: signaling pathways in neuromuscular junction assembly. *Development* 137, 1017–1033. <https://doi.org/10.1242/dev.038711>

- Xu, X., Lee, Y.J., Holm, J.B., Terry, M.D., Oswald, R.E., Horne, W.A., 2011. The Ca²⁺ channel beta4c subunit interacts with heterochromatin protein 1 via a PXVXL binding motif. *J Biol Chem* 286, 9677–9687. <https://doi.org/10.1074/jbc.M110.187864>
- Yadava, R.S., Mandal, M., Mahadevan, M.S., 2024. Studying the Effect of MBNL1 and MBNL2 Loss in Skeletal Muscle Regeneration. *Int J Mol Sci* 25, 2687. <https://doi.org/10.3390/ijms25052687>
- Yang, N., Das, D., Shankar, S.R., Goy, P.-A., Guccione, E., Taneja, R., 2022. An interplay between BRD4 and G9a regulates skeletal myogenesis. *Front. Cell Dev. Biol.* 10. <https://doi.org/10.3389/fcell.2022.978931>
- Yang, X., Arber, S., William, C., Li, L., Tanabe, Y., Jessell, T.M., Birchmeier, C., Burden, S.J., 2001. Patterning of Muscle Acetylcholine Receptor Gene Expression in the Absence of Motor Innervation. *Neuron* 30, 399–410. [https://doi.org/10.1016/S0896-6273\(01\)00287-2](https://doi.org/10.1016/S0896-6273(01)00287-2)
- Yoon, J.K., Olson, E.N., Arnold, H.H., Wold, B.J., 1997. Different MRF4 knockout alleles differentially disrupt Myf-5 expression: cis-regulatory interactions at the MRF4/Myf-5 locus. *Dev Biol* 188, 349–362. <https://doi.org/10.1006/dbio.1997.8670>
- Yuan, S.H., Arnold, W., Jorgensen, A.O., 1991. Biogenesis of transverse tubules and triads: immunolocalization of the 1,4-dihydropyridine receptor, TS28, and the ryanodine receptor in rabbit skeletal muscle developing in situ. *J Cell Biol* 112, 289–301. <https://doi.org/10.1083/jcb.112.2.289>
- Zammit, P.S., 2017. Function of the myogenic regulatory factors Myf5, MyoD, Myogenin and MRF4 in skeletal muscle, satellite cells and regenerative myogenesis. *Semin Cell Dev Biol* 72, 19–32. <https://doi.org/10.1016/j.semcdb.2017.11.011>
- Zamponi, G.W., Striessnig, J., Koschak, A., Dolphin, A.C., 2015. The Physiology, Pathology, and Pharmacology of Voltage-Gated Calcium Channels and Their Future Therapeutic Potential. *Pharmacol Rev* 67, 821–870. <https://doi.org/10.1124/pr.114.009654>
- Zetoune, A.B., Fontanière, S., Magnin, D., Anczuków, O., Buisson, M., Zhang, C.X., Mazoyer, S., 2008. Comparison of nonsense-mediated mRNA decay efficiency in various murine tissues. *BMC Genet* 9, 83. <https://doi.org/10.1186/1471-2156-9-83>
- Zhang, B., Liang, C., Bates, R., Yin, Y., Xiong, W.-C., Mei, L., 2012. Wnt proteins regulate acetylcholine receptor clustering in muscle cells. *Molecular Brain* 5, 7. <https://doi.org/10.1186/1756-6606-5-7>
- Zhang, X., Xie, J., Zhu, S., Chen, Y., Wang, L., Xu, B., 2017. Next-generation sequencing identifies pathogenic and modifier mutations in a consanguineous Chinese family with hypertrophic cardiomyopathy. *Medicine (Baltimore)* 96, e7010. <https://doi.org/10.1097/MD.0000000000007010>
- Zhang, Y., Yamada, Y., Fan, M., Bangaru, S.D., Lin, B., Yang, J., 2010. The beta subunit of voltage-gated Ca²⁺ channels interacts with and regulates the activity of a novel isoform of Pax6. *J Biol Chem* 285, 2527–2536. <https://doi.org/10.1074/jbc.M109.022236>
- Zhou, W., Saint-Amant, L., Hirata, H., Cui, W.W., Sprague, S.M., Kuwada, J.Y., 2006. Non-sense mutations in the dihydropyridine receptor beta1 gene, CACNB1, paralyze zebrafish relaxed mutants. *Cell Calcium* 39, 227–236. <https://doi.org/10.1016/j.ceca.2005.10.015>

Zhu, B., Ramachandran, B., Gulick, T., 2005. Alternative pre-mRNA splicing governs expression of a conserved acidic transactivation domain in myocyte enhancer factor 2 factors of striated muscle and brain. *J Biol Chem* 280, 28749–28760. <https://doi.org/10.1074/jbc.M502491200>

APPENDICES

Mini review – Vergnol et al. 2022

New Insights in $Ca_v\beta$ Subunits: Role in the Regulation of Gene Expression and Cellular Homeostasis

Amélie Vergnol, Massiré Traoré, France Pietri-Rouxel and Sestina Falcone*

INSERM U974, Center of Research in Myology-Sorbonne University, Paris, France

* Corresponding author. s.falcone@institut-myologie.org



New Insights in CaV β Subunits: Role in the Regulation of Gene Expression and Cellular Homeostasis

Amélie Vergnol, Massiré Traoré, France Pietri-Rouxel and Sestina Falcone*

INSERM U974, Center of Research in Myology-Sorbonne University, Paris, France

The voltage-gated calcium channels (CaVs or VGCCs) are fundamental regulators of intracellular calcium homeostasis. When electrical activity induces their activation, the influx of calcium that they mediate or their interaction with intracellular players leads to changes in intracellular Ca²⁺ levels which regulate many processes such as contraction, secretion and gene expression, depending on the cell type. The essential component of the pore channel is the CaV α_1 subunit. However, the fine-tuning of Ca²⁺-dependent signals is guaranteed by the modulatory role of the auxiliary subunits β , $\alpha_2\delta$, and γ of the CaVs. In particular, four different CaV β proteins (CaV β 1, CaV β 2, CaV β 3, and CaV β 4) are encoded by four different genes in mammals, each of them displaying several splice variants. Some of these isoforms have been described in regulating CaV α_1 docking and stability at the membrane and controlling the channel complex's conformational changes. In addition, emerging evidences have highlighted other properties of the CaV β subunits, independently of α_1 and non-correlated to its channel or voltage sensing functions. This review summarizes the recent findings reporting novel roles of the auxiliary CaV β subunits and in particular their direct or indirect implication in regulating gene expression in different cellular contexts.

Keywords: CaV β s, CaV subunits, gene expression, calcium, cell homeostasis, diseases

OPEN ACCESS

Edited by:

Marielle Saclier,
Institut Pasteur, France

Reviewed by:

Wenjun Xie,
Xi'an Jiaotong University, China

*Correspondence:

Sestina Falcone
s.falcone@institut-myologie.org

Specialty section:

This article was submitted to
Molecular and Cellular Pathology,
a section of the journal
Frontiers in Cell and Developmental
Biology

Received: 21 February 2022

Accepted: 16 March 2022

Published: 06 April 2022

Citation:

Vergnol A, Traoré M, Pietri-Rouxel F
and Falcone S (2022) New Insights in
CaV β Subunits: Role in the Regulation
of Gene Expression and
Cellular Homeostasis.
Front. Cell Dev. Biol. 10:880441.
doi: 10.3389/fcell.2022.880441

INTRODUCTION

Voltage-gated calcium channels (CaVs or VGCCs) are transmembrane ion channel proteins that act as major regulator of calcium-related cell functions. Their primary role is to mediate transmembrane calcium influx in response to membrane depolarization. Depending on their sensitivity to membrane depolarization, the activation of CaVs requires either a high or low threshold of membrane potential, dividing CaVs in High- and Low-voltage activated channels (HVA and LVA respectively) (Carbone and Lux, 1984; Fedulova et al., 1985). The crucial component of the channel pore is CaV α_1 , for which ten variants have been identified and classified based on their pharmacological properties and pore-opening kinetic: CaV1 and CaV2 for HVA, and CaV3 for LVA (Tsien et al., 1988; Catterall, 2011; Zamponi et al., 2015).

The CaV of skeletal muscle, also called dihydropyridine receptor (DHPR), was the first to be purified and cloned (Curtis and Catterall, 1984; Tanabe et al., 1987). In skeletal muscle fibers, CaV has a dual function of calcium channel and of voltage sensor of excitation-contraction coupling that controls, through a direct interaction, the opening of RyR1 (Ryanodine Receptor type 1), the Ca²⁺ release channel of the sarcoplasmic reticulum (Allard, 2018). Such a voltage sensor function for CaV and a direct interaction between CaV and RyR have also been described in neurons (Allard, 2018).

The main subunits of CaV, the α_1 subunits, are associated with auxiliary subunits that modulate expression and/or functional properties of the channel. In skeletal muscle, CaV1 is composed of five subunits: α_1S (or CaV1.1), β_1 , $\alpha_2\delta$, and γ (Hagiwara and Naka, 1964).

The function of both CaV1 and CaV2, members of HVA channels, needs the association of the auxiliary CaV β subunit for their plasma membrane docking and proper gating (Schredelseker et al., 2005; Dayal et al., 2013), while the function of LVA class of channel (CaV3) is independent of this subunit (Zhang et al., 2013).

CaV β are intracellular proteins that can either interact with the channel or be in their soluble form (Buraei and Yang, 2013).

Four different proteins, namely CaV β 1, CaV β 2, CaV β 3, and CaV β 4 encoded by four genes, exist in mammals, each of them having several splice variants (Buraei and Yang, 2010). All CaV β subunits are membrane-associated guanylate kinase (MAGUK) family members, with SH3 and GK domains as conserved domains whereas hook region, N- and C-terminal sequences are variables (Buraei and Yang, 2013). Hence, splice variants originate from alternative exon splicing and harbor different amino acid compositions of variable regions, leading to specificities in protein interaction (Subramanyam et al., 2009; Obermair et al., 2010), subcellular targeting properties, and cellular localization, all influencing channel complexes stability, and activity (Campiglio et al., 2013).

Intracellular Ca²⁺ changes account for eukaryotic cell adaptation to external stimuli by modifying gene expression. By controlling Ca²⁺ influx into the cell, CaVs are therefore at the key position to mediate excitation-transcription (E-T) coupling. In point of fact, the mechanisms leading to CREB (cyclic AMP response element-binding) or NFAT (nuclear factor of activated T-cells) activation require the CaVs-dependent Ca²⁺ signaling (Dolmetsch et al., 2001; Hernández-Ochoa et al., 2007; Zhao et al., 2007). Noteworthy, if the role of CaVs in E-T coupling is mainly restricted to the initiation of the subsequent transcriptional activity of Ca²⁺, other mechanisms have been demonstrated to initiate gene regulation by generating a shorter isoform of the CaV1.2 pore forming subunit, which relocated to the nucleus and held a transcription factor activity, (Gomez-Ospina et al., 2006; Gomez-Ospina et al., 2013). or by mobilizing intracellular CaV β subunit after conformational changes upon membrane depolarization (Servili et al., 2018). Indeed, CaV β 2 subunit was recently demonstrated to be the mediator of CaV1.2-dependent E-T coupling, by interacting with H-Ras, which in turn activated MAPK (Mitogen Activated Protein Kinase)/ERK (Extracellular Signal-Regulated Kinase) pathway to induce CREB-directed gene expression in human neuronal SH-SY5Y cells (Servili et al., 2018). Nevertheless, the possibility that CaVs auxiliary subunits may be directly implicated as transcription factors has become an emerging hypothesis in the last 2 decades (Barbado et al., 2009).

This review will focus on CaV β s newly and less broadly described insights by illustrating their nuclei tracking in line with their role as regulators of gene expression.

CAV β AS A SELF-SUFFICIENT NUCLEAR PROTEIN

After the initial cloning of CaV β 1 in skeletal muscle [CaV β 1D formerly known as CaV β 1A (Traoré et al., 2019)] (Ruth et al., 1989), further works described several variants of CaV β 1 expressed in muscle and other tissues CaV β 1 (Hibino et al., 2003; Hullin et al., 2003; Foell et al., 2004; Harry et al., 2004; Cohen et al., 2005), lacking the domain required for its interaction with CaV α _{1S} at

the α -Interaction Domain (AID domain). These reports suggested for the first time that some CaV β subunits isoforms may have a CaV-independent function. Subsequently, several studies have demonstrated the capability of CaV β s to translocate to the nucleus, giving additional indications toward a role for CaV β distinct from its well-known function as modulator of CaV channels.

If not all, at least some isoforms of CaV β 1, CaV β 2, CaV β 3 and CaV β 4 proteins display nuclear localization properties upon appropriate conditions (Buraei and Yang, 2010). For both CaV β 1, in skeletal muscle (Traoré et al., 2019), and CaV β 4, in neurons (Subramanyam et al., 2009; Etemad et al., 2014), this nuclear localization has been demonstrated to be linked to electrical activity. Indeed, our recent study showed that in adult skeletal muscle, after nerve damage, the embryonic isoform CaV β 1E was expressed and localized to the nuclei and near the Z-lines, while the constitutive adult muscle variant, CaV β 1D, remained associated with CaV1.1 at the sarcolemma (Traoré et al., 2019). Similarly, it has been reported that in neurons, CaV β 4A and CaV β 4B translocated to the nuclei when electrical activity was aborted, whereas CaV β 4E did not display nuclear localization. Additionally, a decrease in nuclear targeting of CaV β 1E (Traoré et al., 2019) and CaV β 4 (isoforms A and B) (Etemad et al., 2014) has been correlated with the onset of electrical activity throughout development in muscle fibers and neurons. Interestingly, the proportion of CaV β 4 isoforms targeted to nuclei has been associated with their activity as gene regulators (CaV β 4B > CaV β 4A > CaV β 4E) (Etemad et al., 2014). The mechanism originating the nuclear localization of CaV β 2 and CaV β 3 has not been clearly characterized, however, it can be hypothesized that they follow the same depolarization-sensitive process.

As previously mentioned, the capacity to get to the nucleus is not held by all the CaV β 1, CaV β 2, CaV β 3 and CaV β 4 splicing variants. The mechanisms underlying the specificities of the nucleus-targeted proteins could be passive diffusion through nuclear membrane for small proteins, while large ones need a Nuclear Localization Sequence (NLS), allowing their binding to Importins, or require the association with nuclear proteins as a shuttle. The molecular aspects behind CaV β s translocation to the nucleus are still not fully understood. For CaV β 1 (Buraei and Yang, 2010; Taylor et al., 2014) and CaV β 4 (Tadmouri et al., 2012) the SH3 domain of the protein has been described to exhibit the functional features leading to nuclear shuttling. An additional aspect was highlighted for CaV β 1E which have been described to display a putative NLS signal in its sequence (Taylor et al., 2014; Traoré et al., 2019), suggesting that its nuclear targeting was occurring through its binding to Importin proteins. However, modified genetic constructions lacking the putative NLS sequence did not prevent CaV β 1 to enter the nucleus. As an example, Subramanyam and colleagues showed that a specific double-arginine motif at the N-terminal was necessary and sufficient to induce the recruitment of the CaV β 4B variant toward the nuclei in mouse brain (Subramanyam et al., 2009). Nevertheless, this domain was subsequently demonstrated to be only partially involved in CaV β 4B docking to the nucleus, and that SH3/GK protein interaction domain was required to control its nuclear targeting. If these data were confirmed by several studies, a supplemental and non-exclusive mechanism came up with the demonstration of a PxxP binding motif in the SH3 domain of CaV β 1, raising the possibility that

CaV β proteins might also bind to proteins that themselves shuttle to the nucleus (Buraei and Yang, 2010). An instance supporting this hypothesis is CaV β 4C, which interaction with HP1 γ has been shown as mandatory to localize to the nucleus in mammalian cells (Hibino et al., 2003), while the truncation of a large part of its GK domain cut off the exclusive requirement of SH3/GK interaction for nuclear docking of CaV β s proteins. The molecular aspects of nuclear targeting were less studied for CaV β 2 and CaV β 3, for which some studies mentioning their binding with chaperone proteins may be relevant in supporting their tackling to the nuclei (Zhang et al., 2010; Pickel et al., 2021).

The evidence of the nuclear localization/translocation of several CaV β variants spotted these proteins with an undeniable CaV α ₁ independent function and pinpointed their putative role in the modulation of gene expression. The next part of this review will summarize the mechanisms described for the CaV β auxiliary subunits in the regulation of gene transcription.

CAV β S AS FACTORS CONTROLLING GENE EXPRESSION

CaV-Independent Role of CaV β in Calcium-Mediated Gene Expression

As mentioned, a large set of intracellular processes are driven through Ca²⁺ signaling and therefore dependent on the free cytosolic calcium. Either CaVs-related Ca²⁺ entry from the extracellular space or mobilization of intracellular Ca²⁺ stock can modulate its cytosolic concentration and originate this signaling. As an auxiliary subunit, CaV β has been described to regulate Ca²⁺ influx into the cell by modulating CaVs activity (Buraei and Yang, 2010), however, this protein was also reported to regulate intracellular Ca²⁺ in a CaV-independent way by acting on Ca²⁺ stores. Indeed, in both pancreatic cells (Berggren et al., 2004; Becker et al., 2021) and fibroblasts (Belkacemi et al., 2018), it has been demonstrated that CaV β 3 could interfere with Inositol 3-Phosphate (IP3)-induced Ca²⁺ release from the Endoplasmic Reticulum (ER) by binding IP3 Receptor (IP3R), therefore desensitizing cells to low IP3 concentration (Berggren et al., 2004; Belkacemi et al., 2018; Becker et al., 2021). In this process, CaV β 3 acted as a “brake” on Ca²⁺ release, affecting glucose-triggered insulin exocytosis in β -pancreatic cells (Berggren et al., 2004; Becker et al., 2021) and cellular mobility in fibroblasts (Belkacemi et al., 2018). These studies illustrated an effect of CaV β subunits in affecting gene expression by regulating free cytosolic calcium concentration (Figure 1A)

Interaction With Various Transcription Factors

CaV β 3 has been reported by Zhang and colleagues to co-localize with Pax6(S) in the nucleus and the interaction of these two proteins has been described to account for a ~ 50% decrease in Pax6(S) transcriptional activity (demonstrated in *Xenopus* oocytes by reporter system *in vitro*) without impairing CaV channel properties (Zhang et al., 2010). More generally, Pax6 proteins are composed of two DNA-binding domains: a paired-domain (PD) and a homeodomain (HD), allowing the binding to the cis-elements of target genes to regulate their transcription

rate, and a proline/serine/threonine (PST)-rich C-terminal domain, holding a trans-activation function. The work of Zhang and colleagues highlighted that Pax6(S) presented intact PD and HD domains while its C-terminal domain was truncated, resulting in a weaker Pax6(S) trans-activity. This isoform also differed from canonical Pax6 by a unique S-tail, originating its interaction with CaV β 3. This work suggested a novel function of CaV β 3 in negatively regulating Pax6(S) protein activity, although the precise mechanism, supposed to occur either by CaV β 3 allosteric hindrance or by Pax6(S) removal from DNA binding sites, remained undefined. More importantly, this report showed for the first time a full-length CaV β protein having a role in the channel function, acting also directly as a modulator of gene transcription (Zhang et al., 2010) (Figure 1B).

In 2003, Hibino and colleagues identified from chicken cochlea the CaV β 4C variant, a truncated CaV β 4 isoform which is also expressed in the brain, eye, heart and lung, concomitantly with the full-length isoforms CaV β 4A and CaV β 4B. However, in contrast with these two isoforms, CaV β 4C was described to lack a large part of the GK domain necessary to associate with CaV α ₁ (Chen et al., 2004), having therefore little effect on Ca²⁺ channel activity (Hibino et al., 2003). This -by then- newly identified variant showed a direct interaction with the chromo shadow domain (CSD) of the chromo box protein 2/heterochromatin protein 1 γ (CHCB2/HP1 γ), a nuclear protein that modulates the transcription of several genes by regulating heterochromatin conformation and therefore gene silencing. Noteworthy, the binding of HP1 γ to DNA regions of euchromatin was shown to correlate with gene repression. Hibino's study reported that when co-expressed with HP1 γ , CaV β 4C was recruited to the nucleus, dramatically lowering the CHCB2/HP1 γ gene-silencing activity *in vitro* (Hibino et al., 2003). This was the very first time that a CaV β protein was described to translocate to the nucleus and act as a transcriptional regulator.

A few years later, the existence of CaV β 4C was revealed in the human brain and observed to also interact with the CSD of HP1 γ (Xu et al., 2011). In addition, this interaction was shown to occur *via* a CSD binding motif, the PXVXL consensus sequence. Consistently with Hibino and colleagues' work, the binding of human CaV β 4C to HP1 γ was demonstrated to lead its nuclear translocation where it markedly reduces the gene-silencing activity of HP1 γ *in vitro* (Xu et al., 2011). These studies illustrated a first manner for CaV β subunits to indirectly modulate gene expression by affecting the activity of proteins involved in DNA compaction, like HP1 γ (Figure 1C).

The first report of nuclear localization of the CaV β 4B full-length isoform has been achieved by Subramanyam and colleagues in neurons and muscle cells, where this nuclear localization was reported to negatively relate on electrical activity (Subramanyam et al., 2009). The comprehension of the localization-related role of this protein has been realized later, with the demonstration that it acted as an organizing platform of a group of proteins which controlled transcription (Tadmouri et al., 2012). Among the complex-forming proteins, B56 δ , the regulatory subunit of the PP2A phosphatase induced histone dephosphorylation and HP1 γ restructured

heterochromatin. The last defined component of this complex was a transcription factor able to bind DNA at the promoter regions, allowing B56δ and HP1γ activity (Tadmouri et al., 2012). The gene that has been demonstrated to be modulated through this mechanism is Tyrosine hydroxylase (TH), the corresponding transcription factor being thyroid hormone receptor alpha (TRα) (Tadmouri et al., 2012). This situation was different from the previously described CaVβ4C effect on HP1γ activity, since CaVβ4B was, in this case, the element enabling the complex B56δ/HP1γ/TRα to access their activity site rather than modulating their function itself (Figure 1D). If Subramanyam and colleagues demonstrated a negative correlation between neuronal excitability and V5-tagged CaVβ4B positioning at the nucleus, this report showed that the endogenous CaVβ4B association with B56δ, originating their nucleus translocation, was consecutive to electrical activity, suggesting that the V5 tag might have hindered the pathways leading to CaVβ4B nuclear localization (Tadmouri et al., 2012).

Two further studies, aimed at investigating the property of CaVβ4 variants in controlling the expression of cell cycle-related genes, demonstrated that nuclear CaVβ4 full-length was able to inhibit cell proliferation, while its epileptogenic mutant, lacking C-term, had no impact. The effects of CaVβ4 on cell cycle were

related to the ability of the CaVβ4 to interact to either B56δ or T-cell factor 4 (TCF4) transcription factors. In the first case, B56δ recruitment to the nuclei by CaVβ4 was suggested to mediate the repression of genes involved in cell proliferation (Rima et al., 2017a). On the other hand, the binding of CaVβ4 to TCF4 was demonstrated to prevent its interaction with β-catenin, as additional mechanism to inhibit the activation of β-catenin-Wnt-dependent gene expression and cell cycle (Rima et al., 2017b). These reports established the ability of a CaVβ isoform to control gene expression, autonomously from CaVs, either dependently on or independently of electrical activity.

Interaction With Regulatory DNA Sequence

A study, published in 2014 by Taylor and colleagues, pinpointed that CaVβ1 was able to translocate to the nuclei and bind at the promoter region of 952 genes in muscle precursor cells (MPCs). Importantly, it showed that the absence of CaVβ1 resulted in changes in the expression of several genes, either positively or negatively misregulated, designating this subunit as having a transcription factor function (Taylor et al., 2014). This role was more deeply confirmed for myogenin which was up-regulated in the absence of CaVβ1, preventing a correct myogenic development (Schuster-Gossler et al., 2007; Ho et al., 2011;

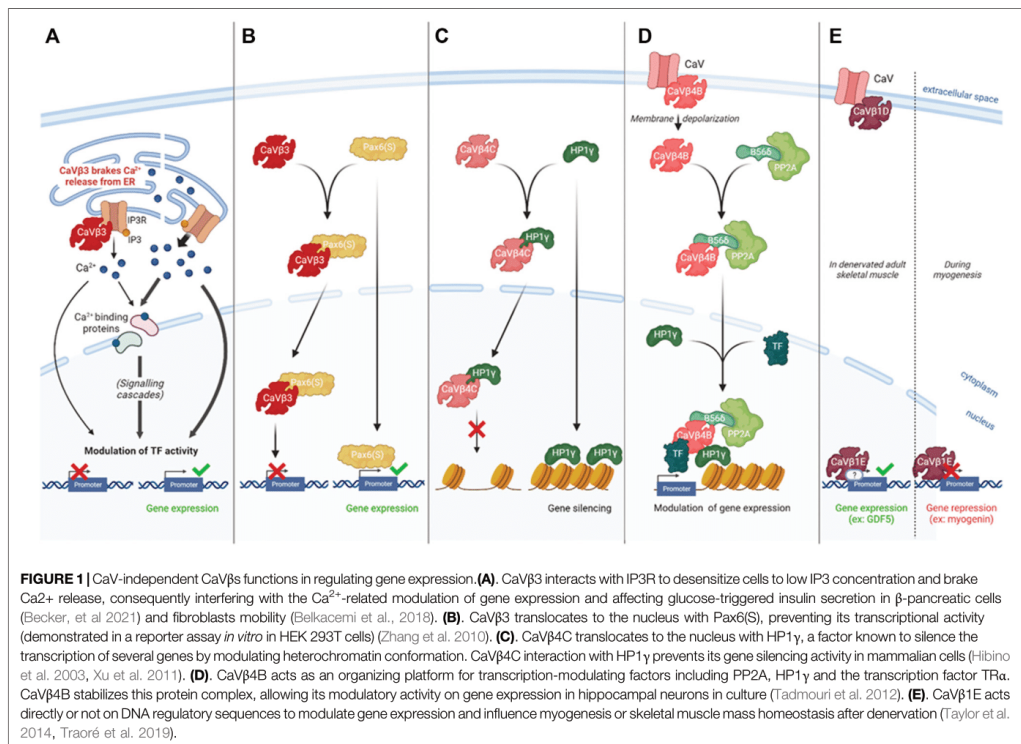


TABLE 1 | CaVβs associated disorders.

	Pathology/Pathological features	CACNB gene	References–CaVβ in the pathological context	
			Description	CaV-independent disorders
Heart	Brugada Syndrome (BrS), Type 4	CACNB2 (causal mutation)	Carbone and Lux (1984); Fedulova et al. (1985)	—
	Hypertrophic cardiomyopathy (HCM)	CACNB2 (gene modifier)	—	Catterall (2011) CaVβ2 regulates cardiomyocytes hypertrophy
Brain	Episodic Ataxia, Type 5	CACNB4 (causal mutation)	Tsien et al. (1988); Zamponi et al. (2015)	—
	Epilepsy, Idiopathic generalized 9 Epilepsy, Myoclonic Juvenile		Tsien et al. (1988)	— Curtis and Catterall (1984) The human CACNB4 mutation prevents CaVβ4 to gets to the nucleus and modulates gene expression
Skeletal muscle	Epilepsy, Myoclonic Juvenile	CACNB1E (age-related decline of expression)	—	Tanabe et al. (1987) Restoration of CaVβ1E rescues GDF5 expression and prevents age-related skeletal muscle wasting

Taylor et al., 2014). In this study, the CaVβ1A was the isoform described as a transcription factor, while our study published in 2019, rather indicated that the capacity to localize to the nucleus and exert a transcription factor role was actually carried by CaVβ1E which was identified as the main CaVβ1 isoform in C2C12 myoblast cell line, consistent with what observed in MPCs (Traoré et al., 2019). In addition, our work showed that the CaVβ1E played a crucial role in adult muscle mass homeostasis, when electrical activity was impaired, by regulating directly or indirectly the GDF5 promoter to trigger its transcriptional activity (Traoré et al., 2019) (Figure 1E).

By all these studies, CaVβs proteins have emerged as key players in regulating gene expression through Ca²⁺ signaling, DNA remodeling, modification of transcription factors activity or by acting as transcription factors themselves. When these functions are lost, multiple cellular functions are disturbed, involving CaVβ proteins in pathological conditions independently of the CaV-related aspect.

IMPLICATION OF CAVβS IN PATHOLOGICAL CONDITIONS

Although isoforms of CaVβ1, CaVβ2, CaVβ3, and CaVβ4 are expressed in several regions of the brain (Buraei and Yang, 2013), ablation of CaVβ1, CaVβ2 and CaVβ3 have no major impact on neuronal function (Ball et al., 2002). On the contrary, the relevance of CaVβ4 in the nervous system physiology was shown in the *lethargic (lh)* mouse model, having ataxic and epileptic phenotype (Burgess et al., 1997). Its implication in the pathophysiology of neuronal disorders was confirmed in Humans, after the discovery that missense and coding mutations, affecting the N-terminal region of the protein, were associated with epilepsy and ataxia, respectively (Escayg et al., 2000; Tadmouri et al., 2012). In the cerebellum, CaVβ4 is the most expressed and the major auxiliary subunit, together with α2δ-2, of the CaV2.1 calcium channel. Interestingly, mutations in all three proteins have been reported to lead to an epileptic and

ataxic phenotype. Therefore, CaVβ4 involvement in such pathological conditions was first linked with its CaV-associated role (Escayg et al., 2000).

However, an additional mechanism to further elucidate such pathologies came from the CaV-independent role of CaVβ4. Indeed, at the molecular level, human epilepsy and ataxia-associated mutations were found to prevent CaVβ4 to shuttle toward nuclei by disrupting the SH3/GK domains interaction and indicated that mis-regulated CaVβ4-dependent gene transcription may have a key relevance in the pathophysiology of these neurological disorders (Tadmouri et al., 2012) (Table 1).

In 2017, the importance of CACNB2 (gene coding for CaVβ2) as a genetic modifier of a Hypertrophic CardioMyopathy (HCM), in which the causal gene was MYBPC3 (Myosin-Binding Protein C), has been described for the first time (Zhang et al., 2017). The authors hypothesized that the potential mechanism modifying disease phenotype was based on the attenuation of CaV-dependent Ca²⁺ current associated with CACNB2 mutations. However, an additional possibility came out a few years later with a study that correlated the reduced cardiomyocyte hypertrophy to a CaV-independent CaVβ2 function (Pickel et al., 2021). CaVβ2 localization and activity in cardiomyocyte nuclei were shown to significantly regulate Calpain activity and Calpastatin expression (Pickel et al., 2021), a pro-hypertrophic protease and its inhibitor, respectively. Even though these events have not been explicitly linked to the reduction of cardiomyocyte hypertrophy, a correlation between the two might be hypothesized and would need to be further studied (Table 1).

Our recent work demonstrated the key role played by CaVβ1E in the context of age-related muscle wasting. We showed that CaVβ1E/GDF5 pathway counteracted the loss of muscle mass after denervation and that this signaling was defective in aged muscle fibers. Importantly, we overexpressed CaVβ1E in aged mouse muscles leading to increased GDF5 expression and activation of its signaling and therefore enabling the prevention of muscle mass loss and force decline during aging (Traoré et al., 2019). Importantly, the expression of an analogous of CaVβ1E has been also discovered in human muscle, decreasing

in an age-related manner, indicating that the defective hCaVβ1E signaling might also be impaired in sarcopenic patients and suggesting the CaVβ1E/GDF5 axis having a therapeutic potential in muscle aging and linked pathologies (Traoré et al., 2019) (Table 1).

Nevertheless, little is known about the causes behind the decrease of CaVβ1E expression in aged muscles. One hypothesis we assessed, was a damaged neuro-muscular junction (NMJ), but we did not detect any NMJ changes in the 78-week old mice involved in the study which could have testified toward changes in electrical activity and modifications in basal CaVβ1E levels (Traoré et al., 2019). Chromatin methylation/demethylation events or other epigenetic alterations could further explain the unbalanced CaVβ1E/GDF5 axis in old muscle and should be investigated in future works.

To summarize, mutations in CaVβs encoding genes have currently been associated with disorders and, even if the pathological mechanisms have not always been fully characterized, both CaVβs roles linked or unlinked to CaVs can be argued. Brugada Syndrome type 4 and Episodic ataxia type 5 present causative mutations in genes coding for CaVβs proteins and other CaV subunits (CACNA2D1 and CACNA1A, and CACNA1A respectively—MalaCard database), corroborating CaVβ involvement in pathological mechanisms in a CaV-linked way (Table 1). Nevertheless, and as described above, CaVβ may also originate or modify pathological features independently of CaVs and an underestimation of these situations can be hypothesized.

CONCLUSION

While CaVβs have long been considered to present exclusively CaVs' linked functions, we depicted in this review the elements

REFERENCES

- Allard, B. (2018). From Excitation to Intracellular Ca²⁺ Movements in Skeletal Muscle: Basic Aspects and Related Clinical Disorders. *Neuromuscul. Disord.* 28, 394–401. doi:10.1016/j.nmd.2018.03.004
- Ball, S. L., Powers, P. A., Shin, H.-S., Morgans, C. W., Peachey, N. S., and Gregg, R. G. (2002). Role of the β2 Subunit of Voltage-dependent Calcium Channels in the Retinal Outer Plexiform Layer. *Invest. Ophthalmol. Vis. Sci.* 43, 1595–1603.
- Barbado, M., Fablet, K., Ronjat, M., and De Waard, M. (2009). Gene Regulation by Voltage-dependent Calcium Channels. *Biochim. Biophys. Acta (Bba) - Mol. Cell Res.* 1793, 1096–1104. doi:10.1016/j.bbamcr.2009.02.004
- Becker, A., Wardas, B., Salah, H., Amini, M., Fecher-Trost, C., Sen, Q., et al. (2021). Cavβ3 Regulates Ca²⁺ Signaling and Insulin Expression in Pancreatic β-Cells in a Cell-Autonomous Manner. *Diabetes* 70, 2532–2544. doi:10.2337/db21-0078
- Belkacemi, A., Hui, X., Wardas, B., Laschke, M. W., Wissenbach, U., Menger, M. D., et al. (2018). IP3 Receptor-dependent Cytoplasmic Ca²⁺ Signals Are Tightly Controlled by Cavβ3. *Cel Rep.* 22, 1339–1349. doi:10.1016/j.celrep.2018.01.010
- Berggren, P.-O., Yang, S.-N., Murakami, M., Efanov, A. M., Uhles, S., Köhler, M., et al. (2004). Removal of Ca²⁺ Channel β3 Subunit Enhances Ca²⁺ Oscillation Frequency and Insulin Exocytosis. *Cell* 119, 273–284. doi:10.1016/j.cell.2004.09.033
- Buraei, Z., and Yang, J. (2013). Structure and Function of the β Subunit of Voltage-Gated Ca²⁺ Channels. *Biochim. Biophys. Acta (Bba) - Biomembranes* 1828, 1530–1540. doi:10.1016/j.bbamem.2012.08.028

pointing towards a far more extensive significance in organ and cell homeostasis. CaVβs proteins have been described as efficient modulators of gene expression, either through their effect on Ca²⁺ signaling or through their DNA-related activities enabled by their nuclear localization. Regardless of the molecular mechanisms in which CaVβs are implicated, these proteins have been shown to influence cell and tissue capability to respond to different stimuli and to adapt following environmental changes. In the light of the findings of these two last decades, the impact of CaVβ1 and CaVβ4 on gene expression has been demonstrated several times, whereas CaVβ2 and CaVβ3 are less deeply characterized. A better establishment and appreciation of CaVβs relevance in cell biology will probably strengthen our understanding in a plethora of physiological and pathological mechanisms.

AUTHOR CONTRIBUTIONS

FP-R and SF proposed the concept for the review, the first draft and revised the manuscript; AV wrote the manuscript and drawn figure and table; MT read the manuscript and contributed to the article conception.

FUNDING

First author fellowship is funded by Sorbonne University.

ACKNOWLEDGMENTS

We thank B. Allard for helpful scientific discussion and the reading of the review; A. Muchir and D. Cardoso to have shared their Biorender Licence.

- Buraei, Z., and Yang, J. (2010). The β Subunit of Voltage-Gated Ca²⁺ Channels. *Physiol. Rev.* 90, 1461–1506. doi:10.1152/physrev.00057.2009
- Burgess, D. L., Jones, J. M., Meisler, M. H., and Noebels, J. L. (1997). Mutation of the Ca²⁺ Channel β Subunit Gene Cchb4 Is Associated with Ataxia and Seizures in the Lethargic (Lh) Mouse. *Cell* 88, 385–392. doi:10.1016/s0092-8674(00)81877-2
- Campiglio, M., Di Biase, V., Tuluc, P., and Flucher, B. E. (2013). Stable Incorporation versus Dynamic Exchange of β Subunits in a Native Ca²⁺ Channel Complex. *J. Cel. Sci.* 126, 2092–2101. doi:10.1242/jcs.jcs124537
- Carbone, E., and Lux, H. D. (1984). A Low Voltage-Activated Calcium Conductance in Embryonic Chick Sensory Neurons. *Biophysical J.* 46, 413–418. doi:10.1016/s0006-3495(84)84037-0
- Catterall, W. A. (2011). Voltage-gated Calcium Channels. *Cold Spring Harbor Perspect. Biol.* 3, a003947. doi:10.1101/cshperspect.a003947
- Chen, Y.-H., Li, M.-h., Zhang, Y., He, L.-l., Yamada, Y., Fitzmaurice, A., et al. (2004). Structural Basis of the α1-β Subunit Interaction of Voltage-Gated Ca²⁺ Channels. *Nature* 429, 675–680. doi:10.1038/nature02641
- Cohen, R. M., Foell, J. D., Balijepalli, R. C., Shah, V., Hell, J. W., and Kamp, T. J. (2005). Unique Modulation of L-type Ca²⁺ channels by Short Auxiliary β1 subunit Present in Cardiac Muscle. *Am. J. Physiology-Heart Circulatory Physiol.* 288, H2363–H2374. doi:10.1152/ajpheart.00348.2004
- Curtis, B. M., and Catterall, W. A. (1984). Purification of the Calcium Antagonist Receptor of the Voltage-Sensitive Calcium Channel from Skeletal Muscle Transverse Tubules. *Biochemistry* 23, 2113–2118. doi:10.1021/bi00305a001
- Dayal, A., Bhat, V., Franzini-Armstrong, C., and Grabner, M. (2013). Domain Cooperativity in the β 1a Subunit Is Essential for Dihydropyridine Receptor

- Voltage Sensing in Skeletal Muscle. *Proc. Natl. Acad. Sci. U.S.A.* 110, 7488–7493. doi:10.1073/pnas.1301087110
- Dolmetsch, R. E., Pajvani, U., Fife, K., Spotts, J. M., and Greenberg, M. E. (2001). Signaling to the Nucleus by an L-type Calcium Channel-Calmodulin Complex through the MAP Kinase Pathway. *Science* 294, 333–339. doi:10.1126/science.1063395
- Escayg, A., De Waard, M., Lee, D. D., Bichet, D., Wolf, P., Mayer, T., et al. (2000). Coding and Noncoding Variation of the Human Calcium-Channel β 4-Subunit Gene CACNB4 in Patients with Idiopathic Generalized Epilepsy and Episodic Ataxia. *Am. J. Hum. Genet.* 66, 1531–1539. doi:10.1086/302909
- Etemad, S., Obermair, G. J., Bindeireith, D., Benedetti, A., Stanika, R., Di Biase, V., et al. (2014). Differential Neuronal Targeting of a New and Two Known Calcium Channel 4 Subunit Splice Variants Correlates with Their Regulation of Gene Expression. *J. Neurosci.* 34, 1446–1461. doi:10.1523/jneurosci.3935-13.2014
- Fedulova, S. A., Kostyuk, P. G., and Veselovsky, N. S. (1985). Two Types of Calcium Channels in the Somatic Membrane of New-Born Rat Dorsal Root Ganglion Neurons. *J. Physiol.* 359, 431–446. doi:10.1113/jphysiol.1985.sp015594
- Foell, J. D., Balijepalli, R. C., Delisle, B. P., Yunker, A. M. R., Robia, S. L., Walker, J. W., et al. (2004). Molecular Heterogeneity of Calcium Channel β -subunits in Canine and Human Heart: Evidence for Differential Subcellular Localization. *Physiol. Genomics* 17, 183–200. doi:10.1152/physiolgenomics.00207.2003
- Gomez-Ospina, N., Panagiotakos, G., Portmann, T., Pasca, S. P., Rabah, D., Budzillo, A., et al. (2013). A Promoter in the Coding Region of the Calcium Channel Gene CACNA1C Generates the Transcription Factor CCAAT. *PLOS ONE* 8, e60526. doi:10.1371/journal.pone.0060526
- Gomez-Ospina, N., Tsuruta, F., Barreto-Chang, O., Hu, L., and Dolmetsch, R. (2006). The C Terminus of the L-type Voltage-Gated Calcium Channel CaV1.2 Encodes a Transcription Factor. *Cell* 127, 591–606. doi:10.1016/j.cell.2006.10.017
- Hagiwara, S., and Naka, K.-i. (1964). The Initiation of Spike Potential in Barnacle Muscle Fibers under Low Intracellular Ca⁺⁺. *J. Gen. Physiol.* 48, 141–162. doi:10.1085/jgp.48.1.141
- Harry, J. B., Kobrinsky, E., Abernethy, D. R., and Soldatov, N. M. (2004). New Short Splice Variants of the Human Cardiac Cav β 2 Subunit. *J. Biol. Chem.* 279, 46367–46372. doi:10.1074/jbc.m409523200
- Hernández-Ochoa, E. O., Contreras, M., Cseresnyés, Z., and Schneider, M. F. (2007). Ca²⁺ Signal Summation and NFATc1 Nuclear Translocation in Sympathetic Ganglion Neurons during Repetitive Action Potentials. *Cell Calcium* 41, 559–571. doi:10.1016/j.cca.2006.10.006
- Hibino, H., Pironkova, R., Onwumere, O., Rousset, M., Charnet, P., Hudspeth, A. J., et al. (2003). Direct Interaction with a Nuclear Protein and Regulation of Gene Silencing by a Variant of the Ca²⁺-channel β 4 Subunit. *Proc. Natl. Acad. Sci. U.S.A.* 100, 307–312. doi:10.1073/pnas.0136791100
- Ho, A. T. V., Hayashi, S., Bröhl, D., Auradé, F., Rattenbach, R., and Relaix, F. (2011). Neural Crest Cell Lineage Restricts Skeletal Muscle Progenitor Cell Differentiation through Neuregulin1-ErbB3 Signaling. *Develop. Cell* 21, 273–287. doi:10.1016/j.devcel.2011.06.019
- Hullin, R., Khan, I. F. Y., Wirtz, S., Mohacsi, P., Varadi, G., Schwartz, A., et al. (2003). Cardiac L-type Calcium Channel β -Subunits Expressed in Human Heart Have Differential Effects on Single Channel Characteristics. *J. Biol. Chem.* 278, 21623–21630. doi:10.1074/jbc.m211164200
- Obermair, G. J., Schlick, B., Di Biase, V., Subramanyam, P., Gebhart, M., Baumgartner, S., et al. (2010). Reciprocal Interactions Regulate Targeting of Calcium Channel β Subunits and Membrane Expression of α 1 Subunits in Cultured Hippocampal Neurons. *J. Biol. Chem.* 285, 5776–5791. doi:10.1074/jbc.m109.044271
- Pickel, S., Cruz-Garcia, Y., Bandleon, S., Barkovits, K., Heindl, C., Völker, K., et al. (2021). The β 2-Subunit of Voltage-Gated Calcium Channels Regulates Cardiomyocyte Hypertrophy. *Front. Cardiovasc. Med.* 8, 692. doi:10.3389/fcvm.2021.704657
- Rima, M., Daghni, M., De Waard, S., Gaborit, N., Fajloun, Z., Ronjat, M., et al. (2017). The β 4 Subunit of the Voltage-Gated Calcium Channel (Cacnb4) Regulates the Rate of Cell Proliferation in Chinese Hamster Ovary Cells. *Int. J. Biochem. Cel Biol.* 89, 57–70. doi:10.1016/j.biocel.2017.05.032
- Rima, M., Daghni, M., Lopez, A., Fajloun, Z., Lefrançois, L., Dunach, M., et al. (2017). Down-regulation of the Wnt/ β -Catenin Signaling Pathway by Cacnb4. *MBoC* 28, 3699–3708. doi:10.1091/mbc.e17-01-0076
- Ruth, P., Röhrkasten, A., Biel, M., Bosse, E., Regulla, S., Meyer, H. E., et al. (1989). Primary Structure of the β Subunit of the DHP-Sensitive Calcium Channel from Skeletal Muscle. *Science* 245, 1115–1118. doi:10.1126/science.2549640
- Schredelseker, J., Di Biase, V., Obermair, G. J., Felder, E. T., Flucher, B. E., Franzini-Armstrong, C., et al. (2005). The β 1a Subunit Is Essential for the Assembly of Dihydropyridine-Receptor Arrays in Skeletal Muscle. *Proc. Natl. Acad. Sci. U.S.A.* 102, 17219–17224. doi:10.1073/pnas.0508710102
- Schuster-Gossler, K., Cordes, R., and Gossler, A. (2007). Premature Myogenic Differentiation and Depletion of Progenitor Cells Cause Severe Muscle Hypotrophy in Delta1 Mutants. *Proc. Natl. Acad. Sci. U.S.A.* 104, 537–542. doi:10.1073/pnas.0608281104
- Servili, E., Trus, M., Maayan, D., and Atlas, D. (2018). β -Subunit of the Voltage-Gated Ca²⁺ Channel Cav1.2 Drives Signaling to the Nucleus via H-Ras. *Proc. Natl. Acad. Sci. U.S.A.* 115, E8624–E8633. doi:10.1073/pnas.1805380115
- Subramanyam, P., Obermair, G. J., Baumgartner, S., Gebhart, M., Striessnig, J., Kaufmann, W. A., et al. (2009). Activity and Calcium Regulate Nuclear Targeting of the Calcium Channel Beta4b Subunit in Nerve and Muscle Cells. *Channels* 3, 343–355. doi:10.4161/chan.3.5.9696
- Tadmouri, A., Kiyonaka, S., Barbado, M., Rousset, M., Fablet, K., Sawamura, S., et al. (2012). Cacnb4 Directly Couples Electrical Activity to Gene Expression, a Process Defective in Juvenile Epilepsy. *EMBO J.* 31, 3730–3744. doi:10.1038/emboj.2012.226
- Tanabe, T., Takeshima, H., Mikami, A., Flockerzi, V., Takahashi, H., Kangawa, K., et al. (1987). Primary Structure of the Receptor for Calcium Channel Blockers from Skeletal Muscle. *Nature* 328, 313–318. doi:10.1038/328313a0
- Taylor, J., Pereyra, A., Zhang, T., Messi, M. L., Wang, Z.-M., Heréñú, C., et al. (2014). The Cav β 1a Subunit Regulates Gene Expression and Suppresses Myogenin in Muscle Progenitor Cells. *J. Cell Biol.* 205, 829–846. doi:10.1083/jcb.201403021
- Traoré, M., Gentil, C., Benedetto, C., Hogrel, J.-Y., De la Grange, P., Cadot, B., et al. (2019). An Embryonic CaV β 1 Isoform Promotes Muscle Mass Maintenance via GDF5 Signaling in Adult Mouse. *Sci. Translational Med.* 11, eaaw1131. doi:10.1126/scitranslmed.aaw1131
- Tsien, R. W., Lipscombe, D., Madison, D. V., Bley, K. R., and Fox, A. P. (1988). Multiple Types of Neuronal Calcium Channels and Their Selective Modulation. *Trends Neurosciences* 11, 431–438. doi:10.1016/0166-2236(88)90194-4
- Xu, X., Lee, Y. J., Holm, J. B., Terry, M. D., Oswald, R. E., and Horne, W. A. (2011). The Ca²⁺ Channel β 4c Subunit Interacts with Heterochromatin Protein 1 via a PXVXL Binding Motif. *J. Biol. Chem.* 286, 9677–9687. doi:10.1074/jbc.m110.187864
- Zamponi, G. W., Striessnig, J., Koschak, A., and Dolphin, A. C. (2015). The Physiology, Pathology, and Pharmacology of Voltage-Gated Calcium Channels and Their Future Therapeutic Potential. *Pharmacol. Rev.* 67, 821–870. doi:10.1124/pr.114.009654
- Zhang, X., Xie, J., Zhu, S., Chen, Y., Wang, L., and Xu, B. (2017). Next-generation Sequencing Identifies Pathogenic and Modifier Mutations in a Consanguineous Chinese Family with Hypertrophic Cardiomyopathy. *Medicine (Baltimore)* 96, e7010. doi:10.1097/md.00000000000007010
- Zhang, Y., Jiang, X., Snutch, T. P., and Tao, J. (2013). Modulation of Low-Voltage-Activated T-type Ca²⁺ Channels. *Biochim. Biophys. Acta (Bba) - Biomembranes* 1828, 1550–1559. doi:10.1016/j.bbame.2012.08.032
- Zhang, Y., Yamada, Y., Fan, M., Bangaru, S. D., Lin, B., and Yang, J. (2010). The β Subunit of Voltage-Gated Ca²⁺ Channels Interacts with and Regulates the Activity of a Novel Isoform of Pax6. *J. Biol. Chem.* 285, 2527–2536. doi:10.1074/jbc.m109.022236
- Zhao, R., Liu, L., and Rittenhouse, A. R. (2007). Ca²⁺ Influx through Both L- and N-type Ca²⁺ Channels Increases C-Fos Expression by Electrical Stimulation of Sympathetic Neurons. *Eur. J. Neurosci.* 25, 1127–1135. doi:10.1111/j.1460-9568.2007.05359.x

Conflict of Interest: The authors declare that the research was conducted in the absence of any commercial or financial relationships that could be construed as a potential conflict of interest.

Publisher's Note: All claims expressed in this article are solely those of the authors and do not necessarily represent those of their affiliated organizations, or those of the publisher, the editors and the reviewers. Any product that may be evaluated in this article, or claim that may be made by its manufacturer, is not guaranteed or endorsed by the publisher.

Copyright © 2022 Vergnol, Traoré, Pietri-Rouxel and Falcone. This is an open-access article distributed under the terms of the Creative Commons Attribution License (CC BY). The use, distribution or reproduction in other forums is permitted, provided the original author(s) and the copyright owner(s) are credited and that the original publication in this journal is cited, in accordance with accepted academic practice. No use, distribution or reproduction is permitted which does not comply with these terms.

2nd author publication – Traoré et al. 2024

(Accepted manuscript)

GDF5 as a rejuvenating treatment for age-related neuromuscular failure

Traoré Massiré^{1†} Noviello Chiara^{1†} **Vergnol Amélie**¹, Gentil Christel¹, Halliez Marius¹, Saillard Lucile¹, Gelin Maxime¹, Forand Anne¹, Lemaitre Mégane², Guesmia Zoheir¹, Cadot Bruno¹, Caldas Eriky³, Marty Benjamin³, Mougnot Nathalie², Messéant Julien¹, Stochlic Laure¹, Sadoine Jeremy⁴, Slimani Lofti⁴, Jolly Ariane⁵, De la Grange Pierre⁵, Hogrel Jean-Yves⁶, Pietri-Rouxel France^{1‡} and Falcone Sestina^{1‡}

¹ Sorbonne Université, INSERM, Institut de Myologie, Centre de Recherche en Myologie, F-75013 Paris, France

² Sorbonne Université, INSERM UMS28, Phénotypage du Petit Animal, Paris 75013, France

³ Institut de Myologie, CEA, Laboratoire d'imagerie et de spectroscopie par RMN, F-75013 Paris, France

⁴ Université de Paris, Plateforme d'Imagerie du Vivant (PIV), Montrouge, France

⁵ GenoSplice, Paris Biotech Santé, Paris, France

⁶ Institut de Myologie, Laboratoire de physiologie et d'évaluation neuromusculaire, Paris, F26 75013 France

†,‡ These authors contributed equally to this work.

GDF5 as a rejuvenating treatment for age-related neuromuscular failure

Traoré Massiré,^{1,†} Noviello Chiara,^{1,†} Vergnol Amélie,¹ Gentil Christel,¹ Halliez Marius,¹ Saillard Lucile,¹ Gelin Maxime,¹ Forand Anne,¹ Lemaitre Mégane,² Guesmia Zoheir,¹ Cadot Bruno,¹ Caldas Eriky,³ Marty Benjamin,³ Mougenot Nathalie,² Messéant Julien,¹ Strohlic Laure,¹ Sadoine Jeremy,⁴ Slimani Lofti,⁴ Jolly Ariane,⁵ De la Grange Pierre,⁵ Hogrel Jean-Yves,⁶ Pietri-Rouxel France^{1,‡} and Falcone Sestina^{1,‡}

^{†,‡}These authors contributed equally to this work.

Abstract

Sarcopenia involves a progressive loss of skeletal muscle force, quality and mass during ageing, which results in increased inability and death; however, no cure has been established thus far. Growth differentiation factor 5 (GDF5) has been described to modulate muscle mass maintenance in various contexts.

For our proof of concept, we overexpressed GDF5 by AAV vector injection in *Tibialis Anterior* (TA) muscle of adult aged (20 months) mice and performed molecular and functional analysis of skeletal muscle. We analysed human *Vastus Lateralis* muscle biopsies from adult young (21-42 years) and aged (77-80 years) donors, quantifying the molecular markers modified by GDF5 overexpression (OE) in mouse muscle. We validated the major effects of GDF5 overexpression using human immortalized myotubes and Schwann Cells (SCs). We established a pre-clinical study by treating chronically (for 4 months) aged mice using recombinant GDF5 protein (rGDF5) in systemic administration and evaluated the long-term effect of this treatment on muscle mass and function.

Here, we demonstrated that GDF5 OE in the old TAs promoted an increase of 16.5% of muscle weight ($P=0.0471$) associated with a higher percentage of 5000-6000 μm^2 large fibres ($P=0.0211$), without the induction of muscle regeneration. Muscle mass gain was associated with an amelioration of 26.8% of rate of force generation ($P=0.0330$) and a better neuromuscular

© The Author(s) 2024. Published by Oxford University Press on behalf of the Guarantors of Brain. All rights reserved. For commercial re-use, please contact reprints@oup.com for reprints and translation rights for reprints. All other permissions can be obtained through our RightsLink service via the Permissions link on the article page on our site—for further information please contact journals.permissions@oup.com. This article is published and distributed under the terms of the Oxford University Press, Standard Journals Publication Model (<https://academic.oup.com/pages/standard-publication-reuse-rights>)

1

1 connectivity ($P=0.0098$). Moreover, GDF5 OE preserved neuromuscular junction (NMJ)
2 morphology (38.5% of nerve terminal area increase, $P<0.0001$) and stimulated the expression of
3 re-innervation-related genes, in particular markers of SCs (fold change 3.19 for S100b gene
4 expression, $P=0.0101$). To further characterize the molecular events induced by GDF5 OE
5 during ageing, we performed a genome-wide transcriptomic analysis of treated muscles and
6 showed that this factor leads to a “rejuvenating” transcriptomic signature in aged mice, as 42%
7 of the transcripts dysregulated by ageing reverted to youthful expression levels upon GDF5 OE
8 ($P<0.05$). Towards a pre-clinical approach, we performed a long-term systemic treatment using
9 rGDF5 and showed its effectiveness in counteracting age-related muscle wasting, improving
10 muscle function (17,8% of absolute maximal force increase, $P=0.0079$), ensuring neuromuscular
11 connectivity and preventing NMJ degeneration (7,96 % of AchR area increase, $P=0.0125$). In
12 addition, in human muscle biopsies, we found the same age-related alterations than those
13 observed in mice and improved by GDF5 and reproduced its major effects on human cells,
14 suggesting this treatment as efficient in humans.

15 Overall, these data provide a foundation to examine the curative potential of GDF5 drug in
16 clinical trials for sarcopenia and, eventually, other neuromuscular diseases.

17

18 **Author affiliations:**

19 1 Sorbonne Université, INSERM, Institut de Myologie, Centre de Recherche en Myologie, F-
20 75013 Paris, France

21 2 Sorbonne Université, INSERM UMS28, Phénotypage du Petit Animal, Paris 75013, France

22 3 Institut de Myologie, CEA, Laboratoire d'imagerie et de spectroscopie par RMN, F-75013
23 Paris, France

24 4 Université de Paris, Plateforme d'Imagerie du Vivant (PIV), Montrouge, France

25 5 GenoSplice, Paris Biotech Santé, Paris, France

26 6 Institut de Myologie, Laboratoire de physiologie et d'évaluation neuromusculaire, Paris, F-
27 75013 France

28

1 Correspondence to: Falcone Sestina
2 Sorbonne Université, INSERM, Institut de Myologie, Centre de Recherche en Myologie, 105
3 boulevard de l'Hôpital, F-75013 Paris, France
4 E-mail: sestinaf@gmail.com

5
6 Correspondence may also be addressed to: Pietri-Rouxel France
7 E-mail: france.pietri-rouxel@upmc.fr

8
9 **Running title:** GDF5 as a rejuvenating treatment

10 **Keywords:** endplate; therapy; musculature

11

12 **Introduction**

Sarcopenia is defined as a progressive age-related loss of strength, quality and mass of muscle inducing adverse outcomes, including frailty, disability and mortality¹. Several mechanisms are proposed to explain the onset and progression of sarcopenia. Studies in rodents and humans suggest that age-related muscle denervation is one of the a major driver of muscle fibre loss and force decline²⁻⁴. A phenomena not associated with motor neuron loss in the spinal cord, indicating that changes in the neuromuscular junction (NMJ) are key⁵. Perisynaptic Schwann cells (SCs), covering physically NMJs, play a critical role during their formation and maintenance, and are involved in neurotransmission and muscle reinnervation after peripheral nerve injury⁶. Interestingly, low reinnervation capacity observed in old muscle is associated with SC degeneration occurring at the NMJ during ageing⁷⁻¹⁰.

13 Nevertheless, many factors are involved in age-related muscle changes, as pro-inflammatory
14 mediators and redox signalling imbalance contributing to muscle wasting^{11,12}. All these aspects
15 have to be considered in a therapeutic perspective for efficient treatments. Today, therapeutic
16 approaches counteracting sarcopenia are limited to caloric restriction and physical exercise
17 which are met with limited patient compliance¹³⁻¹⁷. However, pharmacological strategies have

1 been proposed¹⁸, based on myostatin and activin-A, modulators of muscle growth, to increase
2 muscle mass¹⁹ but clinical trials showed no significant effect on muscle strength or physical
3 performance of sarcopenic patients^{19,20}. Other strategies offered to increase protein intake or
4 vitamin D supplementation; inhibit interleukin-6 or tumour necrosis factor α to reduce inflamm-
5 aging; or hormone administration to enhance anabolism²¹. Nevertheless, none of these treatments
6 alone rescued the neuromuscular failures characterizing sarcopenia²¹. Identification of novel
7 drug to counteract age-related neuromuscular failure is still a challenge.

8 In this context, growth and differentiation factor 5 (GDF5) is of great interest because of its
9 broad functions in neuromuscular system²²⁻²⁴. GDF5 (also called bone morphogenetic protein-
10 BMP 14) belongs to the BMP family activating SMAD (fusion of *Caenorhabditis elegans* Sma
11 and the *Drosophila* Mad, or mothers against decapentaplegic) 1/5 complex phosphorylation
12 leading to transcription of inhibitor of differentiation (Id) genes. BMPs are involved in bone and
13 cartilage development and regeneration^{25,26}. Genetic polymorphisms and *GDF5* mutations are
14 associated with osteoarthritis susceptibility, joint and bone disorders^{27,28}, but also with decreased
15 muscle strength in humans over 65 years of age²⁹. GDF5 can be considered as a pleiotropic
16 factor, modulating physiological processes to shape skeletal tissues, control angiogenesis³⁰,
17 neuronal development and repair^{31,32}, adipose tissue metabolism^{33,34} and as neurotrophic in
18 several studies^{22,32,35,36}. Consistently, *Gdf5* transcript has been shown to be enriched at NMJ
19 regions and its receptors BMPRI1A BMPRI1B expressed in muscle, motor nerve and nerve-
20 associated cells²². After nerve damage, increased GDF5 expression has been shown to be
21 essential to counteract atrophy²³, sustain re-innervation²² and its signalling regulating skeletal
22 muscle mass homeostasis in mice^{23,24,36-40}. Recently, we showed that age-related muscle mass
23 loss is associated with the alteration of the compensatory mechanism involving GDF5 axis in
24 mice and humans and that boosting this signalling prevented aged muscle wasting²⁴.

25 Here, we aimed to unravel the molecular mechanism underlying the beneficial effects of GDF5-
26 based strategies on neuromuscular features during aging. We showed that local GDF5
27 overexpression (OE) in mice, initiated at the onset of age-related muscle atrophy, increased
28 muscle mass and function, inhibited protein degradation and ameliorated neuromuscular
29 connectivity and NMJ morphology. This effect was associated with muscle reinnervation linked
30 to SCs. Whole-transcriptome sequencing of adult/aged muscle overexpressing GDF5
31 demonstrated a “rejuvenating” transcriptomic signature in GDF5-treated aged muscles compared

4

1 to adult/aged controls. To translate this finding to humans, we used systemic administration of
2 recombinant GDF5 protein (rGDF5) in mice and demonstrated its benefits in preventing age-
3 related neuromuscular failure compromising muscle mass and function as well as an age-
4 dependent decrease in the levels of SC-specific markers in human muscle biopsies, strongly
5 suggesting GDF5 administration to promote SC maintenance. Importantly, we provided evidence
6 of human synthetic GDF5 (hsGDF5) effectiveness in inducing human SC proliferation and in
7 decreasing MuRF1-ubiquitin ligase expression in human muscle cells.

8 Altogether, our findings shed light on the benefits of GDF5-based therapies for the
9 neuromuscular system and are the basis of forthcoming medical strategies to counteract
10 sarcopenia and other neuromuscular diseases in humans.

11 **Materials and methods**

12 **Ethics**

13 Animal experimental procedures were approved by ethics committee (MENESR: Project
14 #17975). For human muscle biopsies we received ethical approval and participants provided
15 written informed consent.

16 **Animals**

17 Adult (6-7 months), old (20 months) and very old (26-27 months) C57/BL6 female mice were
18 from Janvier Lab and housed under specific-pathogen-free (SPF) conditions.

19 **Human muscle biopsies**

20 Human *Vastus Lateralis* biopsies from adult/aged healthy volunteers (Table S1) were gathered
21 within the frame of the European project MyoAge⁴¹ (223576-FP7-HEALTH) and by the Institute
22 of Myology Myobank (BB-0033-00012).

23 **Cell culture**

24 hTERT-NF1 cells were cultured in DMEM containing 10% fetal bovine serum (FBS), 0.1%
25 gentamicin and treated for 48h with PBS or hsGDF5 (X'PROCHEM) 10 or 50ng/ml. Cell
26 proliferation was determined by spectrofluorometry (CytoQuant assay, Life technologies).

1 Human healthy immortalized myoblasts (8220 cells)⁴² proliferated in DMEM, 5µg/ml insulin,
2 5ng/ml EGF, 0.5ng/ml bFGF, 0.2µg/ml dexamethasone, 25µg/ml fetuin, 20% FBS and 16%
3 medium 199; differentiated for 5 days in IMDM, 2% HS⁴², then treated 72h with hsGDF5
4 (50ng/ml) or PBS .

5 ***In vivo* gene transfer**

6 AAV2/1 (Adeno-Associated Virus) vectors were prepared as described⁴³. AAV2/1-Scramble or -
7 GDF5 were injected in *Tibialis Anterior* (TA) muscle of old (20 months) mice at 5.10⁹vg/TA.
8 Further details are provided in the Supplementary material.

9 **rGDF5 administration**

10 20-month-old mice were injected intraperitoneally thrice a week during four months with mouse
11 rGDF5 (Merck) or vehicle (PBS-0.1% bovine serum albumin (BSA)).

12 **Hematoxylin-Eosin staining**

13 10µm muscle cryosections were fixed on glass-slides in 4% paraformaldehyde (PFA) and stained
14 with Hematoxylin (BIOGNOST) and Eosin (ScyTek Lab).

15 **Immunofluorescence**

16 Cryosections were fixed in 4% PFA, permeabilized with 0.5% Triton X-100 and blocked in 10%
17 HS, 0.2% Triton, 5% BSA-PBS, incubated overnight at 4°C with primary antibodies (Table S6).
18 Sections were incubated with secondary antibodies (Table S7) for 1 hour at room temperature
19 and mounted with Fluoromont-G (Invitrogen). Further details are provided in the Supplementary
20 material.

21 **Neuromuscular-junction morphology**

22 Isolated muscle fibres were fixed 1 hour in 4% PFA, blocked in 4% BSA, 5% goat serum, 0.5%
23 Triton-PBS and incubated overnight at 4°C with Neurofilament antibody (Table S6). After
24 washes in 0.1% Triton-PBS, fibres were incubated overnight at 4°C with a secondary antibody
25 (Table S7) and α -Bungarotoxin-Alexa FluorTM-594. Isolated fibres were mounted on glass-slide
26 with mounting medium. Further details are provided in the Supplementary material.

1 **Immunoblotting**

2 400µm muscle cryosections were homogenized (Dounce) in lysis buffer (Ozyme)/phosphatase
3 inhibitors (Roche). Proteins were denatured at 95°C for 5 min with Laemmli buffer, separated by
4 electrophoresis (Nu-PAGE 4–12% Bis-Tris gel) and transferred to nitrocellulose membranes.
5 Membranes were blocked with 5% milk or 5% BSA and incubated overnight at 4°C with primary
6 antibodies (Table S6). Membranes were incubated with secondary antibodies (Table S7). Images
7 were acquired with ChemiDoc™ MP (Bio-Rad) and band intensity quantified using Image Lab
8 software (Bio-Rad).

9 Protein synthesis was measured using the *in vivo* SUnSET method* followed by
10 immunoblotting^{44,45}

11 **RNA-Sequencing**

12 mRNA libraries were realized following manufacturer's recommendations (Ultra2 mRNA-New
13 England Biolabs). 12 sample-pooled library preparations were sequenced on Novaseq6000 from
14 ILLUMINA with SP-200 cycles cartridge (2x800Millions of 100 bases reads). Further details are
15 provided in the Supplementary material.

16 **RNA isolation and quantitative real-time PCR (qRT-PCR)**

17 Total RNA was extracted from muscle using Trizol/Direct-zol RNA MiniPrep w/ Zymo-Spin IIC
18 Columns (Ozyme) and from cells using NucleoSpin RNA Columns (Macherey-Nagel). Reverse
19 transcription was performed using Superscript II Reverse transcriptase kit (TermoFisher
20 Scientific) and real-time qPCR performed on StepOne Plus Real-Time PCR System (Applied
21 Biosystems) using Power SYBR Green PCR MasterMix (TermoFisher Scientific). Data were
22 analyzed using $\Delta\Delta CT$ method and normalized to *RPLPO* (*Ribosomal protein lateral stalk*
23 *subunit P0*) or for hTERT NF1 cells *GAPDH* (*Glyceraldehyde 3-phosphate dehydrogenase*)
24 expression. Primers are in Table S8.

25

26

27

1 ***In situ* muscle force and electroneuromyography measurements**

2 Muscle force was evaluated by measuring *in situ* TA muscle contraction after nerve stimulation²⁴
3 and Electroneuromyography (ENMG) was achieved in TA muscle⁴⁶. Further details are provided
4 in the Supplementary material.

5 **Grip strength**

6 We used grip strength meter (Bioseb) to assess hind- and fore-limb strength. Mice were lifted
7 and held by tail and gently pulled backwards until they released the grid. Mean of four
8 consecutive measurements was determined and normalized to body weight.

9 **Magnetic Resonance Imaging (MRI)**

10 The MRI system consisted of a 7 tesla Bruker BioSpec and a transceiver surface cryoprobe
11 (Bruker BioSpin MRI GmbH). Maximal muscle cross-sectional area (CSA) was determined with
12 ITK-SNAP software⁴⁷. Further details are provided in the Supplementary material.

13 **Whole metabolism exploration and body composition**

14 Mice were housed individually in metabolic cages (Labmaster, TSE systems GmbH) with ad
15 libitum access to food and water. They were acclimated four days before monitoring for the next
16 three days. O₂ consumption, CO₂ production, energy expenditure and respiratory exchange ratio
17 were measured using indirect calorimetry technique. Food and water intake and spontaneous
18 locomotor activity were recorded during the entire experiment. Lean and fat masses were
19 assessed using 7.5-MHz time domain-nuclear magnetic resonance (LF90II MiniSpec; Bruker).

20 **Echocardiography**

21 Mice were lightly anesthetized (0.2%-0.5% isoflurane) and echocardiography was performed on
22 37°C pad with a probe emitting ultrasound at a frequency of 9 to 14 MHz (Vivid7 PRO
23 apparatus; GE Medical System) applied to the chest wall. Cardiac ventricular dimensions and
24 fractional shortening were measured in 2D mode and M-mode.

25

26

1 **Bone micro-computed tomography (Micro-CT)**

2 Dried mouse femurs were scanned using *in vivo* high-resolution X-ray micro-CT instrument
3 (Quantum FX Caliper, Life Sciences, Perkin Elmer) hosted by the life Imaging Facility
4 (URP2496, Montrouge, France). Further details are provided in the Supplementary material.

5 **Statistics analyses**

6 Comparison between two groups was tested for normality using Shapiro–Wilk test followed by
7 parametric (two-tailed paired, unpaired Student’s t-tests) or non-parametric test (Mann-Whitney)
8 to calculate *P* values. For more than two groups, ordinary one or two-ways ANOVA tests
9 followed by appropriated post hoc tests were performed. All statistical analyses were performed
10 with GraphPad Prism 8 software and statistical significance was set at $P < 0.05$.

11

12 **Results**

13 **GDF5-OE prevents the neuromuscular system decline during ageing** 14 **in mice**

15 We characterized neuromuscular features by analysing parameters defining muscle mass and
16 function and denervation markers, in younger adult (7m), old (20m), and very old (26-27m)
17 mice. We found that from 20 months, the masses of the *Tibialis Anterior* (TA) and
18 *Gastrocnemius* (GAS) were progressively reduced, without significant body weight loss (Fig
19 1A), whereas *Extensor Digitorum Longus* (EDL) and *Soleus* (Sol) were less affected by ageing
20 (Fig S1A). Muscle fibre’s quantification revealed a diminution of fibre size (Fig S1B),
21 particularly of fast-twitch glycolytic MyHC-IIB fibres, and not a reduction in their number (Fig
22 S1C).

23 To establish whether muscle atrophy was associated with impaired function, we measured limb
24 muscle grip strength, *in situ* tetanic force generation and *in vivo* neuromuscular transmission by
25 electroneuromyography (ENMG) assessing compound muscle action potentials (CMAPs)^{48,49}.

26 We found that grip strength was diminished early in old as well in very old compared to younger
27 (7-month-old) mice (Fig 1B), absolute maximal force generated by TAs was lower in very old

9

1 while not different between older and younger adult animals (Fig S1D). Nevertheless, we found
2 no difference in tetanic force normalized on TA weight, meaning that force generation was
3 directly dependent on muscle mass. Interestingly, we measured a slower rate of force production
4 in muscles of very old mice, indicating contractile system impairment⁵⁰ (Fig S1D). Consistently,
5 ENMG revealed a CMAP decrement in very old mice (Fig 1C), evidencing neuromuscular
6 fatigability in these animals⁴⁸. Altogether, these results show that ageing affects muscle
7 contractility and neuromuscular function without modifying specific force generation.

8 To assess NMJ denervation of aged muscle, the mRNA expression of related markers such as
9 acetylcholine receptor (AChR) subunits (*Chrna1*, *-b1*, *-d*, and *-g*) and *Musk*^{10,24} was measured.
10 We observed a trend towards increased expression of most of these markers beginning at 20
11 months, while *Chrmg* levels were significantly higher ($P=0.0429$) in very old mice (Fig 1D)
12 suggesting the presence of NMJ instability and/or remodeling beginning in old mice.

13 Altogether, these data reveal that muscle mass loss precedes alterations in force generation and
14 neuromuscular connectivity during ageing.

15 **GDF5-OE stimulates muscle hypertrophy and protein synthesis in** 16 **old mice**

17 Our findings could define a time window to take action with therapeutic strategies to prevent
18 signs of sarcopenia. In this aim, we injected TAs of 20-month-old mice with AAV-GDF5 or -
19 scramble and analysed these muscles 4 weeks after injection (Fig 1E). First, transcripts and
20 protein GDF5-OE was confirmed by RT-qPCR and Western blotting (WB), respectively (Fig
21 S1E). GDF5-dependent signalling activation was validated by the quantification of higher
22 number of phosphorylated SMAD1/5-positive nuclei after AAV-GDF5 than after -scramble
23 injection by immunofluorescence (IF). Accordingly, transcription of *Id1*, *2*, *3* and *4*, GDF5 gene
24 targets^{24,51,52} was induced upon GDF5-OE (Fig S1F). Analysis of muscle weight, fibre size and
25 number showed hypertrophy of GDF5-OE TAs (Fig 1E) with a higher percentage of large fibres
26 without fibre number change (Fig 1F). The regeneration process was not involved in mass gain
27 as quantification of the number of myonuclei, indicating muscle cell proliferation, and of the
28 centrally nucleated fibre, showed no variation in GDF5-OE muscle compared to control (Fig
29 2A). Furthermore, the expression of satellite cell marker *Pax7*⁵³ and of myogenic regulatory

1 factors *MyoD*, *Myogenin* and *Myf6*⁵³ was not modified by GDF5-OE (Fig 2B). Finally, to
2 establish whether GDF5 could target specific fibre type size, we measured the cross-sectional
3 area (CSA) of MyHC-IIA-, MyHC-IIB- and MyHC-IIX-positive fibres, without finding
4 difference in the mean size of any single type (Fig S2A, B). These results suggest that GDF5-OE
5 leads to hypertrophy of muscle at the early stage of ageing.

6 Since muscle mass homeostasis is regulated by the balance between protein degradation and
7 synthesis⁵⁴, we determined active protein synthesis after GDF5-OE by *in vivo* Sunset assay¹⁷. We
8 found increased puromycin incorporation into GDF5-OE TA extracts (Fig 2C), indicating that
9 hypertrophy might be partially due to increased anabolism. However, we did not observe
10 AKT/m-TOR/RpS6 phosphorylation, canonically associated with protein synthesis⁵⁵ (Fig 2D,
11 S2C). To investigate protein breakdown we quantified the mRNA expression of atrogenes as
12 *MuRF1*, *Atrogin1* and *Musa1*²³ and showed a significant decrease ($P=0.0437$) in only *MuRF1*
13 transcript level in GDF5-OE TAs (Fig 2E). Accordingly, we observed increased levels of MyHC
14 and actin, two proteins directly targeted by MuRF1^{56,57} for degradation and higher α -actinin
15 protein level also reported as associated with MuRF1 downregulation⁵⁸ in GDF5-OE TAs
16 compared to scramble (Fig 2F). In addition, to explore eventual effect of GDF5-OE on the
17 proteasome-ubiquitin system, we quantified protein poly-ubiquitination⁵⁹ and found a decrease in
18 its levels in GDF5-OE TA extracts *versus* scramble (Fig 2G), indicating a global inhibitory effect
19 of GDF5 against proteasome-ubiquitin-dependent protein degradation. Autophagy/mitophagy
20 pathway has been described as contributing to proteostasis and to be deregulated during
21 aging^{60,61}. We thus investigated the gene expression of autophagic markers *Sequestome1* (*p62*
22 also known as *SQSTM1*), *Microtubule-associated protein 1A/1B-light chain 3* (*lc3b*), *Gamma-*
23 *Aminobutyric Acid Receptor-Associated Protein-Like 1* (*Gabarapl*), *Beclin1* (*Becn1*), *Bcl-*
24 *2/adenovirus E1B 19 kDa protein-interacting protein 3* (*Bnip3*) and lysosomal *Cathepsin L*⁶² as
25 well as the protein levels of lipidated LC3 (LC3-I/LC3-II), p62/SQSTM1 and Beclin1, which
26 increase is associated to autophagy/mitophagy activation⁶¹. We showed that GDF5-OE did not
27 induce muscle mass gain through modifications in gene (Fig S2D) and protein expression of all
28 these autophagy/mitophagy players (Fig 2H, S2E).

29 Here, our data reveal that the GDF5-OE hypertrophic effect is promoted by Akt-independent
30 protein synthesis and by the inhibition of MuRF1 and ubiquitin-dependent protein degradation
31 without modulation of autophagy/mitophagy.

11

1 **GDF5-OE improves neuromuscular transmission, NMJ morphology** 2 **and Schwann cell marker expression**

3 To investigate the effects of GDF5 on muscle contraction through NMJ stimulation, we
4 measured the peak of tetanic force and the rate of force generation in old mouse TAs. We found
5 no difference in absolute or specific maximal force after nerve stimulation between GDF5-OE
6 and scramble conditions. However, the rate of muscle force production was higher after GDF5-
7 OE, indicating a faster development of contraction⁶³ than in scramble (Fig 3A, S3A). In addition,
8 ENMG confirmed that GDF5 improved CMAP in old mice (Fig 3B), showing that one of its
9 major effect is the maintenance of the neuromuscular transmission.

10 These results provide extensive description of the effects of GDF5-OE during the earliest phase
11 of age-related muscle wasting and validate its effectiveness in modulating neuromuscular
12 function.

13 The evidence of GDF5-OE benefit on NMJ activity strongly suggested its impact on NMJ
14 remodelling. Thus, we analysed the morphology of muscle synapses using ImageJ-based
15 workflow⁶⁴, and found that GDF5-OE improved NMJ morphology in 21-month-old mice by a
16 slight increase of endplate area ($P= 0.0577$) associated with a significant rise of AChR area ($P=$
17 0.0145). The pre-synaptic compartment showed increased nerve terminal area and pre- and post-
18 synaptic overlap percentage (Fig 3C). However, AChR compactness and fragmentation were not
19 significantly affected (Fig S3B), nor was the expression of *Chrmg*, one of the hallmark of NMJ
20 instability/remodeling (Fig S3C).

21 To assess the effects of GDF5 on NMJ players, we quantified the transcript levels of the SC-
22 specific glial markers, as *S100b*, *Myelin basic protein (Mbp)*, *Myelin protein zero (Mpz)*, and
23 *Peripheral myelin protein 22 (Pmp22)* related to SC-dependent endplate stability⁶⁵⁻⁶⁸; *Growth-*
24 *associated protein 43 (Gap43)*, associated with axon and SC regeneration; and *Fibroblast growth*
25 *factor binding protein-1 (Fgfbp-1)*, a trophic factor protecting NMJs from degradation^{10,65,68}.
26 Strikingly, we found that GDF5 increased mRNA levels of all of them (Fig 3D). To investigate
27 whether it was accompanied by changes in neurotrophic gene expression, we measured *Nerve*
28 *growth factor (Ngf)*, *Brain-derived neurotrophic factor (Bdnf)*, *Neurotrophin 3 (Nt3)*, *Glial cell*
29 *line-derived neurotrophic factor (Gdnf)*, and *Ciliary neurotrophic factor (Cntf)* transcript levels.

1 We observed that GDF5-OE increased *Ngf* expression (Fig S3D), suggesting that its effect might
2 also be mediated by this neurotrophin involved in axon maintenance/guidance⁶⁶.

3 Overall, our data show GDF5-OE benefit on the integrity of NMJs, its role in modulating SC
4 markers and *Ngf* expression indicating its therapeutic interest in disorders involving SCs and/or
5 axonal degeneration as peripheral demyelinating neuropathies.

6 **Aged human muscle is potential target of GDF5-based therapies**

7 We investigated whether GDF5-based therapy could be useful in humans against sarcopenia. In
8 that purpose, we collected biopsies from quadriceps of adult young (21-42 years) and aged (77-
9 80 years) volunteers²⁴ (Table S1) and assessed some relevant readouts established in mice. First,
10 the expression of SC-related markers was measured, revealing *SI00b* and *MPZ* mRNA levels
11 significantly lower in aged than in young muscle biopsies ($P=0.0396$ and $P=0.0166$
12 respectively) (Fig 4A). We then treated human immortalized SCs with 10 and 50ng/ml of human
13 synthetic GDF5 (hsGDF5) for 48h (Fig 4B) and observed a significant increased rate of their
14 proliferation ($P=0.0002$; $P<0.0001$ respectively) evaluated by spectrofluorometry and by RT-
15 qPCR quantification of *Ki67* transcript (Fig 4B). In addition, hsGDF5 induced the differentiation
16 of these cells, as confirmed by the increased mRNA levels of early myelin-associated markers
17 *Early growth response gene 2 (EGR2)*, *Proteolipid protein (PLP1)*, and *PMP22* (Fig 4C).
18 However, the expression of *MPZ* and *MBP*, mature myelinating SC markers, did not change
19 under the tested conditions (Fig S4A). Altogether, these data strongly suggest direct GDF5 effect
20 on SCs playing fundamental roles in sustaining NMJ formation and preservation⁶⁹.

21 One of the relevant effects of GDF5 on aged mouse muscle from mass wasting was *MuRF1*
22 expression decrease. We treated differentiated human immortalized myotubes with hsGDF5 for
23 72h and found a significantly decreased *MuRF1* expression ($P=0.0125$), confirming the ability of
24 GDF5 in inhibiting this protein breakdown mediator in human muscle cells (Fig 4D).

25 These results provide evidence of therapeutic potential of GDF5 in humans and identify probable
26 targets of the treatment as both SCs and muscle cells, crucial for neuromuscular connectivity and
27 muscle mass.

1 **GDF5-OE rejuvenates transcriptomic profile in aged mouse muscle**

2 To further decipher the effects of GDF5-OE in muscle, we performed a genome-wide
3 transcriptomic analysis using RNA from TAs of 21-month-old mice overexpressing GDF5 (Old-
4 GDF5) compared to RNA from scramble-injected TAs of 7-month-old (Adult-Scra) and 21-
5 month-old mice (Old-Scra) (Tables S2, S3). Principal component analysis revealed distinct gene-
6 expression profiles among groups, however the Old-GDF5 group clustered more with the Adult-
7 Scra than the Old-Scra group (Fig 5A) and this was confirmed by unsupervised, hierarchical
8 clustering analysis (Fig 5B). Remarkably, out of 587 genes affected by ageing, 247 genes
9 differentially expressed in the Old-Scra reverted to youthful expression levels in the Old-GDF5
10 (42% of the dysregulated transcripts) (Fig 5C, Tables S4). This reversal was also observed for the
11 expression of macrophage-specific as well as mitochondrial metabolism- and redox balance-
12 related genes, the alterations of which have been reported to contribute to skeletal muscle
13 disorders and ageing⁷⁰⁻⁷³.

14 To validate these data, we quantified by RT-qPCR the expression of some of most relevant genes
15 modulated upon GDF5-OE on RNA extracts used for transcriptomic analysis. Among
16 macrophage-associated genes, in the Old-GDF5 group we observed upregulation of monocyte-
17 macrophage marker *Colony stimulating factor 1 receptor*, *Csf1r*⁷⁴, and M2 anti-inflammatory
18 macrophage markers *Cd163*, *Cd209* and *Mgl2* (Fig 5D), known to support tissue repair and
19 muscle mass maintenance^{75,76}. In addition, GDF5-OE improved the expression of *Uncoupling*
20 *protein2* (*Ucp2*)⁷⁷⁻⁷⁹ and *Superoxide* dismutase3 (*Sod3*)⁸⁰ genes, implicated in energy
21 expenditure, and *Negative regulator of reactive oxygen species* (*Nrros*), limiting ROS generation
22 and oxidative damage (Fig 5D)⁸¹. We also found increased levels of other markers not altered by
23 ageing, as *F4/80*, *CD68*, *CD206* (macrophage markers), and *catalase*, *Gpx1*, and *Hmox1*
24 (antioxidant-related genes) (Fig S5A), suggesting that these modulations are applicable to GDF5
25 protective function against muscle wasting. Interestingly, *Apelin* and *Follistatin* expression, both
26 described as beneficial in preventing age-related muscle decline and secreted after physical
27 exercise^{17,82,83}, was increased upon GDF5-OE (Fig 5E). We also investigated the expression of
28 *PGC-1a*, another factor involved in oxidative energy balance, exercise adaptation, myokine
29 modulation and NMJ formation^{84,85}. We found that *PGC-1a* transcription was not modified upon
30 GDF5-OE in our experimental conditions (Fig S5 B).

1 To go further, as mitochondrial alterations are associated to sarcopenia⁸⁶, we analyzed
2 mitochondrial content and morphology in TAs overexpressing GDF5. We did not measured
3 significant changes in mitochondrial DNA amount and succinate dehydrogenase complex subunit
4 A (Sdha-Complex II), Cytochrome b-c1 complex subunit 2 (Uqcrc-Complex III) and Voltage-
5 Dependent Anion selective Channel (Vdac) protein expression (Fig S5 C, D), nor in the volume
6 and gross morphology of mitochondria (Fig S5 E). Accordingly, the expression of *dynamin-*
7 *related protein 1 (drp1)*, *fission 1 protein (fis1)*, *optic atrophy1 (opa1)* and *mitofusin 1 and 2*
8 (*mfn1 and 2*) regulating mitochondrial fission and fusion⁸⁷ was not modified by GDF5-OE (Fig
9 S5 F).

10 These results represent an important data set on the wide therapeutic potential of GDF5 in
11 modulating various mechanisms contributing to muscle ageing but also involved in several
12 muscular and neuromuscular diseases.

13 **rGDF5 is a potential therapy for age-related muscle wasting**

14 With the goal of generate patient-relevant preclinical data to be used against sarcopenia, we set
15 up a protocol based on recombinant mouse GDF5 protein (rGDF5). We treated old mice (20
16 months) with rGDF5 (0.2 mg/kg) or vehicle thrice a week systemically (Fig 6A) as we validated
17 that SMAD1/5 signalling was activated in TAs 48h post-injection (Fig S6A). Four weeks later,
18 we evaluated the expression of genes related to reinnervation and myokines and analysed the
19 long-term effect of the treatment on age-related muscle wasting and neuromuscular features (Fig
20 6A). We observed SC marker upregulation, including *S100b*, *Mbp*, *Mpz*, *Gap43* and also *Fgfbp1*
21 and *Ngf*, as well as *Apelin* and *Follistatin* levels (Fig 6B) in old treated TAs confirming the
22 ability of GDF5 to promote these markers and myokine expression.

23 Efficacy of chronic rGDF5 treatment was evaluated by magnetic resonance imaging
24 measurement, an *in vivo* outcome applicable to future clinical studies. We found that total hind
25 limb muscle CSA was higher after treatment compared to vehicle condition. Accordingly, GAS,
26 TA, EDL, and Sol muscle masses were higher in very old mice (24 months) after rGDF5 *versus*
27 vehicle treatment. Histological analysis of the GAS revealed that this increase was not due to
28 changes in fibre number (Fig 6C) but increased MyHC-IIB- and MyHC-IIX-positive fibre size
29 (Fig 6D), rescuing their age-related phenotype. rGDF5 effect on muscle mass was independent of
30 body weight as a slight effect was observed on body composition of fat and lean mass ($P=0.4919$)

15

1 and $P=0.2366$ respectively) (Fig S6B). The metabolic phenotyping showed that rGDF5
2 treatment did not affect food and water intake, ambulatory activity nor energy expenditure or
3 respiratory rate. Furthermore, we did not detect modifications in heart weight (Fig S6D) or
4 function measured by echocardiography (Table S5). Considering the impact of GDF5 on bone
5 homeostasis²⁶, we measured *ex vivo* femur microarchitecture by micro-CT imaging and did not
6 observe any difference between rGDF5 and vehicle-treated groups (Fig S6E).

7 Chronic rGDF5 administration effects on muscle function was evaluated by *in situ* TA force
8 generation that showed increase in both absolute and specific force and a significant higher rate
9 of force generation *versus* vehicle ($P=0.0006$) (Fig 6E), indicating ameliorated neuromuscular
10 connectivity. NMJ morphological analysis revealed no difference in nerve terminal area, overlap
11 percentage, compactness and AChR fragmentation, however, rGDF5 treatment led to higher
12 endplate and AChR areas in very old mice ($P=0.0211$ and 0.0125 respectively) (Fig 6F).

13 In summary, our findings demonstrate the effectiveness of chronic rGDF5 administration in
14 counteracting age-related muscle wasting, improving muscle function, ensuring neuromuscular
15 connectivity and preventing NMJ.

16

17 Discussion

18 Sarcopenia, a widespread age-related disease strongly impacting life quality and representing a
19 public health issue, is a multifactorial pathology with no cure to date. Here, we aimed at
20 identifying a potential therapeutic strategy for this disease by deciphering the mechanisms
21 underlying GDF5 ability to preserve aged muscle. Our data support its major dual action on both
22 skeletal muscle and NMJ at the earlier stage of ageing, by increasing muscle mass, ameliorating
23 neuromuscular connectivity and endplate structure. We dissected the effect of GDF5 on different
24 pathways as protein synthesis/degradation, innervation and potential mechanisms related to
25 inflammation, metabolism and redox equilibrium. We confirmed that GDF5-OE reduces the
26 expression *MuRF1*, involved in protein breakdown⁸⁸, and increases protein synthesis. While
27 muscle wasting was likely prevented by rebalanced protein catabolism, the canonical protein
28 synthesis-associated pathway was not affected, consistently with previous observations

16

1 indicating transient/limited impact of Akt/mTor signalling on muscle mass preservation in
2 different conditions⁸⁹⁻⁹¹.

3 Regarding muscle innervation parameters, we showed that GDF5-OE induced the expression of
4 nerve regeneration- and SC-related re-innervation genes. This finding is consistent with other
5 studies showing GDF5 as neurotrophic factor protecting dopaminergic neurons from
6 neurotoxicity *in vitro* and *in vivo*^{32,92} and promoting neurite complexity in cultured neurons^{93,94}.
7 However, we pointed out a more prominent effect of this factor on SCs, essential for NMJ
8 integrity and neuromuscular maintenance⁶, which are affected by ageing⁸.

9 Overall, our data demonstrated GDF5 rejuvenating effects with reversed expression of several
10 genes altered in aged muscle, particularly those linked to impaired inflammation, macrophages
11 and oxidative balance. Indeed, the steadiness between ATP/heat productions is crucial to regulate
12 ROS production rates for tissue maintenance. In this context, UCPs, which physiological role is
13 to dissipate energy by decreasing mitochondrial membrane potential, are of interest.
14 Mitochondrial uncoupling reduces free radical generation and has protective function in several
15 tissues⁹⁵⁻⁹⁹. Notably, UCP2 expression, upregulated by GDF5, has been described to correlate
16 with life span in humans^{78,100}. Here, we showed that mitochondrial content and morphology was
17 not modified and that metabolic phenotyping was also unaffected by GDF5 treatment. However,
18 further extensive studies are needed to deeper analyze the possible impact of GDF5-based
19 treatment on bioenergetics and redox capacity of muscle and their eventual relationship to
20 performance and mass homeostasis. Furthermore, macrophages, essential in muscle
21 regeneration^{101,102}, are altered during ageing^{70,71} contributing to inadequate repair and muscle
22 wasting¹⁰³. The expression of other markers associated with both macrophages and antioxidant
23 responses, yet not significantly modified during early ageing, was increased upon GDF5-OE,
24 suggesting that it positively modulates inflammation and redox equilibrium. Noteworthy, a
25 beneficial effect similar to those observed upon physical exercise in humans¹⁰⁴⁻¹⁰⁶ has been
26 induced by GDF5-OE such as the myokines Apelin and Follistatin increased expression.
27 Functions and modulations of these factors have been only partially explored thus far¹⁰⁷⁻¹⁰⁹ and
28 despite their apparent trophic effect in the neuromuscular systems^{17,82,110-112}, their molecular
29 triggers is quite lacking^{17,111,113}.

We addressed the challenge of developing a therapeutic approach using systemic rGDF5 administration giving promising data on its benefits against sarcopenia. We revealed the efficacy of hsGDF5 in human cells in promoting nerve regeneration/re-innervation markers and proliferation of SCs, found decreased in aged human muscle, indicating a potential medical use. In addition, we confirmed an inhibited *MuRF1* expression in human myotubes.

1 Here, we provide bases for effective medical approach for ageing muscle and strongly suggests
2 that GDF5 therapeutic potential of is not limited to sarcopenia, but applicable to neuromuscular
3 disorders involving SC degeneration and NMJ dismantling as motoneuron diseases (ALS, spinal
4 muscular atrophy) and demyelinating neuropathies. Consistently, SMAD1/5-dependent pathway
5 activation has been described as beneficial for motor neuron dysfunction in a drosophila ALS
6 model¹¹⁴. In addition, we show that GDF5 influences macrophages, inflammation and oxidative
7 balance, disclose its possible benefit in several conditions considering that altered inflammatory
8 responses and oxidative stress play a key role on muscle wasting following critical illness, cancer
9 cachexia, and immobilization but also in muscular and neuromuscular diseases, including
10 muscular dystrophies^{115–119}.

11 Overall, our results establish that GDF5 effects might be exploited for the treatment of different
12 pathological conditions affecting the neuromuscular system as a whole.

13

14 **Data availability**

15 The authors confirm that the data supporting the findings of this study are available within the
16 article and its Supplementary material.

17

18 **Acknowledgements**

19 We thank A. Lacombe for expertise in indirect calorimetry experiments; B. Matot for MRI
20 analysis; S. Vasseur and M. Chapart for collecting human muscles at Myology Institute
21 Myobank; P. Meunier and S. Benkhelifa-Ziyyat from the MyoVector technical platform of the
22 Centre of Research in Myology-UMRS974 (Paris, France) for AAV production; Y. Marie for
23 RNA sequencing; S. Rosanna Casati and C. De Palma for expertise in mitochondria field; I.

18

1 Akrouf, N. Vignier and V. Allamand for helpful technical advice; Inovarion for technical service;
2 P. Smeriglio and L. Giordani for scientific discussions.

3

4 **Funding**

5 Association Institute of Myology (to FPR and SF), and Association Française contre les
6 myopathies AFM-Telethon (to FPR and SF).

7

8 **Competing interests**

9 The authors declare that they have no competing interests.

10

11 **Supplementary material**

12 Supplementary material is available at *Brain* online.

13

14 **References**

- 15 1. Cruz-Jentoft, A.J., Bahat, G., Bauer, J., Boirie, Y., Bruyère, O., Cederholm, T., Cooper, C.,
16 Landi, F., Rolland, Y., Sayer, A.A., et al. (2019). Sarcopenia: revised European consensus
17 on definition and diagnosis. *Age Ageing* 48, 601. 10.1093/ageing/afz046.
- 18 2. Spendiff, S., Vuda, M., Gousspillou, G., Aare, S., Perez, A., Morais, J.A., Jagoe, R.T., Filion,
19 M.-E., Glicksman, R., Kapchinsky, S., et al. (2016). Denervation drives mitochondrial
20 dysfunction in skeletal muscle of octogenarians. *J. Physiol. (Lond.)* 594, 7361–7379.
21 10.1113/JP272487.
- 22 3. Gousspillou, G., Picard, M., Godin, R., Burelle, Y., and Hepple, R.T. (2013). Role of
23 peroxisome proliferator-activated receptor gamma coactivator 1-alpha (PGC-1 α) in
24 denervation-induced atrophy in aged muscle: facts and hypotheses. *Longev Healthspan* 2,
25 13. 10.1186/2046-2395-2-13.

- 1 4. Piasecki, M., Ireland, A., Piasecki, J., Stashuk, D.W., Swiecicka, A., Rutter, M.K., Jones,
2 D.A., and McPhee, J.S. (2018). Failure to expand the motor unit size to compensate for
3 declining motor unit numbers distinguishes sarcopenic from non-sarcopenic older men. *The*
4 *Journal of Physiology* 596, 1627–1637. 10.1113/JP275520.
- 5 5. Chai, R.J., Vukovic, J., Dunlop, S., Grounds, M.D., and Shavlakadze, T. (2011). Striking
6 denervation of neuromuscular junctions without lumbar motoneuron loss in geriatric mouse
7 muscle. *PLoS ONE* 6, e28090. 10.1371/journal.pone.0028090.
- 8 6. Jablonka-Shariff, A., Lu, C.-Y., Campbell, K., Monk, K.R., and Snyder-Warwick, A.K.
9 (2020). Gpr126/Adgrg6 contributes to the terminal Schwann cell response at the NMJ
10 following peripheral nerve injury. *Glia* 68, 1182–1200. 10.1002/glia.23769.
- 11 7. Fuertes-Alvarez, S., and Izeta, A. (2021). Terminal Schwann Cell Aging: Implications for
12 Age-Associated Neuromuscular Dysfunction. *Aging Dis* 12, 494–514.
13 10.14336/AD.2020.0708.
- 14 8. Ludatscher, R.M., Silbermann, M., Gershon, D., and Reznick, A. (1985). Evidence of
15 Schwann cell degeneration in the aging mouse motor end-plate region. *Exp Gerontol* 20,
16 81–91. 10.1016/0531-5565(85)90043-9.
- 17 9. Snyder-Warwick, A.K., Satoh, A., Santosa, K.B., Imai, S., and Jablonka-Shariff, A. (2018).
18 Hypothalamic Sirt1 protects terminal Schwann cells and neuromuscular junctions from
19 age-related morphological changes. *Aging Cell* 17, e12776. 10.1111/accel.12776.
- 20 10. Aare, S., Spendiff, S., Vuda, M., Elkrief, D., Perez, A., Wu, Q., Mayaki, D., Hussain,
21 S.N.A., Hettwer, S., and Hepple, R.T. (2016). Failed reinnervation in aging skeletal muscle.
22 *Skeletal Muscle* 6, 29. 10.1186/s13395-016-0101-y.
- 23 11. Dalle, S., Rossmeislova, L., and Koppo, K. (2017). The Role of Inflammation in Age-
24 Related Sarcopenia. *Front Physiol* 8, 1045. 10.3389/fphys.2017.01045.
- 25 12. Fulle, S., Protasi, F., Di Tano, G., Pietrangelo, T., Beltramin, A., Boncompagni, S., Vecchiet,
26 L., and Fanò, G. (2004). The contribution of reactive oxygen species to sarcopenia and
27 muscle ageing. *Experimental Gerontology* 39, 17–24. 10.1016/j.exger.2003.09.012.
- 28 13. Valdez, G., Tapia, J.C., Kang, H., Clemenson, G.D., Gage, F.H., Lichtman, J.W., and Sanes,
29 J.R. (2010). Attenuation of age-related changes in mouse neuromuscular synapses by

20

- 1 caloric restriction and exercise. *Proc. Natl. Acad. Sci. U.S.A.* *107*, 14863–14868.
2 10.1073/pnas.1002220107.
- 3 14. Kern, H., Hofer, C., Loeffler, S., Zampieri, S., Gargiulo, P., Baba, A., Marcante, A.,
4 Piccione, F., Pond, A., and Carraro, U. (2017). Atrophy, ultra-structural disorders, severe
5 atrophy and degeneration of denervated human muscle in SCI and Aging. Implications for
6 their recovery by Functional Electrical Stimulation, updated 2017. *Neurol. Res.* *39*, 660–
7 666. 10.1080/01616412.2017.1314906.
- 8 15. Kern, H., Barberi, L., Löfler, S., Sbardella, S., Burggraf, S., Fruhmann, H., Carraro, U.,
9 Mosole, S., Sarabon, N., Vogelauer, M., et al. (2014). Electrical stimulation counteracts
10 muscle decline in seniors. *Front Aging Neurosci* *6*, 189. 10.3389/fnagi.2014.00189.
- 11 16. Mosole, S., Carraro, U., Kern, H., Loeffler, S., Fruhmann, H., Vogelauer, M., Burggraf, S.,
12 Mayr, W., Krenn, M., Paternostro-Sluga, T., et al. (2014). Long-term high-level exercise
13 promotes muscle reinnervation with age. *J. Neuropathol. Exp. Neurol.* *73*, 284–294.
14 10.1097/NEN.0000000000000032.
- 15 17. Vinel, C., Lukjanenko, L., Batut, A., Deleruyelle, S., Pradère, J.-P., Gonidec, S.L.,
16 Dortignac, A., Geoffre, N., Pereira, O., Karaz, S., et al. (2018). The exerkinine apelin reverses
17 age-associated sarcopenia. *Nature Medicine*, *1*. 10.1038/s41591-018-0131-6.
- 18 18. Kim, J.W., Kim, R., Choi, H., Lee, S.-J., and Bae, G.-U. (2021). Understanding of
19 sarcopenia: from definition to therapeutic strategies. *Arch. Pharm. Res.* *44*, 876–889.
20 10.1007/s12272-021-01349-z.
- 21 19. Lee, S.-J. (2021). Targeting the myostatin signaling pathway to treat muscle loss and
22 metabolic dysfunction. *J Clin Invest* *131*. 10.1172/JCI148372.
- 23 20. Rooks, D., Swan, T., Goswami, B., Filosa, L.A., Bunte, O., Panchaud, N., Coleman, L.A.,
24 Miller, R.R., Garcia Garayoa, E., Praestgaard, J., et al. (2020). Bimagrumab vs Optimized
25 Standard of Care for Treatment of Sarcopenia in Community-Dwelling Older Adults: A
26 Randomized Clinical Trial. *JAMA Network Open* *3*, e2020836.
27 10.1001/jamanetworkopen.2020.20836.
- 28 21. Tournadre, A., Vial, G., Capel, F., Soubrier, M., and Boirie, Y. (2019). Sarcopenia. *Joint
29 Bone Spine* *86*, 309–314. 10.1016/j.jbspin.2018.08.001.

- 1 22. Macpherson, P.C.D., Farshi, P., and Goldman, D. (2015). Dach2-Hdac9 signaling regulates
2 reinnervation of muscle endplates. *Development* 142, 4038–4048. 10.1242/dev.125674.
- 3 23. Sartori, R., Schirwis, E., Blaauw, B., Bortolanza, S., Zhao, J., Enzo, E., Stantzou, A.,
4 Mouisel, E., Toniolo, L., Ferry, A., et al. (2013). BMP signaling controls muscle mass.
5 *Nature Genetics* 45, 1309–1318. 10.1038/ng.2772.
- 6 24. Traoré, M., Gentil, C., Benedetto, C., Hogrel, J.-Y., De la Grange, P., Cadot, B., Benkhelifa-
7 Ziyayat, S., Julien, L., Lemaitre, M., Ferry, A., et al. (2019). An embryonic Ca ν β 1 isoform
8 promotes muscle mass maintenance via GDF5 signaling in adult mouse. *Science*
9 *Translational Medicine* 11, eaaw1131. 10.1126/scitranslmed.aaw1131.
- 10 25. Chijimatsu, R., and Saito, T. (2019). Mechanisms of synovial joint and articular cartilage
11 development. *Cell. Mol. Life Sci.* 76, 3939–3952. 10.1007/s00018-019-03191-5.
- 12 26. Jin, L., and Li, X. (2013). Growth differentiation factor 5 regulation in bone regeneration.
13 *Curr. Pharm. Des.* 19, 3364–3373. 10.2174/1381612811319190003.
- 14 27. Farooq, M., Nakai, H., Fujimoto, A., Fujikawa, H., Kjaer, K.W., Baig, S.M., and
15 Shimomura, Y. (2013). Characterization of a novel missense mutation in the prodomain of
16 GDF5, which underlies brachydactyly type C and mild Grebe type chondrodysplasia in a
17 large Pakistani family. *Hum Genet* 132, 1253–1264. 10.1007/s00439-013-1330-3.
- 18 28. Reynard, L.N., Bui, C., Syddall, C.M., and Loughlin, J. (2014). CpG methylation regulates
19 allelic expression of GDF5 by modulating binding of SP1 and SP3 repressor proteins to the
20 osteoarthritis susceptibility SNP rs143383. *Hum. Genet.* 133, 1059–1073. 10.1007/s00439-
21 014-1447-z.
- 22 29. Jones, G., Trajanoska, K., Santanasto, A.J., Stringa, N., Kuo, C.-L., Atkins, J.L., Lewis,
23 J.R., Duong, T., Hong, S., Biggs, M.L., et al. (2021). Genome-wide meta-analysis of muscle
24 weakness identifies 15 susceptibility loci in older men and women. *Nat Commun* 12, 654.
25 10.1038/s41467-021-20918-w.
- 26 30. David, L., Feige, J.-J., and Bailly, S. (2009). Emerging role of bone morphogenetic proteins
27 in angiogenesis. *Cytokine Growth Factor Rev.* 20, 203–212. 10.1016/j.cytogfr.2009.05.001.

- 1 31. Sullivan, A.M., and O’Keeffe, G.W. (2005). The role of growth/differentiation factor 5
2 (GDF5) in the induction and survival of midbrain dopaminergic neurones: relevance to
3 Parkinson’s disease treatment. *J. Anat.* *207*, 219–226. 10.1111/j.1469-7580.2005.00447.x.
- 4 32. Sullivan, A.M., Opacka-Juffry, J., Pohl, J., and Blunt, S.B. (1999). Neuroprotective effects
5 of growth/differentiation factor 5 depend on the site of administration. *Brain Res.* *818*, 176–
6 179. 10.1016/s0006-8993(98)01275-x.
- 7 33. Saltiel, A.R. (2016). New therapeutic approaches for the treatment of obesity. *Science*
8 *Translational Medicine* *8*, 323rv2-323rv2. 10.1126/scitranslmed.aad1811.
- 9 34. Hinoi, E., Nakamura, Y., Takada, S., Fujita, H., Iezaki, T., Hashizume, S., Takahashi, S.,
10 Odaka, Y., Watanabe, T., and Yoneda, Y. (2014). Growth differentiation factor-5 promotes
11 brown adipogenesis in systemic energy expenditure. *Diabetes* *63*, 162–175. 10.2337/db13-
12 0808.
- 13 35. Hegarty, S.V., Collins, L.M., Gavin, A.M., Roche, S.L., Wyatt, S.L., Sullivan, A.M., and
14 O’Keeffe, G.W. (2014). Canonical BMP-Smad signalling promotes neurite growth in rat
15 midbrain dopaminergic neurons. *Neuromolecular Med.* *16*, 473–489. 10.1007/s12017-014-
16 8299-5.
- 17 36. Sartori, R., Hagg, A., Zampieri, S., Armani, A., Winbanks, C.E., Viana, L.R., Haidar, M.,
18 Watt, K.I., Qian, H., Pezzini, C., et al. (2021). Perturbed BMP signaling and denervation
19 promote muscle wasting in cancer cachexia. *Sci Transl Med* *13*, eaay9592.
20 10.1126/scitranslmed.aay9592.
- 21 37. Stantzou, A., Schirwis, E., Swist, S., Alonso-Martin, S., Polydorou, I., Zarrouki, F.,
22 Mouisel, E., Beley, C., Julien, A., Grand, F.L., et al. (2017). BMP signaling regulates
23 satellite cell-dependent postnatal muscle growth. *Development* *144*, 2737–2747.
24 10.1242/dev.144089.
- 25 38. Uezumi, A., Ikemoto-Uezumi, M., Zhou, H., Kurosawa, T., Yoshimoto, Y., Nakatani, M.,
26 Hitachi, K., Yamaguchi, H., Wakatsuki, S., Araki, T., et al. (2021). Mesenchymal Bmp3b
27 expression maintains skeletal muscle integrity and decreases in age-related sarcopenia.
28 10.1172/JCI1139617.

- 1 39. Sader, F., and Roy, S. (2022). Tgf- β superfamily and limb regeneration: Tgf- β to start and
2 Bmp to end. *Dev Dyn* 251, 973–987. 10.1002/dvdy.379.
- 3 40. Winbanks, C.E., Chen, J.L., Qian, H., Liu, Y., Bernardo, B.C., Beyer, C., Watt, K.I.,
4 Thomson, R.E., Connor, T., Turner, B.J., et al. (2013). The bone morphogenetic protein axis
5 is a positive regulator of skeletal muscle mass. *J. Cell Biol.* 203, 345–357.
6 10.1083/jcb.201211134.
- 7 41. McPhee, J.S., Hogrel, J.-Y., Maier, A.B., Seppet, E., Seynnes, O.R., Sipilä, S., Bottinelli, R.,
8 Barnouin, Y., Bijlsma, A.Y., Gapeyeva, H., et al. (2013). Physiological and functional
9 evaluation of healthy young and older men and women: design of the European MyoAge
10 study. *Biogerontology* 14, 325–337. 10.1007/s10522-013-9434-7.
- 11 42. Mamchaoui, K., Trollet, C., Bigot, A., Negroni, E., Chaouch, S., Wolff, A., Kandalla, P.K.,
12 Marie, S., Di Santo, J., St Guily, J.L., et al. (2011). Immortalized pathological human
13 myoblasts: towards a universal tool for the study of neuromuscular disorders. *Skelet Muscle*
14 1, 34. 10.1186/2044-5040-1-34.
- 15 43. Rivière, C., Danos, O., and Douar, A.M. (2006). Long-term expression and repeated
16 administration of AAV type 1, 2 and 5 vectors in skeletal muscle of immunocompetent adult
17 mice. *Gene Ther* 13, 1300–1308. 10.1038/sj.gt.3302766.
- 18 44. Schmidt, E.K., Clavarino, G., Ceppi, M., and Pierre, P. (2009). SUnSET, a nonradioactive
19 method to monitor protein synthesis. *Nat Methods* 6, 275–277. 10.1038/nmeth.1314.
- 20 45. Goodman, C.A., Mabrey, D.M., Frey, J.W., Miu, M.H., Schmidt, E.K., Pierre, P., and
21 Hornberger, T.A. (2010). Novel insights into the regulation of skeletal muscle protein
22 synthesis as revealed by a new nonradioactive in vivo technique. *The FASEB Journal* 25,
23 1028–1039. 10.1096/fj.10-168799.
- 24 46. Boëx, M., Cottin, S., Halliez, M., Bauché, S., Buon, C., Sans, N., Montcouquiol, M.,
25 Molgó, J., Amar, M., Ferry, A., et al. (2022). The cell polarity protein Vangl2 in the muscle
26 shapes the neuromuscular synapse by binding to and regulating the tyrosine kinase MuSK.
27 *Sci Signal* 15, eabg4982. 10.1126/scisignal.abg4982.
- 28 47. Yushkevich, P.A., Piven, J., Hazlett, H.C., Smith, R.G., Ho, S., Gee, J.C., and Gerig, G.
29 (2006). User-guided 3D active contour segmentation of anatomical structures: significantly

- 1 improved efficiency and reliability. *Neuroimage* 31, 1116–1128.
2 10.1016/j.neuroimage.2006.01.015.
- 3 48. Sheth, K.A., Iyer, C.C., Wier, C.G., Crum, A.E., Bratasz, A., Kolb, S.J., Clark, B.C.,
4 Burghes, A.H.M., and Arnold, W.D. (2018). Muscle strength and size are associated with
5 motor unit connectivity in aged mice. *Neurobiol. Aging* 67, 128–136.
6 10.1016/j.neurobiolaging.2018.03.016.
- 7 49. Wu, G., Xu, S., Chen, B., and Wu, P. (2017). Relationship between changes in muscle fibers
8 and CMAP in skeletal muscle with different stages of aging. *Int J Clin Exp Pathol* 10,
9 11888–11895.
- 10 50. Sun, Y.-B., Lou, F., and Edman, K. a. P. (1995). The effects of 2,3-butanedione monoxime
11 (BDM) on the force-velocity relation in single muscle fibres of the frog. *Acta Physiologica*
12 *Scandinavica* 153, 325–334. 10.1111/j.1748-1716.1995.tb09870.x.
- 13 51. Nakahiro, T., Kurooka, H., Mori, K., Sano, K., and Yokota, Y. (2010). Identification of
14 BMP-responsive elements in the mouse *Id2* gene. *Biochemical and Biophysical Research*
15 *Communications* 399, 416–421. 10.1016/j.bbrc.2010.07.090.
- 16 52. Bradford, S.T.J., Ranghini, E.J., Grimley, E., Lee, P.H., and Dressler, G.R. (2019). High-
17 throughput screens for agonists of bone morphogenetic protein (BMP) signaling identify
18 potent benzoxazole compounds. *J Biol Chem* 294, 3125–3136. 10.1074/jbc.RA118.006817.
- 19 53. Zammit, P.S., Partridge, T.A., and Yablonka-Reuveni, Z. (2006). The Skeletal Muscle
20 Satellite Cell: The Stem Cell That Came in From the Cold. *J Histochem Cytochem.* 54,
21 1177–1191. 10.1369/jhc.6R6995.2006.
- 22 54. Sartori, R., Gregorevic, P., and Sandri, M. (2014). TGF β and BMP signaling in skeletal
23 muscle: potential significance for muscle-related disease. *Trends in Endocrinology &*
24 *Metabolism* 25, 464–471. 10.1016/j.tem.2014.06.002.
- 25 55. Blaauw, B., Canato, M., Agatea, L., Toniolo, L., Mammucari, C., Masiero, E., Abraham, R.,
26 Sandri, M., Schiaffino, S., and Reggiani, C. (2009). Inducible activation of Akt increases
27 skeletal muscle mass and force without satellite cell activation. *FASEB J* 23, 3896–3905.
28 10.1096/fj.09-131870.

- 1 56. Peris-Moreno, D., Taillandier, D., and Polge, C. (2020). MuRF1/TRIM63, Master Regulator
2 of Muscle Mass. *Int J Mol Sci* 21, 6663. 10.3390/ijms21186663.
- 3 57. Cohen, S., Brault, J.J., Gygi, S.P., Glass, D.J., Valenzuela, D.M., Gartner, C., Latres, E., and
4 Goldberg, A.L. (2009). During muscle atrophy, thick, but not thin, filament components are
5 degraded by MuRF1-dependent ubiquitylation. *J Cell Biol* 185, 1083–1095.
6 10.1083/jcb.200901052.
- 7 58. Liang, Q., Cai, M., Zhang, J., Song, W., Zhu, W., Xi, L., and Tian, Z. (2020). Role of
8 Muscle-Specific Histone Methyltransferase (Smyd1) in Exercise-Induced Cardioprotection
9 against Pathological Remodeling after Myocardial Infarction. *International Journal of*
10 *Molecular Sciences* 21, 7010. 10.3390/ijms21197010.
- 11 59. Kitajima, Y., Suzuki, N., Yoshioka, K., Izumi, R., Tateyama, M., Tashiro, Y., Takahashi, R.,
12 Aoki, M., and Ono, Y. (2020). Inducible Rpt3, a Proteasome Component, Knockout in
13 Adult Skeletal Muscle Results in Muscle Atrophy. *Front Cell Dev Biol* 8, 859.
14 10.3389/fcell.2020.00859.
- 15 60. Chen, S., Chen, J., Wang, C., He, T., Yang, Z., Huang, W., Luo, X., and Zhu, H. (2023).
16 Betaine attenuates age-related suppression in autophagy via Mettl21c/p97/VCP axis to
17 delay muscle loss. *J Nutr Biochem* 125, 109555. 10.1016/j.jnutbio.2023.109555.
- 18 61. Chen, Y., Ma, Y., Tang, J., Zhang, D., Zhao, Q., Liu, J., Tang, H., Zhang, J., He, G., Zhong,
19 C., et al. (2023). Physical exercise attenuates age-related muscle atrophy and exhibits
20 anti-ageing effects via the adiponectin receptor 1 signalling. *J Cachexia Sarcopenia Muscle*
21 14, 1789–1801. 10.1002/jcsm.13257.
- 22 62. Piétri-Rouxel, F., Gentil, C., Vassilopoulos, S., Baas, D., Mouisel, E., Ferry, A., Vignaud,
23 A., Hourdé, C., Marty, I., Schaeffer, L., et al. (2010). DHPR alpha1S subunit controls
24 skeletal muscle mass and morphogenesis. *EMBO J.* 29, 643–654. 10.1038/emboj.2009.366.
- 25 63. Peczkowski, K.K., Rastogi, N., Lowe, J., Floyd, K.T., Schultz, E.J., Karaze, T., Davis, J.P.,
26 Rafael-Fortney, J.A., and Janssen, P.M.L. (2020). Muscle Twitch Kinetics Are Dependent
27 on Muscle Group, Disease State, and Age in Duchenne Muscular Dystrophy Mouse
28 Models. *Frontiers in Physiology* 11, 1203. 10.3389/fphys.2020.568909.

- 1 64. Jones, R.A., Reich, C.D., Dissanayake, K.N., Kristmundsdottir, F., Findlater, G.S.,
2 Ribchester, R.R., Simmen, M.W., and Gillingwater, T.H. (2016). NMJ-morph reveals
3 principal components of synaptic morphology influencing structure-function relationships
4 at the neuromuscular junction. *Open Biol* 6, 160240. 10.1098/rsob.160240.
- 5 65. Shadrach, J.L., and Pierchala, B.A. (2018). Semaphorin3A Signaling Is Dispensable for
6 Motor Axon Reinnervation of the Adult Neuromuscular Junction. *eNeuro* 5.
7 10.1523/ENEURO.0155-17.2018.
- 8 66. Davis-Lopez de Carrizosa, M.A., Morado-Diaz, C.J., Morcuende, S., de la Cruz, R.R., and
9 Pastor, A.M. (2010). Nerve Growth Factor Regulates the Firing Patterns and Synaptic
10 Composition of Motoneurons. *Journal of Neuroscience* 30, 8308–8319.
11 10.1523/JNEUROSCI.0719-10.2010.
- 12 67. Höke, A., Redett, R., Hameed, H., Jari, R., Zhou, C., Li, Z.B., Griffin, J.W., and Brushart,
13 T.M. (2006). Schwann Cells Express Motor and Sensory Phenotypes That Regulate Axon
14 Regeneration. *J. Neurosci.* 26, 9646–9655. 10.1523/JNEUROSCI.1620-06.2006.
- 15 68. Taetzsch, T., Tenga, M.J., and Valdez, G. (2017). Muscle Fibers Secrete FGFBP1 to Slow
16 Degeneration of Neuromuscular Synapses during Aging and Progression of ALS. *J*
17 *Neurosci* 37, 70–82. 10.1523/JNEUROSCI.2992-16.2016.
- 18 69. Barik, A., Li, L., Sathyamurthy, A., Xiong, W.-C., and Mei, L. (2016). Schwann Cells in
19 Neuromuscular Junction Formation and Maintenance. *J. Neurosci.* 36, 9770–9781.
20 10.1523/JNEUROSCI.0174-16.2016.
- 21 70. Kawanishi, N., and Machida, S. (2021). Alterations of macrophage and neutrophil content
22 in skeletal muscle of aged versus young mice. *Muscle Nerve* 63, 600–607.
23 10.1002/mus.27158.
- 24 71. Cui, C.-Y., Driscoll, R.K., Piao, Y., Chia, C.W., Gorospe, M., and Ferrucci, L. (2019).
25 Skewed macrophage polarization in aging skeletal muscle. *Aging Cell* 18, e13032.
26 10.1111/accel.13032.
- 27 72. Zhao, R.-Z., Jiang, S., Zhang, L., and Yu, Z.-B. (2019). Mitochondrial electron transport
28 chain, ROS generation and uncoupling (Review). *International Journal of Molecular*
29 *Medicine* 44, 3–15. 10.3892/ijmm.2019.4188.

- 1 73. Börsch, A., Ham, D.J., Mittal, N., Tintignac, L.A., Migliavacca, E., Feige, J.N., Rütegg,
2 M.A., and Zavolan, M. (2021). Molecular and phenotypic analysis of rodent models reveals
3 conserved and species-specific modulators of human sarcopenia. *Commun Biol* 4, 1–15.
4 10.1038/s42003-021-01723-z.
- 5 74. Grabert, K., Sehgal, A., Irvine, K.M., Wollscheid-Lengeling, E., Ozdemir, D.D., Stables, J.,
6 Luke, G.A., Ryan, M.D., Adamson, A., Humphreys, N.E., et al. (2020). A Transgenic Line
7 That Reports CSF1R Protein Expression Provides a Definitive Marker for the Mouse
8 Mononuclear Phagocyte System. *J Immunol* 205, 3154–3166. 10.4049/jimmunol.2000835.
- 9 75. Walton, R.G., Kosmac, K., Mula, J., Fry, C.S., Peck, B.D., Groshong, J.S., Finlin, B.S.,
10 Zhu, B., Kern, P.A., and Peterson, C.A. (2019). Human skeletal muscle macrophages
11 increase following cycle training and are associated with adaptations that may facilitate
12 growth. *Sci Rep* 9, 969. 10.1038/s41598-018-37187-1.
- 13 76. Shook, B.A., Wasko, R.R., Rivera-Gonzalez, G.C., Salazar-Gatzimas, E., López-Giráldez,
14 F., Dash, B.C., Muñoz-Rojas, A.R., Aultman, K.D., Zwick, R.K., Lei, V., et al. (2018).
15 Myofibroblast proliferation and heterogeneity are supported by macrophages during skin
16 repair. *Science* 362, eaar2971. 10.1126/science.aar2971.
- 17 77. Amara, C.E., Shankland, E.G., Jubrias, S.A., Marcinek, D.J., Kushmerick, M.J., and
18 Conley, K.E. (2007). Mild mitochondrial uncoupling impacts cellular aging in human
19 muscles in vivo. *Proc Natl Acad Sci U S A* 104, 1057–1062. 10.1073/pnas.0610131104.
- 20 78. B. Andrews, Z. (2010). Uncoupling Protein-2 and the Potential Link Between Metabolism
21 and Longevity. *Current Aging Science* 3, 102–112.
- 22 79. Rose, G., Crocco, P., Rango, F.D., Montesanto, A., and Passarino, G. (2011). Further
23 Support to the Uncoupling-to-Survive Theory: The Genetic Variation of Human UCP Genes
24 Is Associated with Longevity. *PLOS ONE* 6, e29650. 10.1371/journal.pone.0029650.
- 25 80. Cui, R., Gao, M., Qu, S., and Liu, D. (2014). Overexpression of superoxide dismutase 3
26 gene blocks high-fat diet-induced obesity, fatty liver and insulin resistance. *Gene Ther* 21,
27 840–848. 10.1038/gt.2014.64.

- 1 81. Noubade, R., Wong, K., Ota, N., Rutz, S., Eidenschenk, C., Valdez, P.A., Ding, J., Peng, I.,
2 Sebrell, A., Caplazi, P., et al. (2014). NRROS negatively regulates reactive oxygen species
3 during host defence and autoimmunity. *Nature* 509, 235–239. 10.1038/nature13152.
- 4 82. Iyer, C.C., Chugh, D., Bobbili, P.J., Iii, A.J.B., Crum, A.E., Yi, A.F., Kaspar, B.K., Meyer,
5 K.C., Burghes, A.H.M., and Arnold, W.D. (2021). Follistatin-induced muscle hypertrophy
6 in aged mice improves neuromuscular junction innervation and function. *Neurobiol Aging*
7 104, 32–41. 10.1016/j.neurobiolaging.2021.03.005.
- 8 83. Liu, X., Zhang, N., Sun, B., and Wang, B. (2022). Time-specific effects of acute eccentric
9 exercise on myostatin, follistatin and decorin in the circulation and skeletal muscle in rats.
10 *Physiol Res* 71, 783–790. 10.33549/physiolres.934833.
- 11 84. Brandt, N., Dethlefsen, M.M., Bangsbo, J., and Pilegaard, H. (2017). PGC-1 α and exercise
12 intensity dependent adaptations in mouse skeletal muscle. *PLoS ONE* 12, e0185993.
13 10.1371/journal.pone.0185993.
- 14 85. Mills, R., Taylor-Weiner, H., Correia, J.C., Agudelo, L.Z., Allodi, I., Kolonelou, C.,
15 Martinez-Redondo, V., Ferreira, D.M.S., Nichterwitz, S., Comley, L.H., et al. (2017).
16 Neurturin is a PGC-1 α -controlled myokine that promotes motor neuron recruitment and
17 neuromuscular junction formation. *Mol Metab* 7, 12–22. 10.1016/j.molmet.2017.11.001.
- 18 86. Vue, Z., Garza-Lopez, E., Neikirk, K., Katti, P., Vang, L., Beasley, H., Shao, J., Marshall,
19 A.G., Crabtree, A., Murphy, A.C., et al. (2023). 3D reconstruction of murine mitochondria
20 reveals changes in structure during aging linked to the MICOS complex. *Aging Cell* 22,
21 e14009. 10.1111/accel.14009.
- 22 87. De Palma, C., Falcone, S., Pisoni, S., Cipolat, S., Panzeri, C., Pambianco, S., Pisconti, A.,
23 Allevi, R., Bassi, M.T., Cossu, G., et al. (2010). Nitric oxide inhibition of Drp1-mediated
24 mitochondrial fission is critical for myogenic differentiation. *Cell Death Differ.* 17, 1684–
25 1696. 10.1038/cdd.2010.48.
- 26 88. Sartori, R., Schirwis, E., Blaauw, B., Bortolanza, S., Zhao, J., Enzo, E., Stantzou, A.,
27 Mouisel, E., Toniolo, L., Ferry, A., et al. (2013). BMP signaling controls muscle mass. *Nat*
28 *Genet* 45, 1309–1318. 10.1038/ng.2772.

- 1 89. Roy, A., and Kumar, A. (2022). Supraphysiological activation of TAK1 promotes skeletal
2 muscle growth and mitigates neurogenic atrophy. *Nat Commun* *13*, 2201. 10.1038/s41467-
3 022-29752-0.
- 4 90. Baehr, L.M., West, D.W.D., Marcotte, G., Marshall, A.G., De Sousa, L.G., Baar, K., and
5 Bodine, S.C. (2016). Age-related deficits in skeletal muscle recovery following disuse are
6 associated with neuromuscular junction instability and ER stress, not impaired protein
7 synthesis. *Aging (Albany NY)* *8*, 127–146. 10.18632/aging.100879.
- 8 91. Sandri, M., Barberi, L., Bijlsma, A.Y., Blaauw, B., Dyar, K.A., Milan, G., Mammucari, C.,
9 Meskers, C.G.M., Pallafacchina, G., Paoli, A., et al. (2013). Signalling pathways regulating
10 muscle mass in ageing skeletal muscle. The role of the IGF1-Akt-mTOR-FoxO pathway.
11 *Biogerontology* *14*, 303–323. 10.1007/s10522-013-9432-9.
- 12 92. Hurley, F.M., Costello, D.J., and Sullivan, A.M. (2004). Neuroprotective effects of delayed
13 administration of growth/differentiation factor-5 in the partial lesion model of Parkinson's
14 disease. *Experimental Neurology* *185*, 281–289. 10.1016/j.expneurol.2003.10.003.
- 15 93. Hegarty, S.V., O'Keefe, G.W., and Sullivan, A.M. (2013). BMP-Smad 1/5/8 signalling in
16 the development of the nervous system. *Progress in Neurobiology* *109*, 28–41.
17 10.1016/j.pneurobio.2013.07.002.
- 18 94. Osório, C., Chacón, P.J., Kisiswa, L., White, M., Wyatt, S., Rodríguez-Tébar, A., and
19 Davies, A.M. (2013). Growth differentiation factor 5 is a key physiological regulator of
20 dendrite growth during development. *Development* *140*, 4751–4762. 10.1242/dev.101378.
- 21 95. Normoyle, K.P., Kim, M., Farahvar, A., Llano, D., Jackson, K., and Wang, H. (2015). The
22 emerging neuroprotective role of mitochondrial uncoupling protein-2 in traumatic brain
23 injury. *Transl Neurosci* *6*, 179–186. 10.1515/tnsci-2015-0019.
- 24 96. Robbins, D., and Zhao, Y. (2011). New Aspects of Mitochondrial Uncoupling Proteins
25 (UCPs) and Their Roles in Tumorigenesis. *Int J Mol Sci* *12*, 5285–5293.
26 10.3390/ijms12085285.
- 27 97. de Oliveira Bristot, V.J., de Bem Alves, A.C., Cardoso, L.R., da Luz Scheffer, D., and
28 Aguiar, A.S. (2019). The Role of PGC-1 α /UCP2 Signaling in the Beneficial Effects of
29 Physical Exercise on the Brain. *Front Neurosci* *13*, 292. 10.3389/fnins.2019.00292.

- 1 98. Montez, P., Vázquez-Medina, J.P., Rodríguez, R., Thorwald, M.A., Viscarra, J.A., Lam, L.,
2 Peti-Peterdi, J., Nakano, D., Nishiyama, A., and Ortiz, R.M. (2012). Angiotensin receptor
3 blockade recovers hepatic UCP2 expression and aconitase and SDH activities and
4 ameliorates hepatic oxidative damage in insulin resistant rats. *Endocrinology* *153*, 5746–
5 5759. 10.1210/en.2012-1390.
- 6 99. Sullivan, P.G., Dubé, C., Dorenbos, K., Steward, O., and Baram, T.Z. (2003). Mitochondrial
7 uncoupling protein-2 protects the immature brain from excitotoxic neuronal death. *Ann*
8 *Neurol* *53*, 711–717. 10.1002/ana.10543.
- 9 100. Dietrich, M.O., and Horvath, T.L. (2010). The role of mitochondrial uncoupling proteins in
10 lifespan. *Pflugers Arch* *459*, 269–275. 10.1007/s00424-009-0729-0.
- 11 101. Rigamonti, E., Zordan, P., Sciorati, C., Rovere-Querini, P., and Brunelli, S. (2014).
12 Macrophage Plasticity in Skeletal Muscle Repair. *BioMed Research International* *2014*,
13 e560629. 10.1155/2014/560629.
- 14 102. Roux-Biejat, P., Coazzoli, M., Marrazzo, P., Zecchini, S., Di Renzo, I., Prata, C., Napoli, A.,
15 Moscheni, C., Giovarelli, M., Barbalace, M.C., et al. (2021). Acid Sphingomyelinase
16 Controls Early Phases of Skeletal Muscle Regeneration by Shaping the Macrophage
17 Phenotype. *Cells* *10*, 3028. 10.3390/cells10113028.
- 18 103. van Beek, A.A., Van den Bossche, J., Mastroberardino, P.G., de Winther, M.P.J., and
19 Leenen, P.J.M. (2019). Metabolic Alterations in Aging Macrophages: Ingredients for
20 Inflammaging? *Trends in Immunology* *40*, 113–127. 10.1016/j.it.2018.12.007.
- 21 104. Hangelbroek, R.W.J., Fazlzadeh, P., Tieland, M., Boekschoten, M.V., Hooiveld, G.J.E.J.,
22 van Duynhoven, J.P.M., Timmons, J.A., Verdijk, L.B., de Groot, L.C.P.G.M., van Loon,
23 L.J.C., et al. (2016). Expression of protocadherin gamma in skeletal muscle tissue is
24 associated with age and muscle weakness. *Journal of Cachexia, Sarcopenia and Muscle* *7*,
25 604–614. 10.1002/jcsm.12099.
- 26 105. Lavin, K.M., Perkins, R.K., Jemiolo, B., Raue, U., Trappe, S.W., and Trappe, T.A. (2020).
27 Effects of aging and lifelong aerobic exercise on basal and exercise-induced inflammation
28 in women. *J Appl Physiol (1985)* *129*, 1493–1504. 10.1152/jappphysiol.00655.2020.

- 1 106. Raue, U., Trappe, T.A., Estrem, S.T., Qian, H.-R., Helvering, L.M., Smith, R.C., and
2 Trappe, S. (2012). Transcriptome signature of resistance exercise adaptations: mixed
3 muscle and fiber type specific profiles in young and old adults. *J Appl Physiol* (1985) *112*,
4 1625–1636. 10.1152/jappphysiol.00435.2011.
- 5 107. Armand, A.-S., Della Gaspera, B., Launay, T., Charbonnier, F., Gallien, C.L., and Chanoine,
6 C. (2003). Expression and neural control of follistatin versus myostatin genes during
7 regeneration of mouse soleus. *Dev. Dyn.* *227*, 256–265. 10.1002/dvdy.10306.
- 8 108. Bagheri, R., Moghadam, B.H., Church, D.D., Tinsley, G.M., Eskandari, M., Moghadam,
9 B.H., Motevalli, M.S., Baker, J.S., Robergs, R.A., and Wong, A. (2020). The effects of
10 concurrent training order on body composition and serum concentrations of follistatin,
11 myostatin and GDF11 in sarcopenic elderly men. *Experimental Gerontology* *133*, 110869.
12 10.1016/j.exger.2020.110869.
- 13 109. Ivanov, M.N., Stoyanov, D.S., Pavlov, S.P., and Tonchev, A.B. (2022). Distribution,
14 Function, and Expression of the Apelinergic System in the Healthy and Diseased
15 Mammalian Brain. *Genes* *13*, 2172. 10.3390/genes13112172.
- 16 110. Chugh, D., Iyer, C.C., Bobbili, P., Blatnik, A.J., Kaspar, B.K., Meyer, K., Burghes, A.H.,
17 Clark, B.C., and Arnold, W.D. (2021). Voluntary wheel running with and without follistatin
18 overexpression improves NMJ transmission but not motor unit loss in late life of C57BL/6J
19 mice. *Neurobiology of Aging* *101*, 285–296. 10.1016/j.neurobiolaging.2021.01.012.
- 20 111. Kwak, S.E., Cho, S.C., Bae, J.H., Lee, J., Shin, H.E., Di Zhang, D., Lee, Y.-I., and Song, W.
21 (2019). Effects of exercise-induced apelin on muscle function and cognitive function in
22 aged mice. *Experimental Gerontology* *127*, 110710. 10.1016/j.exger.2019.110710.
- 23 112. Kasai, A., Kinjo, T., Ishihara, R., Sakai, I., Ishimaru, Y., Yoshioka, Y., Yamamuro, A.,
24 Ishige, K., Ito, Y., and Maeda, S. (2011). Apelin Deficiency Accelerates the Progression of
25 Amyotrophic Lateral Sclerosis. *PLOS ONE* *6*, e23968. 10.1371/journal.pone.0023968.
- 26 113. Hofmann, M., Schober-Halper, B., Oesen, S., Franzke, B., Tschan, H., Bachl, N., Strasser,
27 E.-M., Quittan, M., Wagner, K.-H., and Wessner, B. (2016). Effects of elastic band
28 resistance training and nutritional supplementation on muscle quality and circulating
29 muscle growth and degradation factors of institutionalized elderly women: the Vienna

- 1 Active Ageing Study (VAAS). *Eur J Appl Physiol* 116, 885–897. 10.1007/s00421-016-
2 3344-8.
- 3 114. Held, A., Major, P., Sahin, A., Reenan, R.A., Lipscombe, D., and Wharton, K.A. (2019).
4 Circuit Dysfunction in SOD1-ALS Model First Detected in Sensory Feedback Prior to
5 Motor Neuron Degeneration Is Alleviated by BMP Signaling. *J Neurosci* 39, 2347–2364.
6 10.1523/JNEUROSCI.1771-18.2019.
- 7 115. Guttenplan, K.A., Weigel, M.K., Adler, D.I., Couthouis, J., Liddelow, S.A., Gitler, A.D.,
8 and Barres, B.A. (2020). Knockout of reactive astrocyte activating factors slows disease
9 progression in an ALS mouse model. *Nat Commun* 11, 3753. 10.1038/s41467-020-17514-9.
- 10 116. Brohawn, D.G., O'Brien, L.C., and Bennett, J.P. (2016). RNAseq Analyses Identify Tumor
11 Necrosis Factor-Mediated Inflammation as a Major Abnormality in ALS Spinal Cord. *PLoS*
12 *One* 11, e0160520. 10.1371/journal.pone.0160520.
- 13 117. Bouredji, Z., Argaw, A., and Frenette, J. (2022). The inflammatory response, a mixed
14 blessing for muscle homeostasis and plasticity. *Front Physiol* 13, 1032450.
15 10.3389/fphys.2022.1032450.
- 16 118. Park, H.T., Kim, Y.H., Lee, K.E., and Kim, J.K. (2020). Behind the pathology of
17 macrophage-associated demyelination in inflammatory neuropathies: demyelinating
18 Schwann cells. *Cell Mol Life Sci* 77, 2497–2506. 10.1007/s00018-019-03431-8.
- 19 119. Ransohoff, R.M. (2016). How neuroinflammation contributes to neurodegeneration.
20 *Science* 353, 777–783. 10.1126/science.aag2590.

21

22 **Figure legends**

23 **Figure 1 Age-related neuromuscular failure and GDF5 overexpression in muscle.** **A:** Weight
24 of *Tibialis anterior* (TA) and *Gastrocnemius* (GAS) of adult (7 months; $n=10$), old (20 months;
25 $n=12$) and very old (26-27 months; $n=14$) mice normalized to body weight. **B:** Grip strength
26 mean of adult ($n=8$), old ($n=12$) and very old ($n=10$) mice normalized to body weight. **C:**
27 Representative electroneuromyography (ENMG) traces recorded in TAs across ages and
28 amplitudes of compound muscle action potentials (CMAP) (adult $n=11$; old $n=12$; very old

33

1 $n=16$). **D**: RT-qPCR for *Chrm1*, *Chrn1*, *Chrnd*, *Chrmg* and *Musk* in TAs across ages (adult
 2 $n=4$; old $n=8$; very old $n=9$). **E**: Experimental design: AAV-Scramble (Scra) or -GDF5 (GDF5)
 3 were injected in 20-month-old mouse TA. Representative picture of TAs injected four weeks
 4 with Scra or GDF5 (21-month-old). Weight of TAs was normalized to body weight (Scra $n=12$;
 5 GDF5 $n=10$). **F**: Representative images of 21-month-old TAs injected with Scra or GDF5,
 6 immunostained with laminin (grey) and DAPI (blue), scale bar 100 μm . Size distribution of TA
 7 fibres and mean of myofibre number were determined in Scra ($n=10$) or GDF5 ($n=8$) conditions.
 8 All data are mean \pm SEM ($*P < 0.05$, $**P < 0.01$, $***P < 0.001$). (**A-D**) P values were
 9 calculated by ordinary one-way ANOVA followed by Tukey's multiple comparison test or (**E, F**)
 10 unpaired t-test.

11

12 **Figure 2 Local GDF5 overexpression in old mice leads to muscle hypertrophy. A**:
 13 Representative images of TAs cryosections from 21-month-old mice injected with AVV-Scra
 14 (Scra) or -GDF5 (GDF5), stained with hematoxylin and eosin, scale bar 100 μm . Number of
 15 myonuclei per fibre and proportion of centro-nucleated fibres were determined using ImageJ-
 16 based machine learning algorithm (Scra $n=10$; GDF5 $n=8$). **B**: RT-qPCR for *Pax7*, *Myod*, *Myog*,
 17 and *Myf6* analyzed in TAs injected with Scra ($n=7$) or GDF5 ($n=7$). **C**: Representative western
 18 blot showing the level of puromycin-labeled proteins in TAs injected with Scra or GDF5.
 19 Relative signal intensity of puromycin-labeled proteins was determined (Scra $n=6$; GDF5 $n=5$).
 20 Ponceau S staining was used as loading control. **D**: Representative western blot showing the
 21 level of phosphorylated and total Akt, m-TOR and Rps6 proteins in TAs injected with Scra or
 22 GDF5. **E**: RT-qPCR for *MurF1*, *Atrogin1* and *Musal* analyzed in TAs injected with Scra ($n=7$)
 23 or GDF5 ($n=7$). **F**: Representative western blot showing the level of MyHC, Actin and α -Actinin
 24 proteins in TAs injected with Scra or GDF5. Relative signal intensity of proteins was determined
 25 (Scra $n=6$; GDF5 $n=6$). Ponceau S staining was used as loading control. **G**: Representative
 26 western blot showing the level of ubiquitinated proteins in TAs injected with Scra or GDF5.
 27 Relative signal intensity of ubiquitinated proteins was determined (Scra $n=6$; GDF5 $n=5$).
 28 Ponceau S staining was used as loading control. **H**: Representative western blot showing the
 29 level of LC3-I, LC3-II, p62 and Beclin1 proteins in TAs injected with Scra or GDF5. Ponceau S
 30 staining was used as loading control. All data are shown as the mean \pm SEM ($*P < 0.05$, $**P <$
 31 0.01 , $***P < 0.001$). (**A-H**) P values were calculated by unpaired t-test.

34

1 **Figure 3 GDF5 overexpression improves neuromuscular connectivity and NMJ**
2 **morphology.** **A:** Absolute tetanic force and rate of force production measured in TAs from 21-
3 month-old mice injected with AAV-Scra (Scra $n=9$) or -GDF5 (GDF5 $n=10$). **B:** Representative
4 ENMG traces and CMAPs amplitudes recorded in TAs injected with Scra ($n=9$) or -GDF5
5 ($n=10$). **C:** Representative images of neuromuscular junction (NMJ) from TAs injected with Scra
6 or GDF5, immunostained with neurofilament (NF: yellow) and bungarotoxin (BTX: purple),
7 scale bar 10 μm . Endplate area, acetylcholine receptor (AChR) area, nerve terminal area, and
8 overlap (nerve terminal area/AChR area ratio) parameters were determined in Scra ($n=4$) or
9 GDF5 ($n=3$) using ImageJ-based workflow. **D:** RT-qPCR for *S100 β* , *Mbp*, *Mpz*, *Pmp22*, *Gap-43*,
10 and *Fgfp1* analyzed in TAs injected with Scra ($n=6$) or GDF5 ($n=6$). All data are shown as the
11 mean \pm SEM (* $P < 0.05$, ** $P < 0.01$, *** $P < 0.001$). (**A**, **B**, **D**) P values were calculated by
12 unpaired t-test or (**C**) by Mann-Whitney test.

13

14 **Figure 4 hsGDF5 enhances human Schwann cell proliferation and decreases MuRF1**
15 **expression in human muscle cells.** **A:** RT-qPCR for *S100 β* and *MPZ* analyzed in human
16 quadriceps biopsies from Adult (21-42 years; $n=6$) and Aged (77-80 years; $n=10$) healthy
17 volunteers. **B:** Graphical representation of *in vitro* experiment. Human Schwann cells (hTERT
18 NF1) were treated with human synthetic GDF5 (hsGDF5) or PBS (control) and 48h after rate of
19 cell proliferation and gene expression experiments were performed. Representative images
20 showing hTERT NF1 cell nuclei after treatment for 48h with PBS or hsGDF5 at 10 or 50 ng/ml,
21 scale bar 100 μm . hTERT NF1 cell proliferation rate evaluated by CyQuant assay 48h after
22 treatment and *KI-67* expression analyzed by RT-qPCR ($n=4$ per condition). **C:** RT-qPCR for
23 *EGR2*, *PLP1* and *PMP22* analyzed in hTERT NF1 cells treated 48h with hsGDF5 or PBS ($n=4$
24 per condition). **D:** Graphical representation of *in vitro* experiment using human differentiated
25 muscle cells (8220) treated 72h with hsGDF5 (50 ng/ml) or PBS (control). RT-qPCR for *MuRF1*
26 was performed in 8220 cells treated 72h with hsGDF5 or PBS ($n=3$ per condition). All data are
27 shown as the mean \pm SEM (* $P < 0.05$, ** $P < 0.01$, *** $P < 0.001$). (**A**, **D**) P values were
28 calculated by unpaired t-test or (**B**, **C**) by ordinary one-way ANOVA followed by Dunnett's
29 multiple comparison test.

30

1 **Figure 5 GDF5 overexpression rejuvenates old whole muscle transcriptomic profile. A:**
 2 Principal component analysis (PCA) for gene expression patterns analyzed in TAs from 7-month
 3 adult and 21-months old mice injected with AAV-Sera (Adult-Sera $n=4$, Old-Sera; $n=4$) or -
 4 GDF5 (Old-GDF5; $n=4$). **B:** Graphical representation of unsupervised hierarchical sample
 5 clustering across groups. **C:** Heatmap showing 247 dysregulated genes in Old-Sera compared to
 6 Adult-Sera which are normalized in Old-GDF5 condition. **D:** RT-qPCR for *Csflr*, *Cd163*,
 7 *Cd209*, *Mgl2*, *Sod3*, *Ucp2* and *Nrros* analyzed in TAs of Adult-Sera ($n=6$), Old-Sera ($n=7$) and
 8 Old-GDF5 ($n=6$). **E:** RT-qPCR for *Apelin* and *Follistatin* analyzed in TAs of Old-Sera ($n=7$) and
 9 Old-GDF5 ($n=6-7$). All data are shown as the mean \pm SEM. * $P < 0.05$, ** $P < 0.01$, *** $P <$
 10 0.001 . **(D)** P values were calculated by ordinary one-way ANOVA followed by Dunnett's
 11 multiple comparison test or **(E)** by unpaired t-test.

12

13 **Figure 6 Chronic rGDF5 systemic administration in ageing mice preserves against age-**
 14 **related muscle wasting and improves NMJ morphology. A:** Graphical representation of *in*
 15 *vivo* experimental design. Recombinant mouse GDF5 (rGDF5) or control vehicle (Veh) were
 16 administered intraperitoneally into 20-months old mice. Four weeks after repetitive injections,
 17 gene expression was analyzed in TAs and the therapeutic effect was evaluated four months after
 18 the beginning of the treatment. **B:** RT-qPCR for *S100 β* , *Mbp*, *Mpz*, *Pmp22*, *Gap-43*, *Fgfp1*, *Ngf*,
 19 *Apelin* and *Follistatin* analyzed in TAs of mice treated four weeks with Veh ($n=8$) or rGDF5
 20 ($n=8$). **C:** Quantification of maximal muscle CSA determined by Magnetic Resonance Imaging
 21 (MRI) in hind limbs of mice treated four months with Veh ($n=12$) or rGDF5 ($n=10$), scale bar: 1
 22 mm. Muscle/body weight ratio of *Gastrocnemius* (GAS), *Tibialis anterior* (TA), *Extensor*
 23 *digitorum longus* (EDL), and *Soleus* (SOL) of mice treated four months with Veh ($n=12$) or
 24 rGDF5 ($n=10$). Mean of myofibre number was determined in GAS of mice treated four months
 25 with Veh ($n=5$) or rGDF5 ($n=4$). **D:** Representative images of GAS cryosections immunostained
 26 with laminin (grey), MyHC-IIB (purple), MyHC-IIA (yellow), and MyHC-IIX (black). Hybrid
 27 MyHC fibres express both MyHC-IIB and MyH-IIA (purple and yellow), MyHC-I expressing
 28 fibres are absent in GAS, scale bar 100 μ m. Mean of myofibre CSA for each fibre type was
 29 determined in GAS of mice treated with Veh ($n=5$) or rGDF5 ($n=4$) using ImageJ-based machine
 30 learning algorithm. **E:** Absolute tetanic force, specific force and rate of force production
 31 measured in TAs from mice treated with Veh ($n=12$) or rGDF5 ($n=10$). **F:** Representative images

36

1 of NMJ from EDLs immunostained with neurofilament (NF: yellow) and bungarotoxin (BTX:
 2 purple), scale bar 10 μ m. Endplate area and acetylcholine receptor (AChR) area parameters were
 3 determined in mice treated with Veh ($n=4$) or rGDF5 ($n=5$). All data are shown as the mean \pm
 4 SEM ($*P < 0.05$, $**P < 0.01$, $***P < 0.001$). (A-E) P values were calculated by unpaired t-test
 5 or (F) by Mann-Whitney test.
 6

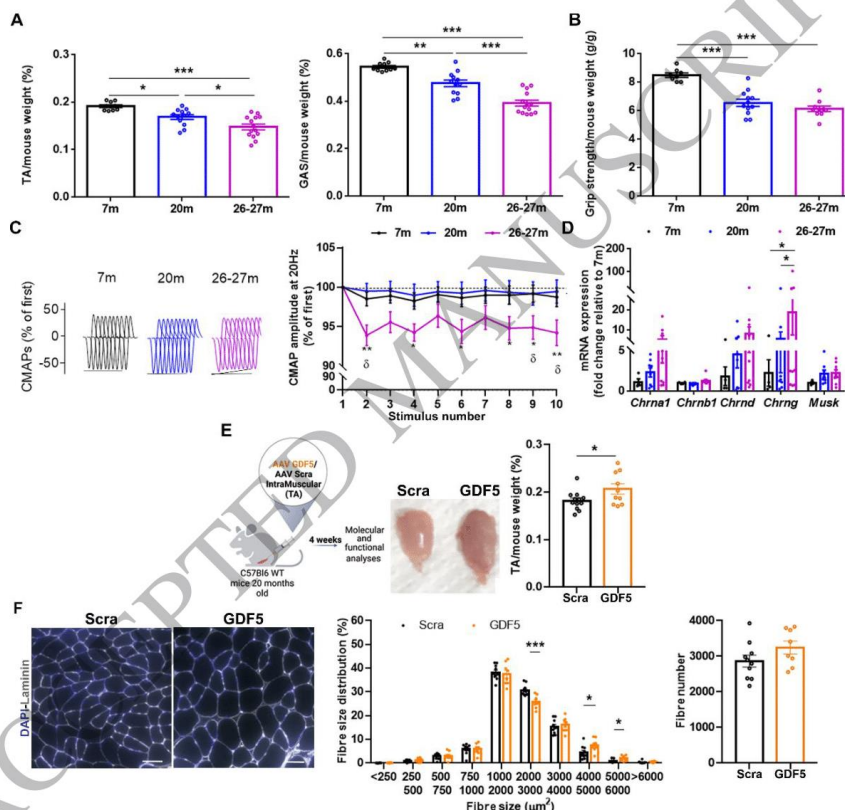


Figure 1
 150x144 mm (x DPI)

7
 8
 9
 10

Downloaded from https://academic.oup.com/brain/advance-article/doi/10.1093/brain/awae107/7641954 by CEREMES user on 31 July 2024

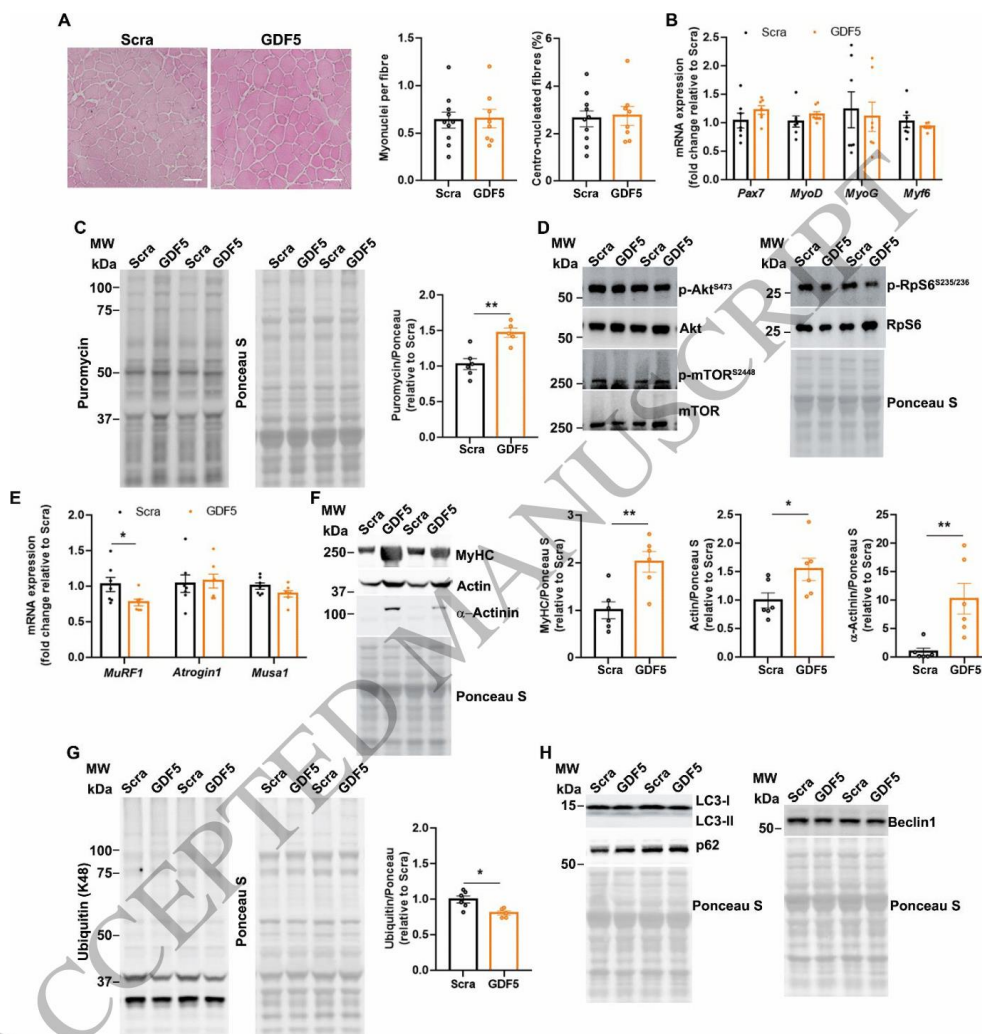


Figure 2
175x183 mm (x DPI)

1
2
3
4

Downloaded from https://academic.oup.com/brain/advance-article/doi/10.1093/brain/awae107/7641954 by CEREMES user on 31 July 2024

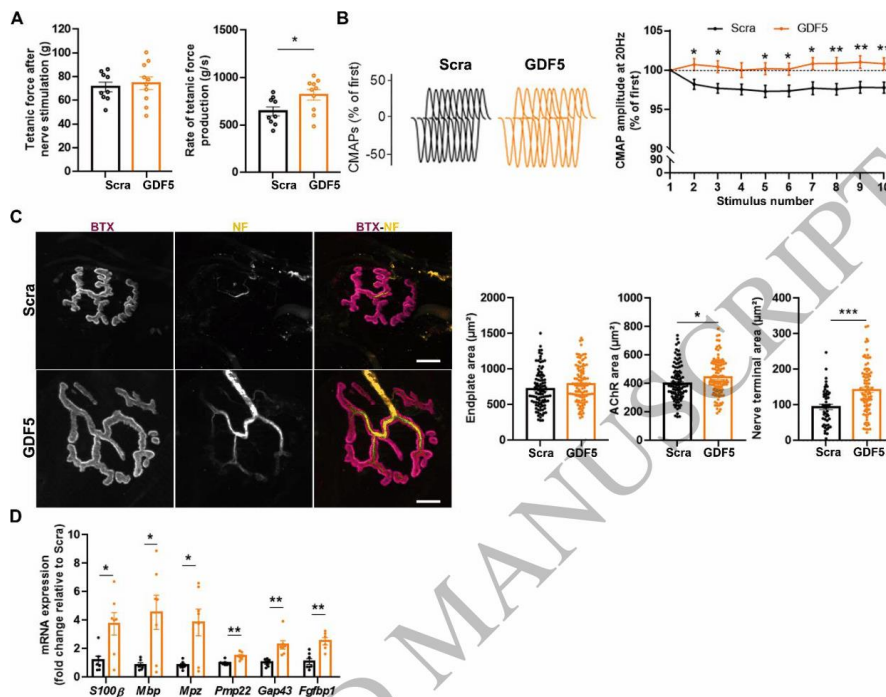


Figure 3
182x125 mm (x DPI)

1
2
3
4

Downloaded from https://academic.oup.com/brain/advance-article/doi/10.1093/brain/awae107/7641954 by CERMIES user on 31 July 2024

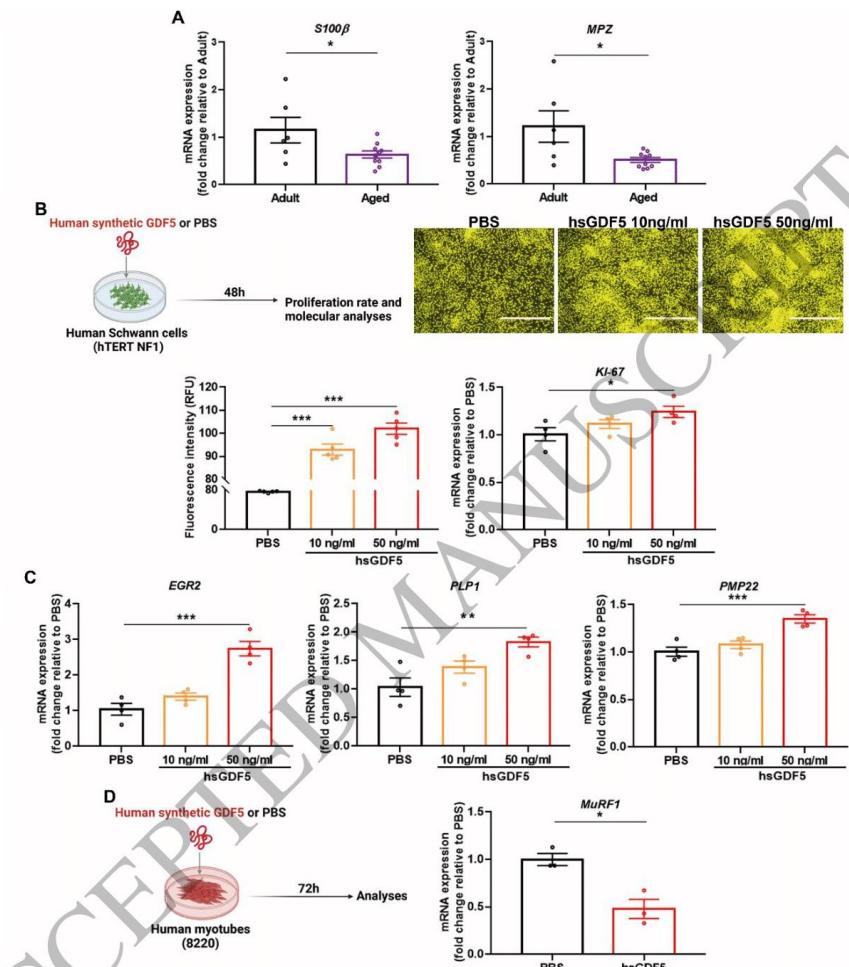


Figure 4
153x172 mm (x DPI)

1
2
3
4

Downloaded from https://academic.oup.com/brain/advance-article/doi/10.1093/brain/awae107/7641954 by CERMIES user on 31 July 2024

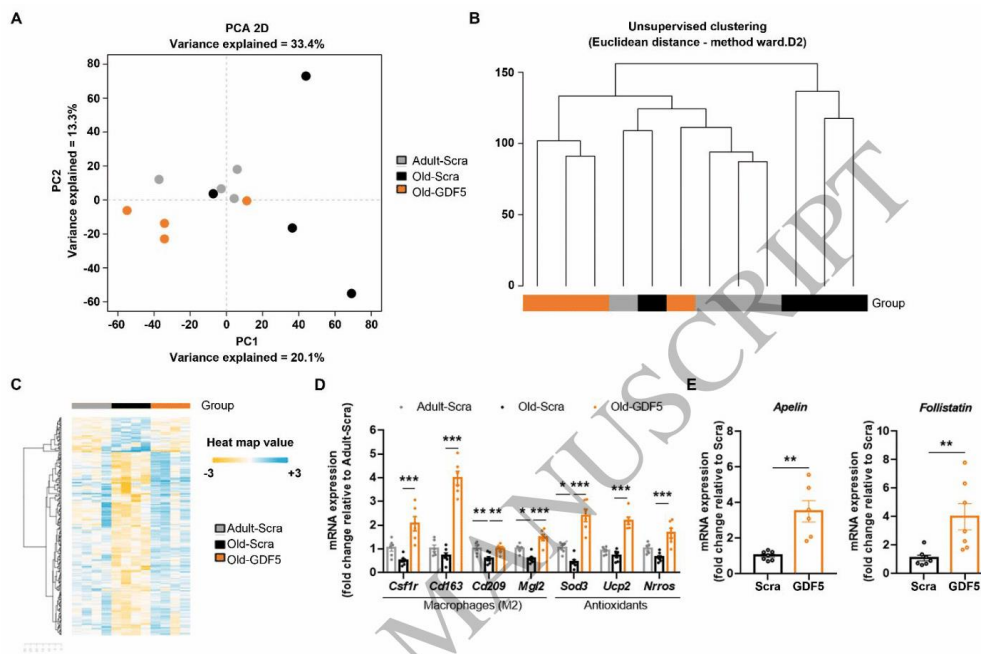
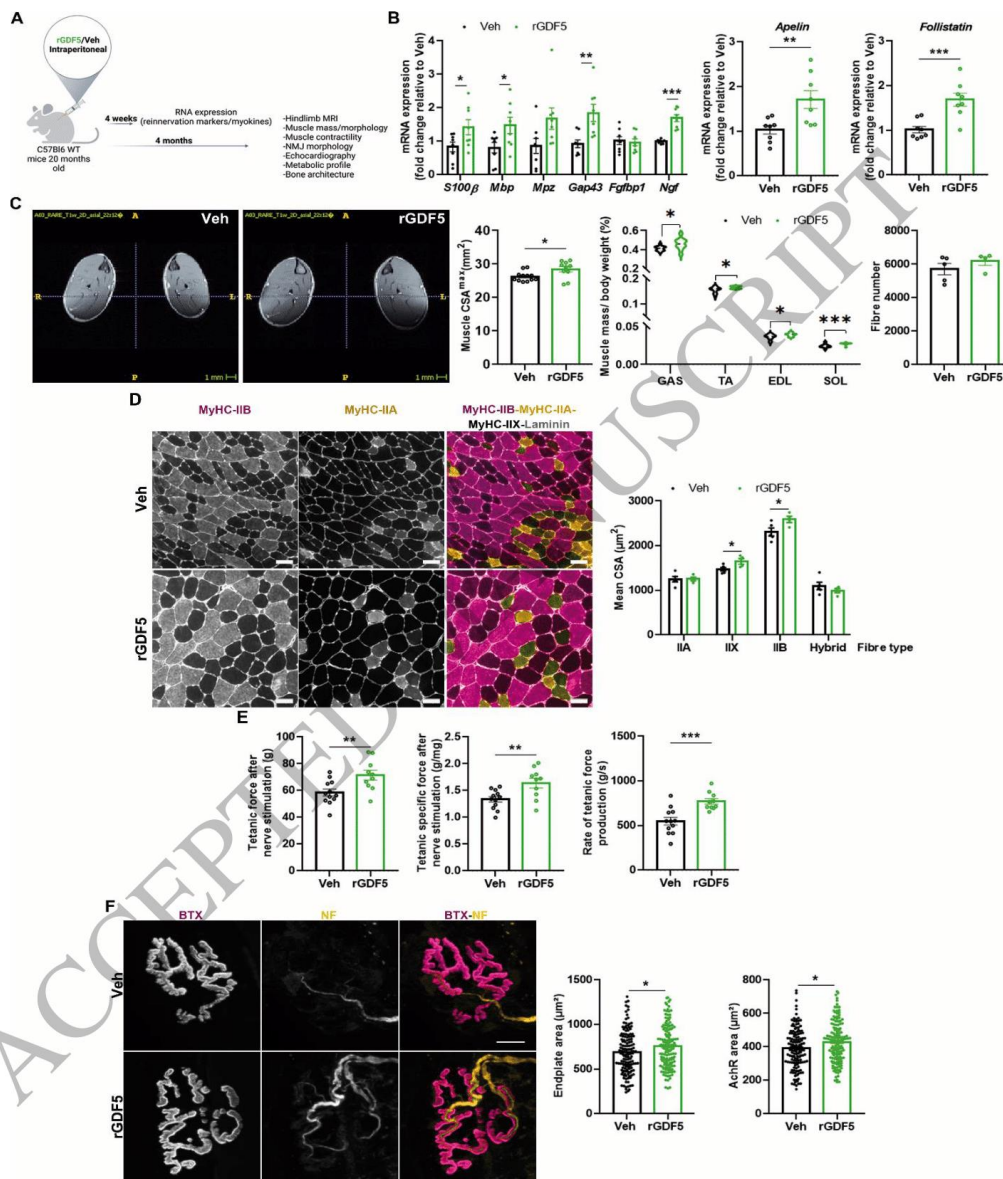


Figure 5
178x117 mm (x DPI)

1
2
3
4

Downloaded from https://academic.oup.com/brain/advance-article/doi/10.1093/brain/awae107/7641954 by CEREMES user on 31 July 2024



Downloaded from https://academic.oup.com/brain/advance-article/doi/10.1093/brain/awae107/7641954 by CEREMES user on 31 July 2024

1
2
3

Figure 6
179x224 mm (x DPI)